APICOMPLEXAN PARASITE INTERACTIONS WITH HOST ORGANELLES: RECRUITMENT, LIPID SCAVENGING, AND CONSEQUENCES

by

Sabrina Jane Nolan

A dissertation submitted to the Johns Hopkins University in conformity with the requirements for the Degree of Doctor of Philosophy

Baltimore, Maryland

April, 2016

ABSTRACT

Apicomplexa parasites are harmful pathogens of humans and animals. They invade mammalian cells wherein they reside within a parasitophorous vacuole (PV) that protects them from cytosolic destructive pathways but forms a physical barrier from host-derived nutrients. Among Apicomplexa, *Toxoplasma gondii* has proficiently evolved to recruit host organelles to its PV to facilitate nutrient uptake. Almost nothing is known about the intracellular development of *Neospora caninum*, a closely relative of *Toxoplasma*. We show that *N. caninum* is also able to attract host organelles (ER, Golgi, endosomes) to its PV from which it retrieves cholesterol and ceramides, revealing conserved strategies among these parasites to exploit nutrient-filled host organelles. We next explore the role of host lipid droplets (LD) as sources of neutral lipids for *Toxoplasma*. We demonstrate that host LD cluster around the PV, and infection leads to an increase, then decrease in host LD numbers, suggesting a manipulation of these structures by *Toxoplasma*. Indeed, *Toxoplasma* is able to scavenge lipids from host LD, in part through the interception of Rab vesicles associated with LD and the translocation of host LD into its PV. Ectopic addition of oleic acid (OA) up to 1 mM (non toxic concentration for mammalian cells) stimulates LD biogenesis. When exposed to 0.2 mM OA, *Toxoplasma* scavenges this fatty acid in excess, channels it to LD that accumulate in the cytoplasm, as a result of increased transcription of its enzymes generating neutral lipids. However, this condition slows down both parasite replication and egress. By comparison, 0.2 mM palmitic acid does not affect the parasite's intracellular development. Interestingly, ultrastructural analyses of OA-loaded *Toxoplasma* reveal for the first time, the presence of coated pits at the plasma membrane and structures potentially involved in endocytosis. More dramatically, addition of 0.4 mM OA to the medium results in massive accumulation of lipid deposits in the PV and the parasite, leading to replication defects and death. This highlights the high sensitivity of *Toxoplasma* towards

deleterious effects of accumulating fatty acids. Deciphering the lipotoxic response of the parasite would reveal new vulnerabilities amenable to controlling *Toxoplasma* infections.

Advisor: Dr. Isabelle Coppens, department of Molecular Microbiology and Immunology

Thesis Advisory Committee: Dr. Carolyn Machamer, Dr. J. Marie Hardwick, Dr. Valeria Culotta, and Dr. Andrew Pekosz

Alternates: Dr. Thomas Hartung and Dr. Sean Prigge

PREFACE

To my parents and brother, whose endless love, wisdom, kindness and unconditional support have allowed me to be where I am today, doing what I love; To my friends that I cherish dearly, whose presence, advice and love helped ensure that life is led to the fullest.

ACKNOWLEDGEMENTS

To my PhD thesis advisor and mentor, I thank Dr. Isabelle Coppens for giving me the opportunity to work with her, as well as all her insight, inspiration and discussions throughout the past four years. She is very supportive, has guided me through the field of *Toxoplasma*, cell biology and lipids, has taught me manuscript-writing, all with patience and kindness. Thank you for allowing me to pursue my own project and believing in me. It has been a real joy working with you.

I thank Dr. Julia Romano who has been an invaluable friend, mentor and colleague since I started working in the lab. She has given me never-ending support, both personally and professionally, as well as plenty of insight, encouragement, laughs and discussions, both in and out of lab. I do not think I could have achieved everything I have these past 4 years without you. Thank you for editing this thesis, as well as my other manuscripts. I know that although my time at Hopkins is nearly over, our friendship will endure and I look forward to it. Thank you.

I thank the members of my thesis committee: Dr. Carolyn Machamer, Dr. J. Marie Hardwick, Dr Valeria Culotta, Dr. Sean Prigge, and Dr. Andy Pekosz for all their scientific advice, suggestions and ideas. Thank you for giving me your time as I worked through this thesis.

I thank Dr. Karen Ehrenman, who is always available and willing to offer her help or advice with whatever problem I, or others encounter. You are so kind and are an invaluable member of the Coppens lab. I would also like to thank Dr. Vera Sampels, Dr. Christiane Voss, Dr. Dominique Promeneur, Eric Hartman and Jeff Danielson for being wonderful lab mates and friends, for making every day interesting and making me look forward to arriving in lab every day.

I thank Dr. Arturo Casadevall, the chair of the MMI department, who has always made time to listen to me and genuinely discuss any and all matters during my time as President of the MMI Student Group. He is also an amazing mentor, a sincere intellectual and an incredibly insightful man. I feel very fortunate to be collaborating with him as he kindly opened up the field of Mycology to me.

I thank all the MMI staff, in particular our academic coordinator, Gail O'Connor who is always available to help all students, with any administrative and student-related issue. You do such hard work and we appreciate you. Thank you also to Thom Hitzelberger, Maryann Smith, Leonid Shats and Genevieve Nixon.

I thank all the professors of MMI, especially Dr. Sabra Klein, Dr. Richard Markham and Dr. Doug Norris for giving me the opportunity to TA their class for 4 years. To Dr. Peter Agre for challenging me on the treadmill, and all MMI professors who are always helpful with an open-door policy.

I thank Dr. Thomas Hartung, who, without really knowing me, gave me an opportunity to work with him at the Center for Alternatives to Animal Testing at JHSPH. Thank you for being trusting, kind, generous, and above all, for inspiring others to live life to its full extent. I'm sure we will meet again, either here or in Italy.

I thank my MMI PhD cohort that I cherish dearly: Nicola Diny, James Gordy, Olivia Hall, Hugo Jhun and Kate Stevens. I am so lucky to have found such wonderful people to have shared classes with, milestones, and the continuous ups and the downs innate to the PhD life. But also, more importantly, to have friends with whom we could talk about anything: life, science, politics, and anything from the intellectual to the mundane. This occurring either indoors with a bottle of wine and board games, and at random bars, or outdoors: camping, hiking or traveling

across the East coast. Thank you for this journey we have shared, for your support and friendship.

I thank my very good friends Sean Doughty, Ashley Gordy (and little RJ) and Thomas Luechtefeld, who have made a lasting impact on me by making my life in Baltimore more enjoyable than I could have imagined and unforgettable. I am glad to have found people with interests so similar as my own, with whom I know will be lifelong friends. To my flatmate, Dr. Daniel Berg, for always having someone to come home to. To all my MMI friends (Nina Martin, Ben Blumberg, Amanda Balaban, Nick Wohlgemuth, Raul Saraiva, Tim Wang, Zach Stolp, Eric Jung, Ashley Nelson, Dr. Kyle Metz) for the laughs, the games, the late night drinking, the fun outdoors, helping with the MMI student group, keeping me company in the microscope facility, and the Daily Grind chats. To all my other friends across the U.S.A. and the world, thank you for sharing your life with me.

I thank Vanessa Sponar for being my lifelong friend and for us always finding each other no matter where we are. Your unconditional support and love has helped me through countless challenges and I appreciate you to no end. You have always believed in me and inspired me to reach higher like none other.

I thank all my family in Ireland and England, it is hard not being able to see you very often but every time I do see you, I feel like I am back home. No matter what, every single one of you can be relied upon and I am so lucky to be able to call you all as my family. Especially my two grandmothers, Nana and Maudie.

I thank my dear brother, Ciaran Nolan. Growing up together, we shared so many experiences, both good and bad, and they have all made us who we are. I am so proud to have you as my brother, and I treasure you more than you could know. You are one of the few who

can genuinely make me laugh any time, and you possess so many qualities I wish I had. I continue to strive to be as open, caring, and honest as you.

Finally, I dedicate this PhD thesis to my parents: My father, Dr. Canice Nolan and my mother Helen Kerrison. You have both made me who I am today and I cannot thank you enough for your unwavering love. Throughout my teenage years to late teen/early 20s doubts, to where I am today, you trusted me and supported me. It has not been easy living so far away from you, but you have always been only a phone call away, always with time to give. I miss you both all the time.

Mum, thank you for your endless optimism and encouragement, always seeing the positive no matter the circumstances. Your love and care know no bounds.

Dad, thank you for inspiring me to be who I am. A long time ago when I was five and you brought me to lab, probably shaped my future more than you could possibly have realized at the time. You always pushed me to go beyond and given me the confidence that I could do and be anything. I truly believe I have achieved all that I have thanks to you. I love you both.

TABLE OF CONTENTS

LIST OF FIGURES

Chapter 1:

Chapter 2:

Chapter 3:

Chapter 4:

Chapter 5:

LIST OF TABLES

MAIN ABBREVIATIONS USED

ACAT	acyl-CoA:Cholesterol Acyltransferase
ADRP	adipocyte differentiation-related protein
AS	autophagic structures
ATGL	adipose triglyceride lipase
CE	cholesteryl ester
CoA	Coenzyme A
DAG	diacylglycerol
DGAT	acyl-CoA:diacylglycerol Acyltransferase
EM	electron microscopy
ER	endoplasmic reticulum
FA	fatty acid
FAS	fatty acid synthase
FFA	free fatty acids
GPI	glycophosphatidylinositol
HFF	human foreskin fibroblasts
hLD	host lipid droplet
IFA	immunofluorescence assay
IMC	inner membrane complex
IVN	intra-vacuolar network
LD	lipid droplet(s)
LDL	low-density lipoprotein
MAMs	mitochondria associated membranes
MT	microtubules

MTOC	microtubule-organizing center
NL	neutral lipids
NO	nitric oxide
NPC1	Niemann-Pick type C1-related protein
OA	oleic acid
p.i.	post invasion
PA	palmitic acid
PC	phosphatidylcholine
PCC	Pearson's Correlation Coefficient
PDM	product differences of the mean
PE	phosphatidylethanolamine
PLINs	perilipins
PM	plasma membrane
Pru	Prugniaud Type II strain of *Toxoplasma*
PS	phosphatidylserine
PV	parasitophorous vacuole
PVM	parasitophorous vacuole plasma membrane
RFP	red fluorescent protein
ROS	reactive oxygen species
SE	steryl ester
TAG	triacylglycerol

CHAPTER 1

TOXOPLASMA GONDII AND *NEOSPORA CANINUM*: LIFE CYCLE, INTRACELLULAR DEVELOPMENT AND LIPID SCAVENGING

1. INTRODUCTION

Our laboratory focuses on the intracellular development of several parasites in the phylum of Apicomplexa, including *Toxoplasma gondii*, *Plasmodium* spp., *Cryptosporidium parvum,* and *Neospora caninum*. The Apicomplexa represent a diverse phylum with more than 5,000 species, and encompass important pathogens of both humans and animals, which cause toxoplasmosis (*Toxoplasma*), malaria (*Plasmodium spp.*), diarrhea (*Cryptosporidium spp.*), East Coast Fever in cattle (*Theileria*), coccidiosis in chickens (*Eimeria*), and neosporosis (*Neospora*). *Plasmodium falciparum* is the most clinically relevant parasite among the Apicomplexa, and is responsible for over 200 million infections and 500,000 deaths per year as estimated last year (WHO, 2015). However, in terms of worldwide infections, *Toxoplasma gondii* leads the charge with an estimated 25-35% of the world's population being infected (CDC, 2013).

All Apicomplexa are exclusively obligate intracellular parasites of either vertebrates or invertebrates, developing in a parasitophorous vacuole (PV) within the cytoplasm of their host cell (Blader *et al*, 2015). Apicomplexan parasites have a distinctive polarized cell structure featuring a complex arrangement of unique organelles at their apical end, e.g., the rhoptries, micronemes and the apicoplast (Dubey *et al*, 1998).

Toxoplasma gondii and *Neospora caninum* are the focus of this thesis and their life cycles, pathogenesis, basic biology, host cell-parasite interactions and nutrient uptake, e.g. lipids, will be described in detail in this introductory chapter. Despite the large range of hosts infected by *T. gondii*, it is the only species belonging to the *Toxoplasma* genus (Sibley and Boothroyd, 1992). Therefore, from here onwards, due to its status as a single species, *T. gondii* will be referred to as *Toxoplasma*.

1.2. Discovery of *Toxoplasma gondii* and *Neospora caninum*

Toxoplasma was discovered over a century ago but it took until 1932 for the parasite to be classified as the pathogenic agent causing toxoplasmosis (Nicolle and Manceaux, 1908; Robert Gangneux and Dardé, 2012). The genus was named *Toxoplasma* due to its arc-like shape (in greek: *toxon* is "bow") and the species was named "*gondii*" after *Ctenodactylus gundi*, the rodent in which it was initially discovered.

Toxoplasma is closely related to another pathogen, *Neospora caninum*, both of which are cyst-forming coccidians (Blader *et al*, 2015). Until 1988, *N. caninum* was misclassified as *Toxoplasma gondii*, due to its similar life cycle, transmission and morphology (Dubey *et al*, 1988; Dubey *et al*, 2007). It was originally discovered in dogs in Norway as a cyst-forming pathogen causing encephalitis (Bjerkås *et al*, 1984). Both parasites have highly conserved, orthologous genomes with nearly a one-to-one pattern between most protein-coding genes (Reid *et al*, 2012).

1.3. Life cycle

Like many parasites, *Toxoplasma* and *N. caninum* have complex life cycles, involving intermediate and definitive hosts where they undergo asexual and sexual replication, respectively. Asexual reproduction in the intermediate host is thought to be advantageous to achieve wider distribution in order to increase the probability of being taken up by the definitive host where sexual replication occurs.

Dubey and colleagues deciphered the lifecycle of *Toxoplasma* and Felidae are recognized as the definitive host (Dubey *et al*, 1970). In contrast to *Toxoplasma,* the Canidae are the definitive host of *Neospora* spp. Besides differences in their definitive hosts, the second

difference between the two parasites is the narrower range of intermediate hosts for *N. caninum,* largely restricted to dogs and cattle, and never found in humans.

Due to the similarity between the lifecycles of *Toxoplasma* and *N. caninum*, only the life cycle of *Toxoplasma* is described, and differences with *N. caninum* highlighted (Fig. 1-1). Following oocyst ingestion by an intermediate host such as a mouse, human or cattle, the sporozoites of *Toxoplasma* or *N. caninum* are released in the small intestine, where they infect the intestinal epithelium and where they transform into tachyzoites. After several rounds of replication, they penetrate the cell wall to reach the bloodstream, the quickest way to reach their target tissues. These tachyzoites (in Greek: *tachys* is "fast"), i.e. the rapid proliferative forms of the parasite, target the central nervous system (CNS) as well as muscle tissue to invade and replicate via endodyogeny, where two daughter cells form from one mother cell. (Fig. 1-1, blue area).

The large increase in parasite numbers due to the fast replication triggers the immune system. The immune response to *Toxoplasma* is orchestrated primarily by interferon gamma (IFNγ) and interleukin-12 (IL-12) – the chief players of the Th1 cell-mediated response. The immune response, in particular IFNγ, causes the tachyzoites to differentiate into the quiescent, slow growing form of the parasite, the bradyzoite (in Greek: *brady* is "slow"). These cysts remain indefinitely in the CNS, eye or muscle tissue (skeletal and cardiac, preferentially), essentially invisible to the immune system. If the host's immune system is compromised and immune stress is relieved, the bradyzoites re-differentiate back into tachyzoites, their rapid proliferation leading to destruction in the brain or muscle areas.

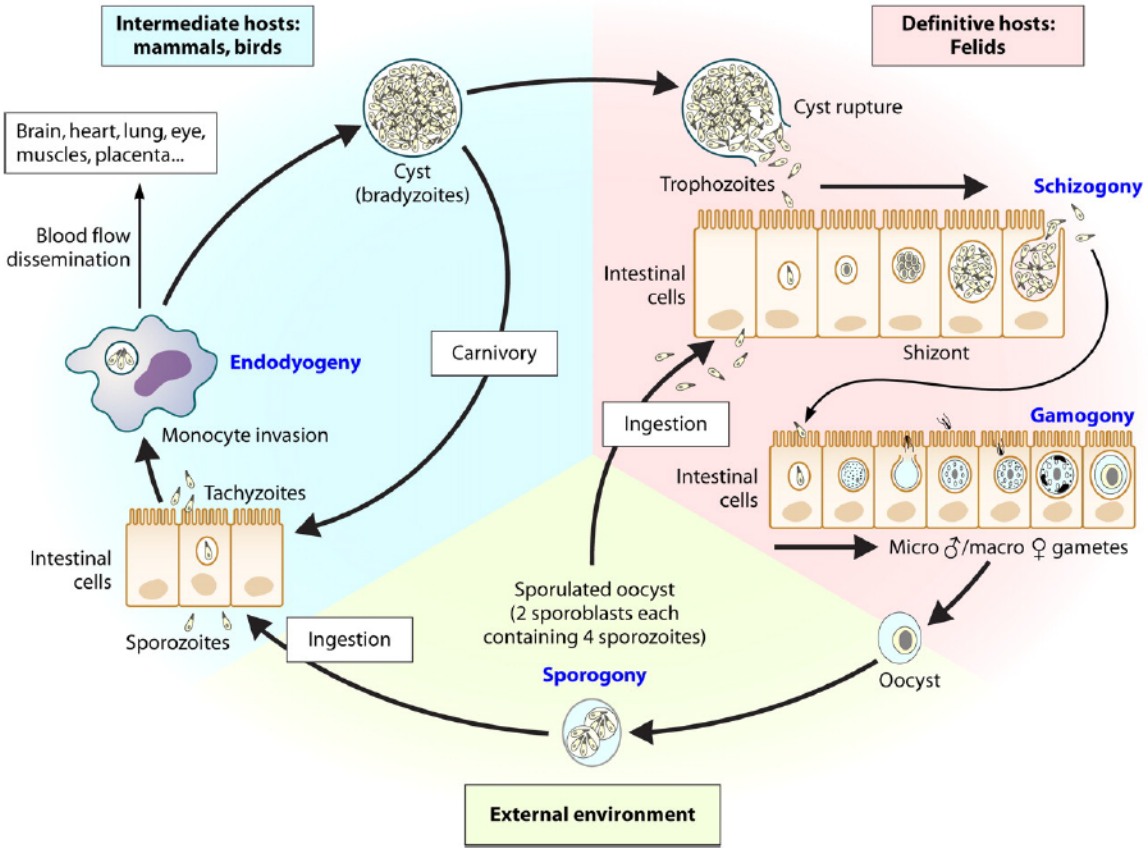

Figure 1-1. Life cycle of *Toxoplasma*

The three infectious forms of the parasite are shown in their corresponding hosts. Following the release of oocysts in cat feces, sporogony occurs in the environment whereupon 4 infectious sporozoites are formed (green area). Upon ingestion by an intermediate host or another felid, sporozoites penetrate the small intestine, enter the bloodstream or the lymph to reach the CNS, heart, eye or the skeletal musculature where they multiply by endodyogeny (blue area). If ingested by a felid, they remain in the small intestine area (see below). The fast growing form, the tachyzoite is quickly targeted by the host's immune system and differentiates into the slow, cyst-forming form of the parasite, the bradyzoite. Upon ingestion of these cysts by felids (pink area), the cyst ruptures and following several rounds of asexual replication in the cat's intestinal cells, the parasite differentiates into female macrogametes or male microgametes. These two forms can fuse and form a diploid zygote which will become an oocyst, and released to the environment, thereby completing the life cycle. Image is taken and adapted from Robert-Gangneux and Dardé, 2012.

1.4. Epidemiology and clinical relevance

1.4.1. Transmission

There exist four ways by which *Toxoplasma* is transmitted to either humans or animal hosts: 1) foodborne, 2) zoonotic, 3) congenital transmission and 4) organ transplantation. Firstly, the parasite can encyst in muscle tissues which can be transmitted to a new host should that individual consume raw or undercooked meat. Secondly, transmission occurs by ingestion of the oocyst form of *Toxoplasma*, released by the definitive host, Felidae. This occurs by drinking contaminated water, ingestion of contaminated soil (vegetables, grass), or contamination with cat feces due to improper hygiene. Thirdly, transmission can occur congenitally via the placenta, from mother-to-child during pregnancy. A fourth, much rarer form of transmission is during organ transplantation procedures. A recipient of a *Toxoplasma*-positive organ will become infected with *Toxoplasma*, and actually succumb to severe disease due to the immune-suppressive regimen (CDC, 2013). The primary way *N. caninum* is transmitted is congenitally, particularly in livestock animals and through oocyst shedding by the definitive host, Canidae.

1.4.2. Pathogenesis

Toxoplasma is a pathogen of neonates and is opportunistic in immunocompromised individuals. In healthy individuals, it is a self-limiting disease but bradyzoites in the CNS, heart or musculature may re-differentiate should the immune system ever become compromised. In neonates infected via congenital transmission, *Toxoplasma* causes severe disease ranging from spontaneous abortion to blindness and mental retardation if the fetus is carried to term (Black and Boothroyd, 2000). This only occurs if the mother's first infection occurs during pregnancy

due to the lack of immunity to the parasite. The tissue tropism of *Toxoplasma* is similar as in adults, and targets the CNS of the developing fetus.

In children and adults, toxoplasmosis manifests itself as retinochoroiditis or myorcarditis if the parasite encysts in the eye or heart respectively. If the encystation process occurs in the brain, encephalitis occurs resulting from cerebral focal lesions due to tachyzoite growth and cellular destruction, which is fatal if left untreated (Blader *et al*, 2015). Such clinical manifestations occur in previously infected individuals with compromised immunity such as AIDS patients or patients undergoing organ transplantation or heavy chemotherapy. Unfortunately, no drug exists for the treatment of latent *Toxoplasma* cysts, however acute toxoplasmosis can be treated with pyrimethamine, trimethaprim or sulfonamides (CDC, 2013).

N. caninum seems to not cause disease in humans despite the presence of antibodies in the blood. Infection of *N. caninum* is primarily in animals, particularly livestock. Neosporosis is the number one cause of cattle abortions worldwide and is therefore of great economic burden (Esteban-Redondo and Innes, 1997; Graham *et al*, 1999; Almería and Lópes-Gatius, 2013).

1.5. *Toxoplasma*, as a model Apicomplexan parasite

Toxoplasma is widely studied in the field of cell biology in regards to members of the Apicomplexa phylum. There are several reasons behind this, the first being the genetic malleability as compared to other Apicomplexa such as *Plasmodium* and *Cryptosporidium*. The genome of *Toxoplasma* has been completely characterized and is composed of 14 chromosomes, with a total of 8×10^7 base pairs (Cornelissen *et al*, 1984). Research on the parasite is usually performed on the tachyzoite or bradyzoite stage, which is haploid, allowing easier genetic manipulation. Prior to CRISPR-Cas9 gene modification and concurrent gain in popularity, the generation of such strains was primarily done through integration by

homologous recombination of plasmids into gene loci (Fox *et al*, 2009; Huynh and Carruthers, 2009). In 2002, the tetracycline inducible system was created to allow the conditional expression of genes, including essential genes that cannot be knocked out due to the haploid nature of the genome (Meissner *et* al, 2002).

Replication time and ease of culture is the second reason why the parasite is regarded as a good model for research. *In vitro* replication by endodyogeny can occur in any nucleated cell of warm-blooded animals with a doubling time every ~ 6-8 hours.

Finally, *Toxoplasma* is a large Apicomplexan parasite, allowing easy viewing of organelles or structures by microscopy.

1.6. Ultrastructure of *Toxoplasma* and *Neospora caninum*

As a eukaryote, *Toxoplasma* possesses most organelles typical of eukaryotes such as a nucleus, an endoplasmic reticulum (ER), a Golgi apparatus and a single mitochondrion. *Toxoplasma* tachyzoites are polarized, measure around 7 µm in length and are crescent-shaped. The maintenance of the parasite's shape is conserved amongst Apicomplexa and is determined by structures of microtubules as well as unique specialized secretory organelles such as micronemes, rhoptries, and dense granules (Fig. 1-2).

1.6.1. Apical complex and conoid

The apical complex surrounds the conoid and consists of tubulin fibers and a microtubule-organizing center (MTOC) from which microtubules spiral down the parasite. Two thirds of the parasite are covered by these subpellicular fibers which are vital for preserving the form and polarity of the parasite (Hu *et al*, 2006).

The conoid is a tubulin basket, surrounded by several apical rings at the apex of the parasite and is extruded out during invasion and egress in a calcium-dependent manner (Carruthers and Boothroyd, 2007).

1.6.2. Inner Membrane Complex

From the apical complex to the basal end is the inner membrane complex (IMC) that runs beneath the plasma membrane along the parasite's body. It is composed of a double-membrane system comprising many alveolar vesicles, which, along with IMC proteins, provides the cortical cytoskeleton of the parasite and its shape (Blader *et al*, 2015). The IMC is also linked to a structure termed the glideosome, which is an actin/myosin based machinery involved in gliding motility.

1.6.3. Micronemes

The micronemes (from the greek, "small threads") are small secretory organelles located at the apex of the parasite. The release of micronemal proteins is involved in parasite motility, migration, host cell attachment and invasion (Black and Boothroyd, 2000).

1.6.4. Rhoptries

The rhoptries (from the greek "club-shaped") are also located at the apical tip and secrete proteins involved in invasion, establishment of the parasitophorous vacuole (PV) and immune evasion (Boothroyd and Dubremetz, 2008).

1.6.5. Dense Granules

The dense granules are found throughout the cytoplasm of the parasite and are released when the invasion process is nearing completion as they are primarily involved in the biogenesis and maintenance of the PV.

1.6.6. Apicoplast

The apicoplast is a unique organelle surrounded by four membranes thought to have originated through secondary endosymbiosis. Both fatty acid (FA) (through FA synthase [FAS] II machinery) and isoprenoid synthesis are two of the major metabolic activities in the apicoplast (Sheiner *et al*, 2013).

1.6.7. Acidocalsisomes and plant-like vacuoles

Also found in the cytosol are acidocalcisomes which are organelles involved in microneme secretion, invasion and extracellular survival of *Toxoplasma* (Liu *et al*, 2014). Acidocalcisomes are capable of Ca^{2+} and fatty acid (FA) storage, as well as ion regulation via proton transporters (Rohloff *et al*, 2011). Plant-like vacuoles are also hypothesized to perform similar functions as acidocalcisomes (unpublished data, Moreno SN).

1.6.8. Endosomal compartments

Endosomal compartments are thought to be vesicles containing material from the Golgi that still requires sorting or maturation (Jackson *et al*, 2013).

1.6.9. Basal complex

The cytoskeleton of the parasite is capped at the basal end by a structure termed the basal complex and the posterior cup. This structure is important for cytokinesis as it functions as a contractile ring, leading to the bud tapering during the separation of the two daughter parasites (Blader *et al*, 2015).

1.7. Intracellular, lytic cycle (tachyzoite)

Extracellular *Toxoplasma* and *N. caninum* move through the blood and tissues using a form of active motility termed gliding motility (Keeler and Soldati, 2004), a type of movement involving sliding as opposed to conformational changes. This energy dependent movement relies on actin/myosin machinery located in between the IMC and the parasite's plasma membrane (Fig. 1-2) and enables the parasite to reach speeds between 1 and 10 µm per second.

Both *Toxoplasma* and *N. caninum* reside in a PV, formed during invasion using lipids from the host cell's plasma membrane (PM). The organization of the parasites within their PV differs: whereas *Toxoplasma* is organized in a rosette, *N. caninum* has a disordered intravacuolar organization (Fig. 1-3).

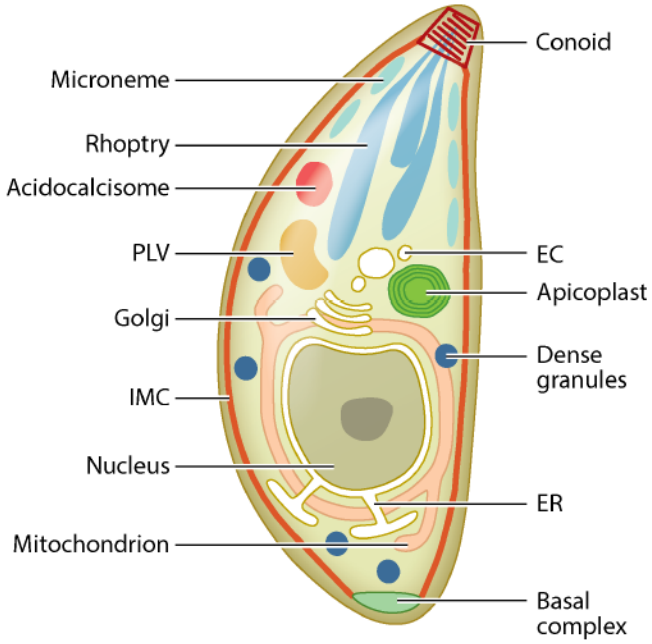

Figure 1-2. Ultrastructure of *Toxoplasma gondii* and *Neospora caninum* tachyzoites.
Abbreviations: PLV: plant-like vacuole; IMC: inner-membrane complex; EC: endocytic compartment; ER: endoplasmic reticulum. Image taken and adapted from Blader *et al*, 2015.

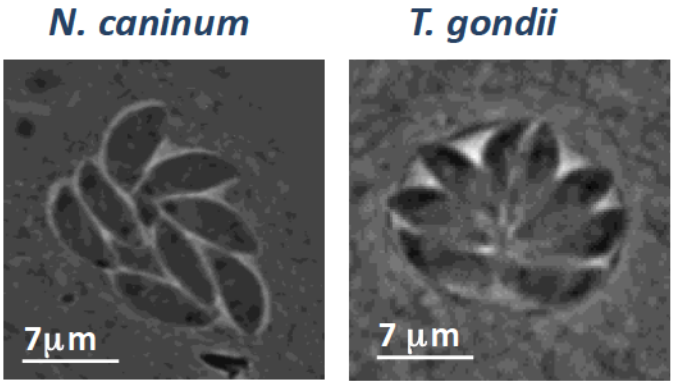

Figure 1-3. Morphology of *Toxoplasma gondii* and *Neospora caninum* PV.
Brightfield microscopy of intracellular *Neospora caninum* (left) and *Toxoplasma gondii* (right) inside their respective parasitophorous vacuoles (PV) in Human Foreskin Fibroblast (HFF) with 100x objective.

1.7.1. Invasion

For an intracellular parasite, contact with the host cell is paramount to initiate invasion. This is achieved through the low-affinity lateral contact of the parasite's surface antigens (SAGs) and SAG-related sequence proteins with the host cell PM (Carruthers and Boothroyd, 2007). SAG proteins are found all over the surface of the parasite and are anchored by glycosylphosphatidylinositol (GPI) to the PM. SAG recognizes and binds to sulfated proteoglycans on the host cell PM (He *et al*, 2002).

This physical attachment leads to the calcium-dependent secretion of micronemes and conoid protrusion, leading to the formation of a unique complex, termed the Moving Junction (MJ) at the apical end of the parasite (Alexander *et al*, 2005; Tyler *et al*, 2011). The MJ allows a tighter parasite-cell interaction and helps the parasite to move through the host cell PM at which point rhoptry proteins are released, initiating the formation of the PV. The PV, originally formed using the host cell's PM is then modified by the addition of *Toxoplasma* rhoptry-derived proteins and removal of host cell proteins and lipid rafts (Mordue *et al*, 1999; Cesbron-Delaum *et al,* 2008; Nam, 2009). This process is essential in order to avoid recognition and destruction by the host endo-lysosomal pathway.

The actin cytoskeleton of the host cell represents a mechanical obstruction for cellular entry, which is subverted by *Toxoplasma* via the secretion of Toxofilin from rhoptries (Delorme-Walker *et al*, 2012). Other rhoptry proteins secreted by the parasite can localize to the nucleus to interfere with host cell transcription or can localize to the PV membrane (PVM) to provide structural integrity or to alter defense-related signaling pathways for PV degradation (Carruthers and Boothroyd, 2007; Boothroyd and Dubremetz, 2008). The invasion process lasts about one minute (Carruthers and Boothroyd, 2007).

1.7.2. Replication

Following invasion, *Toxoplasma* and *N. caninum* migrate to the perinuclear region of the host cell to replicate by endodyogeny in which two daughter cells are formed within the confines of the mother cell, which will get consumed at the end of the process (Blader *et al*, 2015). Tachyzoites have a very rapid doubling time, every 6-8 h, and as such need to modify the host cell in order to support its replication. This is achieved through modulating the immune system to avoid degradation, but also by interacting with host organelles and structures. The parasite can synthesize most of the building blocks it requires for the formation of daughter cells but not in enough quantities to support the rapid doubling time. As such, *Toxoplasma* also scavenges nutrients from the host cell, a process that is mediated through the interaction of the PV with host cell organelles, which will be described in greater detail in a later section (Coppens *et al*, 2000; Romano and Coppens, 2013; Romano *et al* 2013).

1.7.3. Egress

When the parasites have reached maturity or sufficient numbers, egress ensues which involves several parasite effectors (Fig. 1-4). Egress can be triggered by a decrease in pH and changes in calcium and potassium levels. Parasite replication acidifies the PV leading to micronemal secretion and potassium ion motility (Roiko *et al*, 2014). When a certain pH is reached, the micronemal protein, perforin-like protein 1 (PLP1), is secreted and inserts in the PVM and host PM, creating pores and allowing the passage of ions, e.g., calcium and potassium, that induce egress (Kafsack *et al*, 2009). In addition, another family of proteins are secreted into the PV called nucleotide triphosphate-degrading enzymes (NTPases) that are involved in egress. The mechanism by which these enzymes trigger egress is unknown but is hypothesized to involve potassium ion signaling, similarly to PLP1.

Cytoplasmic calcium (Ca^{2+}) is an important secondary messenger heavily involved in *Toxoplasma* egress. Calcium is stored in the parasite in the acidocalcisome (Fig. 1-2) and the ER. The addition of calcium ionophores increases motility and micronemes secretion, stimulates egress as well as enhances invasion (recent review: Nagamune *et al,* 2008; Plattner *et al*, 2012).

The immune system of the host cell may also trigger egress, such as Fas/FasL mediated signaling by cytotoxic $CD8^+$ T cells (Persson *et al*, 2007).

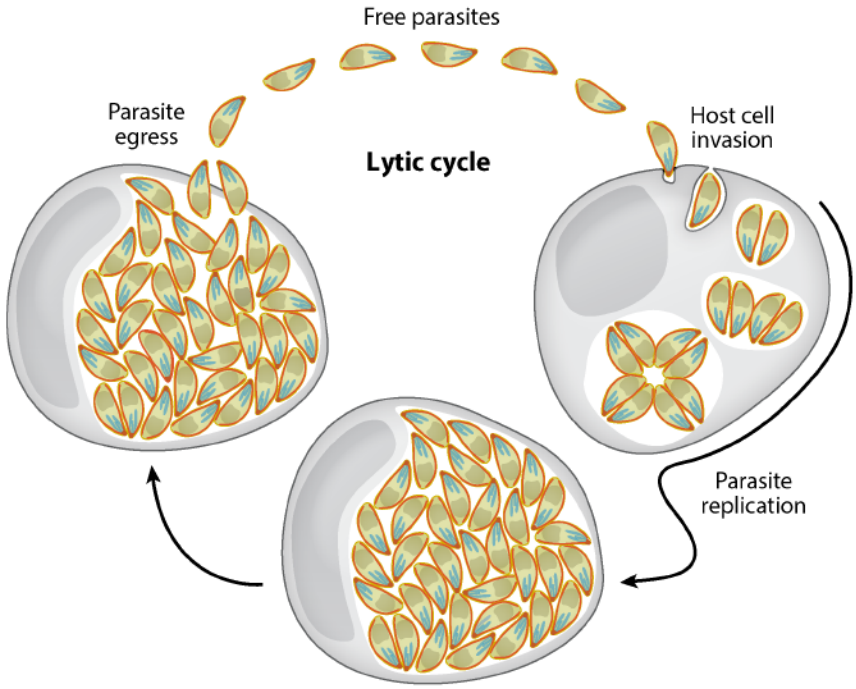

Figure 1-4. The lytic cycle of *Toxoplasma gondii* and *Neospora caninum* tachyzoites.
Freshley egressed parasites actively invade any nucleated cell, and establish a replicative niche within the parasitophorous vacuole (PV). Here, the parasites divide by endodyogeny, a process whereby two daughter cells are formed within the confines of the mother cell. Following several rounds of replication, and when the PV has reached a critical mass, parasites trigger egress from the host cell, a process dependent on calcium signaling. Figure taken and adapted from Blader *et al*, 2015.

1.8. Modification of the host cell

1.8.1. Transcriptional changes

Microarray studies in *in vitro* conditions have revealed that infection with *Toxoplasma* leads to a wide variety of gene expression changes in both the host and parasite. During the first two hours post infection of human fibroblasts, nearly half of host gene expression variation are associated with the immune response, for example, chemokines, cytokines, cell matrix and adhesion proteins and transcriptional regulatory factors such as NF-κB (Blader *et al*, 2001). By 24 h post infection, the major category of genes up-regulated are the host glycolytic and mevalonate metabolism genes. Since *Toxoplasma* scavenges glucose and cholesterol from its host cell (Sinai *et al*, 1997; Coppens *et al*, 2006), it is not surprising that these pathways are up-regulated. Other gene categories that are increased include protein synthesis, cell signaling, cell adhesion and cytoskeleton and transcriptional regulation (Blader *et al*, 2001).

1.8.2. Immune evasion

One aspect that intracellular pathogens must master is immune evasion in order to successfully replicate. *Toxoplasma* has developed many ways in which to interfere with the host's immune response.

1.8.2.1. Evasion of IFNγ-mediated defenses

IFNγ is absolutely essential for *Toxoplasma* control in both the innate and adaptive arm of the immune response by controlling the expression of two effectors. The first is the activation of IFNγ-regulated GTPases (IRGs) for subsequent autophagy-dependent degradation of the PVM and the second is the degradation of vital nutrients for the parasite such as tryptophan by

indoleamine dioxygenase expression (Choi *et al*, 2014; Collazo *et al*, 2001; Pfefferkorn, 1984). Rhoptry proteins such as ROP, ROP1, ROP5, ROP17 and ROP18 are secreted by the parasite shortly after invasion and inactivate IRGs. These rhoptry genes are highly polymorphic between *Toxoplasma* strains and ROP5 is known to be a major virulence determinant in mice (Reese *et al*, 2011).

Another way by which *Toxoplasma* avoids IFNγ-related killing is by inhibiting the binding of the transcription factor STAT1 to its promoter sites in the nucleus. STAT1 is phosphorylated upon IFNγ expression and is another factor critical for host survival during *Toxoplasma* infection (Schneider *et al*, 2013). It is still unknown which *Toxoplasma* effectors are involved in this process.

1.8.2.2. Prevention of degradation by autophagy

Since IRGs are thought to be pseudogenes in higher primates and thus thought not to be important in humans, *Toxoplasma* has another set of proteins to avoid PVM and PV destruction by host cell autophagy machinery. CD40 is a member of the Tumor Necrosis Family receptor superfamily and can stimulate the buildup of autophagy-related proteins on the PVM of *Toxoplasma* after binding to its ligand CD154 (Andrade *et al*, 2006). The parasite can prevent autophagosome formation through the activation and subsequent signaling of epidermal growth factor (EGF) receptor (Muniz-Feliciano *et al*, 2013).

1.8.3. Interaction with host cell organelles

Organelle-organelle interactions within cells are vital for the exchange of material or transmission of signals that regulate, sustain and balance processes involved in metabolism,

signaling, cellular maintenance, regulation of programmed cell death and intracellular microbe defense (Schrader *et al*, 2015). There are 3 mechanisms by which these interactions can occur: 1) vesicular transport; 2) metabolite exchange by diffusion; and 3) physical contact via specific membrane contact sites.

Toxoplasma and *N. caninum* both reside within a PV, allowing the parasites to grow comfortably without hindrance from the immune system. This protection comes at a cost however, since the parasite cannot easily access the abundant reserves of nutrients found in the host cell. In order to acquire host cell-derived resources, *Toxoplasma* have engineered ways by which they can sculpt the host intracellular environment in their benefit. Nothing is known for *N. caninum*.

1.8.3.1. Host cytoskeleton

The spatial distribution and host microtubular network is dramatically modified upon *Toxoplasma* infection as the PV is completely wrapped with host microtubules (Coppens *et al*, 2006; Walker *et al*, 2008) (Fig. 1-5, multiple PVs, 1 parasite per PV). The microtubule rearrangement around the PV of *Toxoplasma* is important for intracellular replication as well as invasion. In the former, it is hypothesized that microtubule wrapping around the PV could help for the association of organelles to the PV, as well as interception of nutrients traveling along the microtubule network. The wrapping of the microtubular network around the PV is important for successful *Toxoplasma* replication (Coppens *et al*, 2006).

The microtubule-organizing center (MTOC) is the site where the host microtubule network nucleation site is located and is the hub for the organization of the mitotic or meiotic spindle apparatus, essential during cell division. During interphase, most animal cells have one MTOC also referred to as the centrosome), often located on the nuclear envelope. The MTOC is

often detached from this envelope upon *Toxoplasma* infection and is relocated to the PVM (Romano *et al*, 2013) (Fig. 1-5, MTOC, green; PV, red). In addition to the observation by immunofluorescence assays (IFA) of MTOC localization to the PVM, centrosomal material is detected at the PV surface (Coppens *et al*, 2006; Romano *et al*, 2013; Walker *et al*, 2008; Wang *et al*, 2010).

Functionally, MTOC localization to the PV may allow these pathogens to disturb the host cell cycle by stalling it prior to cytokinesis in order to ensure a large, spacious cell in which to replicate (Walker *et al*, 2008; Romano and Coppens, 2013).

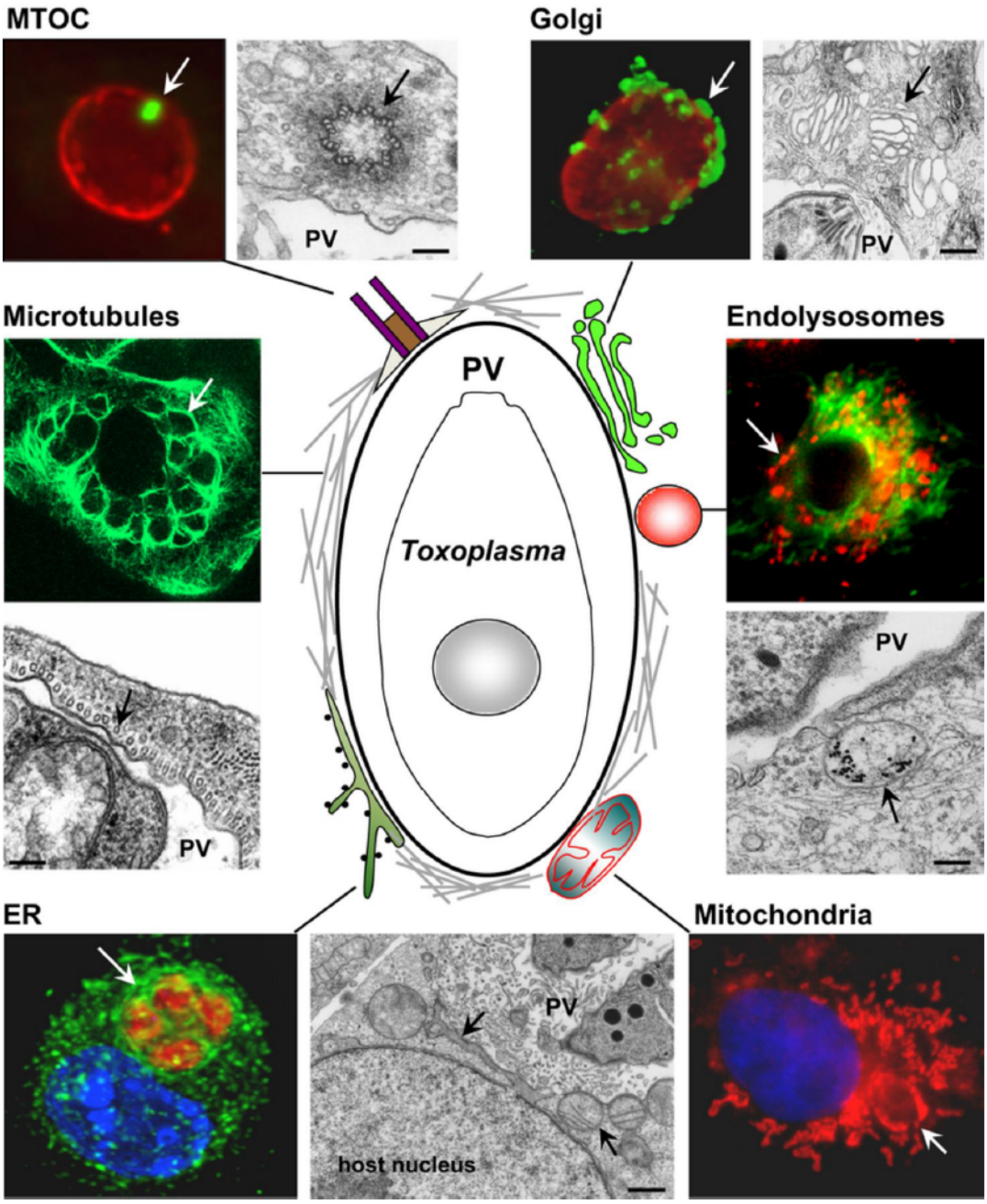

Figure 1-5. Model for the interaction of *Toxoplasma* PV with host organelles and structures.
Immunofluorescence (IFA) and electron microscopy (EM) images highlight the various interactions between the PV (depicted in the middle) and host cell organelles and structures. The endo-lysosome EM image contains LDL-gold particles. EM scale bars are 150nm. Abbreviations: MTOC: microtubule-organizing center; PV: parasitophorous vacuole; ER: endoplasmic reticulum. Image from Romano and Coppens, 2013.

1.8.3.2. Host Mitochondria

Mitochondria are dynamic organelles involved in a broad range of cellular processes including ATP generation, programmed cell death (PCD), autophagy, immunity, calcium homeostatis, and phospholipid metabolism (Shaughnessy *et al*, 2014). They can also physically associate with the ER through Mitochondria-Associated Membranes (MAMs) for lipid exchange between the two organelles (Pagliarini and Rutter, 2013). Due to their involvement in many cellular processes, particularly as resources for lipids and energy, it is not surprising that many intracellular pathogens have developed ways to interact and manipulate host cell mitochondria (Sinai *et al*, 2004; Ashida *et al*, 2011; Anand and Tikoo, 2013; Lartigue and Faustin, 2013).

Shortly after cell invasion, *Toxoplasma* (type I strain) infection leads to a vivid change in the spatial distribution of host mitochondria which concentrate around the PV and associate with the PVM (Sinai *et al*, 1997; Pernas *et al*, 2014) (Fig. 1-5, arrow pointing to PV with 1 parasite). This recruitment is strain dependent as type II strains do not associate as strongly. Recently in 2014, Pernas and colleagues discovered Mitochondria-associated factor 1 (TgMAF1) in type I strains, expressed at the PVM, which is at least partially responsible for the association of mitochondria to the PV and has been shown to regulate cytokine levels *in vivo*.

The biological consequence of mitochondria associating with the PV of *Toxoplasma* is unknown. It could be for lipid exchange as is the case in ER-mitochondria association through MAMs, or could be for energy uptake, PCD or autophagy avoidance, or immune evasion.

1.8.3.3. Host secretory pathway: Endoplasmic reticulum and Golgi apparatus

The spatial distribution of the rough ER is also modified shortly following *Toxoplasma* invasion as ER elements surround, and are in very close association to the PV by 4 h post infection (Sinai *et al*, 1997) (Fig. 1-5, IFA, ER in green; PV in red. EM: arrow). Indeed, the PV becomes stably

connected to the host perinuclear region by the anchoring the PVM to the ER network, which is contiguous with the nuclear envelope (Romano *et al*, 2008).

The functional significance of ER association to the PV could be two-fold. Firstly, the association of *Toxoplasma* PV with the ER could aid in non-vesicular uptake of lipids such as ceramides (Romano *et al*, 2013), or N-glycan precursors for protein incorporation (Bushkin *et al*, 2010). The second potential benefit to close ER association could be for disruption of the host cell's antigen presentation pathway (Goldszmid *et al*, 2009).

Infection with *Toxoplasma* leads to both the clustering of the Golgi apparatus around the PV, as well as its fragmentation into mini-stacks later during infection (Fig. 1-5, EM and IFA of Golgi in green; PV in red. Arrow shows mini-stacks) (Romano *et al*, 2013). Similarly as to with the ER, the clustering of the Golgi and subsequent fragmentation into mini-stacks could aid in the scavenging of nutrients to the PV such as sphingolipids (Romano *et al*, 2013; reviewed in Coppens, 2013).

Toxoplasma can scavenge ceramide and sphingolipids from the host Golgi, a mechanism at least partially mediated through the uptake of Rab GTPases containing the aforementioned lipids (Romano *et al*, 2013).

1.8.3.4. Host endocytic pathway: Endolysosomes

Endocytic organelles and lysosomes represent an extremely rich source of nutrients due to their intrinsic capabilities for transporting catabolic resources from the interior of the cell or from the extracellular medium. These organelles are also part of the autophagic pathway, a recycling mechanism employed by cells to degrade unwanted material or in times of stress or starvation, to ensure cellular functions remain undisrupted.

The MTOC is an area in the cell where host endo-lysosomes accumulate, conveniently hijacked to the PVM, as previously discussed, by *Toxoplasma*. The host mTORC2-Akt signaling pathway is manipulated by *Toxoplasma* leading to an endo-lysosome accumulation around its PV (Wang *et al*, 2010). Additionally, the microtubule network is disrupted by *Toxoplasma* and indeed, invaginations in the PVM caused by this disruption contain host endo-lysosomes (Coppens *et al*, 2006). The sequestration of endo-lysosomes in the PV containing low-density lipoprotein (LDL)-gold shows that the parasite is capable to scavenging nutrients such as cholesterol from the host cell, previously destined for host lysosomal recycling (Fig. 1-6) (Coppens *et al*, 2000).

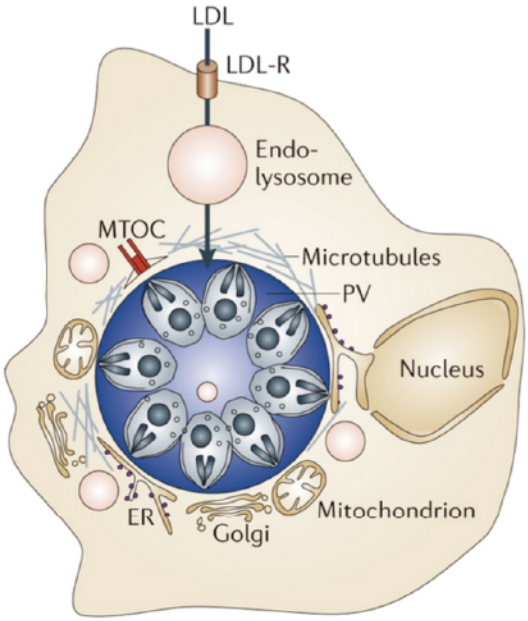

Figure 1-6. Cholesterol uptake to the *Toxoplasma* PV.

Exogenously added cholesterol-containing low-density lipoprotein (LDL) is endocytosed by the host cell via LDL receptor (LDL-R). Endo-lysosomes containing LDL are diverted to the PV and are taken up to the PV lumen. Image adapted from Coppens, 2013.

1.8.4. Autophagy

Infection of mammalian fibroblasts and epithelial cells with *Toxoplasma* has been shown to cause an increase in autophagy, in a calcium-dependent and mTOR independent-process, completely induced by the parasite (Wang *et al*, 2009; Lee *et al*, 2013; Gao *et al*, 2015; Selleck *et al*, 2015). Autophagosomes accumulate around the PV, potentially to enhance access of nutrients for *Toxoplasma* (Selleck *et al*, 2015). Any disruption in autophagy activation results in a decrease in *Toxoplasma* replication when grown in starvation conditions (Wang *et al*, 2009). As of yet, the induction of autophagy and its contribution to the intracellular development is still unknown.

1.9. Lipid synthesis and salvage in *Toxoplasma*

Toxoplasma is capable of both synthesizing most lipids itself, but has also been shown to salvage a variety of lipids from the host cell. An overview of all the lipids that can be scavenged by the parasite is seen in Fig. 1-7, and each lipid species will be discussed in greater detail below. It is not known whether the parasite can scavenge lipids or lipoate originating from the mitochondria and further research will be needed to elucidate this possibility. Prior to this work in chapter 2, nothing was known about the capacity of *N. caninum* to scavenge lipids, nor its ability to synthesize lipids. Since *N. caninum* shares many genes with *Toxoplasma*, nearly at a one-to-one orthologous level, the biosynthetic pathways are hypothesized to be similar (Reid *et al*, 2012).

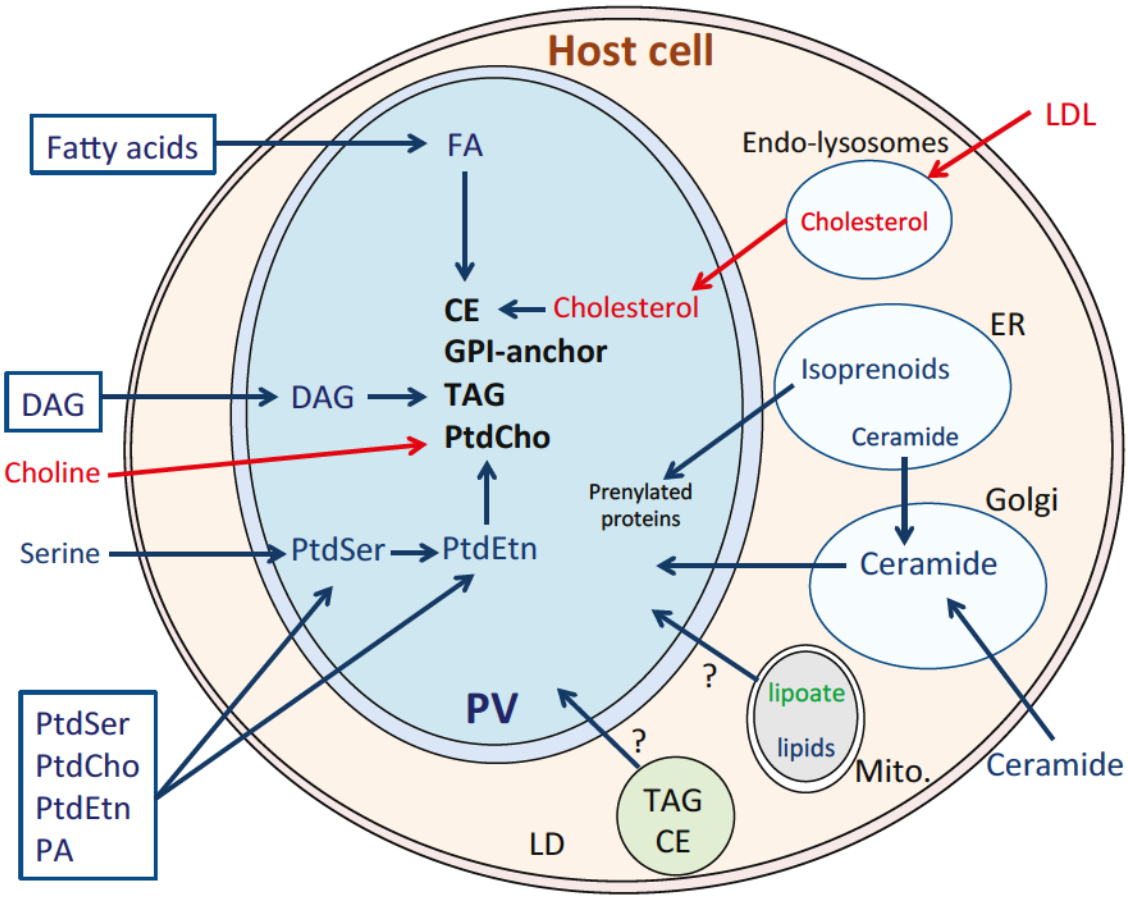

Figure 1-7. Lipid salvaging pathways by *Toxoplasma*.

The metabolites and products that the parasite can both synthesize and salvage are shown in blue, whereas those that must be salvaged are shown in red. Lipoate, in green, is synthesized and salvaged by the parasite but is used for different purposes depending on its origin. The uptake of lipoate or lipids from mitochondria to the PV is unknown. Metabolites and molecules shown to be scavenged from the extracellular environment can also be scavenged by the parasite if found inside the cell. PV: parasitophorous vacuole; ER, endoplasmic reticulum; LDL: low-density lipoprotein; DAG: diacylglycerol; TAG: triacylglycerol; FA: fatty acids; PA: phosphatidic acid; CE: cholesterol ester.

1.9.1. Cholesterol

Cholesterol is the main sterol molecule present in all mammalian cells and plays key roles in the organization of signaling lipids and proteins within membranes by regulating the fluidity of the membrane. Mammalian cells can synthesize cholesterol *de novo* via the mevalonate pathway in the ER or can uptake it from plasma LDL (Goldstein and Brown, 1990).

Toxoplasma contains cholesterol in its membranes and in its rhoptries (Foussard *et al*, 1991; Coppens *et al*, 2000; Coppens and Joiner, 2003). Interestingly, the parasite cannot synthesize cholesterol *de novo*, so therefore must scavenge it from the host cell, a process at least partially mediated through the uptake of host endocytic vesicles to the PV (Coppens *et al*, 2006). In fact, *Toxoplasma* cholesterol scavenged from the host cell gets incorporated into its membranes or esterified into lipid droplets (Coppens *et al*, 2000; Nishikawa *et al*, 2005).

Uptake of host endo-lysosomes containing resources such as cholesterol is essential for *Toxoplasma* since disruption of LDL endocytosis, lysosomal degradation of LDL or cholesterol translocation across membranes is detrimental for the parasite (Coppens *et al*, 2006).

1.9.2. Sphingolipids and ceramides

In mammalian cells, ceramides are synthesized in the ER then transported to the Golgi for modification (e.g. glycosylation) and conversion to sphingomyelin, diacylglycerol or sphingosine. Sphingolipids produced in the Golgi can then be transported to various cell membranes (Pagano *et al*, 1991). Sphingolipids are found in all eukaryotic cell membranes and help protect the cell by stabilizing the outer leaflet of the PM. Additionally, ceramides can act as signaling molecules for cellular development or stress response.

Toxoplasma has over 20 different species of sphingolipids and has the machinery for ceramide and sphingolipid synthesis *de novo* (Zinecker *et al*, 2001). The parasite can also

scavenge ceramides from the host Golgi through the uptake of Golgi-derived Rab vesicles (such as Rab14, Rab30 and Rab43), laden with ceramide for future incorporation into its membranes (de Melo and de Souza, 1996; Romano *et al*, 2013). It is as of yet unknown whether *Toxoplasma* can scavenge exogenously-added ceramides directly, without the need for prior incorporation into the host Golgi.

1.9.3. Fatty acids

Membranes are made up primarily of FA, and are also important for the storage of energy for the esterification reactions of cholesterol and diacylglycerol (DAG) into cholesterol esters (CE) and triacylglycerol (TAG), respectively. Fatty acid derivatives have also been shown to be essential for other purposes such as protein post-translational modifications.

Toxoplasma possesses three fatty acid synthase (FAS) pathways: 1) FAS II pathway in the apicoplast producing lipoic, myristic and palmitic acid; 2) FA elongation pathway in the ER for long-chain monounsaturated FA synthesis; 3) a documented but unstudied FAS I pathway. Additionally, the parasite is able to scavenge fatty acids such as palmitic, oleic, linoleic, arachidonic acids from the host cell (Tomavo *et al*, 1989; Quittnat *et al*, 2004; Polonais and Soldati-Favre; 2010) for their incorporation into more complex lipids such as GPI anchors and CE and TAG. FA can also be degraded by β-oxidation in the parasite's mitochondrion (Tomavo *et al*, 1989; Quittnat *et al*, 2004; Charron and Sibley; 2002; Nishikawa *et al*, 2005). The scavenged FA in the PV have been shown to both originate from *de novo* synthesis in the host cell or from exogenous addition to the medium.

1.9.4. Phospholipids

Phospholipids are one of the major components of cellular membranes by arranging themselves into bilayers. Structurally, they are composed of a hydrophilic phosphate headgroup and two hydrophobic FA tails, joined together by glycerol. They are usually synthesized in the cytosol, close to the ER. These complex lipids also play roles in signal transduction. For example, phosphatidylinositol (4,5)-biphosphate can be split by phospholipase C (PLC) into DAG and inositol triphosphate, both of which play roles in signal transduction. DAG can also be esterified into TAG for energy storage in lipid droplets (LD).

The parasite is capable of synthesizing all its phospholipids via the Kennedy pathway (Gupta *et al*, 2005; Sampels *et al*, 2012). Phosphatidylserine (PS) and phosphatidylethanolamine (PE) are synthesized in the parasite through the incorporation of serine or ethanolamine respectively, both of which can be scavenged or synthesized by *Toxoplasma*. Despite having the necessary machinery for the synthesis of these complex lipids, *Toxoplasma* only has the capability of synthesizing 50% of its PS needs and 10% of phosphatidylcholine (PC) for maximal development, highlighting its need to also scavenge these phospholipids from the host cell (Charron and Sibley, 2002; Gupta *et al*, 2005). PE and phosphatidic acid are also scavenged from the host cell.

1.9.5. Isoprenoids

Isoprenoids are important molecules with functions in photosynthesis, respiration, signaling and protein post-translational modifications. The majority of the isoprenoids in *Toxoplasma* are synthesized in the apicoplast through the isopentenyl diphosphate (IPP) and deoxyxylulose-5-phosphate pathways (Seeber and Soldati-Favre, 2010). Farnesylpyrophosphate (FPP) and geranylgeranylpyrophosphate (GGPP) are the two principle precursors of isoprenoids and they

are both generated by a single FPP/GGPP synthase (reviewed in Coppens, 2013; Coppens, 2014). The protein modification farnesylation is mediated by FPP by the protein farnesyltransferase. FPP, where FPP is also the precursor to ubiquinones and dolichols, both of which play roles in mitochondrial respiration and N-glycosylation, respectively (Coppens, 2014). GGPP is the precursor of abscisic acid. Abscisic acid is a molecule that, upon reaching a certain threshold concentration in the PV, can signal parasite egress from the host cell (Nagamune *et al*, 2008).

Toxoplasma is able to synthesize FPP and GGPP but inhibiting the host cell IPP pathway leads to a decrease in parasite growth, suggesting that host-derived isoprenoid precursors are important for optimal parasite growth and are likely scavenged by *Toxoplasma* (Yardley *et al*, 2002; Li *et al*, 2013).

1.9.6. Neutral lipids

The storage of lipids in lipid droplets (LD) is an evolutionary conserved process found in organisms ranging from bacteria to mammals. This storage function serves primarily two roles: 1) storage of lipids for future use should energy resources decrease; and 2) prevention of lipotoxicity by sequestering harmful, excess FA. Lipids must be converted into neutral lipids (NL) first by the generation of cholesterol esters (CE) and triacylglycerol (TAG) from cholesterol and DAG, respectively. The final, rate limiting step of this reaction is catalyzed by Acyl-CoA:Cholesterol Acyltransferases (ACAT) and Acyl-CoA:diacylglycerol Acyltransferase (DGAT), respectively (Goodman *et al*, 1964; Chang *et al*, 2001; Buhman *et al*, 2000).

Both *Toxoplasma* and *N. caninum* possess LD, and have the enzymatic machinery for LD formation despite neither parasite being able to synthesize cholesterol (Nishikawa *et al*, 2005; Charron and Sibley, 2002). The ablation of either ACAT or DGAT is lethal for *Toxoplasma*, emphasizing the importance of lipid storage in the parasite (Quittnat *et al*, 2004; Nishikawa *et*

al, 2005; Lige *et al*, 2013). As of yet, no studies have shown whether the parasite is capable of scavenging NL from its host.

1.10. THESIS OBJECTIVES

Despite growing knowledge on Apicomplexa infections, critical gaps in the basic biology of these parasites remain, including the mechanism by which these parasites exploit and manipulate their host cell. Like *Toxoplasma*, *N. caninum* spends most stages of its lifecycle as an intravacuolar parasite, and survives poorly axenically. Despite this fact, nothing is known about if and how the parasite interacts with host organelles or scavenges lipids. Chapter 2 of this thesis will examine the modification of the host cell by *N. caninum* by investigating the recruitment of host organelles and scavenging of host lipids, as compared to *Toxoplasma*. This will allow us to identify biological differences between *N. caninum* and *Toxoplasma* as well as provide information on whether *N. caninum*'s host specificity is rooted at the intracellular level.

Mammalian lipid droplets are storage structures for NL and may constitute a providential source of essential lipids for *Toxoplasma*. By investigating interactions between *Toxoplasma* and host lipid droplets, our understanding of the parasite and lipid scavenging, in particular neutral lipids, will be expanded. Chapter 3 will explore the role of host lipid droplets for *Toxoplasma* development, by focusing on their lipid content deliverable to the PV and the parasite.

Finally, Chapter 4 will investigate the consequences of exposure of *Toxoplasma* to large amounts of fatty acids in its environment, in order to decipher novel parasite vulnerabilities in lipid salvage and utilization pathways.

CHAPTER 2

NEOSPORA CANINUM RECRUITS HOST CELL STRUCTURES TO ITS PARASITOPHOROUS VACUOLE AND SALVAGES LIPIDS FROM ORGANELLES

This work has been published:

Nolan SJ, Romano JD, Luechtefeld T, Coppens I.
Neospora caninum recruits host cell structures to its parasitophorous vacuole and salvages lipids from organelles.
Eukaryotic Cell. 2015 May;14(5):454-73. doi: 10.1128/EC.00262-14. Epub 2015 Mar 6.

2.1. ABSTRACT

Toxoplasma gondii and *Neospora caninum*, which cause the diseases toxoplasmosis and neosporosis respectively, are two closely related Apicomplexan parasites. They have similar heteroxenous lifecycles and conserved genomes, and share many metabolic features. Despite these similarities, *T. gondii* and *N. caninum* differ in their transmission strategies and zoonotic potential. Comparative analyses of the two parasites are important to identify the unique biological features that underlie the basis of host preference and pathogenicity. *T. gondii* and *N. caninum* are obligate intravacuolar parasites; in contrast to *T. gondii*, post-invasion events that occur during *N. caninum* infection remain largely uncharacterized. We examined the capability of *N. caninum* (Liverpool isolate) to interact with host organelles and scavenge nutrients, in comparison to *T. gondii* (RH strain). *N. caninum* reorganizes the host microtubular cytoskeleton and attracts endoplasmic reticulum, mitochondria, lysosomes, multivesicular bodies and Golgi vesicles to its vacuole, though with some notable differences from *T. gondii*. For example, host ER gathers around the *N. caninum* PV but does not physically associate with the vacuolar membrane; the host Golgi surrounds the *N. caninum* PV but does not fragment into mini-stacks. *N. caninum* relies on plasma lipoproteins and scavenges cholesterol from NPC1-containing endocytic organelles. This parasite salvages sphingolipids from host Golgi Rab14 vesicles that it sequesters into its vacuole. Our data highlight remarkable conservation in the intracellular infection program of *N. caninum* and *T. gondii*. The minor differences between the two parasites related to the recruitment and rearrangement of host organelles around their vacuole likely reflect divergent evolutionary paths.

2.2. INTRODUCTION

Coccidian parasites are obligate intracellular pathogens of the phylum Apicomplexa and are responsible for significant human and veterinary diseases. Among them, *Toxoplasma gondii* and *Neospora caninum* are very closely related tissue-dwelling Coccidia that share many biological features (Dubey *et al*, 2002). The two parasites diverged ~28 million years ago, but their genome's size, gene content and expression have been remarkably conserved; amongst the shared genes by *T. gondii* and *N. caninum*, 40% have no orthologues in any other Apicomplexa (ex. *Plasmodium*, *Cryptosporidium*) (Reid *et al*, 2012). *T. gondii* affects up to one-third of the human population and is responsible for severe infections associated with the central nervous system (Tenter *et al*, 2002). In healthy individuals, toxoplasmosis is usually asymptomatic, with the parasite remaining encysted in brain and muscle cells throughout the host's lifetime. Reactivation of this latent infection occurs in immune deficiency conditions, which can lead to fatal encephalitis (Luft and Remington, 1992). Congenital infection with *T. gondii* can cause neurologic defects in the fetus and abortions in both humans and animals, particularly in sheep and goats (Kieffer and Wallon, 2013; Esteban-Redondo and Innes, 1997). *N. caninum* is the agent of the disease neosporosis, which is associated with neuromuscular degeneration and neonatal mortality in animals, particularly in dogs and cattle (Esteban-Redondo and Innes, 1997; Graham *et al*, 1999; Almería and Lópes-Gatius, 2013). Once in their hosts, *N. caninum* parasites also transform into cyst forms that persist in the brain and muscles (Speer *et al*, 1999). Both *T. gondii* and *N. caninum* have a heteroxenous lifecycle, characterized by asexual replication in an intermediate host and sexually reproduction in the small intestine of a definitive host: *Toxoplasma* completes its sexual cycle in Felidae, *Neospora* in Canidae. While *T. gondii* can infect virtually all warm-blooded animals, *N. caninum* has a more limited host range. Notably, *N.*

caninum does not cause any recognized disease in humans despite the detection of antibodies against *N. caninum* antigens in humans (~6% in healthy individuals and up to 40% in HIV-infected patients; Lobato *et al*, 2006; Ibrahim *et al*, 2009).

The differences between *T. gondii* and *N. caninum* in zoonotic capability and host preferences emphasize the relevance of comparative studies to identify organism-driven mechanisms in the program of infectivity of the two pathogens. Comparisons of genomes and transcriptomes have revealed defining differences between these parasites in gene products with roles in host defense (Reid *et al*, 2012). For example, *N. caninum* has twice as many genes coding for surface glycosylphosphatidylinositol-linked proteins (SAG1-related sequences or SRS) as *T. gondii*. As these proteins mediate attachment to host cells and immune activation (Jung *et al*, 2004), this difference could represent an evolutionary advantage for evolving a narrower host range. A second example involves rhoptry-derived kinases that are secreted by these parasites into host cells to interfere with host signaling pathways; *N. caninum* encodes for fewer of these virulence-associated rhoptry proteins than *T. gondii* (Reid *et al*, 2012). In particular, the ROP18 kinase, which inactivates host immunity-related GTPases that would otherwise disrupt the membrane of the parasitophorous vacuole (PV) (El Hajj *et al*, 2997; Ong *et al*, 2010; Steinfeldt *et al*, 2010; Fentress *et al*, 2010), is reduced to a pseudogene in *Neospora* (Lei *et al*, 2014).

Investigations of host cell invasion by *N. caninum* are largely inspired by studies on *T. gondii*, and small differences in the invasion processes of these parasites have been identified. The proliferative tachyzoite forms of these parasites invade a large variety of cultured cells wherein they multiply in a parasitophorous vacuole (PV). By virtue of their obligate intracellular lifestyle, these parasites cannot survive under axenic conditions, and *N. caninum* tachyzoites are

particularly vulnerable to the harmful effects of extracellular maintenance and rapidly lose their invasibility. Active invasion of mammalian cells by these parasites involves the coordinated release of proteins from the parasite's secretory organelles. First, micronemes release adhesins that mediate the attachment of the parasites to the host plasma membrane (Carruthers and Tomley, 2008). This process is accompanied by the proteolytic cleavage of micronemal proteins by cysteine proteases and rhomboid proteases (Kim, 2004; Binder and Kim, 2004; Carruthers and Blackman, 2005; Dowse and Soldati, 2005)), and *T. gondii* and *N. caninum* differ with regard to their susceptibility to protease inhibitors (Naguleswaran *et al*, 2003). Secondly, proteins from rhoptries are released at the parasite-host cell interface to form a tight junction between the plasma membranes of the invading parasite and the host cell (Bradley and Sibley, 2007). The ring-like moving junction serves as a filter to eliminate host transmembrane proteins from the nascent PV, thereby avoiding subsequent recognition and fusion with host lysosomes. Finally, these parasites modify the environment of their PV by secreting proteins from dense granules (Cesbron-Delauw *et al*, 1996; Hemphill *et al*, 1998; Vonlaufen *et al*, 2004). A striking morphological difference between replicating *T. gondii* and *N. caninum* is their organization inside the PV: *Toxoplasma* parasites form rosettes around a central residual body, with the parasite's apical end facing the PV membrane, while *Neospora* parasites have no specific spatial organization within their PV. One hallmark of a *T. gondii* infection is the ability of the parasite to alter host cell pathways by using the PV membrane as a signaling platform or by secreting bioactive factors into the host cytoplasm and nucleus (Hemphill *et al*, 2006; Sinai, 2008). *T. gondii* is also notorious for interacting with many host cell structures and organelles that surround with the PV (Romano and Coppens, 2013). Despite the discovery of *N. caninum* 30 year ago, many aspects on its intracellular behavior, including host cell-interaction and nutrient uptake, remain understudied.

In this study, we examined the capability of *N. caninum* to modify the host cell interior and recruit mammalian organelles. Our goal is to identify functional differences in the colonization of host cells between *N. caninum* and *T. gondii* to provide unique insights into *Neospora* host specificity and pathogenesis at the cellular level. *N. caninum* spends most stages of its lifecycle as an intravacuolar parasite as it survives poorly axenically. Thus, to effectively control *Neospora* infections, it is important to decipher the steps that lead to its successful intracellular development, which may uncover potential targets for chemotherapeutic intervention as neosporosis is a major root cause of economic loss worldwide (Hemphill and Gottstein, 2000). Here we show that *N. caninum* diverts many host cell structures and organelles to its PV, notably to exploit their nutrient content, hereby demonstrating conserved mechanisms between this parasite and *T. gondii*. However, small differences in the *modus operandi* of these parasites are also observed, e.g., in the rearrangement of host secretory organelles around its PV, which could account for divergence in their respective evolutionary paths, as well as reflect differences in the expression of unique genes.

2.3. MATERIALS AND METHODS

2.3.1. Reagents and antibodies

All chemicals were obtained from Sigma (St Louis, MO) or Fisher (Waltham, MA) unless otherwise stated. The nitrobenzoxadiazole (NBD)-cholesterol and NBD C6-ceramide were obtained from Molecular Probes (Seattle, WA), and BODIPY TR C5-ceramide from Invitrogen (Carlsbad, CA). [^{3}H]uracil was purchased from PerkinElmer (Shelton, CT). The following primary antibodies were used: mouse monoclonal and rabbit polyclonal anti-g-tubulin; rabbit polyclonal anti-giantin (Covance, Emeryville, CA); rabbit polyclonal anti-GRA7 antibodies (Coppens *et al*, 2006); mouse anti-KDEL (Stressgen, Assay Designs); mouse anti-H5C6 Limp (CD63); mouse anti-H4A3 LAMP1 (Developmental Studies Hybridoma Bank, University of Iowa); and mouse monoclonal anti-TOM20 (Santa Cruz, CA). The *N. caninum* mouse anti-NcPIs and 21H7A antibodies were generous gifts from Dr. Vern Carruthers (University of Michigan; Morris *et al*, 2004) and Dr. Peter Bradley (UCLA; Sohn *et al*, 2011), respectively. Secondary antibodies used for immunofluorescence were conjugated to Alexa^{488}, Alexa^{594} or Alexa^{350} (Invitrogen, Carlsbad, CA).

2.3.2. Cell lines and culture conditions

Human foreskin fibroblasts (HFF), HeLa cells and CHO-K1 were obtained from the American Type Culture Collection (Manassas, VA). Bovine turbinate cells (BT24 cells) were generously provided by Dr. Dan Howe (Gluck Equine Research Center, Lexington, KY). The somatic 2-2 mutant CHO cells lacking functional NPC1 was kindly provided by Dr. L. Liscum (Tufts University; Dahl *et al*, 1992). All cells were grown as monolayers and cultivated in α-minimum essential medium

(MEM) supplemented with 10% fetal bovine serum (FBS), 2 mM glutamine and penicillin/streptomycin (100 units/ml per 100 µg/ml), and maintained at 37°C in 5% CO_2. Preparation of LDL and lipoprotein-deficient serum (LPDS) was described (Coppens *et al*, 2000).

2.3.3. Parasite cultivation

The tachyzoites from the Nc-Liv isolate (Liverpool, UK; Barber *et al*, 1993) of *N. caninum* and from RH strain (type I lineage) of *T. gondii* were used throughout this study. In one experiment, the Prugniaud strain (type II lineage) of *T. gondii* was used. The parasites were propagated *in vitro* by serial passage in monolayers of HFF (Roos *et al*, 1994).

2.3.4. Plaque assay

BT24 cells or HFF were grown until confluence in a 6-well plate, as both cell lines have growth contact inhibition. Two hundred parasites were added to each well and the plates were incubated at 37°C for 6 days. The cells were fixed and stained as described previously (Stripen and Soldati-Favre, 2013). The plates were scanned (ScanWizard 5, Microtek) and the area of each plaque was measured using Volocity software (PerkinElmer, Waltham, MA) by tracing each plaque using the 'Region of Interest' (ROI) tool. The mean area and standard deviation of the plaques were calculated from three independent experiments and the *P*-values were calculated using a student *t*-test with Excel software (Microsoft, Redmond, WA). The total number of plaques in each well was also counted and analyzed in the same manner. The mean area and number of plaques were calculated from three independent experiments using three wells of a 6-well plate per experiment and condition.

2.3.5. Uracil incorporation assay

CHO cells were grown until confluent in 24-well plates before infection with $5x10^4$ parasites for 4 h at 37°C, washed with PBS and incubated for 24 h in MEM medium. Cells were then incubated with 1 µCi of [^{3}H]uracil for 2 h at 37°C and the samples were processed as described previously (Roos *et al*, 1994).

2.3.6. Lipid uptake

To monitor the uptake of ceramides by intracellular *N. caninum*, HFF were infected for 24 h, washed with PBS and incubated in serum free-medium containing 5 µM NBD C6-ceramide complexed to BSA for different time points prior to observations by live fluorescence microscopy (Romano *et al*, 2013). To examine cholesterol uptake, HFF were infected for 24 h, washed with PBS and incubated in the presence of the serum containing 1 mM NBD-cholesterol incorporated into lipoproteins for the various time points (Coppens *et al*, 2000).

2.3.7. Mammalian cell transfection with GFP-Rab constructs

The GFP-Rab43, GFP-Rab30 and GFP-Rab14 constructs were generously provided by Dr. John Presley (McGill University, Canada). HFF were used for transfection using the Amaxa nucleofector kit V according to the manufacturer's conditions (Lonza, Basel, Switzerland). Cells were transfected with 2 µg of plasmid DNA and left to recover overnight prior to parasite infections. The cells were infected with *N. caninum* for 45 min at 37°C, washed with PBS to remove extracellular parasites, and incubated for 30 h at 37°C. The cells expressing GFP-Rab14

were incubated with serum free medium containing 5μM BODIPY TR C5-ceramide conjugated to BSA for 20, 30 or 40 min.

2.3.8. Fluorescence microscopy and image analysis

For immunofluorescence assays (IFA), cells were fixed either with 4% formaldehyde (Polysciences, Warrington, PA) plus 0.02% glutaraldehyde in PBS for 15 min, or in cold 100% methanol for 5 min (for immunostaining with g-tubulin and a-tubulin). IFA were performed as described previously (Karsten *et al*, 2004) except that the permeabilization step with 0.3% TritonX-100 in PBS was omitted for samples fixed with methanol. Coverslips were mounted using ProLong anti-fade mounting solution (Invitrogen). The fluorescence dye filipin was used for cytochemical detection of 3b-hydroxysterols within membranes of *N. caninum*-infected cells as described (Coppens *et al*, 2000). LysoTracker Red was used to track the distribution of acidic (endocytic) organelles in live cells according to the manufacturer's instructions (Molecular Probes). Infected HFF expressing a GFP-Rab construct and/or incubated with BODIPY TR C5-ceramide were washed with PBS and fixed with 4% paraformaldehyde (EM grade; Electron Microscopy Sciences, Hatfield, PA) and 0.02% glutaraldehyde (EMS) in PBS for 20 min. Samples were then washed with PBS and mounted using ProLong anti-fade mounting solution (Invitrogen). Cells were viewed with either: 1) a Nikon Eclipse E800 microscope (Nikon, Melville, NY) equipped with an oil-immersion plan Apo 100x NA 1.4 objective, a Spot RT CCD camera (Diagnostic Instruments, Sterling Heights, MI) and Image-Pro-Plus software (Media Cybernetics, Silver Spring, MD), or 2) a Nikon Eclipse 90i equipped with an oil-immersion plan Apo 100x NA 1.4 objective and a Hamamatsu GRCA-ER camera (Hamamatsu Photonics, Hamamatsu, Japan). Optical z-sections with 0.2-μm spacing were acquired using Volocity software (PerkinElmer,

Waltham, MA). The images were deconvolved using an iterative restoration algorithm and the registry was corrected using Volocity software. Photoshop (Adobe) was used to adjust levels, crop and resize images obtained from both microscopes. Pearson Correlation Coefficient (PCC) and the positive product of the differences of the mean (PDM) images were calculated using Volocity software. Thresholds were set automatically using the method of Costes (Costes *et al*, 2004).

2.3.9. Electron microscopy and morphometric analysis

For transmission EM, BT24 cells infected with *N. caninum* or HFF infected with *T. gondii* for 20 h were fixed in 2.5% glutaraldehyde (EMS) in 0.1 M sodium cacodylate buffer (pH 7.4) for 1 h at room temperature, and processed as described (Fölsch *et al*, 2001) before examination with a Philips CM120 Electron Microscope (Eindhoven, the Netherlands) under 80 kV. To track the distribution of host endo-lysosomes, VERO cells infected with *N. caninum* for 30 h were incubated with 0.5 mg/ml of LDL particles adsorbed to 15 nm gold particles as described (Coppens *et al*, 1987) before fixation. To determine the extent of association of host mitochondria with *N. caninum* PV at the ultrastructural level, about 50 images of PV of *N. caninum* in BT24 cells 20 h p.i. were randomly taken at a magnification of 15,000 using a grid containing points spaced at 0.1 cm. Morphometry was performed as followed: the surface densities (membrane surface area in mm^2:volume in mm^3) of each PV (S_vPV) and host mitochondrion associated with the PV membrane (S_vM) were determined by counting the number of points that land on the PV membrane and mitochondrial membranes images. Combining the S_v for each PV and each mitochondrion, the percent of host mitochondria

associated with the PV membrane was obtained by calculating the mean ratios of S_vM/S_vPV. Data were compiled and analyzed using Microsoft Excel 2007.

2.3.10. Quantitative analysis with MetaScopics

We created and used MetaScopics, an image analysis web application developed to provide simple and effective tools for leveraging user input to quantify protein or organelle recruitment, perform morphological analysis, and determine object distances (see illustrations in Fig. 2-1). MetaScopics algorithms operate on a per image basis. After the upload of fluorescent images of infected cells and partitioning into groups (e.g., parasites, timepoints of infection, cell types, etc…), each algorithm quantifies a specific metric over individual images. This metric is then aggregated over each group of images and the group aggregations are compared. To quantify host mitochondria, ER, microtubule and lysosome, MVB recruitment around the PV, we used the MetaScopics algorithm "Intensity by Distance". This operates via user input (e.g., drawing a boundary around an object) and a shell-pixel counting method (e.g., generating concentric 1 pixel-wide layers surrounding the object). First, the user draws a boundary around an object (Fig. 2-1.A; PV in red), selects a color of interest (Fig. 2-1.A; mitochondria in green), and selects a maximum distance (Fig. 2-1.B; 200 pixels, white). Then, the MetaScopics algorithm sums the color intensity of each pixel within a layer (i.e. distance of 1 pixel from the PV or previous layer) and determines the percent intensity by calculating the ratio of pixel intensity per layer to the total pixel intensity of all layers (e.g., Fig. 2-1.B; 200 pixels, white). Each layer corresponds to a given concentric distance from the object boundary in pixels. Fig. 2-1.C shows the percentage of the total intensity of each layer (1 pixel width) surrounding the boundary of the PV in Fig. 2-1.A within a 200 pixel maximum distance (Fig. 2-1.B). Fig. 2-1.D displays the percent intensity of

TOM20 staining (mitochondria) versus distance in pixels averaged over many images of *T. gondii* and *N. caninum* PV. A maximum distance of 100 pixels was used, representing approximately 7 µm, a physiologically relevant distance.

A summary statistic, called average distance, for recruitment is created for each image by finding the average distance for the color of interest weighted by pixel intensity from the user input boundary. This statistic is calculated by summing the product of the total number of pixels of a given color at a given distance (e.g., 100 pixels away; 7 µm away) with that distance and dividing by the total color intensity thus normalizing and ensuring that the quantification is weighted by intensity. In the below equation describing this process $P_{intensity}$ describes the intensity of a pixel and $P_{distance}$ to boundary is the distance of that pixel from the user defined boundary. The summary statistic (intensity weighted distance) is used to compare images from different conditions using box plots:

$$\text{Average Distance} = \frac{\sum^{\text{pixels}} P_{\text{intensity}} \times P_{\text{distance to boundary}}}{\sum^{\text{pixels}} P_{\text{intensity}}}$$

To assess host Golgi proximity to the PV, we used the "Centroid to Surface Distance" algorithm from MetaScopics, which provides another useful metric to determine recruitment. This method is more appropriate than the "Intensity by Distance" algorithm and is used for objects that are compact or are separated by large distances from the PV as the "Intensity by Distance" task is more advantageous for focusing on close interactions with spread organelles or structures. First, the user selects the color of the centroid object (e.g., Golgi) and the color of the other object (e.g., PV). The algorithm finds the centroid of the centroid object by first finding

all pixels with the user selected color (Golgi). Next, the x and y location of these pixels is averaged, arriving at the x and y centroid coordinates. Once the centroid is found, all pixels corresponding to the PV are scanned and the distance from the pixel closest to the centroid is used to define the "Centroid to Surface Distance" metric. This process is visualized in Fig. 2-1.E and F. The "Centroid to Surface Distance" metric provides a good relative metric for recruitment. Because a strongly recruited object may become fragmented or distorted around its recruiter, the centroid provides a heuristic for the point the object is being recruited towards; a centroid need not lie within its generating object. Thus for strong recruitment we frequently see small values for this metric, often a value of zero.

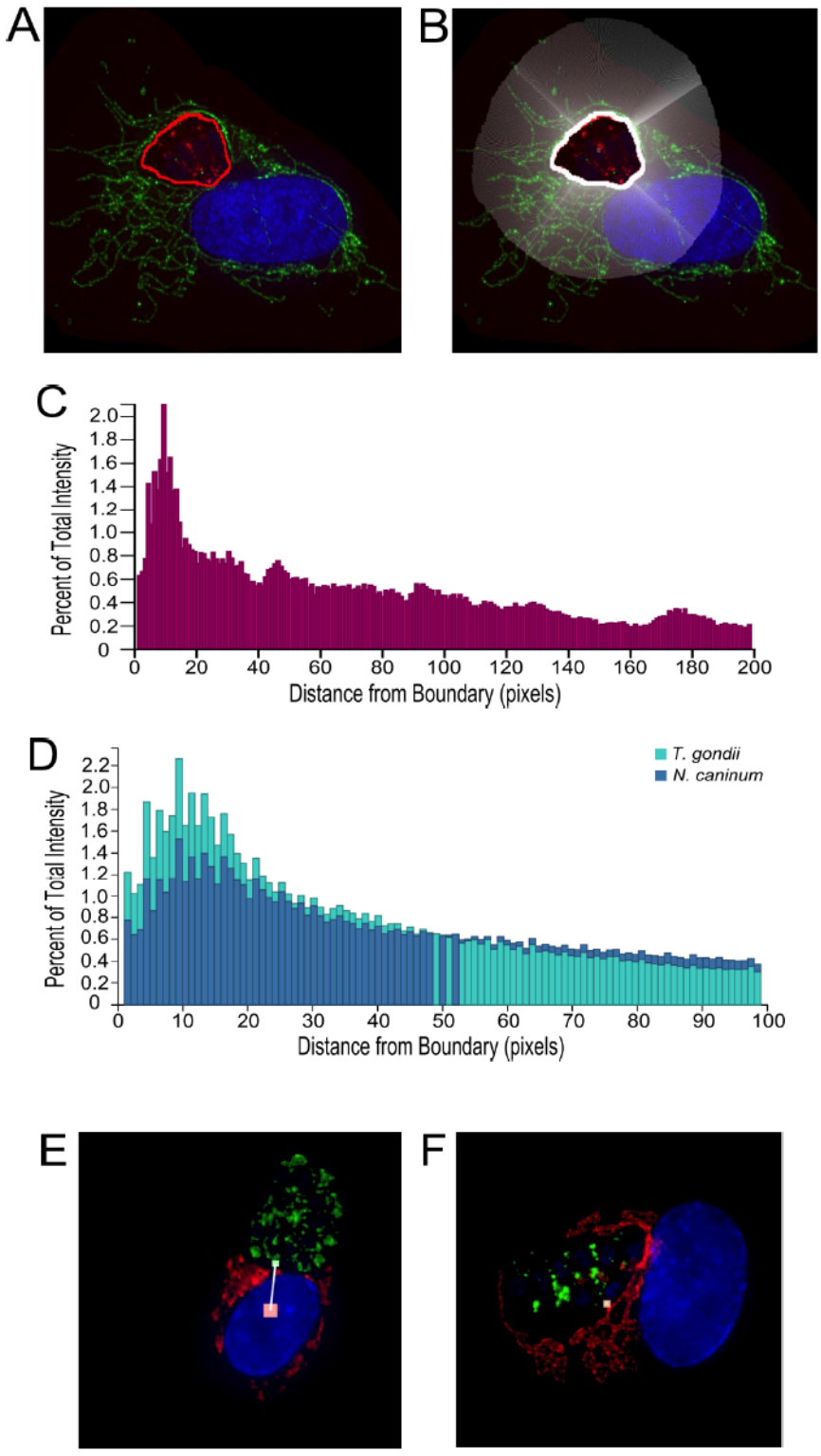

Figure 2-1. Examples of the MetaScopics algorithms "Intensity by Distance" and "Centroid to Surface". **A.** An example of a user-defined boundary in the "Intensity by Distance" algorithm is shown. The user-defined boundary (bold red) delineates the perimeter of the PV in a fluorescent extended focus image of

an *N. caninum*-infected HFF labeled with antibodies to TOM20 (mitochondria, green), 21H7A (PV lumen, red) and DAPI (nuclei, blue).

B. A visualization of the pixels, analyzed by the algorithm, corresponding to a user selected maximum distance of 200 pixels. All of the pixels have a distance less than or equal to the maximum distance. The region corresponding to the pixels is shown (white) superimposed on the fluorescent image from A.

C. The result of the "Intensity by Distance" algorithm for the image in **A** is shown with a maximum distance input of 200 pixels. The algorithm calculated the percent of the total intensity of the TOM20 signal (green in A) as described in the Experimental Procedures. The distance from the user-defined boundary (PV perimeter, bold red in A) corresponds to concentric layers each with a width of 1 pixel that surround the boundary. Relative to Panel A we see that individual images tend to have much greater noise in the distribution of their intensity by distance. In this image the majority of the target organelle (TOM20 signal, mitochondria) lies within 20 pixels of the PV.

D. Shown is the percent of total intensity of the TOM20 signal as a function of distance from the user-defined boundary (PV perimeter) averaged over many images of *T. gondii* and *N. caninum* infected cells. In this example, the PVs of *T. gondii* show greater relative recruitment of host mitochondria than the PVs of *N. caninum* based on the greater left skew in the distance distribution of the TOM20 signal.

E. A result from the MetaScopics algorithm "Centroid to Surface" is shown for a single fluorescent extended focus image of a *N. caninum* infected HFF labeled with antibodies to giantin (host Golgi, red), 21H7A (PV, green) and DAPI (nuclei, blue). In this example, the distance between the host Golgi and PV is calculated as described in the Experimental Procedures and is categorized as moderate. The pink square denotes the centroid of the host Golgi (target organelle). The green square denotes the location of the closest PV pixel. The PV appears fragmented due to a high threshold on the color intensity. MetaScopics is only interested in surface pixels with high intensity.

F. A result from the MetaScopics algorithm "Centroid to Surface" where the distance between the host Golgi (target organelle) and the PV is small. A single fluorescent extended focus image of a *N. caninum*-infected cell labeled with antibodies to giantin (host Golgi, red), 21H7A (PV, green) and DAPI (nuclei, blue) is shown. In this example, the target organelle (host Golgi) is surrounding, or being recruited by, the PV and its centroid lies within the PV surface, resulting in a centroid to surface distance of zero. Both the centroid (pink square) and closest PV surface pixel (green square) lie on top of each other.

2.3.11. Statistical methods

Data were displayed in box plots using Kaleidagraph software (Synergy Software, Reading, PA). Whiskers of the box plots represent the upper and lower values excluding outliers, outliers are marked as open circles, and the line inside the box is the median value. Means and standard deviations were calculated from three independent experiments using Excel (Microsoft). *P*-values were calculated using either student *t*-test in Excel (Microsoft) or from a one-way ANOVA with a post-hoc Bonferroni test in Kaleidagraph (Synergy Software).

2.4. RESULTS

2.4.1. *Neospora caninum* infects and replicates in bovine and human cells with the same efficiency

Our analyses on host cell-parasite interaction were conducted in parallel on *N. caninum* and *T. gondii* in cultured mammalian cells. These studies were performed on the Nc-Liv isolate of *N. caninum* [referred here as Nc-Liv] collected from tissues of infected dogs (Barber *et al*, 1993). Among all the *N. caninum* isolates, Nc-Liv shows the highest proliferative capacity and parasite burden in both the brain and placenta, and therefore has the highest virulence in hosts (Dellarupe *et al*, 2014). The behavior of Nc-Liv *in vitro* was compared with that of the RH strain of *T. gondii* [referred here as *T. gondii* (RH)], which is also the highest virulent strain for this parasite. Since cattle, and never humans, are important intermediate hosts of *N. caninum*, we first wanted to examine whether bovine cells may confer an advantage in supporting the intracellular development of Nc-Liv over human cells. The growth rate of Nc-Liv was monitored in bovine cells (bovine nasal turbinate epithelial cells or BT24 cells) in comparison with human cells (human foreskin fibroblasts or HFF) by parasite enumeration 24 h and 48 h post-infection (p.i.). Fig. 2-2.A shows no significant difference in parasite number between the two cell lines (doubling time of 7.9 ± 1.4 and 10.2 ± 3.9 in BT24 cells and HFF, respectively). In addition, we performed plaque-based assays and measured the size of the lysed area in Nc-Liv-infected monolayers of BT24 cells or HFF. Cells were infected and incubated for 6 days to allow for multiple rounds of replication and egress. No statistical difference was observed in either plaque number or size between Nc-Liv grown in BT24 cells or HFF (Fig. 2-2.B). This suggests that the host cell specificity does not influence the proliferation of Nc-Liv *in vitro*.

2.4.2. Nc-Liv grows slower than *T. gondii* (RH) *in vitro* regardless of cell type

We compared the efficiency of Nc-Liv and *T. gondii* (RH) to infect and lyze cell monolayers (Fig. 2-2.C). Data from plaque assays were normalized with values of plaque number and size during a Nc-Liv infection in BT24 cells or HFF. BT24 cells have been previously used to cultivate *T. gondii*, and no difference was observed for productive infection of the parasite in BT24 cells or HFF (Blais *et al*, 1993). *T. gondii* (RH) formed significantly more abundant and larger lytic areas than observed for Nc-Liv whether inoculated in BT24 cells or HFF. This indicates that Nc-Liv parasites have a slower developmental rate than *T. gondii* (RH) parasites in cultured cells.

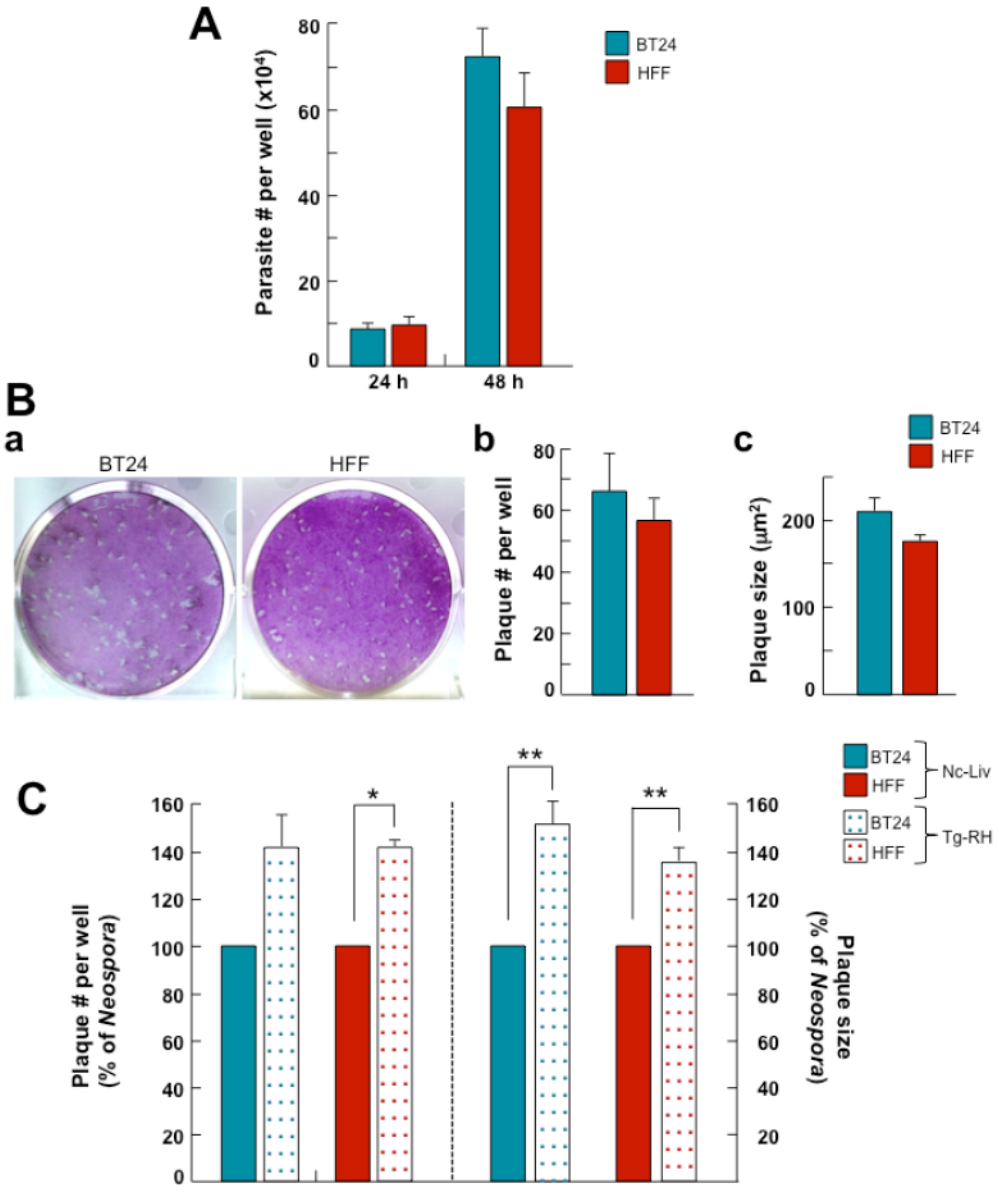

Figure 2-2. Growth specificity of Nc-Liv *in vitro.*

A. Comparison of the replication rate of Nc-Liv in BT24 cells and HFF. Cell monolayers of BT24 cells and HFF seeded in 6-well plates were infected with the same inoculum size of Nc-Liv and then washed after 2 h. Cells were scrapped 24 h or 48 h p.i. and the total number of parasites in each well was assessed using a hemocytometer. Data are means ± S.D., n=3 separate assays. **B.** Comparison of the growth rate of Nc-Liv in BT24 cells and HFF using plaque assays. Panel a illustrates representative area of monolayers of BT24 cells or HFF destroyed by the parasite. The mean number (b) and area (c) of the plaques ± S.D. were calculated from 3 independent experiments. **C.** Comparison of the growth rate of Nc-Liv and *T. gondii* (RH) in BT24 cells and HFF using plaques assays. The mean number and area of the plaques ± S.D. are expressed as percent relative to controls (infection with Nc-Liv), which was set as 100%, for 3 independent experiments. Results were statistically significant (*, $P<0.05$; **, $P<0.01$).

2.4.3. Development of MetaScopics, a new image analysis software for the quantification of host organelle-PV interactions

Using image analysis, we compared the relative ability of *N. caninum* and *T. gondii* to attract host cell structures and organelles to their PV. Mammalian cytoskeletal elements and organelles were fluorescently labeled to track their distribution in infected cells. To compare the intensity of the fluorescent signal around the PV of *N. caninum* and *T. gondii*, and therefore to evaluate the respective competence of these parasites for recruiting host cell structures, we developed a new image analysis program, named MetaScopics (www.metascopics.com). MetaScopics consists of several algorithms for quantitative analysis of microscopy images. Information on computational principles underlying the algorithms of MetaScopics and applications is available Materials and Methods.

One algorithm used in this study named "Intensity by Distance", measures the percent intensity of a fluorescent marker (associated with an organelle) as a function of the distance of this marker from the perimeter of the parasitophorous vacuole (PV), which is labeled with a different fluorescent marker. The output of this algorithm allows the comparison of distances between groups of images. Robust PV association of a given marker correlates with smaller distances between the marker and the PV perimeter. This algorithm is best suited for structures that pervade the cell, e.g., the ER, cytoskeleton, mitochondria, lysosomes or MVB, or that have poorly defined boundaries, e.g., microtubules. In a second algorithm titled "Centroid to Surface Distance", MetaScopics calculates the centroid of a given object (fluorescently-labeled organelle) and measures the distance from the centroid to the nearest surface of the PV stained with a different fluorochrome. By tracking distances between objects designated by fluorescence markers, MetaScopics allows to derive changes in distance attributable to different

experimental conditions. This algorithm is suitable for organelles with well-defined structures or localizations in the cell, e.g., the Golgi apparatus. To validate the "Centroid to Surface Distance" task, we applied the algorithm to a well-known biological event - the change in morphology of the Golgi apparatus upon treatment with Nocodazole. This drug interferes with microtubule polymerization, leading to the destabilization of the microtubular network and change in organelle positioning in cells. In HFF exposed to 300 nM Nocodazole for 90 min, the Golgi apparatus is disrupted and Golgi fragments are spread in a broad area around the nucleus (Cole *et al*, 1996; Fig. 2-3.A). The "Centroid to Surface Distance" task was used to measure the distance between the centroid of the Golgi and the nucleus in drug-treated and control cells. MetaScopics analysis measured the average distance of the Golgi centroid to the nucleus as 3.18 µm in untreated cells and 0.11 µm in nocodazole-treated cells, in accordance with a perinuclear localization of Golgi fragments induced by the drug (Fig. 2-3.B).

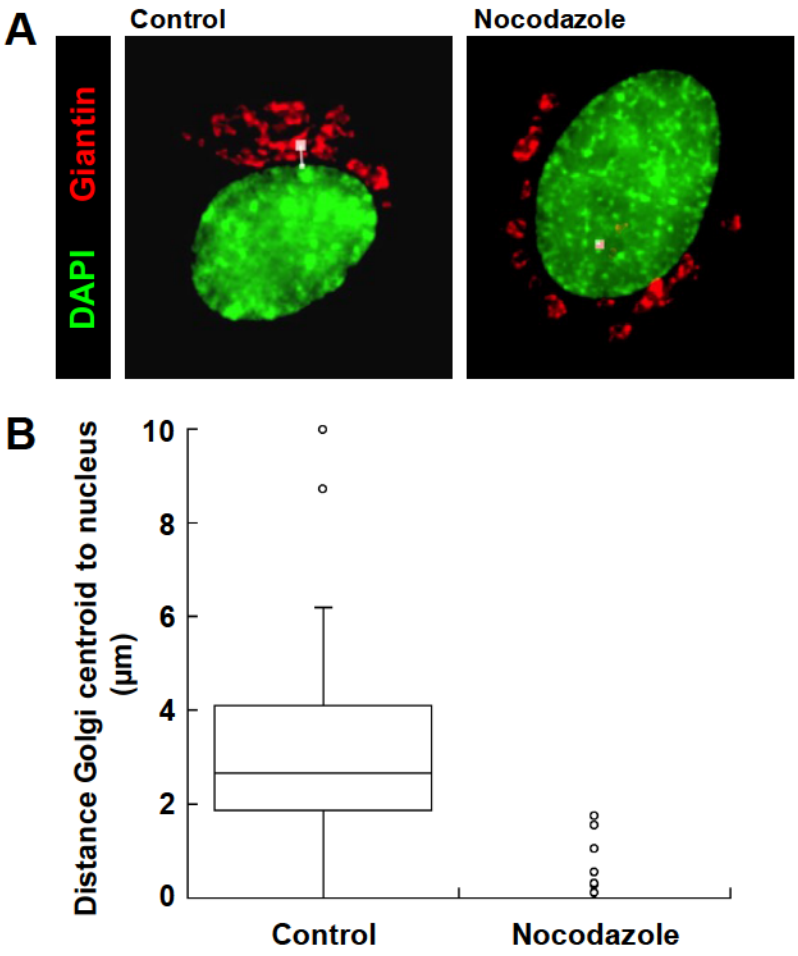

Figure 2-3. Biological validation of the MetaScopics algorithm - Example of the "Centroid to Surface Distance" task

A. IFA of HFF control (DMSO) or treated for 90 min with 300 nM of Nocodazole showing fragmentation of the Golgi and distribution of Golgi elements around the nucleus. The pink squares denote the centroid of the Golgi (target organelle) in both conditions. Nucleus stained with DAPI in green; Golgi immunolabeled for giantin in red. **B.** Quantitative measurement of the Golgi morphology in the absence or presence of Nocodazole using MetaScopics. Box plots show the average distance from the Golgi centroid to the nearest nucleus boundary (data from 50 infected HFF per group). The Golgi centroid distance to the nucleus is significantly lower with Nocodazole (P<0.00001).

2.4.4. Like *T. gondii* (RH), Nc-Liv attracts host mitochondria to its PV and retains these organelles close to the vacuolar membrane

Mitochondria are dynamic organelles involved in a wide range of processes such as ATP generation, cell death, immune signaling, chemotaxis and calcium homeostasis (Shaughnessy *et al*, 2014). These organelles also play a central role in phospholipid metabolism and lipid exchange with the ER (Pagliarini and Rutter, 2013; Sinai *et al*, 2004). Many intracellular pathogens, including *T. gondii* have evolved to manipulate the surveillance or bioenergetic pathways of host mitochondria for their benefit (Sinai *et al*, 2004; Ashida *et al*, 2011; Anand and Tikoo, 2013; Lartigue and Faustin, 2013). Rapidly after penetration into the cell, *T. gondii* (RH) induces a dramatic change in the spatial distribution of host mitochondria. These organelles become concentrated around the PV and closely associate with the vacuolar membrane, with a distance of ~12 nm (Sinai *et al*, 1997). By 4 h and 24 h p.i., 18 and 23 % of the PV membrane, respectively, is covered by host mitochondria.

As *T. gondii* and *N. caninum* share several metabolic features, we evaluated if Nc-Liv co-opts host mitochondria like *T. gondii* (RH). In infected cells, mitochondria were immunolabeled for TOM20 and their distribution was assessed by fluorescence microscopy 24 h p.i. A concentric fluorescent signal was observed around the PV of Nc-Liv in both BT24 cells and HFF, resembling the perivacuolar gathering of host mitochondria in *T. gondii* (RH)-infected cells (Fig. 2-4.A). We used MetaScopics to calculate the intensity-weighed distances of host mitochondria to the PV of Nc-Liv and *T. gondii* (RH). Host mitochondria were statistically closer to the PV of *T. gondii* (RH) than that of Nc-Liv (Fig. 2-4.B). This indicates that these host organelles are more concentrated around the PV of *T. gondii* (RH) than that of Nc-Liv, as calculated within an arbitrary delineated

area of 7 mm radiating from the PV. Identical statistical results were obtained by selecting perimeters of 3.5 and 10 mm around the PV boundary (data not shown).

In *T. gondii*, the recruitment of host mitochondria is strain-dependent. RH parasites express a Mitochondria Association Factor 1 (TgMAF1) at the PV membrane, a mediator of PV association with host mitochondria (Pernas *et al*, 2014). The cystogenic Prugniaud strain of *T. gondii*, however, does not express TgMAF1 and at 12 h p.i. less than 2% of the PV is associated with host mitochondria as observed. We compared the distribution of host mitochondria in HFF infected with Nc-Liv and *T. gondii* (Pru). Early in infection, no interaction of host mitochondria was observed for either parasite (Fig. 2-5). At 24 h p.i., we observed a concentration of host mitochondria that was more intense around the PV of Nc-Liv, as compared to *T. gondii* (Pru) (Fig. 2-6.A), with 54% and 12% of the PV of Nc-Liv and *T. gondii* (Pru), respectively, substantially covered with mitochondria (Fig. 2-6.B). We also examined the localization and morphology of host mitochondria in *N. caninum*-infected BT24 cells at the EM level. Like in *T. gondii* (RH)-infected cells, many host mitochondria gathered around the *N. caninum* PV, often in multiple layers (Fig. 2-4.C, panels a and b, compared to panel e). Observations at high magnification show a close apposition of the outer membrane of the host mitochondria with the PV membrane of Nc-Liv, with a mean distance of 16 ± 4 nm, as similarly documented for *T. gondii* (RH) (Fig. 2-4.C, compare panels c and d with panel f). Morphometric analyses were undertaken to quantify the extent of host mitochondria-PV membrane association in Nc-Liv-infected BT24 cells and ascertain the representativeness of our microscopic observations. The extent of association is presented as the percentage of the PV surface in direct physical contact with host mitochondria as shown in panel d of Fig. 2-4.C. For a 20 h infection, ~8% of the PV membrane was associated with host mitochondria, which is less than that calculated for *T. gondii* (RH) (23% at 24 h; Pernas *et al*, 2014).

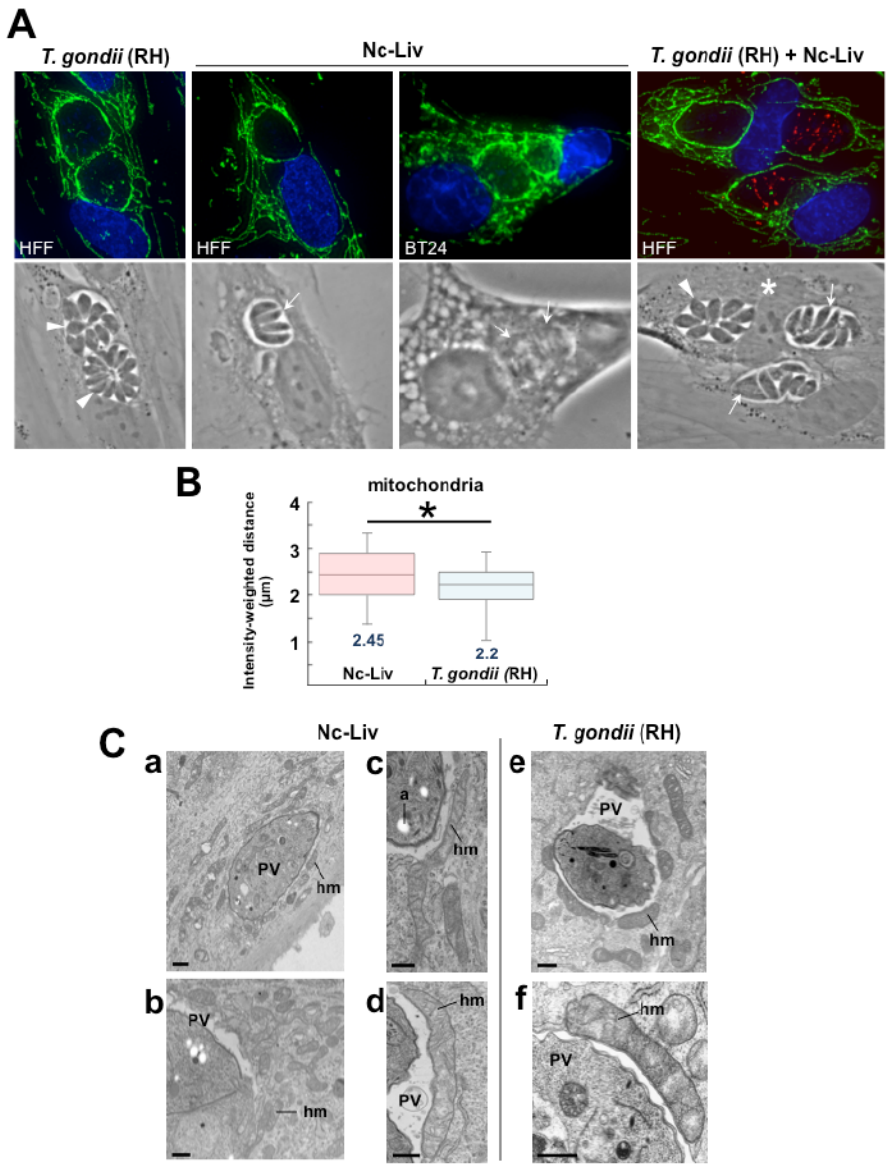

Figure 2-4. Host mitochondria interaction with the PV of Nc-Liv.

A. Immunofluorescence assays (IFA) of host mitochondria in *T. gondii* (RH)- or Nc-Liv-infected cells. HFF or BT24 cells were infected with *T. gondii* (RH) and/or Nc-Liv, fixed and stained with DAPI (blue, nucleus), and antibodies against TOM20 (green, mitochondria). In a co-infection assay, the antibody 21H7A was used to identify Nc-Liv (red, PV). An asterisk identifies a co-infected cell. Representative extended focus images are shown. Arrowheads and arrows pinpoint the PV of *T. gondii* (RH) and Nc-Liv, respectively. **B.** Quantitative comparison of mitochondrion recruitment by Nc-Liv and *T. gondii* (RH) by MetaScopics analysis. Box plots show the average distance, weighted by intensity, of the host mitochondria to the PV boundary, as calculated for host mitochondrial profiles included in a 7 µm radius of the PV (data from 94 infected HFF at 24 h p.i.). The lines inside the box are the median values, the numbers written under the plot are the mean fluorescence intensities. Comparison between the two parasites is statistically significant (*, $P<0.004$). **C.** Ultrastructural analysis of host mitochondria-PV interaction. EM of Nc-Liv-infected BT24 cells (a-d) and *T. gondii* (RH)-infected HFF (e and f) showing the distribution of host mitochondria (hm) relative to the PV. a, amylopectin granule. Scale bars are 0.5 µm.

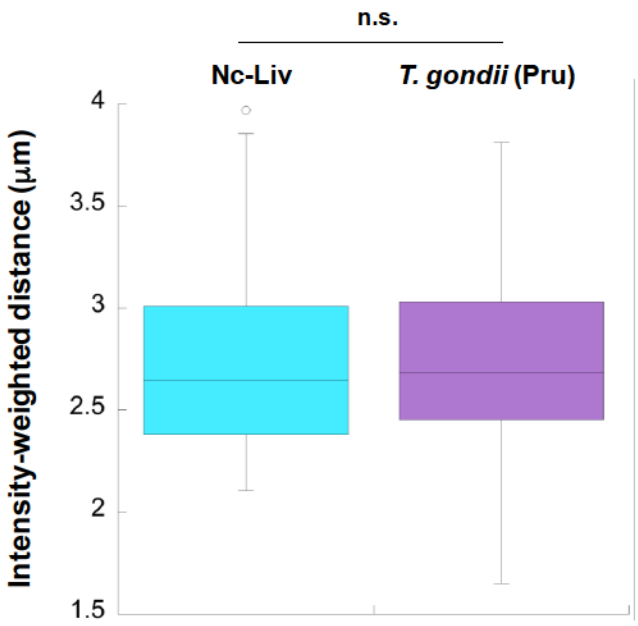

Figure 2-5. Comparison of host mitochondria distribution in cells containing small PV of Nc-Liv and *T. gondii* (Pru)

Box plots show the average distance, weighted by intensity, of the host mitochondria to the PV boundary, as calculated for host mitochondrial profiles included in a 7 µm radius of the PV (data from 35 infected HFF containing PV with one single parasite). The lines inside the box are the median values. No host mitochondria were observed around small PV of either parasite.

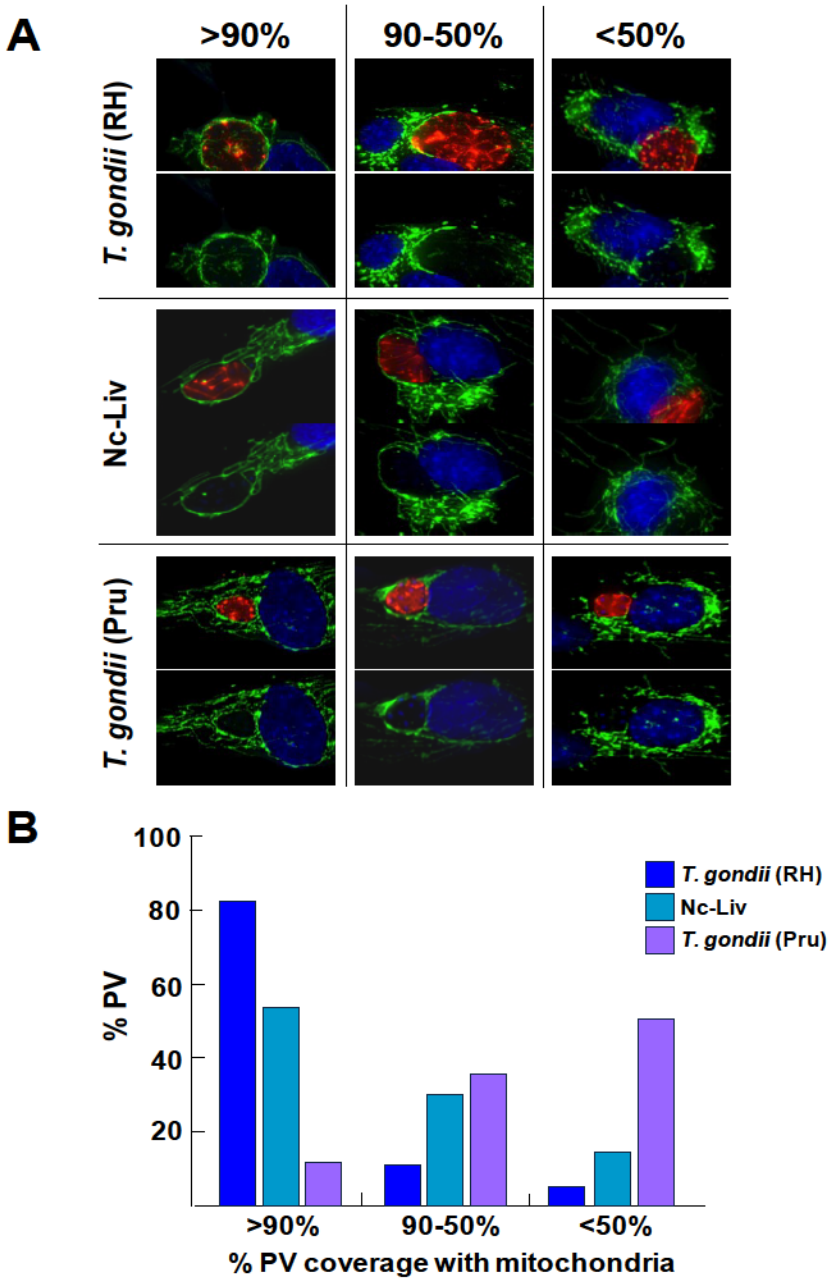

Figure 2-6. Comparison of the interaction of host mitochondria with large PV of Nc-Liv and *T. gondii* (RH) and (Pru)

A. IFA of host mitochondria in *T. gondii* (RH) and (Pru) or Nc-Liv-infected cells. HFF were infected with these parasites for 24 h before fixation and staining. Nucleus stained with DAPI in blue; mitochondria immunolabeled for TOM20 (green, mitochondria); *N. caninum* or *T. gondii* in red. For each parasite, representative extended focus images of PV covered with host mitochondria at more than 90% of the PV surface, from 90 to 50%, and less than 50% are shown. **B.** Class distribution of PV of *T. gondii* (RH) and (Pru), and Nc-Liv per percent coverage with host mitochondria (data from 35 infected HFF).

2.4.5. While host ER elements are closely apposed to with the PV membrane of *T. gondii* (RH), ER elements gather around the Nc-Liv PV but do not tightly associate with the vacuolar membrane

The distribution of the ER is also modified in *T. gondii* (RH)-infected cells as ER elements surround the PV and are in intimate association with the PV membrane (Sinai *et al*, 1997). From 4 h p.i. and onwards, half of the PV membrane is covered by host ER tubules. The perivacuolar ER elements are located within ~20 nm of the vacuolar membrane, and ribosomes are restricted to the opposite face of the ER from the PV. Inspection of the organization of the host ER in Nc-Liv-infected cells by IFA using anti-KDEL antibodies revealed an intense staining around the PV. This perivacuolar fluorescent signal was more pronounced in BT24 cells than in HFF but was similar to the *T. gondii* (RH) PV in fibroblasts (Fig. 2-7.A), suggestive of an interaction between host ER and the Nc-Liv PV. The spatial distribution of host ER elements relative to the Nc-Liv PV was measured using MetaScopics at different time points of infection. The distance between the host ER and the PV decreased significantly between 8 and 24 h p.i. with no significant decrease observed between 24 h and 48 h (Fig. 2-7.B). This suggests that the host ER-PV recruitment occurs prior to 24 h p.i. EM observations of Nc-Liv-infected BT24 cells confirm the bundling of host ER around the PV 20 h p.i. (Fig. 2-7.C, panel a). Perivacuolar ER elements were particularly enlarged (Fig. 2-7.C, panels b and c), compared to the ER in uninfected BT24 cells or in *T. gondii* (RH)-infected cells (Fig. 2-7.C, panel f). Although the amassing of host ER around the PV was impressive, no physical association of ER elements with the PV membrane could be observed, and ribosomes were also distributed on ER tubules facing the PV membrane (Fig. 2-7.C, panels d and e compared to panels g and h). This suggests that either there is no molecular contact between proteins of the PV of Nc-Liv and host ER, or if any, those are transient.

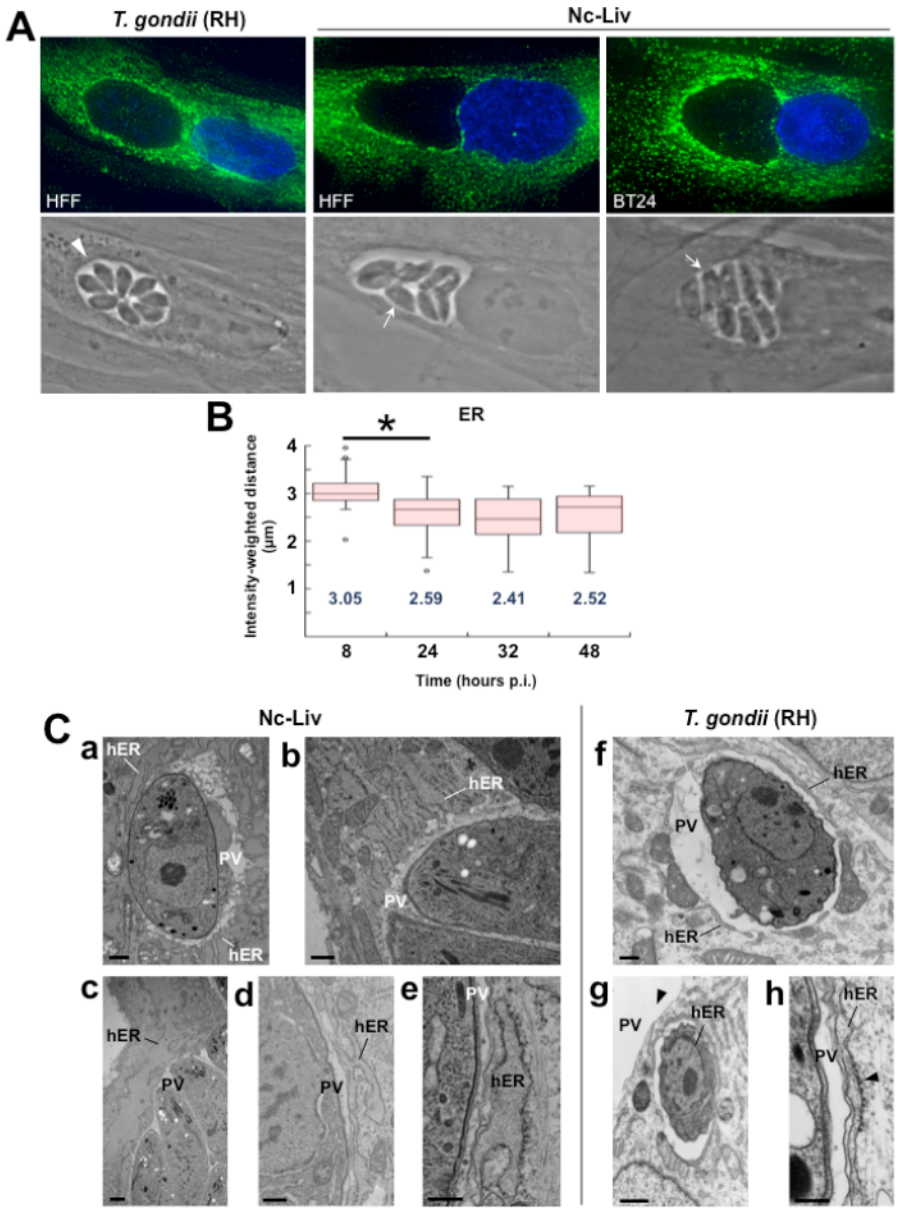

Figure 2-7. Host ER interaction with the PV of Nc-Liv.

A. IFA of host ER in *T. gondii* (RH)- or Nc-Liv-infected cells. HFF or BT24 cells were infected with *T. gondii* (RH) or Nc-Liv, fixed and stained with DAPI (blue, nucleus) and antibodies against KDEL (green, ER). Representative extended focus images are shown. Arrowheads and arrows pinpoint the PV of *T. gondii* (RH) and Nc-Liv, respectively. **B**. MetaScopics analysis of the kinetics of host ER recruitment by Nc-Liv. Box plots show the average distance, weighted by intensity, of host ER to the PV boundary, as calculated for host ER profiles detected within a 7 µm radius of the PV (data from 158 infected HFF at 24 h p.i.). The lines inside the box are the median values, the numbers written under the plot are the mean fluorescence intensities. Comparison between ER distribution at 8 h and 24 h is statistically significant (*, $P<0.0001$). **C.** Ultrastructural analysis of host ER-PV interaction. EM of Nc-Liv-infected BT24 cells (a-e) and *T. gondii* (RH)-infected HFF (f-h) showing the distribution of host ER (hER) relative to the PV. Arrowheads show the distribution of ribosomes on the ER side facing the host cytoplasm, and not the *T. gondii* (RH) PV membrane. Scale bars are 0.5 µM.

2.4.6. Host microtubules concentrate around the Nc-Liv PV but not as extensively as with the *T. gondii* (RH) PV

T. gondii (RH) dramatically modifies the architecture of the host microtubular network as its PV is entirely wrapped by microtubules (Coppens *et al*, 2006; Walker *et al*, 2008). To determine whether the PV of Nc-Liv is comparably surrounded by host microtubules, we examined the distribution of the host microtubular cytoskeleton in Nc-Liv-infected cells by IFA using anti-a-tubulin antibodies, and by EM. Fig. 2-8.A illustrates a concentration of host microtubules around the PV of Nc-Liv in mono-infected cells and in cells co-infected with *T. gondii* (RH). At the ultrastructural level, bundles of host microtubules closely apposed to the PV membrane could be observed (Fig. 2-8.B). Using MetaScopics, we quantified the distribution of host microtubules around the PV of both parasites, and found that host microtubules were more concentrated around the PV of *T. gondii* (RH) than that of Nc-Liv in a statistically significant manner (Fig. 2-8.B). To validate the "Intensity by Distance" task of MetaScopics, we quantified the concentration of host microtubules around the PV of *T. gondii* (RH) and Nc-Liv in the presence or absence of the microtubule-depolymerizing agent Nocodazole (Fig. 2-9). Data show a significant decrease in the fluorescent staining for a-tubulin around the *T. gondii* PV in Nocodazole-treated cells in comparison with untreated cells; no significant decrease was observed for the Nc-Liv PV in treated versus untreated cells. This result is in accordance with our data in Fig. 2-8.A, showing a higher concentration of host microtubules around the PV of *T. gondii* (RH) than of Nc-Liv.

2.4.7. Like *T. gondii* (RH), Nc-Liv displaces the host microtubule-organizing center to its PV

Most animal cells have one microtubule-organizing center (MTOC) during interphase. According to our observations, the MTOC in both HFF and BT24 cells was located on or near the nucleus in 92% and 6% of cells, respectively. *T. gondii* (RH) also hijacks the MTOC or centrosome by detaching this structure from the host nuclear envelope and relocating it to its PV (Romano *et al*, 2013). Evidence for a MTOC-PV association in *T. gondii* (RH)-infected cells is supported by the detection of centrosomal material at the PV surface, including pericentriolar matrix proteins and components of the g-tubulin ring complex, which are all critical for microtubule nucleation (Coppens *et al*, 2006; Romano *et al*, 2013; Walker *et al*, 2008; Wang *et al*, 2010).

The recruitment of the host MTOC by Nc-Liv and the MTOC position relative to the PV was investigated by IFA using anti-g-tubulin antibodies. Occasionally, the host MTOC was present at the PV surface of Nc-Liv (Fig. 2-8.D). Quantitative analysis shows that the host MTOC was: i) associated with ~20% of the PV of Nc-Liv; ii) equidistant to the host nucleus and the PV in ~25% of infected cells; or iii) closer to the host nucleus than the PV in half of the infected cells (Fig. 2-8.E). These distributions are similar to that observed during *T. gondii* (RH) infection. Though Nc-Liv does not recruit microtubules as extensively as *T. gondii* (RH) (Fig. 2-8.B), this parasite is equally proficient in hijacking the host MTOC, perhaps suggesting that the association of the host MTOC and the wrapping of host microtubules around the PV are not necessarily correlated.

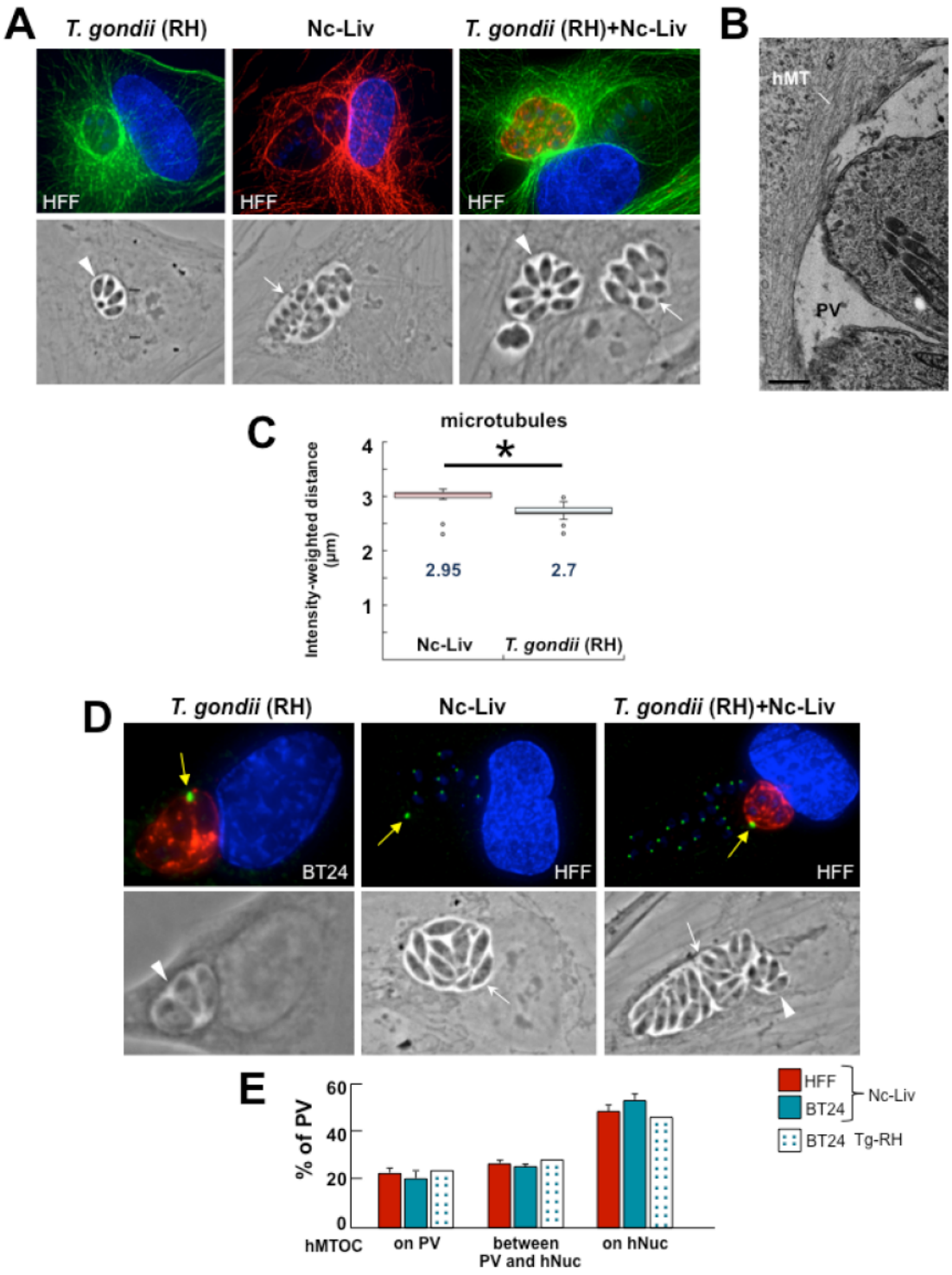

Figure 2-8. Host microtubules and MTOC association with the PV of Nc-Liv.

A. IFA of host microtubules in *T. gondii* (RH)- and/or Nc-Liv-infected cells. HFF were infected with *T. gondii* (RH) or Nc-Liv, fixed and stained with DAPI (blue, nucleus), and antibodies against a-tubulin (green or red, microtubules) during mono-infection, and during a co-infection with anti-GRA7 antibodies to identify *T. gondii* (RH) (red, PV). Representative extended focus images are shown. Arrowheads and arrows pinpoint the PV of *T. gondii* (RH) and Nc-Liv, respectively. **B.** EM of a view of a PV of Nc-Liv in BT24 cells showing

host microtubules (hMT) aligned along the PV membrane. Scale bar is 0.5 µM. **C.** Quantitative comparison of microtubule recruitment by Nc-Liv and *T. gondii* (RH) by MetaScopics analysis. Box plots show the average distance, weighted by intensity, of the host microtubules to the PV boundary, as calculated for host microtubules in a 7 µm radius of the PV (data from 26 infected HFF at 24 h p.i.). The lines inside the box are the median values, the numbers written under the plot are the mean fluorescence intensities. Comparison between the two parasites is statistically significant (*, $P<0.01$). **D.** IFA of host MTOC in *T. gondii* (RH)- and/or Nc-Liv-infected cells. BT24 cells or HFF were infected with *T. gondii* (RH) or Nc-Liv, fixed and stained with DAPI (blue, nucleus), antibodies against g-tubulin as a marker of the MTOC (green) indicated by yellow arrows during mono-infection, and GRA7 to identify *T. gondii* (RH) (red, PV) in a co-infected cell. Note that the anti-γ-tubulin antibodies also label the MTOC/centrosome of Nc-Liv. Representative extended focus images are shown. Arrowheads and arrows pinpoint the PV of *T. gondii* (RH) and Nc-Liv, respectively. **E.** Quantification of the distribution of the PV of Nc-Liv or *T. gondii* (RH) relative to the host nucleus (hNuc). The distribution of the host MTOC has been classified as: on the PV, equidistant to the PV and the host nucleus, and close to the host nucleus. Data expressed in % of PV population, are means ± S.D. of 3 independent assays for Nc-Liv and means for a representative experiment for *T. gondii* (RH), with a minimum of 150 vacuoles counted in each experiment.

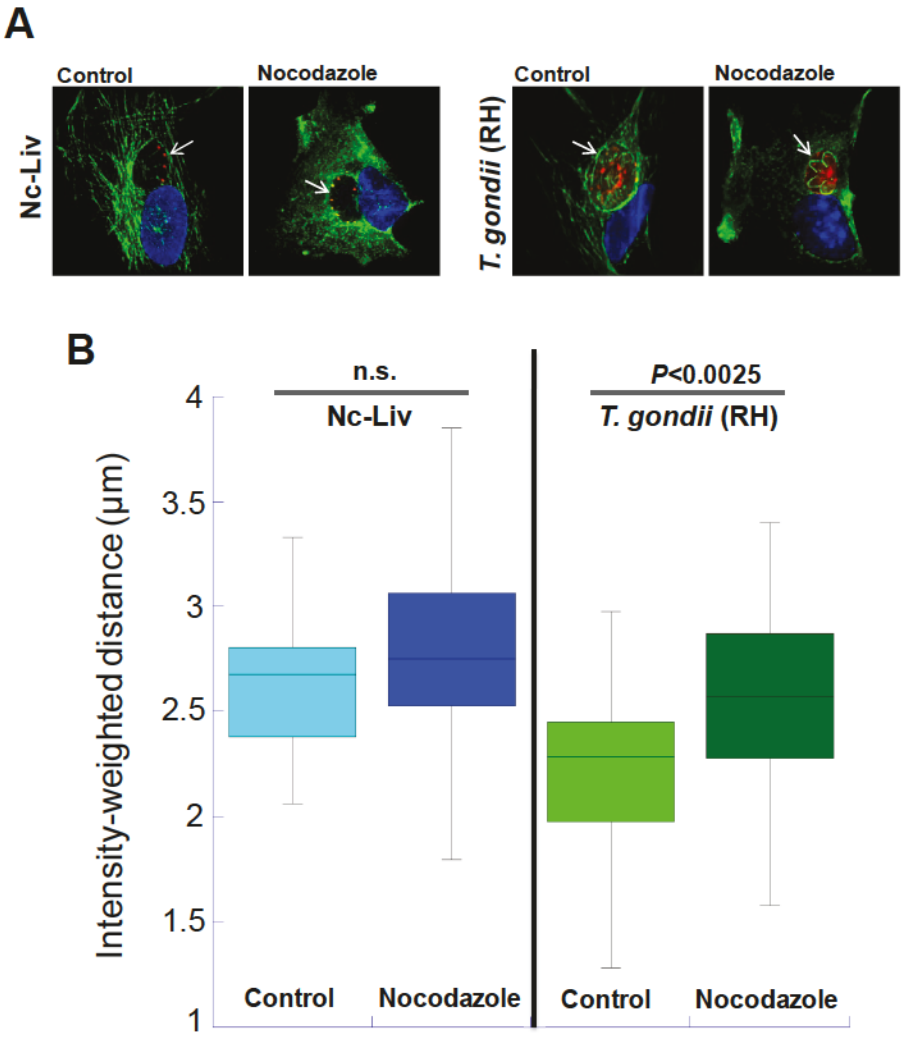

Figure 2-9. Biological validation of the MetaScopics algorithm - Example of the "Intensity by Distance" task

A. IFA of infected HFF control (DMSO) or treated for 90 min with 300 nM of Nocodazole, showing dispersion of depolymerized microtubules throughout the cytoplasm. Concentration of microtubules to the PV of both parasites decreases upon Nocodazole treatment. Nucleus stained with DAPI in blue; microtubules immunolabeled for a-tubulin in green; *N. caninum* or *T. gondii* in red. **B.** Measurement using MetaScopics of host microtubule concentration around the *N. caninum* or *T. gondii* PV in the presence or absence of Nocodazole. Boxplots show the percent of total intensity of the a-tubulin signal as a function of distance from the PV perimeter (data from at least 35 infected HFF per group). Since host microtubules are more abundantly concentrated around the PV of *T. gondii* (RH) than around the Nc-Liv PV, a significant decrease in microtubule distribution around *T. gondii* in treated vs. control cells is solely observed for *Toxoplasma* infection, which validates the algorithm.

2.4.8. Host endocytic organelles and multivesicular bodies concentrate around the PV of both parasites

Host endocytic organelles represent a rich source of nutrients, derived from the extracellular medium, for intracellular pathogens. *Toxoplasma* has developed strategies to attract these organelles while avoiding destruction. The parasite manipulates the host microtubular network to create invaginations of the PV membrane, and through these microtubule-based invaginations, host endo-lysosomes are retained within the PV (Coppens *et al*, 2006). The host mTORC2-Akt signaling is then usurped by *Toxoplasma* to maintain endo-lysosomes around the PV (Wang *et al*, 2010).

We assessed the distribution of host endocytic compartments in Nc-Liv-infected cells using three independent approaches: i) LysoTracker-containing organelles (Fig. 2-10.A); ii) endocytic structures loaded with lipoprotein-gold particles (Fig. 2-10.B); and iii) LAMP1 (Lysosome-Associated Membrane Protein 1)-labeled organelles (Fig. 2-10.C, panel a). Findings were concordant from all of these approaches, illustrating an accumulation of endo-lysosomes around the PV of Nc-Liv. As similarly observed for the *T. gondii* (RH) PV, the gathering of these organelles at the Nc-Liv PV was maintained throughout parasite replication as 58-70% of the LysoTracker-containing structures surrounded the PV 24 h p.i. EM observations illustrate lipoproteins-containing organelles concentrated at the PV of Nc-Liv. MetaScopics analysis comparing the intensity-weighed distances of host endo-lysosomes to the PV of Nc-Liv and *T. gondii* (RH) did not reveal any statistical difference between the two parasites (Fig. 2-10.C, panel b).

Multivesicular bodies (MVB) are temporary storage compartments enriched in sphingolipids and cholesterol at the intersection of the endocytic and exocytic pathways.

Nothing is known about the interaction of host MVB with the PV of *T. gondii* or *N. caninum*. We used antibodies against the MVB protein marker CD63 to analyze the distribution of MVB in *T. gondii* (RH)- or Nc-Liv-infected cells (Fig. 2-10.D, panel a). We observed a distribution of CD63-labeled organelles around the PV of each pathogen, and quantification by MetaScopics indicates a statistically higher concentration of MVB around the PV of *T. gondii* (RH), compared to that of Nc-Liv (Fig. 2-10.D, panel b).

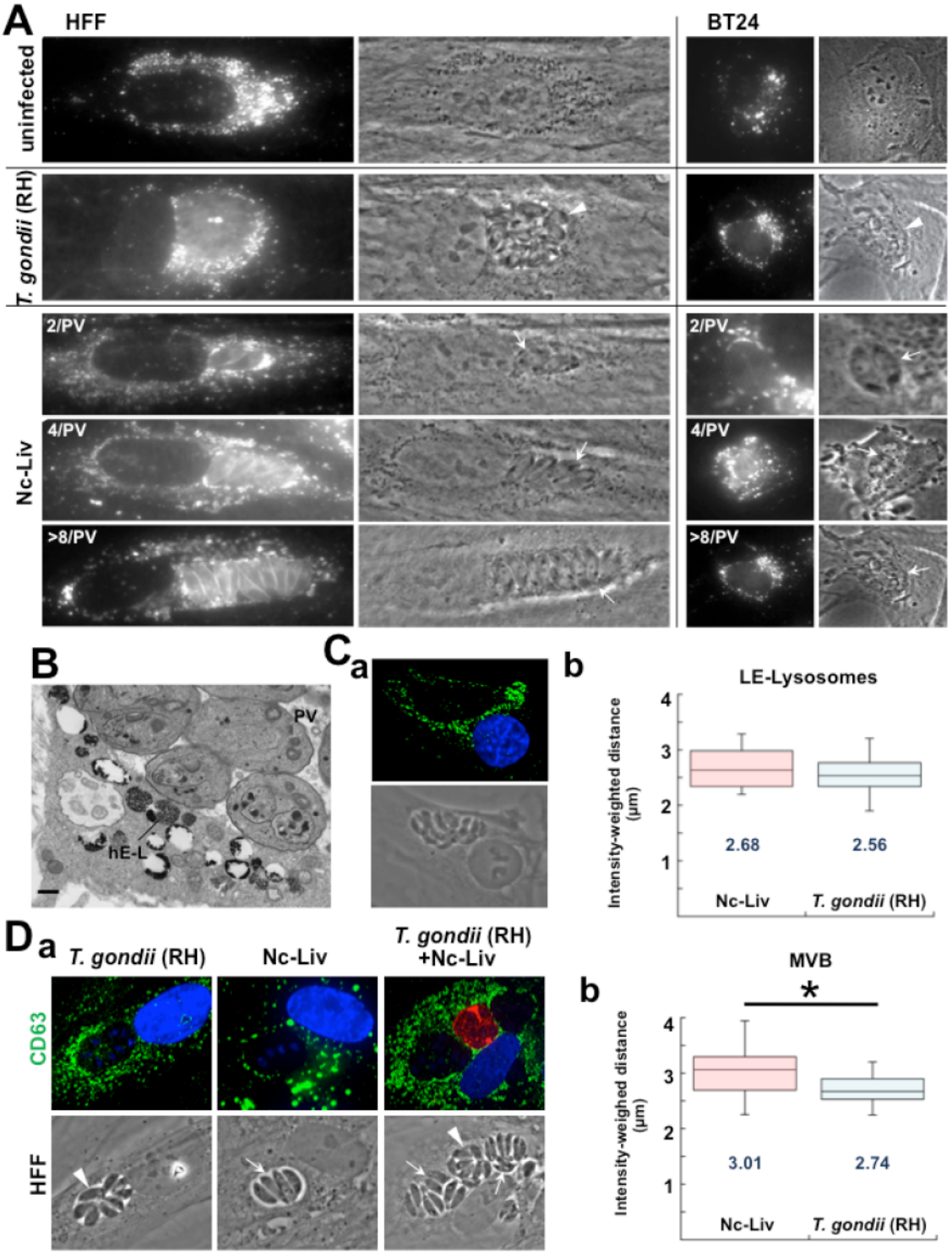
A
HFF
BT24
uninfected
T. gondii (RH)
Nc-Liv
2/PV
4/PV
>8/PV
B
PV
hE-L
Ca
b
LE-Lysosomes
Intensity-weighted distance (µm)
2.68
2.56
Nc-Liv
T. gondii (RH)
Da
T. gondii (RH)
Nc-Liv
T. gondii (RH) +Nc-Liv
CD63
HFF
b
MVB
*
Intensity-weighed distance (µm)
3.01
2.74
Nc-Liv
T. gondii (RH)

Figure 2-10. Host endosomal organelle interaction with the PV of Nc-Liv.

A. Live fluorescence microscopy of cells incubated with Lyso-Tracker. HFF or BT24 cells, uninfected or infected with *T. gondii* (RH) or Nc-Liv, were incubated for 1 h with Lyso-Tracker before observation by live fluorescence microscopy. Arrowheads and arrows pinpoint the PV of *T. gondii* (RH) and Nc-Liv, respectively. **B.** Ultrastructural analysis of Nc-Liv incubated with LDL-labeled organelles. Nc-Liv-infected CHO cells incubated with LDL-gold particles for 24 h, showing the concentration of host LDL-containing endo-lysosomes (hE-L) at the PV membrane. Scale bar is 0.5 µm. **C.** Panel a: IFA of host endocytic structures in Nc-Liv-infected HFF. HFF were infected with Nc-Liv, fixed and stained with DAPI (blue, nucleus) and antibodies against LAMP1 (green, late endosomes/lysosomes). Panel b: Quantitative comparison of host late endosome (LE)-lysosome recruitment by Nc-Liv and *T. gondii* (RH) by MetaScopics analysis. Box plots show the average distance, weighted by intensity, of LAMP1-positive structures to the PV boundary, as calculated for all of these host organelles within in a 7 µm radius of the PV (data from 26 infected cells at 24 h p.i.). **D.** Panel a: IFA of host multivesicular bodies (MVB) in *T. gondii* (RH)- and/or Nc-Liv-infected HFF. HFF were infected with *T. gondii* (RH) or Nc-Liv, fixed and stained with DAPI (blue, nucleus), and antibodies against CD63 (green, MVB) during mono-infection, and during a co-infection with anti-GRA7 antibodies to identify *T. gondii* (RH) (red, PV). Arrowheads and arrows pinpoint the PV of *T. gondii* (RH) and Nc-Liv, respectively. Panel b: Quantitative comparison of host MVB recruitment by Nc-Liv and *T. gondii* (RH) by MetaScopics analysis. Box plots show the average distance, weighted by intensity, of MVB to the PV boundary, as calculated for all of the MVB within in a 7 µm radius of the PV (data from 68 infected HFF at 24 h p.i.). The lines inside the box are the median values, the numbers written under the plot are the mean fluorescence intensities. Comparison between the two parasites is statistically significant (*, $P<0.002$).

2.4.9. Like *T. gondii* (RH), Nc-Liv contains cholesterol that it scavenges from host endocytic compartments

Cholesterol is the major sterol molecule ubiquitously present in mammalian cells, in which it plays key roles in organizing signaling lipids and proteins within membranes. Mammalian cells obtain cholesterol by internalization of plasma low-density lipoproteins (LDL) or from *de novo* synthesis in the ER via the mevalonate pathway (Goldstein and Brown, 1990). *T. gondii* contains cholesterol but cannot synthesize this lipid that it salvages from host endocytic organelles (Coppens *et al*, 2000). *Toxoplasma* recruits the host ER but its growth does not rely on ER-synthesized cholesterol.

To assess the presence and distribution of cholesterol in *N. caninum*, we labeled Nc-Liv parasites with filipin, a fluorescent compound that interacts with the 3b-OH group of sterols within membranes (Volpon and Lancelin, 2000), and viewed the parasite by microscopy (Fig. 2-11.A). Intracellular Nc-Liv parasites exhibited a strong filipin-positive staining (Fig. 2-11.A), as previously observed for *T. gondii* (RH) (Coppens *et al*, 2000). The parasite's plasma membrane and apical elongated organelles displayed the most intense labeling. The morphology of the apical organelles is reminiscent to that of rhoptries, organelles that contain cholesterol in *T. gondii* (Foussard *et al*, 1991; Coppens and Joiner, 2003).

Toxoplasma has the ability to store cholesterol as cholesteryl esters in lipid bodies. To examine whether Nc-Liv has cholesterol stores, we labeled the parasite with Nile Red, a dye that strongly fluoresces in cytoplasmic lipid bodies. Under normal culture conditions (i.e. 10% FBS), *N. caninum* contained an average of 3 ± 1 Nile Red positive-neutral lipid bodies (Fig. 2-11.B), which is comparable to the 4 ± 2 lipid bodies detected in *T. gondii* (Quittnat *et al*, 2004). The availability of host LDL has a direct impact on the development of *T. gondii* (RH). LDL deprivation

(e.g., via interference with LDL endocytosis, LDL lysosomal degradation or cholesterol egress from lysosomes) impairs *Toxoplasma* growth whereas the overabundance of these lipoproteins stimulates parasite replication (Coppens *et al*, 2000; Nishiwaka *et al*, 2011). To determine if Nc-Liv also scavenges cholesterol from host endo-lysosomes, we incubated infected fibroblasts with fluorescent NBD-cholesterol incorporated into lipoproteins for 5, 10 and 20 min at 37°C, and viewed the parasites by live microscopy. We observed an intense labeling of intravacuolar parasites after 5 min of incubation (Fig. 2-11.C). From 10 min and onwards, we noticed the appearance of stained cytoplasmic lipid bodies in the parasites, indicative of storage of NBD-cholesterol. Next, we evaluated whether the growth of Nc-Liv was influenced by the availability of exogenous cholesterol. Infected cells were incubated in medium containing FBS (control), lipoprotein-deficient FBS (LPDS) or excess LDL, and the parasite replication was measured by radioactive uracil incorporation 18 h and 36 h p.i. (Fig. 2-11.D). Removal of lipoproteins from the incubation medium resulted in a significant reduction in uracil incorporation into the parasites, as compared with control parasites. The lower levels of uracil incorporation coincided with the presence of PV containing fewer parasites (data not shown). Addition of excess LDL to the culture medium stimulated Nc-Liv replication 36 h p.i., as previously demonstrated for *T. gondii* (RH) (Coppens *et al*, 2000). To determine if Nc-Liv relies on host endocytic organelles for cholesterol acquisition, we monitored the parasite growth in NPC1-deficient CHO cells. Mammalian Niemann-Pick type C1 (NPC1) cells display defect in cholesterol mobilization from lysosomes (Ko *et al*, 2001). A significant impairment of Nc-Liv growth was observed in NPC1 mutant cells as compared to CHO wild-type, a phenomenon similarly reported for *T. gondii* (RH) (Coppens and Joiner, 2003). EM studies of parasites infecting NPC1 mutant cells showed abnormal parasite division and accumulation of electron-dense multilamellar structures in the vacuolar space, which is suggestive of lipid disorders (Fig. 2-11.E).

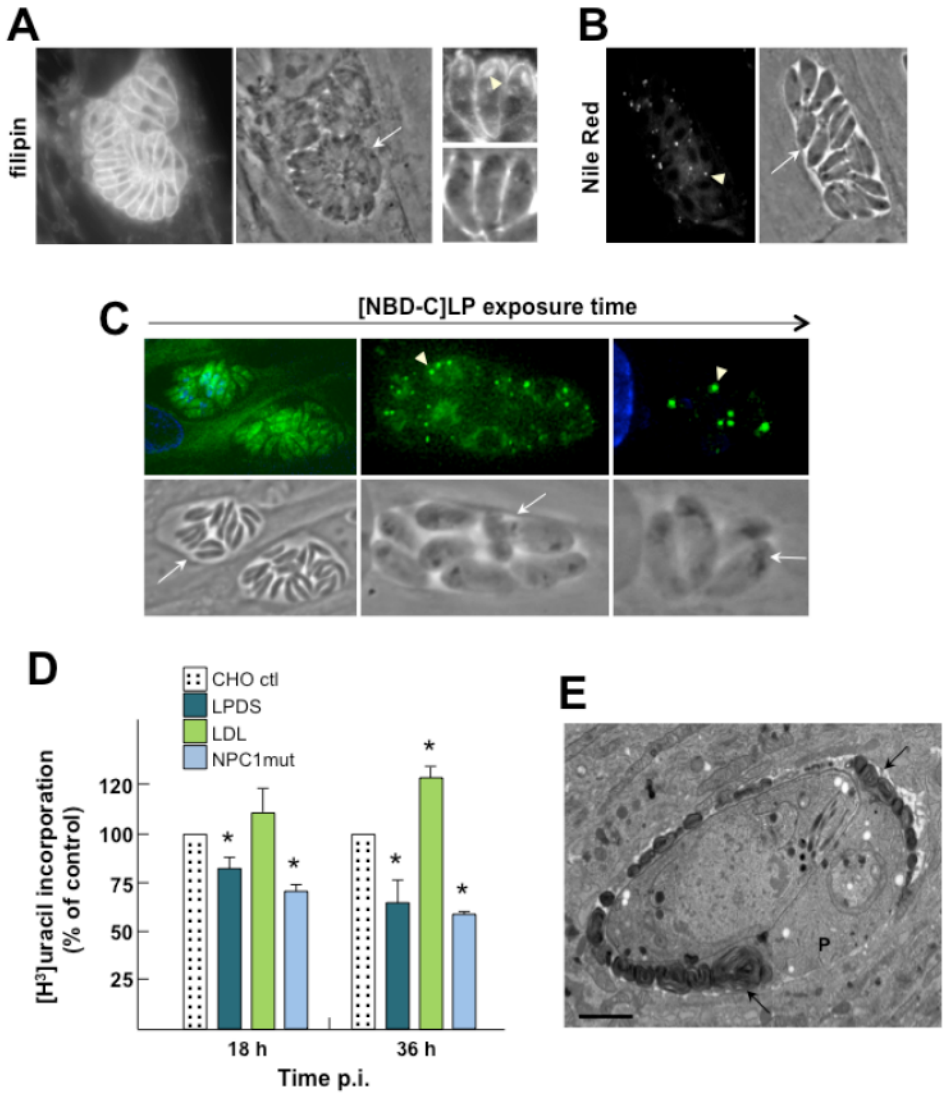

Figure 2-11. Cholesterol uptake and storage by Nc-Liv.

A. Fluorescence microscopy of Nc-Liv-infected HFF labeled with filipin. HFF were infected with Nc-Liv for 24 h, fixed and stained with the fluorescent dye filipin for sterols, showing strong fluorescence associated with the PV (arrow) and the parasite's plasma membrane and rhoptries (arrowhead). **B.** Fluorescence microscopy of Nc-Liv-infected HFF labeled with Nile Red. HFF were infected with Nc-Liv for 24 h, fixed and stained with Nile Red for lipid bodies (arrowhead). **C.** Live fluorescence microscopy of Nc-Liv-infected HFF incubated with exogenous fluorescent cholesterol. HFF infected with Nc-Liv for 24 h (arrows) were incubated with NBD-cholesterol incorporated into lipoproteins ([NBD-C]-LP) for 5 to 20 min prior to observation by live fluorescence microscopy, showing cholesterol on the plasma membrane, and then in lipid bodies (arrowheads). **D.** Influence of exogenous lipoproteins on Nc-Liv proliferation. Uracil incorporation by *Nc-Liv* 24 h or 36 h p.i. in either CHO cells grown in medium containing: a) 10% FBS (control); b)10% delipidated FBS (LPDS); or c)10% LPDS supplemented with 1 mg/ml of LDL (LDL), or in CHO cells with defective NPC1 (NPC1mut). Data in percent ± S.D. are expressed relative to the control (set as 100%) from 4 separate experiments done in triplicate. Differences between control and experimental groups were statistically significant (*, $P < 0.05$). **E.** Ultrastructural analysis of Nc-Liv-infected NPC1 mutant cells. EM of Nc-Liv (P) incubated 36 h in CHO cells lacking functional NPC1. Small PV size with parasite membrane defects and abnormal lipid accumulation in the PV lumen (arrows) were observed. Scale bar is 0.5 µm.

Jointly, these results highlight the dependence of *N. caninum* on host endocytic structures to access cholesterol and the role of LDL to supply this lipid for the parasite.

2.4.10. *N. caninum* attracts the host Golgi to its PV but induces less Golgi fragmentation than *T. gondii*

The morphology of the host Golgi apparatus is altered in cells infected with *T. gondii* (RH and Prugniaud strains), as this organelle is fragmented into mini-stacks that encircle the PV (Romano *et al*, 2013). To assess the effect of a Nc-Liv infection on the morphology of the host Golgi, we inspected the morphology of this organelle by fluorescence microscopy and EM throughout parasite infection in various mammalian cells. In each of the cell types assayed (HeLa cells, HFF and BT24 cells), the host Golgi associated with and wrapped around the Nc-Liv PV (Fig. 2-12.A). However, the morphology of this organelle remained more compact in Nc-Liv-infected cells as compared to *T. gondii* (RH)-infected cells wherein the host Golgi was severely dismantled and spread all around the PV (Fig. 2-12.A and B; Romano *et al*, 2013). EM observations illustrate the ultrastructure of Golgi stacks in vicinity to the PV of Nc-Liv. These stacks were longer and composed of more cisternae compared to the stacks observed around the *T. gondii* PV (Fig. 2-12.B). We used MetaScopics to assess the association of the host Golgi with the Nc-Liv PV. In BT24 cells, the centroid to surface distance of the host Golgi to the PV was larger when the PV was small and contained few parasites. A similar result was observed in infected HFF cells where the distance from the host Golgi centroid to the PV decreased progressively from 24 h to 48 h p.i. in a statistically significant manner.

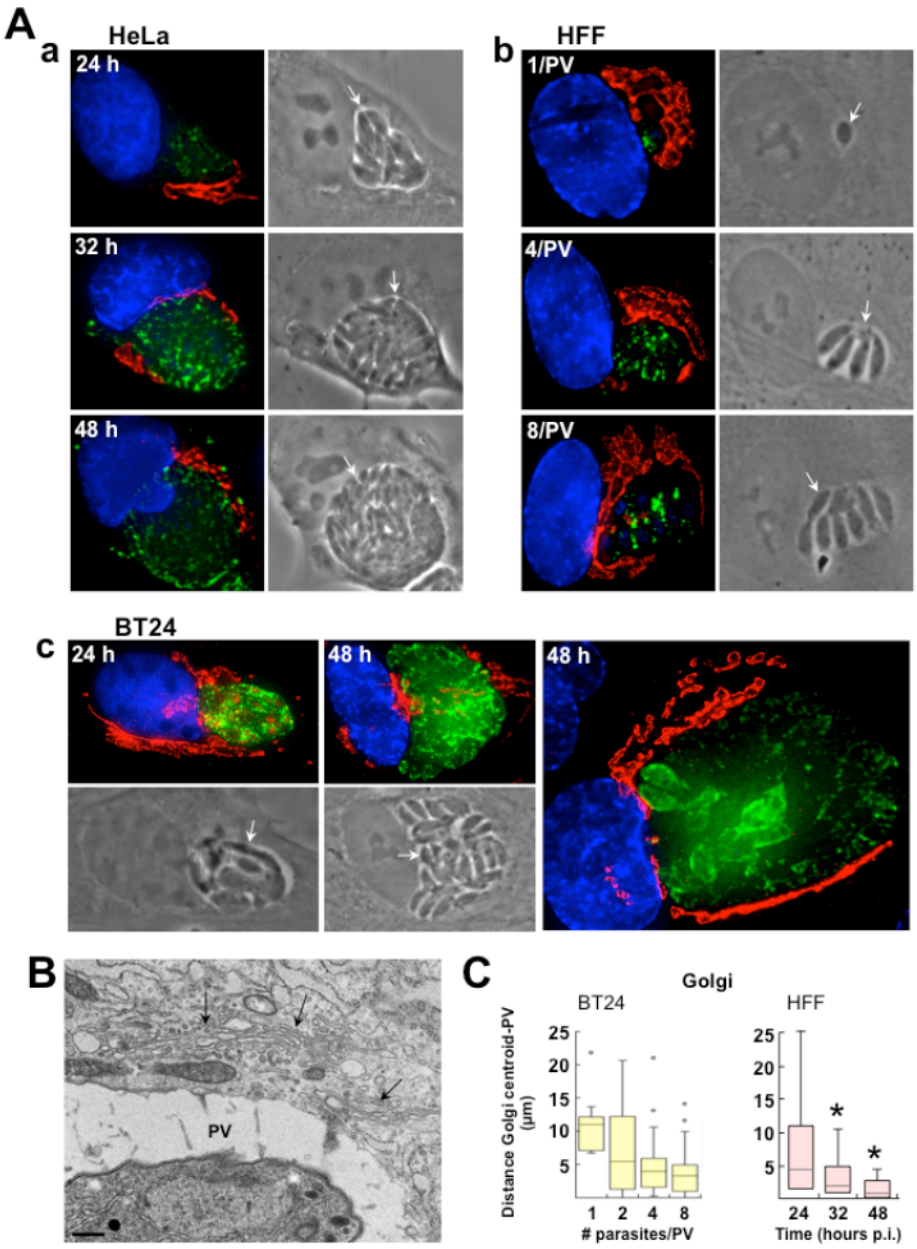

Figure 2-12. Host Golgi interaction with the PV of Nc-Liv

A. IFA of host Golgi in Nc-Liv-infected cells. HeLa cells (panel a), HFF (panel b) or BT24 cells (panel c) were infected with Nc-Liv at the indicated times, fixed and stained with DAPI (blue, nucleus), and antibodies against giantin (red, cis-and medial Golgi) and either 21H7A (green, panels a and b) and NcPIS (green, panel c) to stain the parasite. Representative extended focus images are shown. Arrows pinpoint the PV of Nc-Liv. **B.** Ultrastructural analysis of host Golgi-PV interaction. EM of Nc-Liv-infected BT24 cells showing the gathering of small stacks of Golgi (arrows) around the PV. Scale bar is 0.5 µm. **C.** Quantitative measurement of Golgi recruitment by Nc-Liv using MetaScopics. Box plots show the average distance from the host Golgi centroid to the nearest PV boundary. In BT24 cells, the host Golgi centroid distance to the PV decreased progressively as the PV size increased (data from 90 infected BT24 cells at 24 h p.i). In HFF, the host Golgi centroid distance to the PV decreased progressively in a statistically significant manner between 24 h, 32 h, and 48 h p.i. (157 infected HFF at the indicated times; *, $P<0.001$).

2.4.11. Like *T. gondii*, *N. caninum* scavenges exogenously derived ceramides from the host Golgi

In mammalian cells, ceramides are synthesized in the ER, and then transported to the Golgi for further modifications (e.g., phosphorylation, glycosylation) or conversion to sphingomyelin, diacylglycerol or sphingosine. *Toxoplasma* contains several species of sphingolipids (Welti *et al*, 2007; Lige *et al*, 2010) and scavenges ceramides and ceramide-derived lipids from the host Golgi (Romano *et al*, 2013; de Melo and de Souza, 1996). We investigated whether Nc-Liv also diverts ceramides from the host Golgi by incubating infected cells with NBD labeled C6-ceramide. Uninfected fibroblasts exposed 15 min to the lipid dye showed fluorescent staining of the Golgi complex (Fig. 2-13). Correspondingly, Nc-Liv-infected HFF displayed fluorescent labeling of host Golgi, which surrounds the PV. As the incubation time increased from 30 to 120 min, a gradual staining of the parasites was observed, with a concentration of the fluorescent signal on the parasite's plasma membrane and Golgi. In addition, egressed Nc-Liv parasites contained NBD-labeled lipids. These observations indicate that Nc-Liv, like *T. gondii* scavenges ceramides or lipids derived from the host Golgi and incorporates these lipids into its membranes. To ascertain that Nc-Liv is actively involved in the scavenging of host Golgi-derived sphingolipids, we pretreated infected cells with the anti-parasitic drug pyrimethamine, which inhibits dihydrofolate reductase, thus affecting the parasite's metabolism. Pyrimethamine-treated, infected cells contained small PV with misshapen parasites, and following NBD C6-ceramide incubation, the Nc-Liv PV were barely fluorescent, confirming that an active metabolism of the parasite is required lipid uptake from the host Golgi.

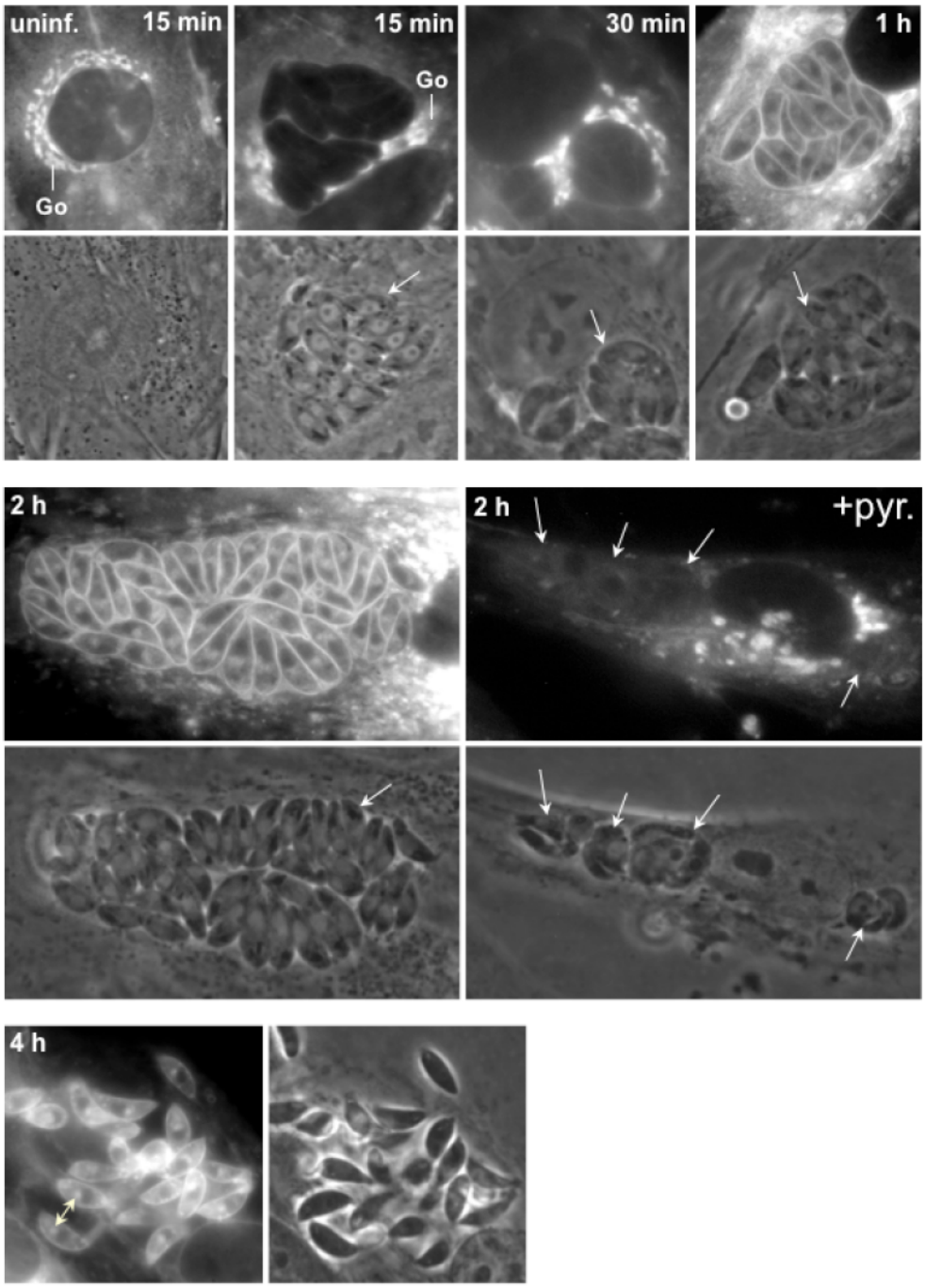

Figure 2-13. Sphingolipid uptake by Nc-Liv.

Live fluorescence microscopy of HFF incubated with fluorescent ceramides. HFF, uninfected or infected with Nc-Liv for 24 h, were incubated with NBD C6-ceramide complexed to BSA at the indicated times and washed before live microscopy observations. Staining was gradually observed on the host cell Golgi (Go) from 15 min, then on the PV (arrows) from 30 min, and the parasite's plasma membrane from 1 h and Golgi (double arrows). In parallel assays, infected HFF were treated with 10 µM pyrimethamine (+pyr.) for 24 h prior to the addition of fluorescent ceramides for 2 h, showing negligible PV staining (arrows). Egressed parasites also displayed fluorescent staining in internal structures (4 h).

2.4.12. Similarly to *T. gondii*, Nc-Liv intercepts host Rab Golgi-derived vesicles to access their sphingolipid content

Ceramides converted into major sphingolipids in the Golgi are transported to various cell membranes via Golgi-derived Rab-associated vesicles (Lipsky and Pagano, 1985; Pagano *et al*, 1991). We previously showed that *Toxoplasma* (RH and Prugniand strains) diverts several host Golgi-derived vesicles to its PV (Romano *et al*, 2013). These vesicles contained Golgi-associated Rab vesicles, including Rab14, which mediates the trafficking between the TGN, endosomes and the plasma membrane, and delivers sphingomyelin to the plasma membrane (Junutula *et al*, 2004; Proikas-Cezanne *et al*, 2006; Kitt *et al*, 2008); Rab30, which is associated with many compartments of the Golgi complex and is involved in the maintenance of Golgi structure and vesicular trafficking (de Leeuw *et al*, 1998; Sinka *et al*, 2008; Thomas *et al*, 2009; Kelly *et al*, 2011); and Rab43, which is located in the *cis*-Golgi (Dejgaard *et al*, 2008). *T. gondii* scavenges sphingolipids from Rab30-, and Rab43-associated Golgi vesicles that accumulate within the PV. This process mirrors the uptake of host endocytic structures by *T. gondii*, which are also delivered intact into the PV lumen (Coppens *et al*, 2006).

The close association of the Nc-Liv PV with the host Golgi may also facilitate the scavenging of sphingolipids present in this organelle by the parasite. For this reason, we examined whether Nc-Liv intercepts the host Rab-mediated vesicular trafficking from the Golgi. We therefore followed the distribution of host Golgi-derived vesicles by focusing on those marked with Rab14, Rab30 or Rab43. HFF were transfected with each of the three GFP-Rab constructs, infected with Nc-Liv and observed by fluorescence microscopy (Fig. 2-14.A). In the infected, transfected fibroblasts, numerous GFP-Rab puncta were concentrated all round the PV. In large PV, the fluorescence signal was particularly intense around to the PV membrane.

Viewing individual optical z-slices demonstrated that GFP-Rab puncta were localized on top of the PV as well as inside the PV, as illustrated for Rab14 vesicles (Fig. 2-14.B). Quantification indicates that the GFP foci were perivacuolar in 77%, 79% and 48% of infected cells expressing GFP-Rab14, -Rab30 and -Rab43, respectively. Similarly, GFP foci were observed intraluminally in 29%, 21% and 2% of infected cells that express GFP-Rab14, -Rab30 and -Rab43, respectively.

To determine whether GFP-Rab14-associated vesicles located within the Nc-Liv PV contain sphingolipids, we monitored the uptake of BODIPY TR C5- ceramide in infected HFF expressing GFP-Rab14. We compared the respective localization of the GFP to BODIPY signal around and inside the PV by fluorescence microscopy and measured the level of co-localization using the Pearson Correlation Coefficient (PCC; Fig. 2-14.B and C). In uninfected cells incubated with BODIPY TR C5- ceramide from 20 to 40 min, the two fluorescent signals partially co-localized with a PCC of ~0.65 (Fig. 2-14.B). In infected cells, several GFP-Rab14 foci that co-localized with red fluorescent puncta were visible at the edge of and within the PV (Fig. 2-14.B). The level of co-localization was greater for GFP-Rab14 foci associated with the PV as the PCC averaged around 0.9 for the GFP and BODIPY TR signals within and on the PV, as compared to PCC of around 0.6 when calculated over the entire cell. These results suggest that the parasite is capable of hijacking selective Golgi-derived vesicles, and host ceramides are, at least partially, contained in these Rab14-associated vesicles.

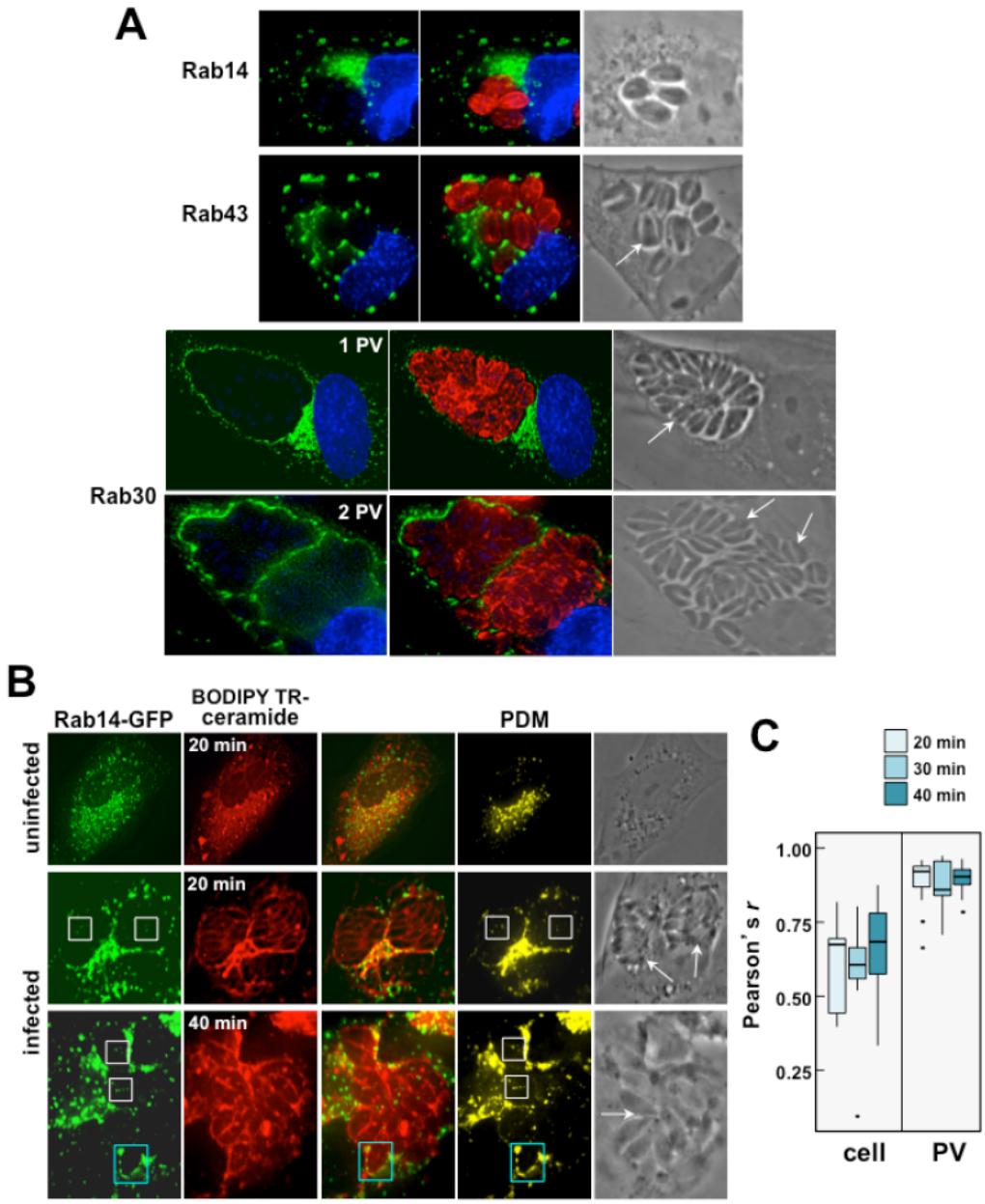

Figure 2-14. Interception of host Golgi-derived vesicles by Nc-Liv.

A. Fluorescence microscopy of Nc-Liv-infected HFF expressing GFP-Rab14, -Rab43 or -Rab30. HFF expressing the GFP-Rab constructs (green) were infected for 24 h or 30 h with Nc-Liv, fixed and stained with DAPI (blue, nucleus) and antibodies against NcPIS (red, parasite). The distribution of GFP-Rab-positive vesicles around individual PV, in mono- or multi-infected cells are shown in extended focus images. **B.** HFF expressing GFP-Rab14 (green), either uninfected or infected with Nc-Liv for 24 h, were incubated in the presence of BODIPY TR C5-ceramide (red) at the indicated times. An optical z-slice is shown for the merged, BODIPY TR C5-ceramide and GFP-Rab14 channels plus the positive PDM. The white and blue boxes contain Rab14-GFP vesicles inside the PV and along the PV membrane, respectively. **C.** Box plots showing the values of the PCC for co-localization of vesicles containing GFP-Rab14 and BODIPY TR C5-ceramide in either the entire cell or solely in the PV membrane and lumen at 20, 30 and 40 min of BODIPY TR C5-ceramide exposure.

2.5. DISCUSSION

This study demonstrates that *N. caninum* (Nc-Liv) re-routes host cell structures to its PV and salvages the nutrient content of organelles, e.g., lipids. Based on these results, we concluded that this parasite has evolved similar strategies as *T. gondii* (RH strain) for manipulating the host cell and exploiting mammalian resources, which emphasizes the remarkable conservation of these processes between the two pathogens. However, we identified small functional differences between Nc-Liv and *T. gondii* (RH), related to the growth rate and rearrangement of host organelles around the PV, which likely reflect divergent evolutionary paths.

As compared to *T. gondii* (RH), Nc-Liv grows slower in cultured cells regardless of their origin. These observations are in accordance with a recent analysis of the transcriptional activities of Nc-Liv that have revealed that after 6 days of adaptation in cultured cells, the parasite shows signs of conversion from the fast-growing tachyzoite to slower growing pre-bradyzoite-like forms, as reflected by a down-regulation of typical tachyzoite markers (SRS genes including *SAG1*) and an up-regulation of bradyzoite-specific mRNA (*BAG1*; Reid *et al*, 2012). During bradyzoite differentiation, *T. gondii* shuts down aerobic respiration in favor of glycolysis and gluconeogenesis, and accumulates amylopectin granules (Tomavo, 2001). Transcriptional profiles of Nc-Liv grown *in vitro* indicate a redirection of pyruvate from the TCA cycle into gluconeogenesis with down-regulation of transcription of pyruvate dehydrogenase and up-regulation of lactate dehydrogenase, pyruvate carboxylase and PEP-carboxylase kinase. Moreover, our EM observations on Nc-Liv illustrate the presence of amylopectin granules in the parasite's cytoplasm. Thus the slower growth rate of Nc-Liv as compared to that of *T. gondii* (RH) could be explained by the bradyzoite-like behavior of *Neospora* during *in vitro* culture.

Like *T. gondii* (RH), Nc-Liv attracts and retains host mitochondria to its PV. In *T. gondii* (RH), the tropism of host mitochondria to the PV is unknown but the retention of these organelles at the PV surface seems to largely be mediated by the parasite Mitochondria Association Factor 1 (TgMAF1; Pernas *et al*, 2014). Earlier studies have suggested that the TgROP2 protein may interact with host mitochondria as it is anchored to the PV membrane via hydrophobic and ionic interactions and contains a matrix mitochondrial targeting signal (Labesse *et al*, 2009; Sinai and Joiner, 2001). However, a *T. gondii* (RH) mutant strain that lacks TgMAF1 mostly lost its ability to recruit host mitochondria while *T. gondii* (RH) parasites deficient in TgROP2 expression did not, indicating that TgMAF1 is one of the prime factors for this function (Pernas and Boothroyd, 2010). The molecular mechanism underlying Nc-Liv PV association with host mitochondria remains to be elucidated. A MAF1 gene is present in the genome of *N. caninum* (accession # XP_003886010.1) and NcMAF1 shares 69% identity with TgMAF1. If NcMAF1 is secreted into the PV, it might be involved in the association of host mitochondria with the PV membrane of Nc-Liv, as TgMAF1 is for *T. gondii* (RH). This would substantiate our observations illustrating that the Nc-Liv PV display a more important coverage with host mitochondria than the PV of *T. gondii* (Pru), a parasite strain lacking TgMAF1 (Pernas *et al*, 2014). A ROP2 gene is also present in *N. caninum* and is expressed by the parasite (Alaeddine *et al*, 2013). NcROP2 shares 47% identity with TgROP2, and possesses features of ROP2 family proteins, including the R-rich amphipathic Helix (RAH) domain at the N-terminus that mediates the anchorage of ROP2 to the PV membrane. NcROP2, however, does not have the putative mitochondrial matrix targeting signal [SAFRRT] present in TgROP2, disputing its possible role in associating host mitochondria with the PV of Nc-Liv. The biological relevance of host mitochondria-PV is still unknown but MAF1 appears to play a role in modulating the host immune response as its deletion results in changes in serum cytokines, thus altering conditions

to be conducive to parasite dissemination in animals (Pernas *et al*, 2014). An additional possibility is that the recruitment of mitochondria may prove beneficial to the parasite by providing metabolites, e.g., lipids and lipoate, synthesized in these organelles (Crawford *et al*, 2006).

The PV of Nc-Liv is enveloped by host ER but does not physically interact with this organelle. In *T.* gondii (RH), host ER elements are closely apposed to the PV membrane (Sinai *et al*, 1997). The molecular machinery of this process is still unknown but two candidates have been proposed: ROP2, which contains an ER-targeting domain exposed to the host cytosol, and GRA3, which interacts with the host ER type II transmembrane protein calcium modulating ligand (CAMLG) (Sinai and Joiner, 2001; Kim *et al*, 2008). A GRA3 gene is present in the genome of *N. caninum*, although transcriptional profiles show a strong down-regulation of GRA3 in cultured *Neospora*. Attraction of the host ER to the PV may facilitate the delivery of ER-derived lipids or glucides to *N. caninum* and *T. gondii*. In fact, the growth of *Toxoplasma* is decreased in cells impaired in ceramide production in the ER (Romano *et al*, 2013; Pratt *et al*, 2013), suggesting an interdependence between parasite infectivity and host sphingolipid metabolism. Also, *T. gondii* synthesizes *N*-glycans from sugar precursors synthesized in the host ER, implying that it has access to ER molecules (Garénaux *et al*, 2008; Bushkin *et al*, 2010).

Nc-Liv has also the ability to cross-talk with the host microtubular cytoskeleton as its PV is encased by microtubules and is often seen close to the host MTOC to the same extent as observed for *T. gondii* (RH). The role of host microtubules recruited by either parasite needs to be clarified but it is known that host microtubules are important for *T. gondii* (RH) intracellular development. These cytoskeletal elements are exploited by *Toxoplasma* to facilitate its invasion into a host cell (Sweeney *et al*, 2010): it has been proposed that host microtubules selectively

concentrated on one side of the moving junction, may help stabilize the site of parasite invasion. After invasion, the PV is positioned at the center of the microtubular network in the host perinuclear region and remains surrounded by host microtubules throughout infection (Coppens *et al*, 2006; Walker *et al*, 2008). The parasite nucleates host microtubule growth via gamma-tubulin-associated sites, which suggests a physical interaction between the PV membrane and host microtubules. EM observations also show invaginations of the PV membrane mediated by host microtubules that serve as conduits to guide host organelles to the PV lumen.

During a *T. gondii* (RH) infection, host centrosome positioning at the PV requires the function of the host mammalian target of rapamycin complex 2 (mTORC2), which activates the Akt signaling pathway (Wang *et al*, 2010). In mTORC2-deficient cells infected with the parasite or cells treated with an Akt inhibitor, the host MTOC-PV association is abolished and the microtubules display an altered distribution. The Akt signaling pathway plays a pivotal role in growth factor regulation of microtubule stability, resulting in the phosphorylation of the glycogen synthase kinase 3b (GSK3b), which is a master regulator of the microtubule cytoskeleton. Moreover, inhibition of GSK3b restores the host centrosome-PV association in infected cells treated with an Akt inhibitor and in mTORC2 deficient cells. Inhibition of GSK3b in untreated cells increases the association of the host MTOC and the PV. It could be interesting to investigate if *N. caninum* also interferes with the host Akt signaling pathway to attract the MTOC or if it operates differently. Controlling MTOC functions may allow these parasites to modulate the host cell cycle by creating centrosomal defects and/or disorganizing mitosis. By stalling host cell division prior to cytokinesis, they may ensure a stable and spacious environment for replication as offered by a multinucleated cell. To this point, infection of quiescent cells with *T. gondii* induces an increase in D and E cyclins, thus promoting progression through G1 and transition into S-phase, respectively (Molestina *et al*, 2008). Therefore, in *Toxoplasma*-infected

cells, there is not only an induction of entry into S-phase triggered by the parasite but also an arrest in cell cycle progression in the S/G2 transition, based on host cyclin expression levels and accumulation in the infected cells. Additionally, usurping MTOC functions may also permit *N. caninum* and *T. gondii* to regulate the movement of host organelles and attract them to their vacuoles. Located at the intersection of the exocytic and endocytic pathways, the MTOC-Golgi region of the cell is rich in both endosomes and lysosomes. Therefore, the location of the PV in the peri-Golgi/MTOC region of the cell could facilitate the interception of host vesicular trafficking, which may help satisfy the pathogens' requirements for nutrients.

We previously documented that the attraction and sequestration of host endo-lysosomal organelles within the PV of *T. gondii* (RH) may facilitate the delivery of a diverse range of molecules supplied by the endocytic circuit to the parasite (Coppens *et al*, 2006). *T. gondii* (RH) also exploits the nutritive function of host autophagic compartments by diverting autophagosomes to its PV (Wang *et al*, 2009; Gao *et al*, 2014). Blocking host lysosomal or autolysosomal functions impairs the parasite's growth under nutrient-limiting conditions. Finally, MVB may represent a prodigious source of nutrients for *T. gondii* and *N. caninum* as reported for *C. trachomatis* that shows growth delay upon inhibition of host MVB biogenesis and disruption of lipid trafficking from MVB to the bacterium (Beatty, 2006; Beatty 2008).

Like *T. gondii* (RH), Nc-Liv is auxotrophic for cholesterol and stores this lipid in lipid bodies. To esterify cholesterol, *T. gondii* expresses two acyl-CoA:cholesterol acyltransferases (ACAT), TgACAT1 and TgACAT2 that share 56% identity with each other. Under condition of excess LDL, the parasite takes up cholesterol proportionally to the LDL concentration but controls the massive supply of cholesterol by increasing the activity of TgACAT1 and TgACAT2 to store excess cholesterol. Pharmacological blockade of cholesteryl ester synthesis with ACAT

inhibitors or genetic ablation of either *TgACAT1 or TgACAT2* is highly deleterious for the parasite growth (Nishikawa *et al*, 2005; Lige *et al*, 2013). The genome of *N. caninum* contains a single gene homologue to an ACAT enzyme. NcACAT shares 71% identity with TgACAT1 and possesses the canonical cholesterol-binding site [HSY], suggesting that *Neospora* has the capacity to synthesize cholesteryl esters for storage in lipid bodies.

The Nc-Liv growth depends on host endocytic structures for cholesterol supply from LDL. We cannot exclude that other sources of cholesterol may be exploited by *N. caninum* as is the case for other Apicomplexa. For example, *Plasmodium berghei* retrieves cholesterol from the *de novo* synthetic pathway (Labaied *et al*, 2011) and *Cryptosporidium parvum* salvages cholesterol originating from micelles (Ehrenman *et al*, 2013). How *N. caninum* accesses host cholesterol from lysosomes and internalizes this lipid remains to be elucidated. *T. gondii* expresses a lipid-translocating importer of the ATP-binding cassette (ABC) transporter G subfamily (ABCG family) at the plasma membrane and in the PV, and this translocator delivers cholesterol to the parasite's interior (Ehrenman *et al*, 2010). A homologue for this *Toxoplasma* ABCG is present in the *N. caninum* genome (76% identity; XP_003881240.1).

Like *T. gondii*, Nc-Liv scavenges exogenously derived ceramides from the host Golgi that is re-organized around the PV. The proximity of the PV of *T. gondii* (RH, Prugniaud) and Nc-Liv to host Golgi elements may facilitate the retrieval of nutrients, e.g., sphingolipids that are manufactured in this organelle. *Toxoplasma* is capable of *de novo* sphingolipid synthesis (Azzouz *et al*, 2002; Sonda *et al*, 2005; Bisanz *et al*, 2006), but it relies on the salvage of host sphingolipids from many sources. Indeed, exogenously added ceramides processed in the Golgi enhance parasite replication whereas blockade of host ceramide production leads to parasite growth impairment (Romano *et al*, 2013). The recruitment of the host Golgi and its size

reduction in Nc-Liv- or *T. gondii* (RH)-infected cells may facilitate the interception of host Golgi-derived vesicles by the parasites. Such a scenario has been described for *C. trachomatis*, which scavenges host Golgi-derived lipids (Hackstadt *et al*, 1995; Hackstadt *et al*, 1996). The bacterium fragments the host Golgi by co-opting the Golgi-specific brefeldin A resistance guanine nucleotide exchange factor 1 (GBF1; Elwell *et al*, 2011), which is required for the assembly of the Golgi stacks and for vesicle-mediated sphingolipid acquisition by the bacterium. *C. trachomatis* also cleaves golgins, which are important for the structural organization of Golgi, leading to the fragmentation of the Golgi (Heuer *et al*, 2009). Interfering with Golgi fragmentation in *C. trachomatis*-infected cells impairs bacteria growth. The mechanism leading to the dismantling of the host Golgi during *Toxoplasma* infection is still unknown but it does not involve the proteolytic cleavage of the Golgi matrix proteins, golgin160 and golgin97 (Romano *et al*, 2013). Finally, the interception of host Golgi Rab vesicles by Nc-Liv followed by the sequestration of these vesicles in the PV to access to their sphingolipid content is also a process shared with *T. gondii*. Many proteins secreted by these parasites are embedded in the PV membrane, and localize thus at the interface between the PV and mammalian cell structures. Identification of specific parasite effectors that interact with host Rab proteins to mediate the docking of Rab vesicles onto the PV membrane would reveal unique molecular players and open new therapeutic approaches to fight against these pathogens.

CHAPTER 3

LIPID DROPLET DYNAMICS IN *TOXOPLASMA GONDII*-INFECTED CELLS AND LIPID SOURCES FOR THE PARASITE

3.1. ABSTRACT

The protozoan *Toxoplasma gondii* is an obligate intracellular parasite, which resides in a parasitophorous vacuole (PV) derived from the plasma membrane of its host cell during invasion. The PV is refractory to fusion with host cell organelles but associates with various host organelles, structures and vesicles to facilitate access to their nutrient content. Previous studies report that *Toxoplasma* can scavenge many lipid species such as cholesterol, sphingolipids, ceramides, phospholipids and fatty acids from its host cell, but the salvaging of neutral lipids such as triacylglycerols and cholesteryl esters has never been studied. Both of these non-polar lipids are found predominantly in cytoplasmic lipid droplets (LD), which are highly evolutionarily conserved structures among organisms ranging from bacteria to humans, whose functions include lipid and energy storage, and prevention of lipotoxicity. Here, we show that *Toxoplasma* attracts host LD to its PV and infection leads to an initial increase, then decrease in LD numbers in the host cell, suggestive of a manipulation of these structures by the parasite. We document that *Toxoplasma* scavenges neutral lipids likely from host LD, in part through the translocation of intact host LD into its PV, and potentially through the interception of Rab7 and Rab18 positive vesicles, proteins known to be anchored on the LD surface. In response to exposure of host cells to excess oleic acid, a monounsaturated fatty acid, *Toxoplasma* accumulates many large LD in its cytosol and increases the transcription of its own enzymes storing neutral lipids. Interestingly, ultrastructural analysis of *Toxoplasma* incubated with excess oleic acid reveals, for the first time, the presence of coated endocytic pits at the parasite plasma membrane. These structures may represent gates of entry by which the material in the PV lumen could be internalized into the parasite.

3.2. BACKGROUND

In this chapter, I describe my investigations into the potential contribution of host neutral lipids (NL) stored in host cell cytoplasmic lipid droplets (LD) to the development of *Toxoplasma* in cultured cells. There is emerging evidence that many intracellular pathogens, including viruses, bacteria and parasites, exploit host LD during infection for replication, nutritional purposes or manipulate these structures as part of an anti-immunity strategy. This section contains general information on LD formation, content and functions in mammalian cells, and on host LD usurpation by pathogens. It also includes current knowledge on lipid metabolism in *Toxoplasma*, with special focus on NL synthesis and storage.

3.2.1. History of lipid droplets

Until recently, lipid droplets (LD) were regarded as little more than inert lipid repositories within cells. They were first described in the late 19th century by Richard Altmann and E.B. Wilson using light microscopy although the first observation of LD or "fat globules in milk" was by van Leeuwenhoek in 1674 using his home-made microscope (Kernohan and Lepherd, 1969). Their high diffraction characteristics made them easily identifiable by microscopy and by the early 20th century, they were coined liposomes (Farese and Walther, 2009). In the 1960s however, the term liposome switched to signify artificial liposomes and since then, LD have been called many different terms including lipid bodies, adiposomes, oil bodies, fat bodies and lipid droplets. These structures remained in the dark and unstudied for many decades until 1991 when the LD-specific protein, Perilipin, was discovered in the laboratory of Constantine Londos (Greenberg *et al*, 1991), which ignited the spark for LD research. The term "lipid droplet" has gained increased acceptance over the past decade and is now the preferred nomenclature for mammalian cells.

From 1991 onwards, the publication rate for LD studies has sharply risen, potentially due to increased awareness of fat-related diseases (e.g., obesity, atherosclerosis), to research into oil production, and to increased number of fields where LD play a role, as well as scientists' innate curiosity to tap into this undiscovered realm (Farese and Walther, 2009).

LD are ubiquitous and evolutionary conserved structures found in virtually all cell types and organisms, ranging from bacteria, to plants and vertebrates. Their primary function is the storage of lipid metabolic energy in the form of neutral (non-polar) lipids. This was thought to serve two purposes: serve as a reservoir of fatty acids (FA) for energy production via β-oxidation of FA and a safe sink of excess FA to prevent lipotoxicity. As amphipathic molecules, FAs can severely affect membrane integrity but are inert and stable when associated with other lipids (Farese and Walther, 2009). The evolutionary conservation of LD throughout the tree of life could be a result of the selective advantage of having energy storage capabilities since resources are rarely constant and continuously fluctuating in the environment.

In the past two decades, significant progress in the LD field has uncovered many aspects relating to the function, maintenance, biogenesis and composition of these unique structures, thereby challenging the traditional viewpoint of simply being lipid depositories. They are now viewed as dynamic structures heavily involved in lipid homeostasis, lipid metabolism, immunity, autophagy and signaling. Despite the multitude of versatile roles recently uncovered, many aspects of LD biology remain unknown but future discoveries will no doubt reveal exciting new functions for this fascinating structure.

3.2.2. Mammalian LD structure and protein composition

In contrast to organelles which are characterized by lipid bilayer membranes, LD have a unique feature in that they have a hydrophobic core consisting predominantly of NL (e.g., triacylglycerol

(TAG) and steryl esters (SE)), which is surrounded by a single layer of amphipathic lipids (essentially a phospholipid monolayer) in which proteins are embedded. In mammalian cells and yeast, the main phospholipids in this monolayer are phosphatidylcholine (PC) (50-60%), phosphatidylethanolamine (PE) (20-30%) and phosphatidylinositol (PI), which are synthesized in the endoplasmic reticulum (ER) (Tauchi-Sato *et al*, 2002).

LD size and TAG to SE ratio are variable in different cell types. The size of mammalian LD range depending on the cell type from as small as 0.5 micron in most cells to 300 microns in white adipocytes, cells specialized in the storage of fat, which have a single, enormous LD. In yeast, LD size ranges from 0.3 to 1.5 micron, whereas in prokaryotes, the range extends from 0.15 to 0.5 micron (Athenstaedt and Daum, 2006). LD sizes are not uniform either within a single cell. Moreover, the ratio of TAG and SE in the core of the LD depends on the cell type. For example, in adipocytes there is more TAG than SE. Conversely, in steroid-synthesizing cells, there tends to be a higher ratio of SE to TAG.

A large number of proteins decorate the LD surface, usually involving amphipathic alpha helices for insertion into the outer lipid layer. In mammals, there are five main LD proteins, collectively belonging to the PAT family – now renamed the Perilipins (PLINs) (Fig. 3-1). These proteins comprise Perilipin/PLIN1, Adipose Differentiation-Related Protein/PLIN2 (ADRP), Tail-Interacting Protein of 47 kiloDaltons/PLIN3 (TIP47), OXPAT/PLIN5 and S3-12/PLIN4 (Bickel *et al*, 2010).

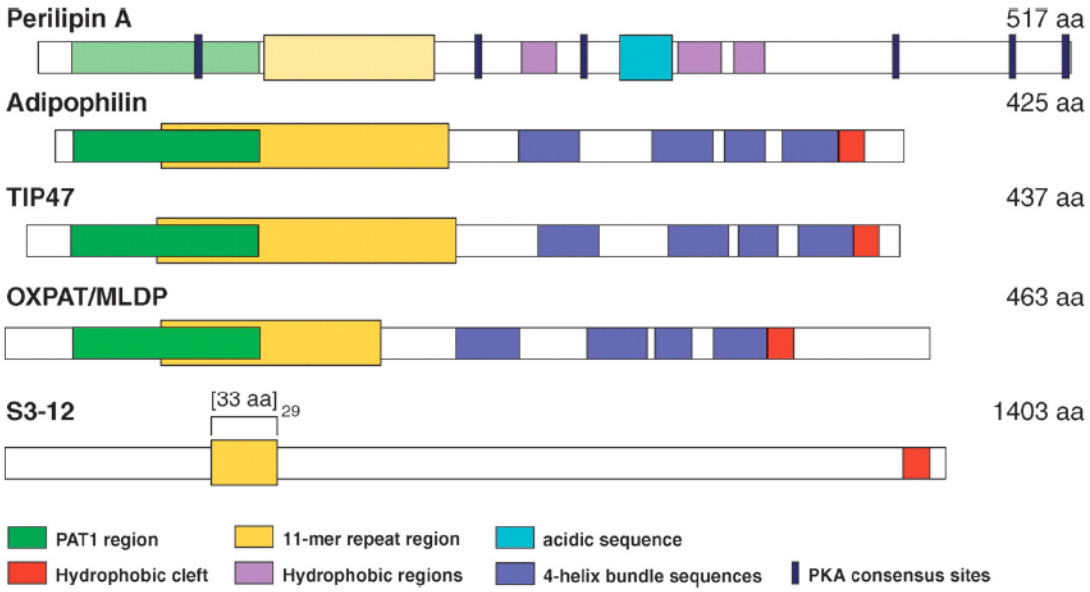

Figure 3-1. Structural representation of the mouse five PAT family members sequences.

Perilipin isoform A, ADRP/Adipophilin, TIP47, OXPAT and S3-12. Common structural characteristics between these proteins are represented by similar colors where more intense color represents higher sequence similarity. In green are the 100 amino acid (aa) N-terminal regions that are shared by all but S3-12 which are overlapped by stretches of 11-mer repeat regions believed to fold into amphipathic helices (yellow). The ADRP/Adipophilin, TIP47 and OXPAT sequences then have 4 stretches predicted to fold into a 4-helix bundle of amphipatic alpha helices (blue). In contrast, perilipin A only has 3 such stretches that are mildly hydrophobic along with a highly acid stretch (cyan). The C-terminal regions of all proteins except for perilipin A are highly conserved (red). Peripilin A, whose activity is regulated by phosphorylation by protein kinase A, displays 6 potential phosphorylation sites (gray). Image from Brasaemle, 2007.

All of these proteins are capable of binding LD, either constitutively or upon induction with various stimuli. ADRP and perilipin usually bind LD constitutively whereas the three others tend to bind LD transiently (Wolins *et al*, 2006). The protein composition of the LD surface is heterogeneous and differs between cells or individual LD within a cell, depending on metabolic circumstances. The ratio of one PLIN protein to another differs depending on the size of LD, PLIN protein affinity for LD binding, PLIN tissue-specific expression, and PLIN protein stability (Bickel *et al*, 2010). Perilipin, OXPAT and S3-12 are only found on LD in specific tissues such as adipose tissue, whereas ADRP and TIP47 are ubiquitous. Here, perilipin and ADRP will be discussed as they are the two most commonly studied PLIN family proteins, with increased emphasis on ADRP due to its ubiquitous LD localization in non-adipocytes.

3.2.2.1. Perilipin

Perilipin (PLIN1), the first LD-related protein discovered, was shown to regulate lipid storage by modulating lipase access to the LD core (Greenberg *et al*, 1991; Bickel *et al*, 2010). There are 3 isoforms (A, B and C), which have different C-termini. Perilipin A is mainly found in adipocytes and is regulated by the Peroxisome Proliferator-Activated Receptor gamma (PPARγ) and the Estrogen-Related Receptor alpha, as well as by phosphorylation via the activity of Protein Kinase A (PKA) (Fig. 3-1, top, perilipin A) (Egan *et al*, 1990). Phosphorylation of perilipin A by PKA allows the lipolytic enzymes, Adipose Triglyceride Lipase (ATGL) and the Hormone Sensitive Lipase (HSL), access to the NL core of LD, leading to the lipolysis of the NL (Bickel *et al*, 2010). Studies in perilipin-KO mice revealed that mice are of normal weight and eat normally, but are resistant to diet-induced obesity (Tansey *et al*, 2001). These mice also have smaller LD as a result of increased basal lipolytic activities due to ATGL and HSL access to the LD core.

3.2.2.2. ADRP/Adipophilin

ADRP (PLIN2) is also a constitutively bound protein of LD and highly expressed in fibroblasts and hepatocytes. In contrast to perilipin, ADRP expression diminishes as the adipocyte matures. Both perilipin and ADRP are degraded via the ubiquitin/proteasome pathway when not associated with LD (Gross *et al*, 2006). Like perilipin, the PPAR nuclear hormone receptor family also regulates ADRP expression. In mice lacking perilipin, ADRP partially compensates for perilipin loss (Tansey *et al*, 2001). In non-adipocytes, ADRP also limits access of lipases such as ATGL to the LD core although the precise mechanism has not been elucidated (Listenberger *et al*, 2007).

Upon ADRP overexpression in fibroblasts, there is a stimulation of LD production, affiliated with an increase in TAG levels. This is a result of decreased TAG hydrolysis since there is decreased ATGL localization to LD (Inamura *et al*, 2002; Listenberger *et al*, 2007). Additionally, overexpression of ADRP leads to decreased association of other PAT proteins with the LD, including TIP47. This is likely due to a predominant overcrowding of ADRP at the LD periphery.

Silencing ADRP leads to a decrease in LD numbers and increased fatty acid β-oxidation in hepatocytes (Magnusson *et al*, 2006). Similarly as in *in vitro* experiments, studies using mice lacking ADRP showed that hepatocytes have decreased numbers of LD and an overaccumulation of TAG in the membrane of the ER, the site of LD formation (Chang *et al*, 2006). This implies a role for ADRP in the initial formation of LD at the ER. It is still unknown how ADRP aids in this process.

In cells incubated with excess FA such as oleic acid (OA), NL stores increase, as does ADRP expression which covers the surface of the newly formed LD (Bickel *et al*, 2010). Additionally, ADRP expression correlates with TAG concentrations in the cell.

3.2.2.3. Other proteins on the LD surface

Recent proteomic studies have revealed several hundred different proteins on the LD surface. In addition to lipid synthetic enzymes (discussed in the next section), membrane trafficking proteins such as Rab GTPases, SNAREs, and Arfs and their coatomers were identified. Signaling proteins such as RalA, Rabp1B and protein kinases as well as molecules involved in protein degradation such as AUP1 and UBXD were also found (Yang *et al*, 2012). Surprisingly, histones are also detected on the LD of *Drosophila* embryos (Li *et al*, 2012).

3.2.3. LD formation and expansion

It is widely believed that the initial formation of LD occurs between the leaflets of the phospholipid bilayer of the ER, however, the precise mechanism of LD biogenesis is not fully understood (Fig. 3-2). In this model, non-polar lipids accumulate within the ER bilayer and upon reaching a certain threshold, are then organized into a fat lens which bulges out into the cytosol. This model also implies the close coordination between TAG/SE synthesis and LD budding from the ER membrane.

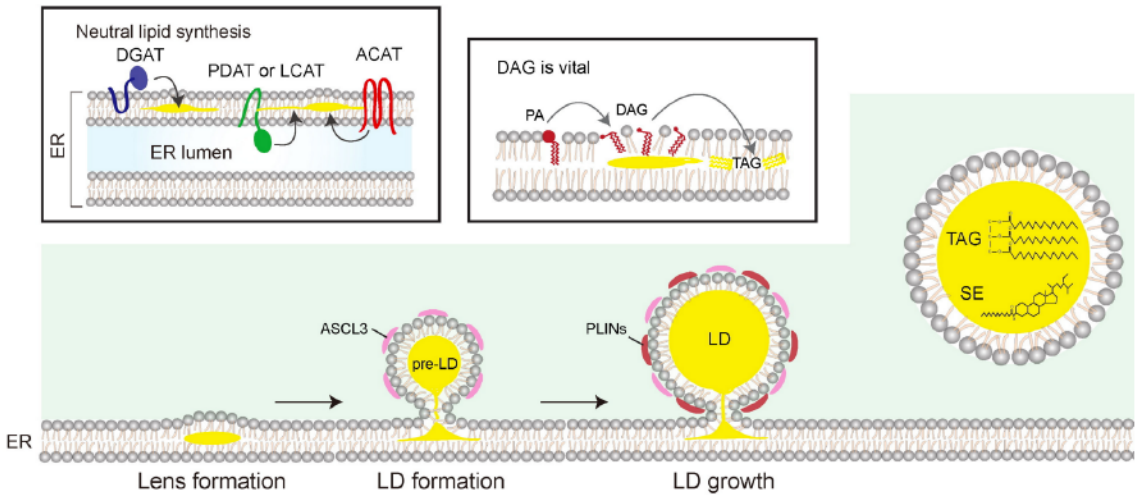

Figure 3-2. Lipid droplet biogenesis at the endoplasmic reticulum.

Neutral lipid synthesis enzymes, such as DGAT or ACAT catalyze TAG or SE synthesis. These neutral lipids accumulate between the leaflets of the ER phospholipid bilayer, reach a threshold concentration and form a fat lens. The pre-LD then bulges out of the ER on the cytosolic face which leads to the formation of a mature LD. The pre-LD bulge requires specific membrane curvature that is generated by DAG which was generated from phosphatidic acid (PA) by Phosphatidate Phosphatase (PAP). Avoidance of phase coalescence is achieved by ensuring PC is incorporated into the LD outer membrane layer and LD-related proteins such as ADRP or other PLINs are bound to the nascent LD. Image adapted from Wang CW, 2015.

3.2.3.1. LD expansion in size

LD enlargement can occur by three independent processes: 1) local synthesis of NL inside the LD; 2) lipid delivery to the LD from organelles; and 3) LD coalescence. Firstly, TAG synthetic enzymes such as Acyl-CoA:diacylglycerol Acyltransferase 2 (DGAT2) are found on LD in non-adipocytes, enabling the in situ production of TAG and LD enlargement (Wilfling *et al*, 2013). Secondly, ER-bound proteins such as FIT1/2 and seipin/BSCL2 can regulate the transfer of TAG from the ER to LD situated in close proximity to this organelle (Szymanski *et al*, 2007). In a similar manner, ADRP and the small GTPase Rab18 may help transport TAG between the ER and LD by regulating ER-LD contact (Ozeki *et al*, 2005). Thirdly, LD-LD fusion can occur. The outer layer of LD are composed of phospholipids that can lead to phase coalescence, reminiscent of SNARE-mediated hemifusion. Fusion requires firstly the close apposition of two LD followed by pore formation connecting the two oil phases and linking the LD (Thiam *et al*, 2013). If the membrane curvature is either positive or negative, the pore will stabilize and expand leading to coalescence. If not, the pore will close due to the energy barrier imposed by curvature mismatch. The phospholipid PC helps prevent phase coalescence as LD devoid of PC are prone to fuse together and are enlarged (Krahmer *et al*, 2011). Membranes rich in cholesterol, DAG or PE will favor coalescence due to their small head groups and negative membrane curvature (Thiam *et al*, 2013).

3.2.4. Neutral lipid biosynthesis in mammalian cells

As NL, TAG and SE do not contain a charged group and therefore by default cannot easily integrate into bilayer membranes. These NL are formed via two elaborated biosynthetic pathways that are relatively well conserved across organisms. Since lipids are essential for all life

forms, this evolutionary conservation further highlights the importance of lipid storage across the tree of life.

As previously discussed, LD arise from the ER where the final step is catalyzed by DGAT1 and DGAT2 which convert diacylglycerol (DAG) and FA into TAG following acyl-CoA activation (Fig. 3-3.A). These enzymes are localized at the ER membrane, which leads to TAG accumulation in between the two ER bilayer membrane leaflets (Athenstaedt and Daum, 2006). Upon reaching a threshold TAG concentration within the ER bilayer, the nascent LD detaches itself from the ER, or may remain connected via a narrow bridge for potential lipid transport between the LD and the ER (Welte, 2015). DGAT2 is only found on the cytoplasmic leaflet side of the ER and diffuses readily onto the nascent LD, eventually residing on the LD itself (Athenstaedt and Daum, 2006). This is relevant as the localization of DGAT2 on LD supports TAG synthesis and continuous LD growth in volume. Despite the DGAT1 and DGAT2 enzymes catalyzing the same reaction, their activities are not completely redundant. While DGAT1 is involved in the recycling of hydrolyzed TAGs by FA esterification and is more active when FA are abundant or lipolysis activity is high, DGAT2 is involved in TAG synthesis when FA levels are lower (Yen *et al*, 2008).

In mammalian cells, the final step of cholesteryl ester (CE) biosynthesis is catalyzed by the Acyl-CoA:Cholesterol Acyltransferases (ACAT), another ER-residing enzyme that esterifies cholesterol (Goodman *et al*, 1964). Mammalian cells possess two ACAT enzymes (ACAT1 and ACAT2); expression of ACAT2 is strictly limited to the liver and small intestines and is involved in CE production destined for plasma lipoproteins secreted by these cells whereas ACAT1 is ubiquitous and responsible for CE synthesis for storage in cytoplasmic LD (Chang *et al*, 2001; Buhman *et al*, 2000).

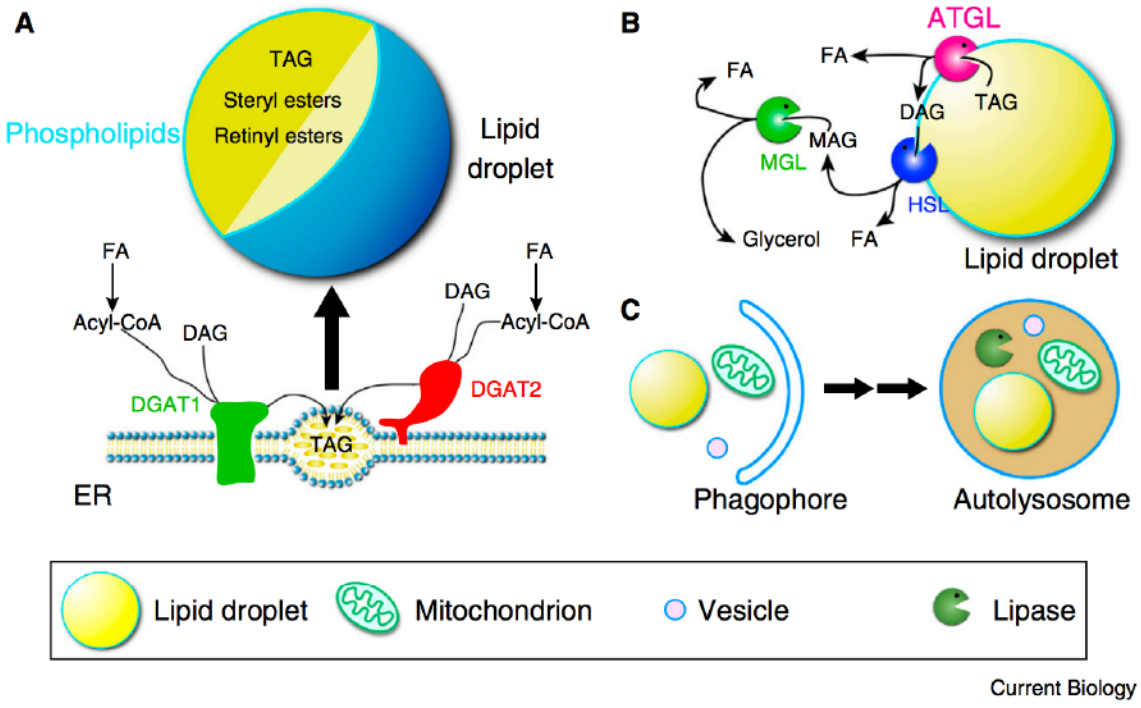

Figure 3-3. *De novo* biogenesis and degradation mechanisms of lipid droplets.

A. LD have a phospholipid monolayer and a hydrophobic core comprising of TAG and SE. These neutral lipids accumulate in between the leaflets of the ER membrane as shown for TAG generated from DAG and FA by DGAT1 and DGAT2, which leads to the formation of nascent LD.

B. LD catabolism is induced by cytosolic lipases. ATGL is bound to LD and hydrolyzes TAG into DAG and FA. DAG is further broken down by HSL, leading to MAG which are then catabolizes by MGL into FA and glycerol as products.

C. Lipophagy. Following phagophore formation and autophagosome engulfment of LD, the autophagosome fuses with lysosomes that contain LAL which break down LD.

Image from Welte, 2015.

Cholesterol is stored as a non-toxic, esterified form and is used for membrane synthesis or hormone production after de-esterification by a cholesterol esterase. Cholesterol is an essential lipid for all eukaryotic organisms since it controls the fluidity and permeability of membranes, in particular phospholipid bilayers. After CE accumulation inside the ER bilayer membranes, the LD bud off. In contrast to DGAT2, the ACAT enzymes remain in the ER and do not localize to mature LD in the cytosol (Athenstaedt and Daum, 2006).

3.2.4.1. LD breakdown

There exist two different processes by which LD may be degraded for FA generation: lipolysis and lipophagy. The first way involves TAG lipases that reside in the cytosol and can bind LD in order to hydrolyze TAG into DAG and FA. In most cells including adipocytes, ATGL is responsible for the majority of TAG conversion to DAG, and when needed, conveniently locates to the LD (Fig. 3-3.B). Perilipin has been shown to act in conjunction with ATGL in adipocytes to allow the enzyme access to the NL core of the LD (Bickel *et al*, 2010). Other lipases such as HSL can hydrolyze DAG into monoacylglycerol (MAG) and FA, then a monoglyceride lipase (MGL) hydrolyzes MAG to glycerol and FA (Athenstaedt and Daum, 2006). The second way by which LD can be catalyzed is via selective autophagy, a process known as lipophagy. Double-membrane phagophores engulf LD and become autophagosomes upon closure. LD-containing autophagosomes then fuse with lysosomes to become autolysosomes where the degradation of LD occurs by hydrolytic enzymes, the main one being the Lysosomal Acid Lipase (LAL) (Fig. 3-3.C). Lipophagy is stimulated upon excess levels of OA in cells (Singh *et al*, 2009). Under these conditions, it has been proposed that LD can also be sources of lipids for initial phagophore and autophagosome formation (Dupont *et al*, 2014). Interestingly, the small GTPase Rab7 has recently been implicated as a principal regulator of lipophagy. In hepatocytes under starvation,

Rab7 becomes highly expressed and activated (Schroeder *et al*, 2015). The Rab7 GTPase is also known to regulate traffic from late endosomes to lysosomes and multivesicular bodies, and promotes early to late endosome maturation, and endosome-to-lysosome transport.

3.2.5. LD homeostasis in mammalian cells

The most widely recognized function of lipid droplets (LD) is the storage of NL in its hydrophobic core. These lipids can then be used, following various metabolic signals, for functions ranging from energy production, membrane biogenesis to support cellular growth, post-acylation of proteins, and signaling, e.g. upon DAG release.

During periods of limited resources or starvation, LD can undergo lipolysis by ATGL activation or consumption by macroautophagy in order to release FA for β-oxidation in mitochondria or peroxisomes (Khor *et al*, 2013; Smirnova *et al*, 2006). Released FA can be used to build membranes for autophagosome formation and signaling lipids such as DAG can be incorporated into PE and PC via the Kennedy pathway (Athenstaedt and Daum, 2006).

Additionally, LD are indispensable for maintaining lipid homeostasis. Free FA can be harmful to the cell as they can interfere with membrane integrity. Indeed it has been shown that defects in the machineries implicated in LD generation or degradation lead to grave physiological defects at the organismal level (Greenberg *et al*, 2011). Protection from lipotoxicity is crucial to control a variety of diseases such as atherosclerosis, type 2 diabetes, cardiomyopathy, fatty liver disease and obesity (Walther and Farese, 2012). Indeed, if excess cholesterol is not stored in LD properly, it can cause ER stress and eventually apoptosis or necrosis in macrophages (Maxfield and Tabas, 2005).

3.2.6. Non-canonical roles of LD

Other LD functions recently uncovered include providing a platform for viral replication and assembly, immunity modulation, lipid transport, intracellular trafficking, chaperone functions, RNA metabolism, cytoskeletal organization, nuclear transcription and histone modulation, and potentially a role in prevention of neurodegeneration (Bickel *et al*, 2010; Welte, 2015).

3.2.6.1. LD in the nucleus

Regarding the involvement of LD in transcriptional activities, two groups have documented the presence of LD inside the nucleus (Uzbekov and Roingeard, 2013; Layerenza *et al*, 2013). In the nucleus, LD have been shown to regulate nuclear transcription by sequestering transcription factors (Ueno *et al*, 2013), regulating the accessibility of proteins and lipids for signaling, as well as sequestering histones to avoid degradation. The LD found in the nucleus are formed independently of cytoplasmic LD and harbor DGAT2, so presumably grow from incorporation of lipids synthesized in the nucleus (Ohsaki *et al*, 2016). In *Drosophila* embryos, this process enables certain histones to be stockpiled early and be available *en masse* for chromatin assembly later during development (Li *et al*, 2012).

3.2.6.2. Roles in protein storage and degradation

It has recently been proposed that LD may serve as a temporary sink for hydrophobic proteins that need to be degraded. In excessive amounts, these proteins could aggregate, leading to inefficient degradation by proteasomes and eventually leading to impaired cellular function and cell death. However, retention of these hydrophobic proteins on LD could prevent the formation of toxic aggregates and aid in proteasome degradation. This has been proposed for

ubiquitinated apolipoprotein B-100 (apoB) in hepatocytes Fujimoto and Ohsaki, 2006), as well as alpha-synuclein, a protein known to aggregate in Parkinson's disease (Cole *et al*, 2002). Indeed, proteosomal subunits have been found on LD, and the LD has been shown to be a crossroads for the autophagy and proteosomal pathways (Fujimoto and Ohsaki, 2006).

3.2.6.3. Immunity

LD can also act as modulators of immunity. The eicosanoid family includes prostaglandins, prostacyclins, leukotrienes and thromboxanes. These are potent and tightly regulated signaling molecules involved in inflammation, immunity and tissue homeostasis in response to cytokines, allergens, growth factors and pathogen peptides (Wyman and Schneiter, 2008). Arachidonic acid (AA) is the main substrate for eicosanoid biosynthesis and is stored in an esterified form in LD (Wang and Dubois, 2010). Upon proper stimuli, such as activation by members of the mitogen-activated protein kinase family (MAP kinases), cytosolic Phospholipase 2 ($cPLA_2$) (Perez-Chacón *et al*, 2009) on the LD surface can mediate AA release from LD for subsequent metabolization into eicosanoids. One common eicosanoid is prostaglandin E2, which is involved in a variety of processes including tumor formation, response to pathogens, inflammation induction, cellular growth and fever (Furuyashiki and Narumiya, 2011). It exerts its activity via the cyclooxygenase, cytochrome P450 monooxygenase or lipoxygenase pathways.

Type I and type II interferons (IFNs) are immune modulators involved in regulating responses to intracellular pathogens. IFNs can induce the expression and activity of hundreds of different IFN-induced genes and proteins (Katze *et al*, 2002). Viperin located on the surface of LD (Saka and Valdivia, 2012), is an IFN-induced protein that plays important roles in anti-viral responses (Hepatitis C Virus, Influenza, Cytomegalovirus, Dengue, Human Immunodeficiency virus) and is upregulated in the presence of lipopolysaccharides. Considering that several viruses

have evolved to use LD as a platform to replicate, it seems likely that cellular immune responses would also involve LD to hinder viral maturation.

Immunity-related GTPases (IRGs) are proteins induced by IFNs in mammalian cells to combat intracellular pathogens. In mice, unlike in humans, these proteins, in particular Irgm3, are indispensable for resistance to various intracellular pathogens including *Toxoplasma gondii*, *Leishmania major* and *Chlamydia trachomatis* (Hunn *et al*, 2011). Upon IFN stimulation, Irgm3 relocalizes from the ER to the LD surface in dendritic cells. In these cells, LD are also involved in the cross presentation of phagocytosed microbial peptides onto MHC class I (Bougneres *et al*, 2010).

3.2.7. LD interactions with cellular organelles

Organelle-organelle interactions are indispensable for the exchange of material or transmission of signals that sustain and balance cellular processes such as metabolism, signaling, cellular maintenance, regulation of programmed cell death and intracellular microbial defense (Schrader *et al*, 2015). These interactions may occur via 3 mechanisms: 1) vesicular transport; 2) metabolite exchange by diffusion; and 3) physical contact via specific membrane contact sites, such as Mitochondria Associated Membranes (MAMs) for ER-mitochondria interactions.

Firstly, some LD-organelle interactions appear to be regulated by specific Rab GTPases (Liu *et al*, 2007; Murphy *et al*, 2009). Varying proportions of Rab proteins are detected on LD, depending on their location in the cytosol. Rab18 association with LD for example is observed on 50% of LD, especially those close to the ER (Ozeki *et al*, 2005). Transport of lipids, in particular, cholesterol, occurs via endosome association to LD for delivery to the lysosomes (Martin and Parton, 2005; Ouimet *et al*, 2011). Fusion between LD or LD and mitochondria has been shown and involves SNARE-mediated homotypic fusion (Goodman, 2008; Olofsson *et al*, 2009).

Secondly, the ER, mitochondria, peroxisomes and endosomes have been shown to associate with LD where metabolite exchange may occur by diffusion (Fujimoto *et al*, 2008; Goodman, 2008; Murphy *et al*, 2009), although this process has not been fully elucidated.

Thirdly, lipid exchange that occurs between the LD and organelles is thought to be mediated by direct physical contact, a mechanism under intense study (Szymanski *et al*, 2007). LD-associated membrane contacts sites, or LAMs, are under investigation but these sites, especially LD-mitochondria LAMs, may be important for the transfer of FA for β-oxidation. Lipid transfer can be bidirectional too since mitochondria or peroxisomes can also provide lipids to LD for membrane replacement or lipid storage (Shaw *et al*, 2008; Binns *et al*, 2006). In the context of immunity, transient association between LD and phagosomes in immune cells such as neutrophils and dendritic cells is seen and appears to play a role in efficient MHC I cross presentation of antigens (Bougneres *et al*, 2010).

Motility of LD is critical in light of the plethora of their roles, such as organelle association or spatial distribution in the cell. They achieve this by using actin for random short-distance motility, and microtubules for long distances (Welte, 2009).

3.2.8. Importance of host lipid droplets upon intracellular infections

3.2.8.1. Viruses

Many viruses including Influenza, Vaccinia virus, Epstein-Barr virus, Ebola virus, HIV, Hepatitis C virus (HCV), Measles and Dengue virus depend on lipids, e.g., cholesterol from the host cell for replication, and some, such as the flaviviridae, exploit LD as a lipid source for viral assembly.

Lipophagy is induced upon Dengue virus infection to boost viral replication. Following the breakdown of LD, FA are liberated from TAG in LD and used for β-oxidation, leading to an

increase in ATP levels beneficial for viral growth (Heaton and Randall, 2010). Inhibition of autophagy decreases viral replication while exogenous addition of free FA restores replication.

A nucleocapsid core protein found in HCV can bind to DGAT1 at the ER where the virus begins its initial assembly. As the LD matures and buds from the ER membrane, the outer layer of the LD contains many core HCV proteins, which can then be released to surround and protect the viral RNA (Moriishi and Matsuura, 2012).

3.2.8.2. Bacteria

Intracellular bacteria can stimulate host LD formation, as in the case of *Mycobacterium* in foamy macrophages and *Chlamydia* sp. in epithelial cells. Macrophages undergo a respiratory burst upon infection with mycobacteria, leading to the generation and release of reactive oxygen species (ROS). ROS can cause the oxidation of FA e.g. from LDL or phospholipids, which eventually leads to the foamy macrophage phenotype. Foamy macrophages have many LD and eventually release lipids and bacteria into their surroundings (Kim *et al*, 2010).

It is thought that foamy macrophages help supply nutrients to the *M. tuberculosis* bacterium during latency in the lung (Palanisamy *et al*, 2012; Neyrolles, 2014). Indeed, macrophages infected with *M. tuberculosis* show a large accumulation of LD, followed by large LD accumulation in the bacterium. This is hypothesized to occur during stress conditions and is a signal for *M. tuberculosis* to induce a dormancy state (Kim *et al*, 2010). The mycobacterial LD accumulation likely results from the uptake of host derived FA and potentially host-derived TAG. *M. tuberculosis* primarily uses TAG as its source of energy and encodes its own TAG synthase enzyme, Tgs1 (triacylglycerol synthase 1) as well as a lipase homologous to mammalian HSL, LipY (Sirakova *et al*, 2006). The presence of these two enzymes, critical for LD biogenesis and

catalysis, emphasizes the significance of LD, even in bacteria. The accumulation of bacterial LD is hypothesized to supply nutrients to the bacteria during dormancy in the lung (Kim *et al*, 2010).

This idea was given further rooting by using *the Dictyostelium discoideum* and *Mycobacterium marinum* model to investigate lipid metabolism in a mycobacterial infection. *Dictyostelium* infection with *M. marinum* led to the accumulation of LD around the vacuole containing the bacteria (Barisch *et al*, 2015). This was concomitant with NL accumulation inside the bacterium, lipid stores at least partially derived from the host. *Dictyostelium* possesses a PLIN2-homolog on its LD and these studies showed that this protein interacts with bacteria having escaped their niche. This interaction is poorly understood but could represent an initial event leading to LD or NL uptake by *M. marinum*.

Chlamydia pneumonia and *C. trachomatis* trigger the formation of host LD and three bacterial proteins (Lda1, Lda2 and Lda3) are involved in the translocation of the host LD into the inclusion where the bacteria replicate (Cocchiaro *et al*, 2008). This translocation involves the removal of ADRP from the LD surface, possibly as a means of accessing the NL core for subsequent degradation. The advantage of LD translocation to the inclusion body is not known. A potential motive could be nutrient scavenging by the bacterium since TAG and SE could aid bacterial growth. Indeed, a boost in replication is observed when *Chlamydia*-infected cells are incubated with OA, a fatty acid known to increase LD numbers in the host cell (Cocchiaro *et al*, 2008). It is also possible that by sequestering host LD, the immune-related functions of the LD cannot be fulfilled and could therefore be an immune system avoidance mechanism by *Chlamydia* spp.

3.2.8.3. Parasites

Cellular infection with protozoan parasites can also lead to an increase in LD in the host mammalian cell. This was first observed for *Trypanosoma cruzi* infecting macrophages, in a TLR-2 dependent manner (de Melo *et al*, 2003; D'avila *et al*, 2011). It was additionally shown in *Plasmodium*-infected murine hepatocytes, where *P. berghei* infection led to an increase in numbers of LD in cells (Pulido-Mendez *et al*, 2006). After several rounds of replication and differentiation in hepatocytes, *Plasmodium*, the causative agent of malaria, leaves the liver and infects erythrocytes where it must digest hemoglobin in order to obtain amino acids for growth. Studies have shown that upon infection with *P. falciparum*, the human-specific species, an increase in TAG and phospholipids in the erythrocyte is detected. This is a result of the parasite's own DGAT enzyme, which is specifically upregulated during the intra-erythrocytic stage despite the parasite's inability to degrade TAG (Palacpac *et al*, 2004). The significance of LD increase in the erythrocyte is unknown. Within the parasite, LD are important as they can act as a sink for heme, which would otherwise be toxic for the parasite (Jackson *et al*, 2004).

An increased LD formation has been observed upon *Toxoplasma* infection in skeletal muscle cells and in mouse peritoneal macrophages, along with concurrent host LD association to the PV membrane (PVM) (Mota *et al*, 2014, Gomes *et al*, 2014).

3.2.9. Neutral lipid synthesis and storage in *Toxoplasma gondii*

Toxoplasma is also a fat accumulator and has between 2-4 LD per cell (Charron and Sibley, 2002; Nishikawa *et al*, 2005). It possesses the enzymatic machinery for NL synthesis. The parasite has a single DGAT enzyme, TgDGAT, and two ACAT enzymes (TgACAT1 and TgACAT2) (Quittnat *et al*, 2004; Nishikawa *et al*, 2005; Lige *et al*, 2013) and all three are located to the ER. Similarly to

their mammalian counterparts, TgDGAT catalyzes the final rate-limiting step of TAG synthesis whereas TgACAT1 and TgACAT2 use fatty acyl-CoA and cholesterol for CE synthesis. TgACAT1 is preferentially used for palmitoyl-CoA incorporation into cholesterol whereas TgACAT2 uses a much broader range of fatty acyls and forms more CE than TgACAT1 (Lige *et al*, 2013). In mammalian cells, cholesteryl oleate is the main CE (Yang *et al*, 1997) whereas *Toxoplasma*'s primary CE is derived from palmitate (Nishikawa *et al*, 2005). Despite preference for palmitate, *Toxoplasma* is also able to incorporate oleate into DAG (Cases *et al*, 1998).

Knockout parasites of *TgACAT1* or *TgACAT2* are viable but have diminished replication whereas a double *TgACAT1/TgACAT2* knockout is lethal (Lige *et al*, 2013). Incubation of infected cells with ACAT inhibitors led to a specific rupture of the parasite's plasma membrane due to overaccumulation of free toxic cholesterol in this membrane (Nishikawa *et al*, 2005). A *TgDGAT* knockout parasite was impossible to generate likely due to the importance of TAG storage for *Toxoplasma*. Indeed, although *Toxoplasma* has the enzymes required for cholesterol esterification and storage, the parasite lacks the ability to synthesize cholesterol *de novo* and must scavenge it from the host cell. Excessive cholesterol in the medium leads to the stimulation of LD in *Toxoplasma* (Coppens *et al*, 2000). The particular sensitivity of *Toxoplasma* towards ACAT inhibitors is likely due to dramatic cholesterol incorporation into its membranes in the absence of physiological acceptors of cholesterol that desorb this lipid from membranes, such as apolipoproteins present in the mammalian host (Coppens and Vielemeyer, 2005).

3.2.10. Lipid scavenging by *Toxoplasma gondii*

Toxoplasma is capable of both *de novo* synthesis of a variety of lipids, but can also scavenge these lipids from their host cell. Table 3-1 summarizes these activities.

	Ability to synthesize	Salvage from host cell	References
Cholesterol	No	Yes (LDL uptake from endolysosomes)	Coppens *et al*, 2006
Sphingolipids	Yes	Yes (Rab14, Rab30, Rab43 vesicles)	Azzouz *et* al, 2002; Sonda *et* al, 2005; de Melo and de Souza, 1996; Romano *et al*, 2013.
Fatty Acids	Yes	Yes	Waller *et al*, 1998; Seeber, 2003; Ramakrishnan *et al*, 2012; Tomavo *et al*, 1989; Quittnat *et al*, 2004; Polonais and Soldati-Favre, 2010.
Phospholipids	Yes (PC, PE, PS)	Yes	Sampels *et al*, 2012; Charron and Sibley, 2002.
Triacylglycerols	Yes	Unknown	Quittnat *et al*, 2004.
Steryl esters	Yes	Unknown	Nishiwaka *et al*, 2005; Charron and Sibley, 2002; Lige *et al*, 2013.

Table 3.1. Summary of the synthesis or scavenging potential of lipids by *Toxoplasma gondii*.
Table showing whether the parasite *Toxoplasma gondii* can synthesize or scavenge various lipids from the host cell. It is unknown whether the parasite can scavenge triacylglycerols or sterol esters from the host cell, both lipids found predominantly in lipid droplets.

One potential mechanism used by the parasite to scavenge lipids from the host cell would be by attracting host organelles that produce and/or store lipids. Shortly after invasion, the host mitochondria and ER associate closely with the PVM (Sinai and Joiner, 2001). A *Toxoplasma*-secreted protein, TgMAF1, was recently recognized as mediating the interaction between host mitochondria and the PVM, at least partially (Pernas *et al*, 2014). It is hypothesized that this close apposition between the PV and host organelles could facilitate lipid transfer to the PV. It is unknown why an increase in host LD and association to the PV could occur in *Toxoplasma*-infected cells. It is also unknown whether this could be beneficial for the parasite. In any case, host LD could represent a proficient source of lipid, and due to the parasite's gluttonous nature, may potentially be scavenged to the PV.

3.2.11. Chapter goals

In this chapter, we have addressed the following questions:

- Does *Toxoplasma* induce LD formation in the host cell?
- Do host LD associate with the PV?
- Does an increase in host LD alter *Toxoplasma*'s neutral lipid content?
- Can the parasite scavenge neutral lipids from the host cell or from LD?
- Can the parasite sequester LD into the PV?
- What are potential mechanisms by which host LD could be scavenged by *Toxoplasma*?

3.3. MATERIALS AND METHODS

3.3.1. Reagents and antibodies

All chemicals were obtained from Sigma (St Louis, MO) or Fisher (Waltham, MA) unless otherwise stated. [^{3}H]Oleic acid was purchased Moravek (Brea, CA). 5-Butyl-4,4-Difluoro-4-Bora-3a,4a-Diaza-*s*-Indacene-3-Nonanoic Acid (C4-BODIPY-C9) was purchased from ThermoFisher Scientific (Waltham, MA) and 4,4-Difluoro-1,3,5,7,8-Pentamethyl-4-Bora-3a,4a-Diaza-*s*-Indacene (BODIPY 493/503) from Life Technologies (Carlsbad, CA). The primary antibody rabbit polyclonal anti-GRA7 antibodies was used (Coppens *et al*., 2006). Secondary antibodies used for immunofluorescence were conjugated to Alexa^{594} or Alexa^{350} (Invitrogen, Carlsbad, CA). For oleic acid (OA) preparations, sodium oleate was dissolved in H_2O at a concentration of 100 mM, then thoroughly mixed by vortexing (3 minutes) with 5% Fatty Acid Free BSA for a final concentration of 10 mM to ensure BSA-OA complexes formation and stored in the dark at 4°C. In our hands, our HFF could tolerate OA up to a concentration of 0.7 mM. Many studies use 0.5 mM and there are reports of no cytotoxicity up to 1.2 mM OA in human erythrocytes (Dwight *et al*, 1992; Mei *et al*, 2011; Thörn and Bergsten, 2010). For palmitic acid (PA) preparations, sodium palmitate was dissolved in 50% ethanol at a concentration of 100 mM and prepared subsequently identically as OA. Cells were incubated in medium with various final OA or PA concentrations.

3.3.2. Cell lines and culture conditions

Human foreskin fibroblasts (HFF) were obtained from the American Type Culture Collection (Manassas, VA). GFP-ADRP HeLa cells were kindly provided by Raphael Valdivia (Duke University, North Carolina, USA; originally made by P. Targett-Adams and J. McLauchlan at the Medical

Research Council Virology Unit, Institute of Virology, Glasgow, UK; Targett-Adams *et al*, 2003). All cell lines were grown as monolayers and cultivated in α-minimum essential medium (MEM) supplemented with 10% fetal bovine serum (FBS), 2 mM glutamine and penicillin/streptomycin (100 units/ml per 100 µg/ml), and maintained at 37°C in 5% CO_2.

3.3.3. Parasite cultivation

The tachyzoites from the RH strain (type I lineage) were used throughout this study. *Toxoplasma* stably expressing RFP was kindly provided by Florence Dzierszinski (McGill University, Montreal, Canada). The parasites were propagated *in vitro* by serial passage in monolayers of HFF (Roos *et al.*, 1994).

3.3.4. Real-Time PCR

Confluent HFF were infected with *Toxoplasma* RH for 30 minutes, followed by PBS washes to remove extracellular parasites then incubated with 0.2 mM OA for various times. The RNA was extracted using *RNeasy Minikit* (Qiagen, Valencia, CA, USA) according to the manufacturer's protocol. The concentration was determined on a NanoDrop 1000 Spectrophotometer (Thermo Scientific, Waltham, MA). Amplified cDNA of the RNA samples was made using SuperScript III First Strand kit (Invitrogen). 100 ng of cDNA per sample was incubated with 2.25 µl each of forward and reverse appropriate primer and 17.5 µl of PowerUp SyBr Green Master Mix (Applied Biosystems) and run on StepOne Plus Real-Time PCR Systems (Applied Biosystems). The data of *TgACAT1, TgACAT2* and *TgDGAT* was normalized to the TgGT1 housekeeping gene whereas the data of *HsACAT, HsDGAT, HsADRP* and *HsATGL* was normalized to *HsGAPDH*. ΔΔCCs

were calculated using as controls RNA from uninfected HFF to assess transcripts levels of *HsACAT, HsDGAT, HsADRP* and *HsATGL* in mammalian cells. In *Toxoplasma* transcript level quantification, ΔΔCCs were calculated using RNA from infected HFF without OA as controls. The following primers were used: *TgACAT1*: (F) CGA CAT CCT CAT TTT CTA CAT TCT C and (R) GTG ACT CCA CTT GTA TCT TTG CTG; *TgACAT2*: (F) ATG CAT TTT TGT ATT CTA GGT GCA and (R) GGA GAA GGA GAA GAG TTG CAA A; *TgDGAT*: (F) GGA AGT GTG CTA TCC CTT ACA C and (R) CTC CCT TAC CAA AGC CGA TAA T; *TgGT1*: (F) GGC TAT TTT GGC ACC TTT CA and (R) AAC GGG AAG ACA AAC CAC AG ; *HsADRP*: (F) CAG TAG TCG TCA CAG CAT CTT and (R) GAT TGA GGA GAG ACT GCC TAT TC ; *HsACAT*: (F) CGG GCT AAC TGA TGT CTA CAA T and (R) GCA TAA GCG TCC TGT TCA TTT C ; *HsDGAT1*: (F) CTGCAG GAT TCT TTA TTC AGC TC and (R) CAT TGC TCA AGA TCA GCA TCA C ; *HsGAPDH*: (F) GGT GTG AAC CAT GAG AAG TAT GA and (R) GAG TCC TTC CAC GAT ACC AAA G ; *HsATGL*: (F) TGT CTG CAG CGG TTT CAT and (R) CTC ATA GCG TGG CAG GTT GTC.

3.3.5. Mammalian cell transfection with Rab constructs

The GFP-Rab7 was kindly provided by Craig Roy (Yale University, School of Medicine, New Haven, CT). The EGFP-Rab18 construct was a gift from Marci Scidmore (Addgene plasmid # 49550) (Huang et al, 2010). The mCherry-Rab7 constructs were generated in the laboratory. Rab7A was amplified by PCR using the forward primer (5' CTGGTGGACAGCAAATGG 3') and reverse primer (5' CCTTCACAAAGATCCCAAGC 3') from pEGFP-Rab7A, generously provided by Craig Roy (Yale University School of Medicine, New Haven, CT). The PCR product was cloned into pmCherry-C1 (Clontech, Mountain View, CA) using *Xho*I and *Hin*dIII. The plasmid DNA was confirmed by sequencing. Only HFF were used for transfections using the Amaxa nucleofector kit V according to the manufacturer's protocol (Lonza, Basel, Switzerland). Cells were

transfected with 2.5 µg of plasmid DNA and left to recover overnight prior to infections with *Toxoplasma* for 30 minutes at 37°C, cascade-washed with PBS to remove extracellular parasites, and incubated for 24 h at 37°C.

3.3.6. [^{3}H]Oleic acid uptake

[^{3}H]Oleic acid was mixed with 100 mM of OA in ethanol, evaporated by N_2 and resuspended in 100 µl DMSO, mixed with 900 µl of 7% fatty acid free BSA for a final concentration of 10 mM [^{3}H]OA. HFF cells were seeded in 24 well plates and incubated with 0.1 or 0.4 mM of [^{3}H]OA to induce the formation of lipid droplets (LD) containing radioactive OA. Excess [^{3}H]OA was thoroughly washed from the medium and the cells were infected with *Toxoplasma* for 24 or 36 h. The calcium ionophore A23187 (20 µM) was added to the cells in order to induce *Toxoplasma* egress. The parasites were subsequently purified from the medium by 3 rounds of washes. The radioactivity specifically associated with the parasite faction was determined by scintillation counting (Multipurpose Scintillation Counter, Beckman, Brea, CA) and cpm values were normalized to the protein concentration of the sample using a Biorad Protein Assay (Biorad, Hercules, CA). These assays were graphed according to the means of means of radioactivity per mg in Excel (Microsoft).

3.3.7. Fluorescence microscopy

For staining with BODIPY dyes, infected HFF pretreated with 0.4 mM OA or not, were incubated with either 10 mM of C4-BODIPY-C9 or BODIPY 493/503 for 24 h, thoroughly washed with PBS then incubated for 2 h with α-MEM medium. These pre-loaded BODIPY-stained hLD cells were

infected with *Toxoplasma* (RH or RFP-RH) for the indicated times prior to fixation, staining or image acquisition. During infection with *Toxoplasma*, 0.2 mM of OA was added to the medium to ensure that hLD would remain as such and would not undergo lipophagy by the host cell.

Immunofluorescence assays (IFA) on fixed cells using 4% formaldehyde (Polysciences, Warrington, PA) plus 0.02% glutaraldehyde in PBS was performed as described previously (Karsten *et al*., 2004) with a 5 minute permeabilization step with 0.3% TritonX-100 in PBS if staining with antibodies. Specific IFA with BODIPY 493/503 labeling was performed after the secondary incubation step for 30 minutes at 1:100 dilution in PBS, followed by three 5 minute PBS washes prior to staining with 4-,6-diamidino-2-phenylindole (DAPI). Coverslips were mounted using ProLong Diamond Antifade Mountant (Life Technologies) to minimize bleaching during microscopy. Cells were viewed with a Nikon Eclipse 90i equipped with an oil-immersion plan Apo 100x NA 1.4 objective and a Hamamatsu GRCA-ER camera (Hamamatsu Photonics, Hamamatsu, Japan). Optical z-sections with 0.2-µm spacing were acquired using Volocity software (PerkinElmer, Waltham, MA). The images were deconvolved using an iterative restoration algorithm and the registry was corrected using Volocity software. The positive product of the differences of the mean (PDM) images were calculated using Volocity software, which was also used to adjust brightness levels, cropping and resizing of the images obtained.

3.3.8. Image analysis

GFP-ADRP HeLa cells were infected with *Toxoplasma* for various amounts of time ranging from 2 h to 36 h and viewed by microscopy to quantify the amassing of host LD around the PV of *Toxoplasma*. The percentage of PV surrounded by host LD was calculated by observation of host

LD around the PV. If over 70% of the PV was surrounded by host LD, the PV was marked as positive and plotted as such in a histogram.

3.3.9. Electron microscopy

For transmission EM, HFF cells infected with *Toxoplasma* RH strain for 24 h (with or without OA) were fixed in 2.5% glutaraldehyde (EM grade; Electron Microscopy Sciences, Hatfield, PA) in 0.1 M sodium cacodylate buffer (pH 7.4) for 1 h at room temperature, and processed as described (Fölsch *et al*., 2001) before examination with a Philips CM120 Electron Microscope (Eindhoven, the Netherlands) under 80 kV.

3.3.10. Statistical methods

Data were displayed in box plots using Kaleidagraph software (Synergy Software) or graphed in Excel (Microsoft) with standard deviations displayed. Whiskers of the box plots represent the upper and lower values excluding outliers, outliers are marked as open circles, and the line inside the box is the median value. Means and standard deviations were calculated from three independent experiments using Excel (Microsoft). *p* values were calculated using either student *t*-test or a Chi-squared test in Excel (Microsoft).

3.4. RESULTS

3.4.1. Host lipid droplets cluster around the PV of *Toxoplasma*

The rapid intracellular multiplication of Apicomplexan parasites such as *Toxoplasma gondii* requires large amounts of lipids for the membrane biogenesis of the new progenies. Hence, the study of lipids is fundamental to understand the biology and pathogenesis of this human pathogen. *Toxoplasma* scavenges many lipids from mammalian host organelles (Coppens *et al*, 2006; Romano *et al*, 2013; Quittnat *et al,* 2004; Charron and Sibley, 2002; Sampels *et al*, 2012), but its ability to salvage lipids stored in host lipid droplets (LD) remains unexplored. LD are found in virtually all cell types and serve primarily as lipid depots for energy (e.g. fatty acids as respiratory substrates), membrane biogenesis (e.g. fatty acids, cholesterol) and/or for the formation of specific lipophilic components, (e.g. steroid hormones) as well as for the prevention of cellular lipotoxicity (Khor *et al*, 2013; Smirnova *et al*, 2006; Athenstaedt and Daum, 2006; Bickel *et al*, 2010). The lipids stored in LD are esterified with a fatty acid (FA) into a neutral lipid (NL) form. The two main lipids present in mammalian LD are cholesteryl esters (CE) and triacylglycerols (TAG).

A hallmark of a *Toxoplasma* infection is the interaction of host organelles with the parasitophorous vacuole (PV) (Coppens *et al*, 2006; Sinai *et al*, 1997; Walker *et al*, 2008; Romano *et al*, 2008; Wang *et al*, 2010; Romano *et al*, 2013; Pernas *et al*, 2014) so we first investigated the spatial distribution of host LD in *Toxoplasma*-infected cells. We stained infected cells with the fluorescent NL dye, BODIPY 493/503 which specifically fluoresces and accumulates in LD. Fluorescence microscopy reveals the partial clustering of host LD around the PV of *Toxoplasma* 24 h post-infection (p.i.) (Fig. 3-4.A, panel a). Culture medium supplemented with 10% serum,

which is referred to here as control medium, contains on average 30 µg/ml of cholesterol and 3 µg/ml oleic acid. Incubation of mammalian cells with oleic acid (OA) at a concentration of 0.2 mM, which corresponds to approximately a 20 fold excess of OA, increased numbers of LD. We investigated the effect of increased OA concentrations on LD association with the PV. In infected cells exposed to 0.2 mM OA, we observed a more dramatic perivacuolar accumulation of host LD as compared to control medium (Fig. 3-4.A, panel b). This feature was further examined by electron microscopy (EM) in which LD can be identified as homogenous electron-dense structures without bilayer membranous profiles. Our ultrastructural observations of *Toxoplasma*-infected cells confirmed the clustering of host LD at the PV, often organized in multilayers (Fig. 3-4.B).

To quantify the amassing of host LD around the PV and examine the dynamics of this process over time, we assessed the percent of PV, from 2 to 32 h p.i., that had greater than 70% of their perimeter ringed by host LD (Fig. 3-4.C). For better visualization of this feature, we used HeLa cells overexpressing the Adipose Differentiation-Related Protein (ADRP) in which the biogenesis of LD is stimulated, as host cells for the *Toxoplasma* infection (Targett-Adams *et al*, 2003). Indeed, as compared to fibroblasts and HeLa cells that produce a median of 23 and 17 LD per cell respectively, ADRP-overexpressing HeLa cells contain a median of 36 LD per cell (Fig. 3-4.D and E). Imaging of fixed samples by microscopy showed that the mean diameter of LD in HFF or HeLa cells ranged between 1 and 3 µm, similarly as reported for a human hepatocyte cell line, Huh7 (Targett-Adams *et al*, 2003). As the infection progresses concomitant with the PV enlargement, a greater number of PVs were surrounded by host LD, with less than 1% of PV at 2 h p.i. and up to ~ 45% of PV by 32 h p.i. (Fig. 3-4.C). Addition of 0.2 mM OA during infection amplified this phenomenon with ~70% of PVs surrounded with hLD by 32 h p.i.

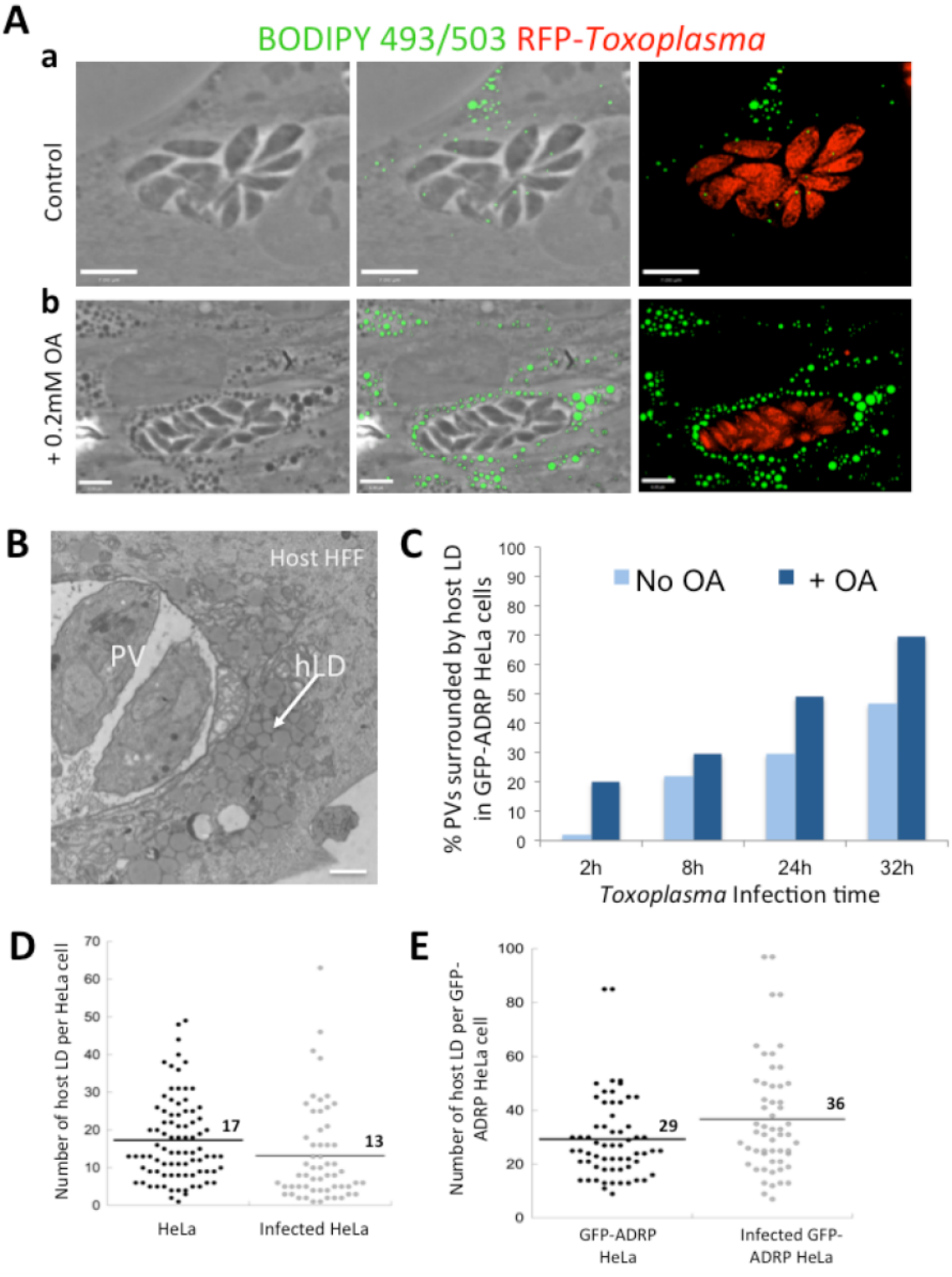
A
BODIPY 493/503 RFP-Toxoplasma
a
Control
b
+ 0.2mM OA
B
Host HFF
PV
hLD
C
No OA
+ OA
% PVs surrounded by host LD in GFP-ADRP HeLa cells
100
90
80
70
60
50
40
30
20
10
0
2h
8h
24h
32h
Toxoplasma Infection time
D
Number of host LD per HeLa cell
70
60
50
40
30
20
10
0
17
13
HeLa
Infected HeLa
E
Number of host LD per GFP-ADRP HeLa cell
100
80
60
40
20
0
29
36
GFP-ADRP HeLa
Infected GFP-ADRP HeLa

Figure 3-4. Dynamic changes of host LD upon *Toxoplasma* infection.
A. Fluorescence microscopy of HFF infected with RFP-expressing *Toxoplasma* for 24 h and stained with BODIPY 493/503 after fixation without oleic acid (OA) (a) or with 0.2 mM OA (b) during infection. Representative images of host lipid droplets (host LD) stained with BODIPY 493/503 (green) surrounding the PV of *Toxoplasma* (red) are shown. Scale bars, 7 µm. **B.** Ultrastructural EM view of an infected HFF with the PV of *Toxoplasma* surrounded by host LD in the presence of 0.2 mM OA. Scale bar, 1 µm. **C.** Quantification of the percent of PVs surrounded by host LD over time, with or without OA. GFP-ADRP-expressing HeLa cells were infected with *Toxoplasma* at the indicated times and stained with BODIPY 493/503 as shown in (A). PVs were scored as LD-associated if over 70% of the PV was surrounded by host LD. Data representative of 2 independent experiments. **D-E.** Enumeration of host LD numbers after 24 h *Toxoplasma* infection in HeLa and GFP-ADRP expressing-HeLa cells. Cells were infected with *Toxoplasma*, fixed and stained with BODIPY 493/503 to count the number of host LD. The boxplot in (D) shows the number of host LD in uninfected and infected HeLa cells at 24 h p.i. whereas the boxplot in (E) shows data from GFP-ADRP expressing-HeLa cells. Data acquired from two independent measurements with n>40.

3.4.2. Host lipid droplet number fluctuates throughout infection

Next, we examined whether there is a fluctuation in the host LD number throughout a *Toxoplasma* infection in cultured cells. The number of parasites per PV is a recognized indicator of infection time since *Toxoplasma* has a doubling time of 6-8 h. In HFF infected with *Toxoplasma,* LD were counted after staining with BODIPY 493/503 (Fig. 3-5). Early during infection (1, 2 or 4 parasites per PV), host LD numbers steadily increased from a median of 23 in uninfected cells to 34 (1/PV), 51 (2/PV) and 50 (4/PV) in infected cells. However, once the PV contained 8 parasites which corresponds to ~ 24 h p.i., host LD numbers abruptly declined to approximately 26 per cell. This suggests a highly dynamic status of host LD upon *Toxoplasma* infection, with a stimulation of LD production up to 16 h p.i., and a slowdown in host LD biogenesis and/or consumption of host LD from 24 h p.i. until parasite egress.

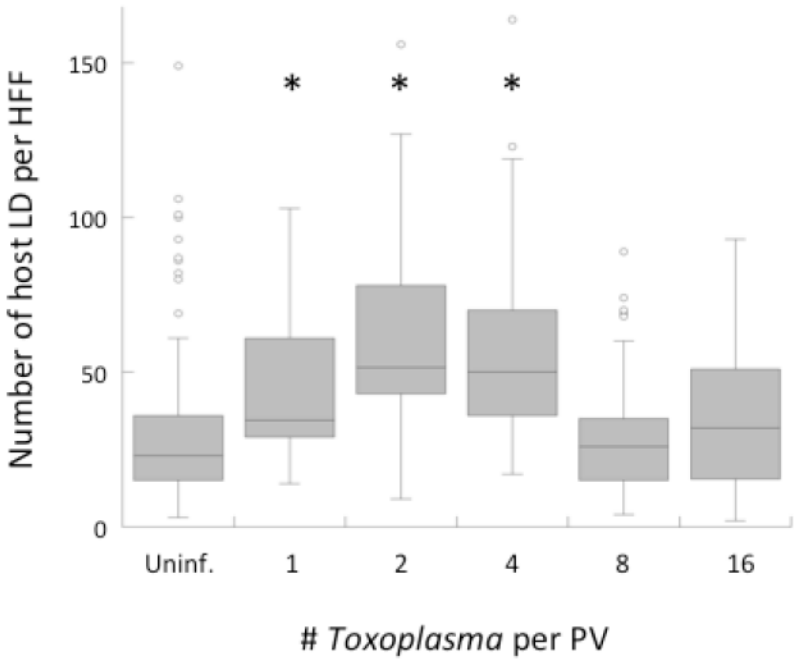

Figure 3-5. Influence of *Toxoplasma* on host LD dynamics.
Enumeration of host LD numbers throughout *Toxoplasma* infection in HFF. HFF were infected with *Toxoplasma*, fixed and stained with BODIPY 493/503 to count the number of host LD. The boxplot shows the number of host LD in infected HFF as infection with *Toxoplasma* progresses. HFF with PVs of 1, 2 or 4 parasites have statistically more host LD than uninfected cells, or HFF with 8 or 16 parasites per PV. Data acquired from two independent experiments, counting >30 PVs per condition per experiment.

3.4.3. Infection with *Toxoplasma* alters the cycle of host neutral lipids

The variability of host LD numbers in *Toxoplasma*-infected cells prompted us to examine potential changes in the NL cycle (synthesis and lipolysis) in LD. To do so, we monitored the transcriptional activities of host *Acetyl-Coenzyme A Acetyltransferase (ACAT), Diacylglycerol O-Acyltransferase 1 (DGAT1)* and *Adipose Triglyceride Lipase* (*ATGL)* in infected fibroblasts for 24 h (Fig. 3-6.A). Infection with *Toxoplasma* led to a statistically significant ($p < 0.05$) decrease in transcript levels for *ACAT* by 2.85 fold, *DGAT1* by 1.25 fold and *ATGL* by 3.44 fold as compared to uninfected control HFF (Fig. 3-6.A).

In parallel, we investigated whether these changes could also occur under conditions of excess OA in the medium. It is known that exogenous addition of OA results in an increase in LD formation and impacts NL content in mammalian cells (Bickel *et al*, 2010; Rohwedder *et al*, 2014). In our system using HFF, addition of 0.2 mM OA to the medium of a confluent layer of HFF for 24 h led to an increase of *ADRP* and *DGAT1* transcription by 3.87 and 1.66 fold, respectively, but no statistically significant increase in *ACAT* nor *ATGL* gene expression (Fig. 3-6.B). Upon excess OA in *Toxoplasma*-infected cells, we observed the decrease of *ACAT*, *DGAT* and *ATGL* transcript levels, to a similar extent as in cells without OA (Fig. 3-6.A). *ADRP* expression does not change with infection but increases with excess OA in both uninfected and infected cells, as previously reported (Ducharme and Bickel, 2008; Mei *et al*, 2011).

These data show that the drop in host LD number 24 h p.i. may be related to decreased ACAT and DGAT activity. However, the reduced ATGL activity would have led to a reduced catalysis of LD and concomitant increase or stabilization in LD and its NL content. This seems to not be the case, as we observe a decline in LD number observed upon 24 h infection, suggestive of a dysregulation in the NL cycle of the host cell during *Toxoplasma* infection.

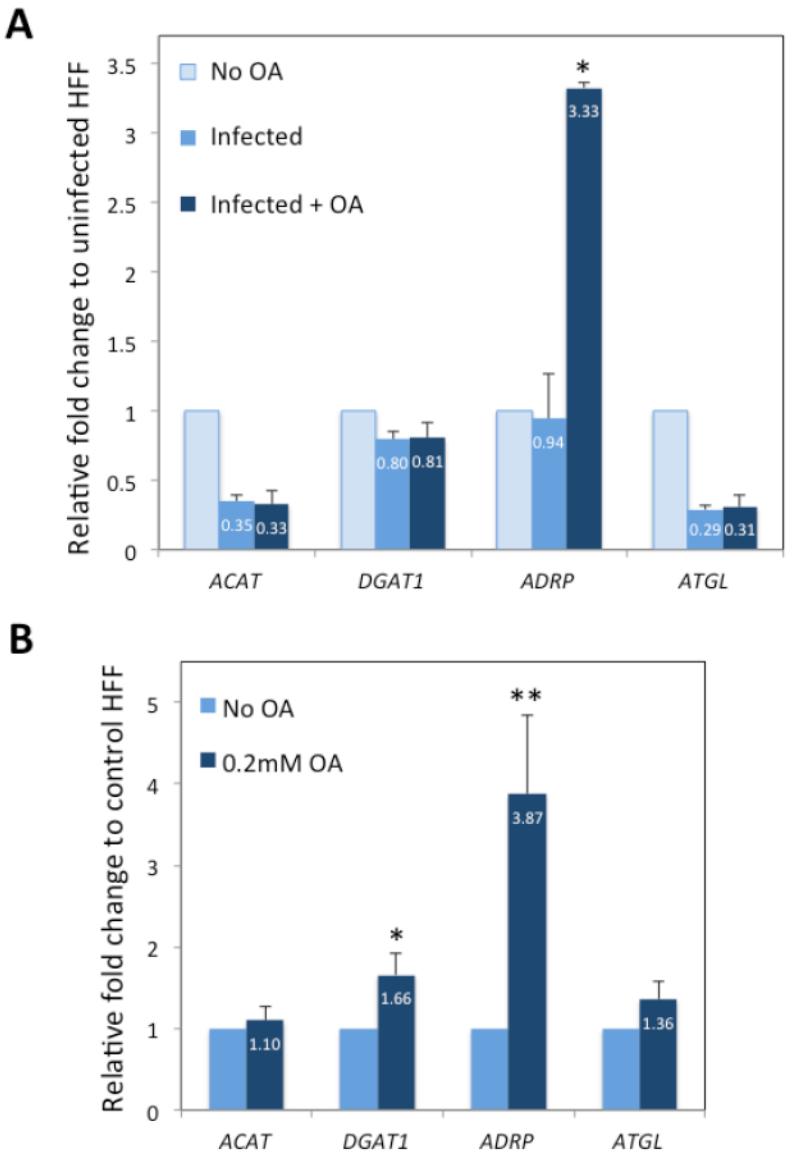

Figure 3-6. Mammalian LD-related gene expression upon OA addition and *Toxoplasma* infection. **A.** Real-time PCR analysis of *Acetyl-Coenzyme A Acetyltransferase* (*ACAT*), *Diacylglycerol O-Acyltransferase 1* (*DGAT1*), *Adipose Differentiation-Related Protein* (*ADRP*) and *Adipose Triglyceride Lipase* (*ATGL*) gene expression in uninfected HFF and HFF infected with *Toxoplasma* for 24 h in the absence or presence of 0.2 mM OA. Means ± SD of assay triplicates. *p <0.001 indicates statistical difference between infected control HFF and infected HFF with 0.2 mM OA.**B.** Real-time PCR analysis of mammalian *ACAT, DGAT1, ADRP,* and *ATGL* gene expression in HFF in the presence of 0.2 mM OA or absence for 24 h. Means ± SD of assays in triplicates. Indicated statistical differences are between control and 0.2 mM OA treated HFF. * p<0.02; ** p <0.03.

3.4.4. Exogenously added oleic acid triggers neutral lipid synthesis and storage in *Toxoplasma.*

Intracellular *Toxoplasma* has the ability to divert various FA present in its environment and incorporate them into major lipids and proteins (Charron and Sibley, 2002; Tomavo *et al*, 1989; Quittnat *et al*, 2004; Polonais and Soldati-Favre, 2010). The parasite has distinct enzymes to catalyze the esterification of cholesterol and DAG. In contrast to mammalian cells, *Toxoplasma* possesses two ACATs (*TgACAT1* and *Tg ACAT2*) differing in FA substrate specificity and one *DGAT*, *TgDGAT* (Quittnat *et al*, 2004; Nishikawa *et al*, 2005; Lige *et al*, 2013). The simultaneous deletion of both *TgACAT* in or deletion of *TgDGAT* is lethal for *Toxoplasma*, emphasizing the importance of NL storage for the parasite (Nishikawa *et al*, 2005; Lige *et al*, 2013).

We examined the physiological response of *Toxoplasma* to excess OA present in the culture medium and stored in host LD. In particular, we sought to determine if the parasite takes advantage of the copious source of exogenous OA by scavenging these lipids, e.g., to boost its replication, and whether it has the capacity to store FA in its LD in case of surplus. To examine whether the parasite is able to access FA accumulated in the host cell, we measured the transcriptional levels of *TgACATs* and *TgDGAT* after 12 or 24 h incubation with excess OA (0.2 mM). No statistically significant variations were observed in all three transcripts at 12 h p.i. as compared to no OA addition (12 h control). At 24 h p.i., a significant increase in *TgACAT2* (1.71 fold) and *TgDGAT* (1.79 fold) expression was observed with 0.2 mM OA compared to the condition without OA added (24 h control) (Fig. 3-7.A). In complement to these assays, we stained infected cells with BODIPY 493/503 to visualize NL stores in *Toxoplasma* during exposure to excess OA (Fig. 3-7.B and 3-7.C). Under control conditions, the parasite contains an average of 1 to 4 LD with a diameter between 0.1 and 0.5µm (Nishikawa *et al*, 2005; Charron and Sibley,

2002; Fig. 3-7.B). Prominent LD accumulation was observed in the PV following incubation with 0.2 mM OA for 24 h (Fig. 3-7.C), consistent with the increase in *TgACAT2* and *TgDGAT* transcript levels. These results suggest that *Toxoplasma* may salvage exogenous OA for storage in LD, via conversion of OA to TAG or CE. Unlike mammalian cells, *TgACAT* transcription increased upon excess OA in the medium. *TgACAT* transcription also increased upon excess cholesterol addition to the medium (Nishikawa *et al*, 2005).

3.4.5. Very large excess OA leads to a dramatic accumulation of lipid droplets in *Toxoplasma*.

We were interested in examining how intracellular *Toxoplasma* would cope when exposed to very large excess of OA in its environment. Upon 0.4 to 1 mM OA incubation, mammalian cells respond by regulating the massive influx of OA mainly by conjugating OA to DAG and storing TAG in newly formed LD (Fig. 3-8.A). After 24 h incubation with 0.4 mM OA, we detected extremely large LD within the parasite with a diameter up to 0.8 µm, confirming that *Toxoplasma* is capable of storing excess lipids retrieved from their environment (Fig. 3-8.A). Most of the parasites had a normal ultrastructure except for large LD and massive accumulations of osmiophilic materials, i.e., lipid deposits, amassed in the residual body, a structure leftover from the mother cell following replication. EM studies revealed that some parasite LD were as large as host mammalian LD regardless of the PV size, and some LD were clustered in the cytosol (Fig. 3-8, panels B-C). The vacuolar space was also characterized by an extensive development of the intravacuolar network (IVN), which is a membranous tubular network derived from vesicles exported by the parasite. Lipidic structures were also present in the vacuolar space, wrapped by the tubules on the IVN (Fig. 3-8.B, inset ii).

We next wanted to use fluorescent microscopy to confirm that the enlarged parasite LD identified by EM contained NL. We infected HFF with RFP-*Toxoplasma* for 24 h with 0.5mM OA, fixed the coverslips and stained with BODIPY 493/503 (Fig. 3-9). Large BODIPY 493/503-containing structures were observed, whose size matched that of the structures observed at the ultrastructural level (Fig. 3-8.B and C), which we ascertain are canonical LD. Parasites were able to form up to 5 large LD per individual parasite.

Altogether, these data revealed that *Toxoplasma* is capable of retrieving OA from the medium with subsequent storage in LD. Additionally, the amount of OA scavenged is proportional to the exogenous OA concentration. It strongly suggests that the parasite does not have the capacity to regulate FA uptake and can store copious amounts of FA in its LD. However, the parasite can also accumulate lipidic structures, putting it at risk for lipotoxicity.

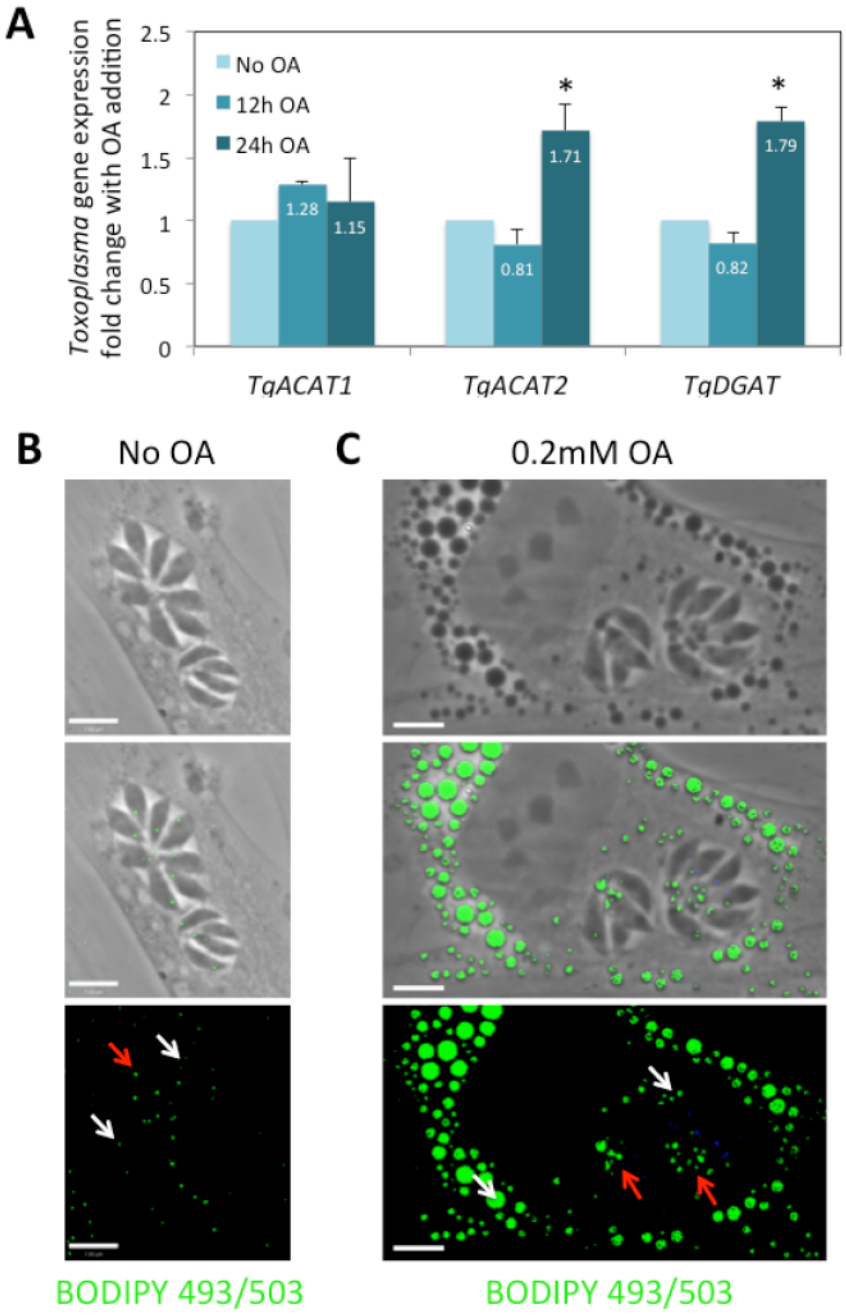

Figure 3-7. Neutral lipid synthesis and storage in *Toxoplasma* with 0.2 mM OA for 24h.
A. Real-time PCR analysis of *Toxoplasma gondii* Acetyl-Coenzyme A Acetyltransferase 1 and 2 (*TgACAT1*, *TgACAT2*), Diacylglycerol O-Acyltransferase 1 (Tg*DGAT*) gene expression in infected HFF grown without OA (control) or with 0.2 mM OA for 12 or 24 h. Means ± SD of assay triplicates. * p <0.001 indicates statistical difference between infected control HFF and infected HFF with 0.2 mM OA.**B-C.** Fluorescence microscopy of *Toxoplasma*-infected HFF grown without OA (B) or with 0.2 mM OA (C) for 24 h and stained with BODIPY 493/503. The green staining is specific for host LD as well as neutral lipid depots in the parasite and PV. White arrows, host LD; Red arrows, *Toxoplasma* LD. Scale bars, 7 µm.

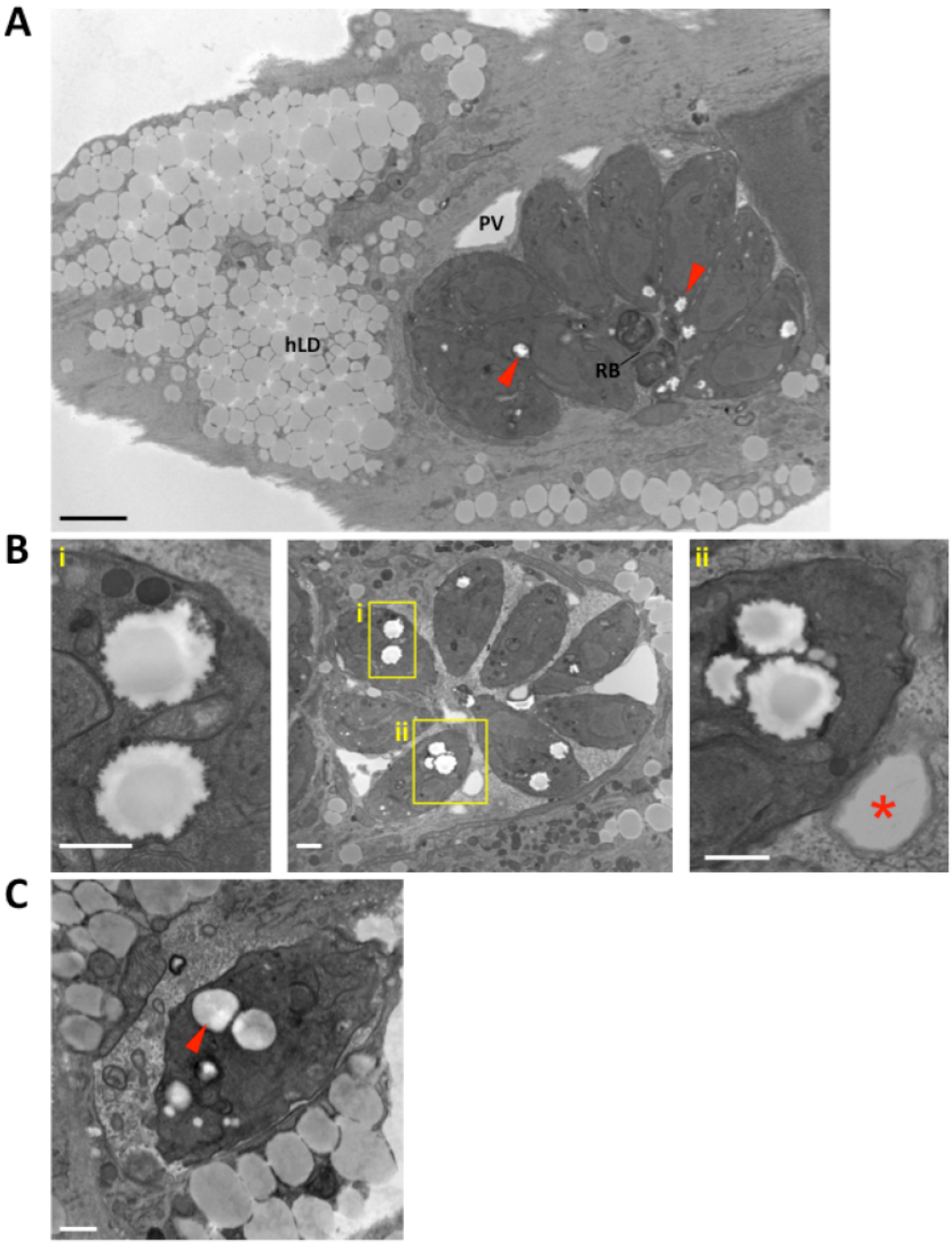

Figure 3-8. Ultrastructural analysis of *Toxoplasma*-infected HFF upon excess OA.
A. EM showing the accumulation of LD in HFF and the parasite with 0.4 mM OA incubation for 24 h. Red arrows point to *Toxoplasma* LD. Scale bar, 3 µm**. B-C**. EM of the PV of *Toxoplasma* in infected-HFF for 24 h with 0.4 mM OA. Large LD accumulate in the parasite (B, inset i) and PV lumen (B, inset ii, red asterisk). LD in the parasite are the same size and morphology as LD in the host cell (C, red arrow). Scale bar, 1 µm. Abbreviations: hLD: host LD; RB: residual body.

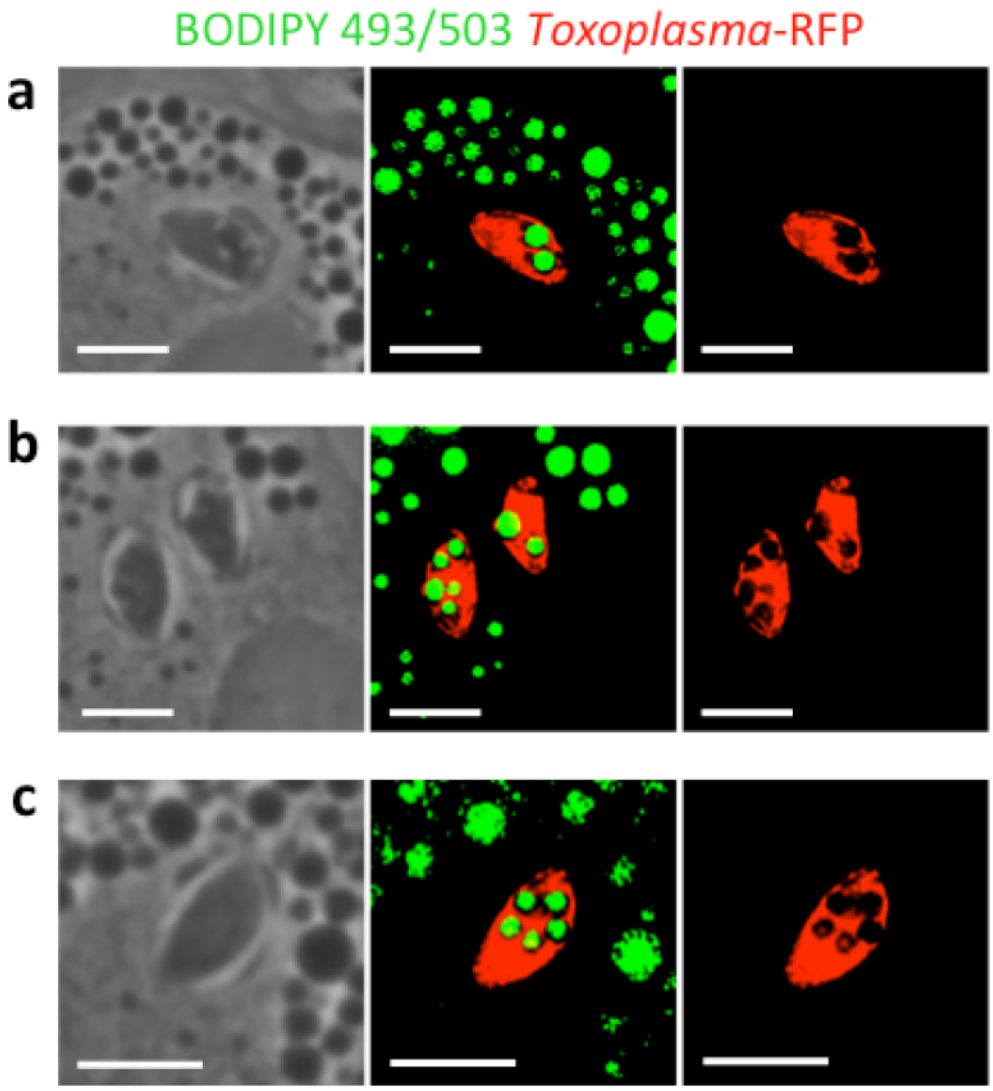

Figure 3-9. Neutral lipid stores in *Toxoplasma* upon excess OA.
Three examples of fluorescence microscopy of HFF infected with RFP-expressing *Toxoplasma* for 24 h in the presence of 0.5mM OA and stained with BODIPY 493/503. Up to **6** very large BODIPY-stained structures can be observed within a single parasite. Scale bars, 7 µm.

3.4.6. *Toxoplasma* scavenges the free fatty acid C4-BODIPY-C9 from host lipid droplets

Previous studies reported lipid scavenging by *Toxoplasma* from host cells (Charron and Sibley, 2002; Quittnat *et al*, 2004; Polonais and Soldati-Favre, 2010; Coppens *et al*, 2006; Romano *et al*, 2013) and our data above highlight the capability of the parasite to scavenge and store lipids when infected cells were incubated in excess OA. We next wanted to determine whether the parasite retrieves NL directly from host LD or from the host cell but not stored in LD.

We incubated *Toxoplasma*-infected cells with the fluorescently-labeled free fatty acid C4-BODIPY-C9 to track the internalization of this lipid into the parasite. Addition of FA C4-BODIPY-C9 and 0.4 mM OA to the medium of infected cells for 2 h led to intensive fluorescent labeling of host LD and internal membranes of the parasite, confirming that *Toxoplasma* scavenges FA (Fig. 3-10.A). At 24 h p.i., we observed fluorescent signals in both the host cell and the parasite (Fig. 3-11.A)

To specifically assess whether the parasite retrieves this lipid from host LD, we incubated HFF with 0.4 mM OA and C4-BODIPY-C9 for 18 h, washing away the excess C4-BODIPY-C9 from the medium, then infected with *Toxoplasma* for 2 h or 24 h in the presence of 0.4 mM OA for sustainment of LD formation (Fig. 3-10.B, Fig. 3-11.B). At 2 h p.i., no fluorescent signal associated with the parasite could be resolved by live fluorescence microscopy (Fig. 3-10.B). At 24 h p.i. however, we observed by live microscopy a dotty intra-parasitic staining resembling LD, as seen on z-stacks images of the PV shown in Fig. 3-11.B. This is suggestive of a trafficking of FA C4-BODIBY-C9 from host LD to parasite LD by 24 h p.i., a phenomenon not observed (or undetectable) at 2 h p.i.

To confirm this process, we devised another experimental protocol that would ensure that lipids found in *Toxoplasma*'s LD contain lipids originating from the host LD. BODIPY 493/503

is not a fluorescently labeled FA, and is instead a lipid dye specific to NL. Only NL within LD fluorescence with this dye thus enabling the tracking of NL. Host LD formation was induced in HFF by incubating with 0.4 mM OA in addition to BODIPY 493/503 for 18 h, and a plethora of LD became fluorescent in HFF. After washing, HFF loaded with BODIPY-stained LD were infected with RFP-expressing *Toxoplasma* for 24 h in the presence of 0.2 mM OA to pressure the host cell to maintain LD (Fig. 3-12). The coverslips were then viewed by live or fixed microscopy (Fig. 3-12 and 3-13, respectively). Remarkably, BODIPY 493/503 staining was observed in *Toxoplasma* LD, and the signal was more prominent on fixed cells. This staining could only have occurred if the parasite had taken up fluorescent lipids derived directly from host LD prior to storage in their own LD.

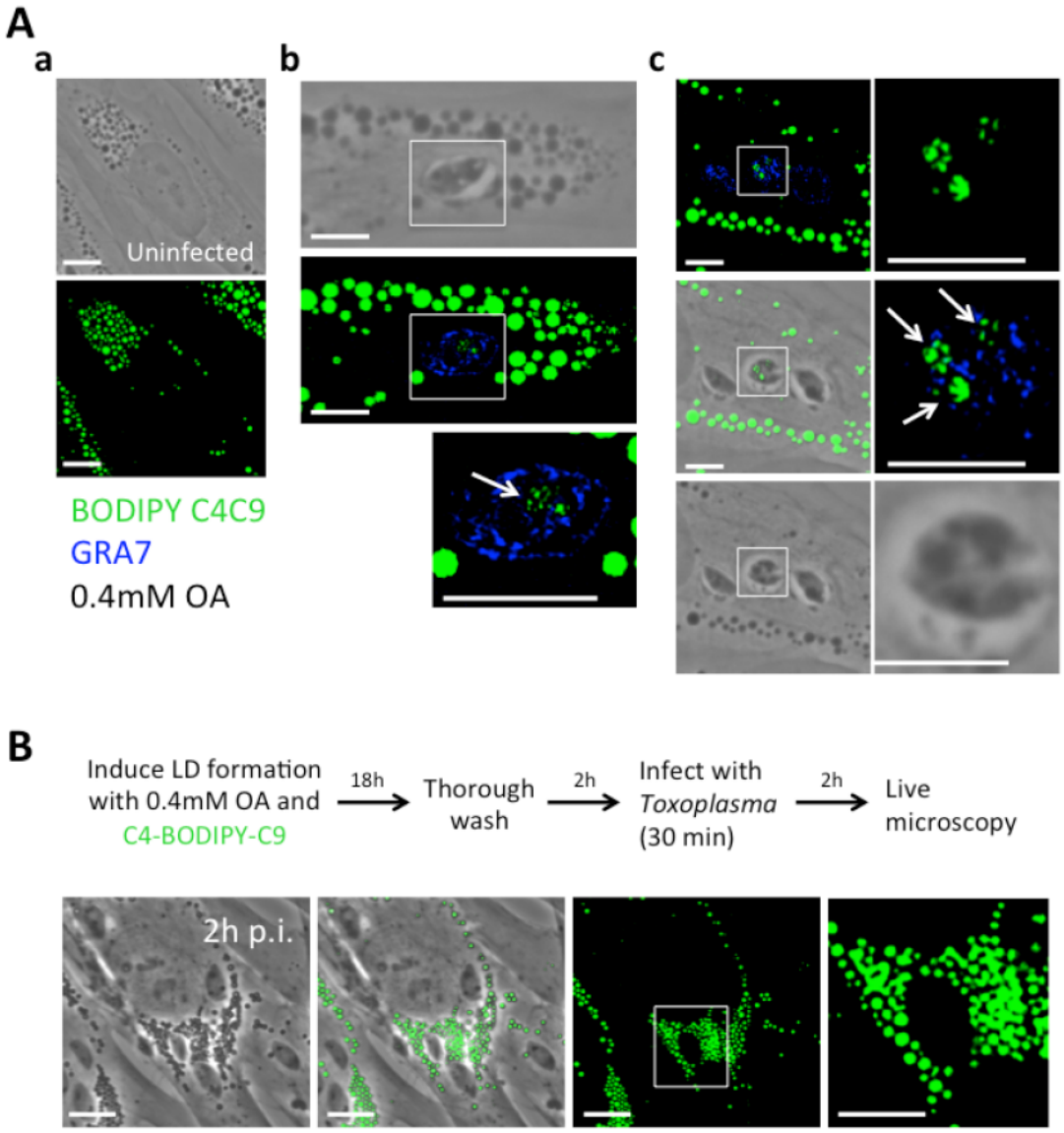

Figure 3-10. Detection of the fatty acid C4-BODIPY-C9 in *Toxoplasma* 2 h p.i.

A. Immunofluorescence microscopy of uninfected (panels a) or infected HFF (panels b, c) for 2 h in the presence of 0.4mM OA and the free fatty acid C4-BODIPY-C9 (10 µM) stained with anti-GRA7 antibody for the PV of *Toxoplasma*. In A, BODIPY-positive structures are visible on parasite membranes and in well as LDs (c). Scale bars, 7 µm. **B.** Schema outlining the experimental protocol for the induction of C4-BODIPY-C9 positive LDs in HFF. Green fluorescent LD formation in HFF was stimulated by incubating cells with 0.4mM OA and 10 µM of C4-BODIPY-C9 for 18 h, followed by a 2 hour chase in normal α-MEM medium. These cells were then infected with *Toxoplasma* and visualized by live microscopy after 2 of infection. Fluorescence microscopy of *Toxoplasma*-infected HFF for 2 h. Host LD labeled with C4-BODIPY-C9 seen in green, are visible around *Toxoplasma* PV, but not inside the parasites. Scale bars, 7 µm.

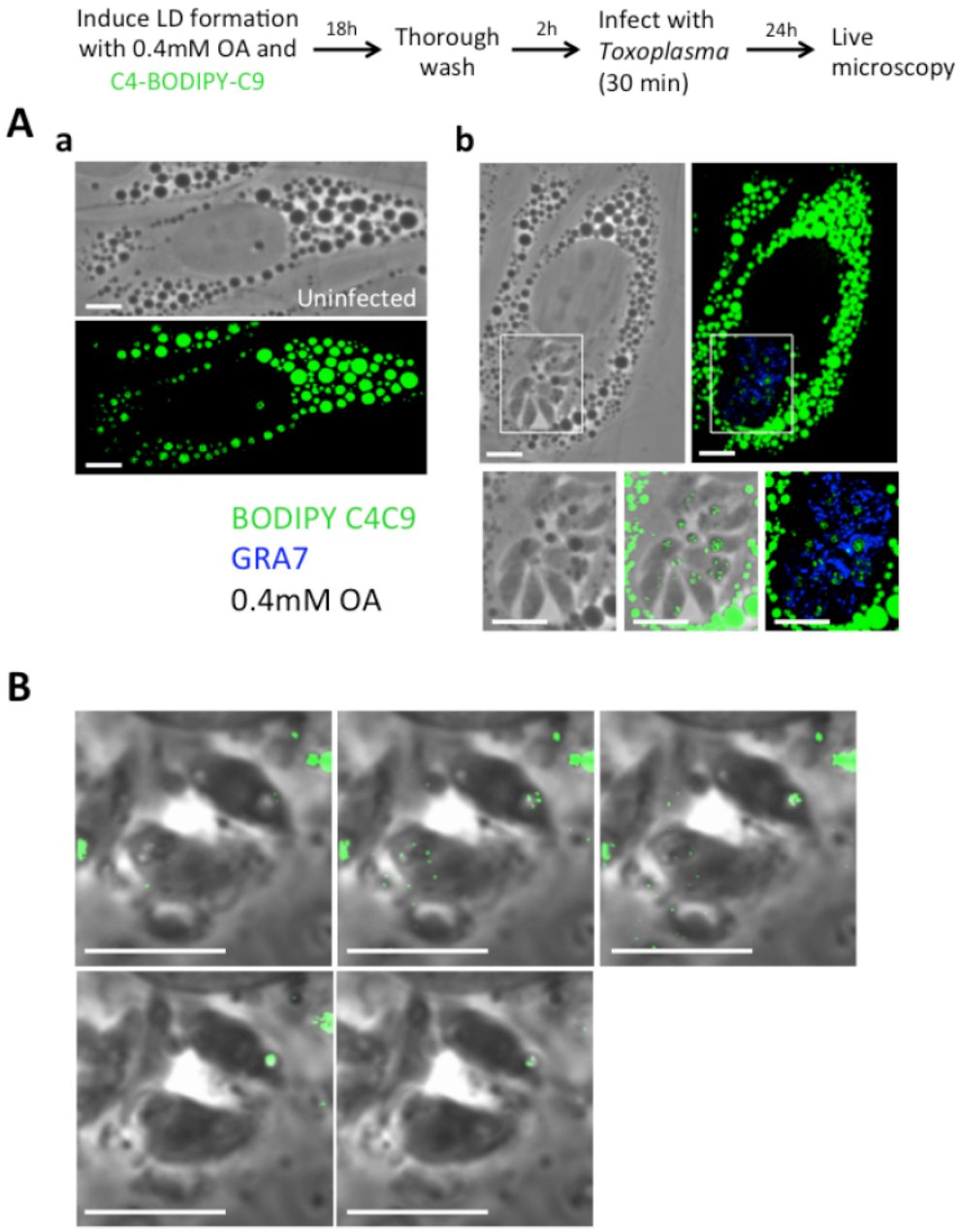

Figure 3-11. Detection of the fatty acid C4-BODIPY-C9 pre-accumulated into host LD in *Toxoplasma*. Schema outlining the experimental protocol for the induction of C4-BODIPY-C9 positive LDs in HFF. Green fluorescent LD formation in HFF was stimulated by incubating cells with 0.4mM OA and 10 µM of C4-BODIPY-C9 for 18 h, followed by a 2 hour chase in normal α-MEM medium. These cells were then infected with *Toxoplasma* and visualized by live microscopy after 24 h of infection**. A.** Immunofluorescence microscopy of uninfected (panels a) or infected HFF (panel b) for 24 h in the presence of 0.4mM OA and the free fatty acid C4-BODIPY-C9 (10 µM), stained with anti-GRA7 antibody for the PV of *Toxoplasma*. In panel b, BODIPY-positive LDs are seen in the PV of *Toxoplasma* demonstrating scavenging of free fatty acid from the host cell and incorporation into LD. Scale bars, 7 µm. **B.** Fluorescence and phase microscopy of *Toxoplasma*-infected HFF for 24 h. Images show individual z-stacks demonstrating the presence of host LD-derived C4-BODIPY-C9 inside *Toxoplasma* LD. Scale bars, 7 µm.

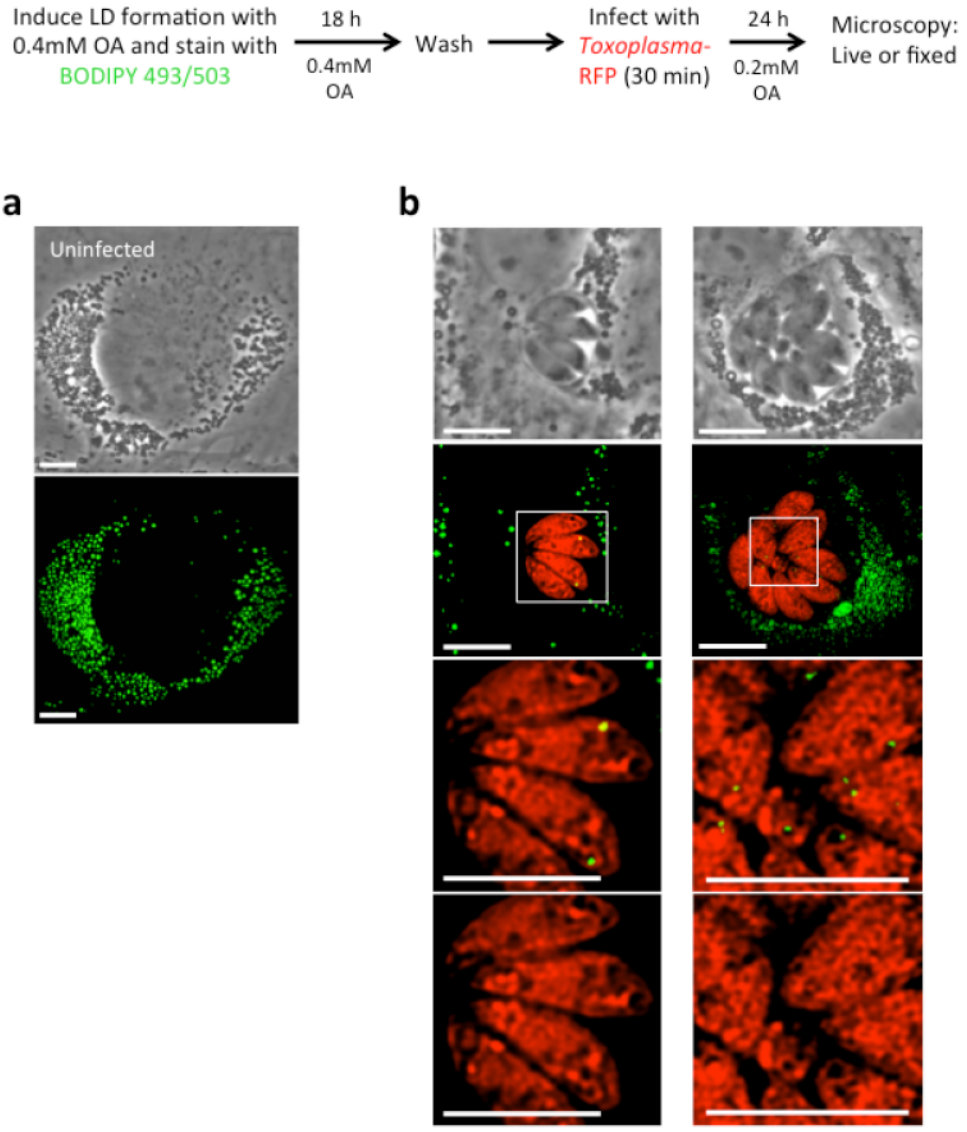

Figure 3-12. Detection of BODIPY 493/503 pre-labeled host LD in *Toxoplasma* (live microscopy)
Schema outlining the experimental protocol for the induction of LD labeled specifically with BODIPY 493/503 in HFF. BODIPY-labeled LD in HFF were induced by incubating with 0.4mM OA and BODIPY 493/503 prior to infection with RFP-expressing *Toxoplasma* for 24 h. **a-b.** Fluorescence microscopy of uninfected (a) and RFP-expressing *Toxoplasma*-infected HFF (b) containing pre-labeled host LD with BODIPY 493/503. BODIPY 493/503 labeling is visible inside individual parasites in z-slices from small or large PV. Scale bars, 7 µm.

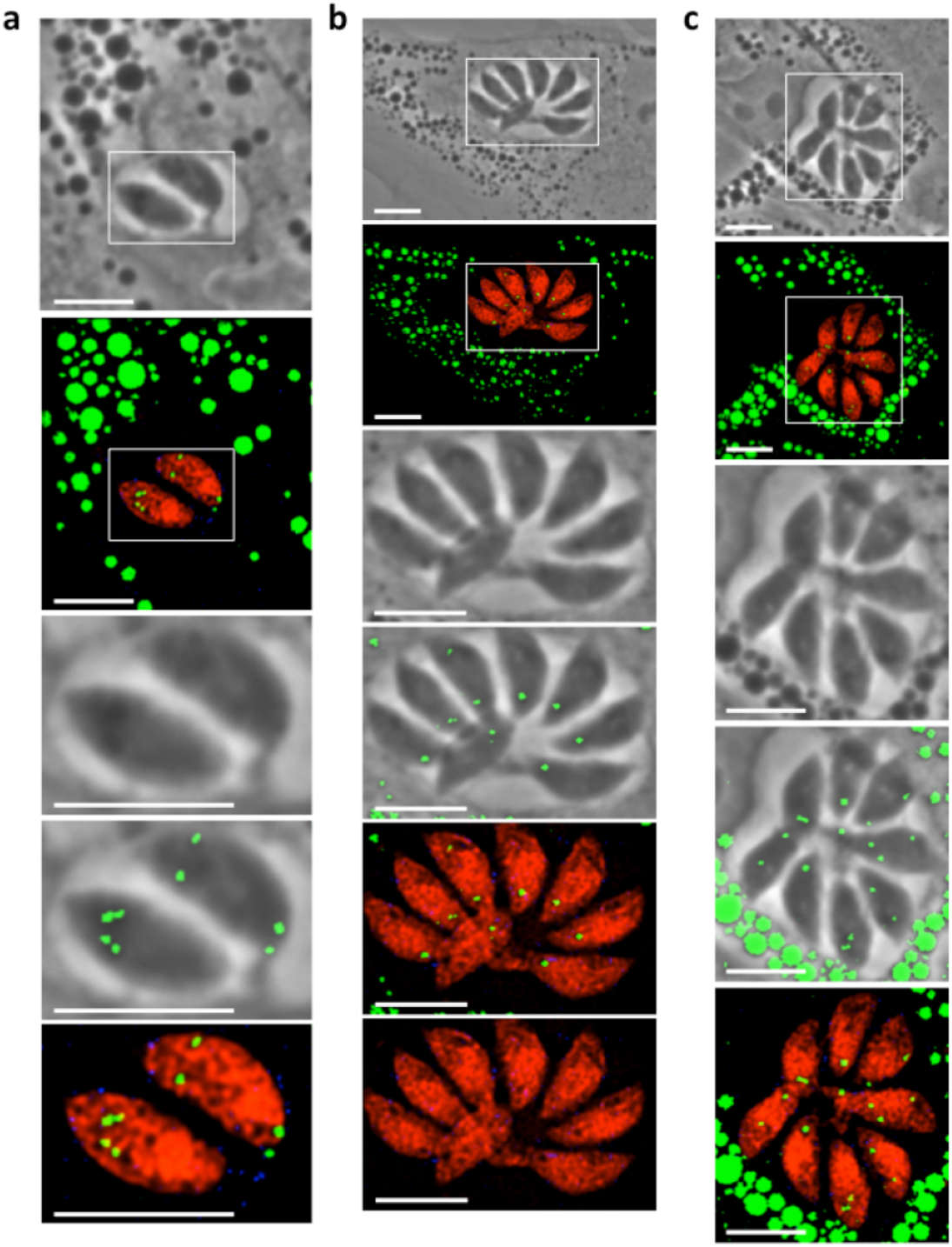

Figure 3-13 Detection of BODIPY 493/503 pre-labeled host LD in *Toxoplasma* (fixed cells).
Fluorescence microscopy of RFP-*Toxoplasma* and BODIPY 493/503 labeled host LD in HFF at 24 h infection. The same protocol displayed in Fig. 3-8 was used to pre-label LD in HFF with BODIPY 493/503 prior to infecting with RFP-expressing *Toxoplasma* for 24 h. Coverslips were fixed prior to viewing by microscopy. Small PV (a) and large PVs (b, c) display green BODIPY labeling, indicating the uptake of neutral lipids directly from host LD. Scale bars, 7 µm.

3.4.7. Quantification of [^{3}H]OA uptake by the parasite

We wanted to quantify the uptake of host derived NL by *Toxoplasma* by measuring the presence of radiolabeled OA originating from host LD, into the parasite. LD were induced in HFF by incubating with either 0.1 mM or 0.4 mM OA mixed with traces of [^{3}H]OA for 24 h. After washing, cells were infected with *Toxoplasma,* and parasite egress was induced at 24 or 36 h p.i. using the calcium ionophore A23817 (Endo *et al*, 1982). Parasites were collected, purified from cellular debris and the radioactivity associated with parasite preparations was determined (Fig. 3-14). Tritiated material was incorporated into *Toxoplasma* proportionally to OA concentration, amounts stored in host LD and the infection time (Fig. 3-14.A). These data provide additional evidence that the parasites can acquire lipids associated with host LD, though, it remains a possibility that *Toxoplasma* can divert radioactive OA from other cell compartments than LD.

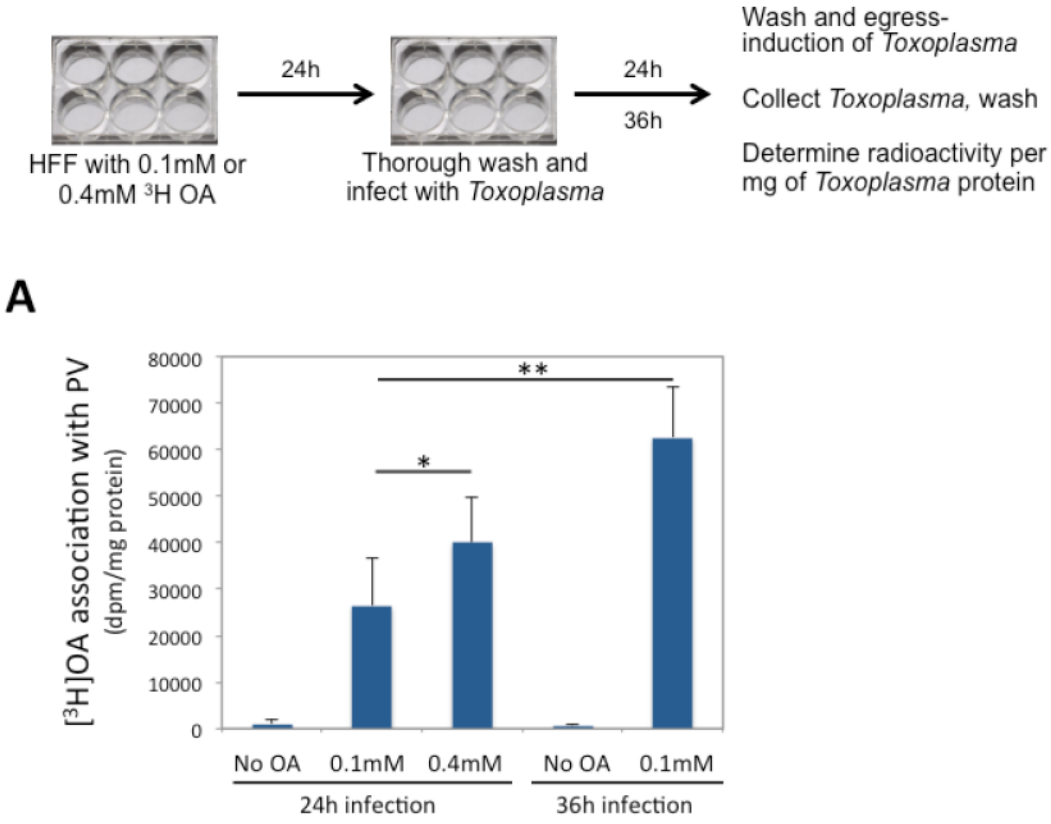

Figure 3-14. Quantification of [^{3}H]OA association with the parasite.

Schema outlining the experimental protocol for the formation of [^{3}H]-labeled LD in HFF, infection with *Toxoplasma* and measurement of [^{3}H]OA association with the parasite. **A.** Quantification of [^{3}H]OA levels in *Toxoplasma*. HFF were incubated with 0.1 mM or 0.4 mM [^{3}H]OA for 24 h, thoroughly washed and infected with *Toxoplasma* for 24 or 36 h before chemically inducing parasite egress. Parasites were collected, washed and purified to determine the radioactivity and protein contents. Means ± SD of assay triplicates. p^* <0.05; . p^{**} <0.001.

3.4.8. Host LD protrude into the PV of *Toxoplasma* and are trapped in the PV lumen

Our data suggests that lipids present in host LD can be detected in the parasite. Several mechanisms could be involved in this process such as the exportation of effectors by the parasite that could retrieve lipids from host LD, or the scavenging of host LD intact into the PV, as observed for other host organelles (Coppens *et al*, 2006; Romano *et al*, 2013). The gathering of host LD around the PV favors the second scenario. We thus conducted ultrastructural studies by EM due to its high resolution in order to visualize the distribution of host LD in *Toxoplasma*-infected cells. HFF infected with *Toxoplasma* were incubated with 0.2 mM OA and then processed for EM. In many instances, we observed host LD in close proximity to the PVM of *Toxoplasma* (Fig. 3-15.A). Some host LD were seen deeply protruding into the PV (Fig. 3-15.B panels a and b) whilst other host LD were found in the PV lumen (Fig. 3-16, panels a and b). Host LD were unmistakently detected within the PV lumen, as characterized by identical size, electron-density and shape as those located in the host cytoplasm. Interestingly, intraluminal LD were surrounded by tubules of the IVN (Fig. 3-16, panel a), a network hypothesized to be involved in nutrient uptake and trafficking within the PV (Coppens *et al*, 2006).

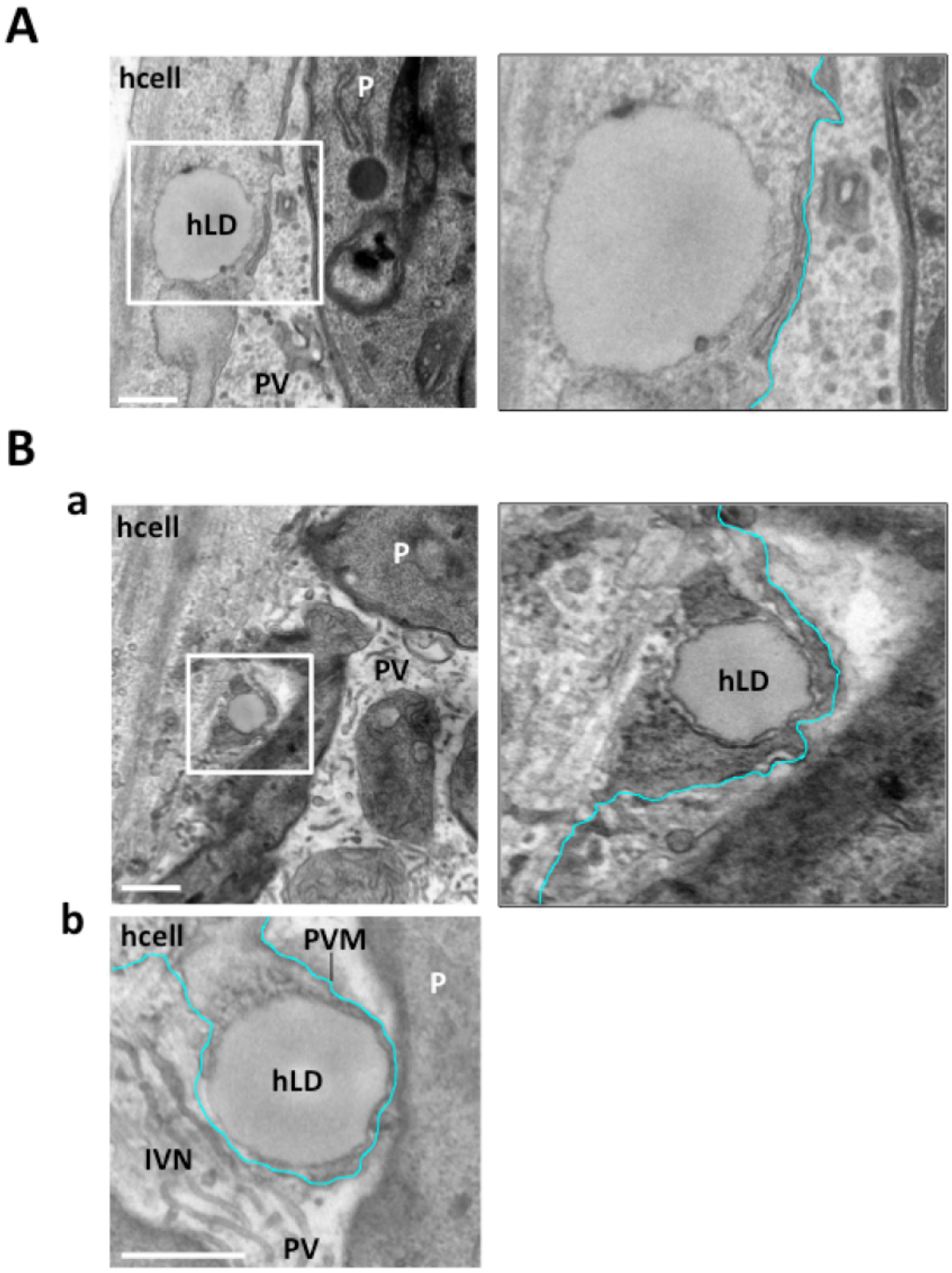

Figure 3-15. Ultrastructural evidence of host LD protrusion to PV.

A-B. EM of infected HFF with 0.2 mM OA showing a host LD in close proximity to the PV (A) or largely protruding to the PV lumen (B) at various degrees, shallow depth (a) and deeper in the PV membrane (PVM) (b). Cyan line in magnified panel represents the PVM of *Toxoplasma*. Scale bar, 0.2 µm.

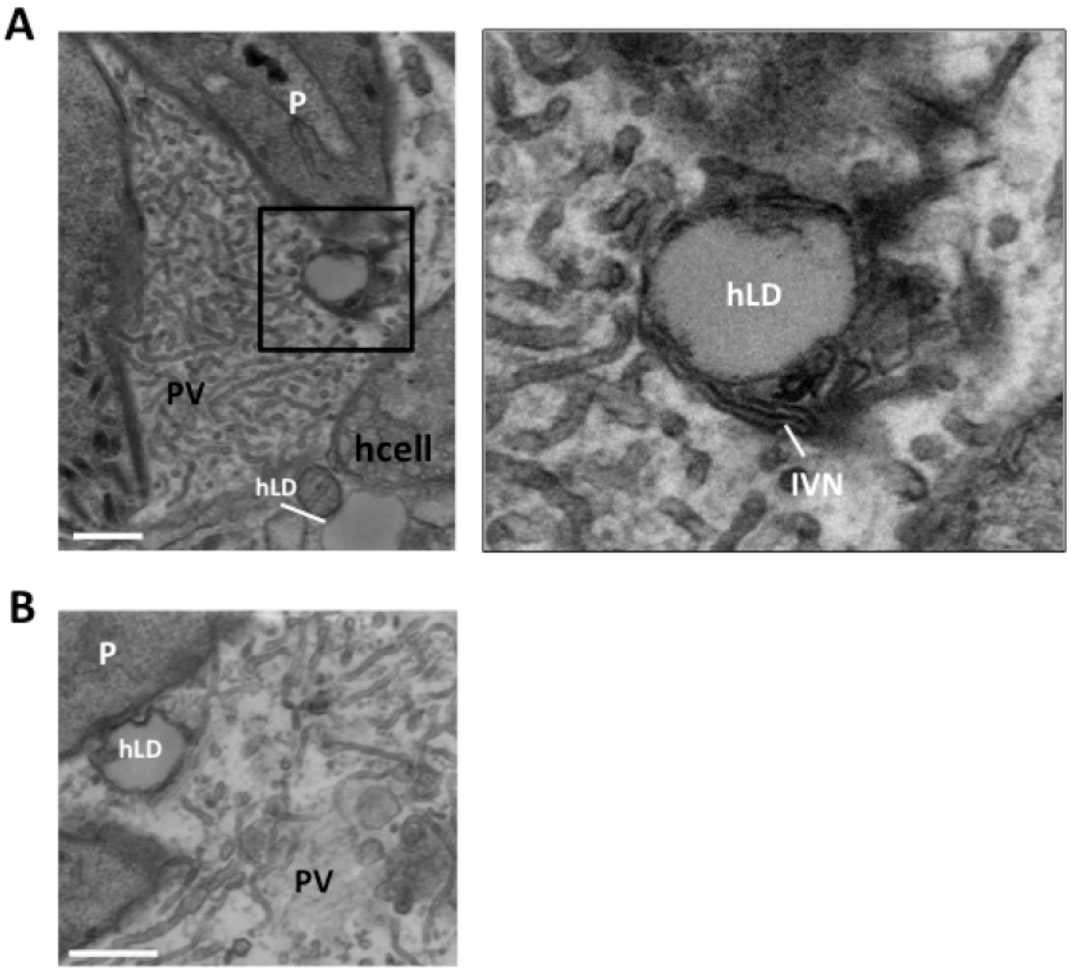

Figure 3-16. Ultrastructural evidence of host LD inside the PV.

A-B. EM of infected HFF with 0.2 mM OA showing host LD wrapped by the intravacuolar network (IVN) within the *Toxoplasma* PV. Host LD trapped in the PV were identified based on their electron density and similar size to LD present in the mammalian cytoplasm. Scale bar, 0.1 µm.

3.4.9. Rab7-GTPase associated with host lipid droplets are trapped in the *Toxoplasma* PV

Our lab previously found that host mammalian Rab14, Rab30 and Rab43 vesicles containing lipids (e.g., ceramides, sphingolipids) can be diverted by intracellular Apicomplexa including *Toxoplasma* and *Neospora caninum,* and sequestered into the PV (Romano *et al*, 2013; Nolan *et al,* 2015). In mammalian cells, several Rab vesicles intersect with LD trafficking pathways as some Rab GTPases proteins have been detected on LD. While Rab7 is known to regulate trafficking and maturation of endosomes it has also been implicated as a principal regulator of lipophagy and is found on 10% of LD (Schroeder *et al*, 2015; Oseki *et al*, 2005). Rab18 localizes to ~ 50 % of LD, especially those located close to the ER, and its presence is negatively correlated with ADRP expression. We thus wanted to investigate whether Rab7- or Rab18-associated LD may selectively be re-routed to the PV allowing *Toxoplasma* to have access to their NL cargo.

Next, we wanted to confirm that Rab7 localizes, at least in part, to LD in our system. HFF were transfected with a plasmid containing an mCherry-Rab7 construct, incubated with 0.2 mM OA for 24 h then fixed for microscopy observations of mCherry-Rab7-vesicles and host LD, stained with BODIPY 493/503. Fig. 3-17.A shows partial colocalization (yellow, PDM) between the red mCherry and the green BODIPY signals (PCC: 0.129), primarily on the surface of the LD., confirming published data (Ozeki *et al*, 2005). mCherry-Rab7-expressing HFF were infected with *Toxoplasma* for 24 h and stained for BODIPY 493/503 and colocalization events could also be observed between host Rab7 vesicles and host LD. Upon the addition of OA, the number of number of foci containing the two signals increased dramatically (Fig. 3-17.B). Quantification of this increase was performed by counting the number of green (LD) foci and yellow (PDM) foci in both uninfected and infected cells. On average, the addition of 0.2 mM OA led to a 3 fold

increase in yellow foci in uninfected HFF, and a 2 fold increase in *Toxoplasma*-infected HFF ($p < 0.005$) (data not shown).

Having confirmed the localization of Rab7 to LD in uninfected cells, we next performed assays to visualize the potential presence of Rab7 foci within the PV of *Toxoplasma*. Since the mCherry-Rab7 construct used in Fig. 3-17 did not emit a strong enough fluorescence signal in our experimental conditions to conclusively detect mCherry-Rab7 inside the PV, we transfected cells with a plasmid containing a GFP-Rab7 construct showing brighter fluorescence in the green channel (Fig. 3-18). GFP-Rab7-expressing HFF were infected with *Toxoplasma* for 24 h with 0.2 or 0.4 mM OA or without OA, fixed and immunostained for GRA7 to delineate the PVM. Several GFP-Rab7 foci were observed inside the PV, as visualized in the XYZ image, in all conditions (Fig. 3-18.A, panels a-c). Quantification of the percent of PVs containing at least one GFP-Rab7 foci showed an average of 60 % of positively stained PV without OA, whilst addition of 0.2 mM or 0.4 mM OA led to a statistically significant increase up to 90 % (Fig. 3-18.B).

In infected GFP-Rab18-expressing HFF we observed GFP-Rab18 positive vesicles inside ~ 40 % of PV of *Toxoplasma* (Fig. 3-19.A, panels a-c). In contrast to GFP-Rab7 assays, there was no significant increase in the percent of PVs containing Rab18 in the presence of 0.2 or 0.4 mM OA (Fig. 3-19.B).

The data show that host Rab7 and Rab18 are present inside the PV. Based on these observations, we hypothesize that if host LD are marked with Rab7 and/or Rab18 and found within the PV, this may represent a way for the parasites to have access to NL.

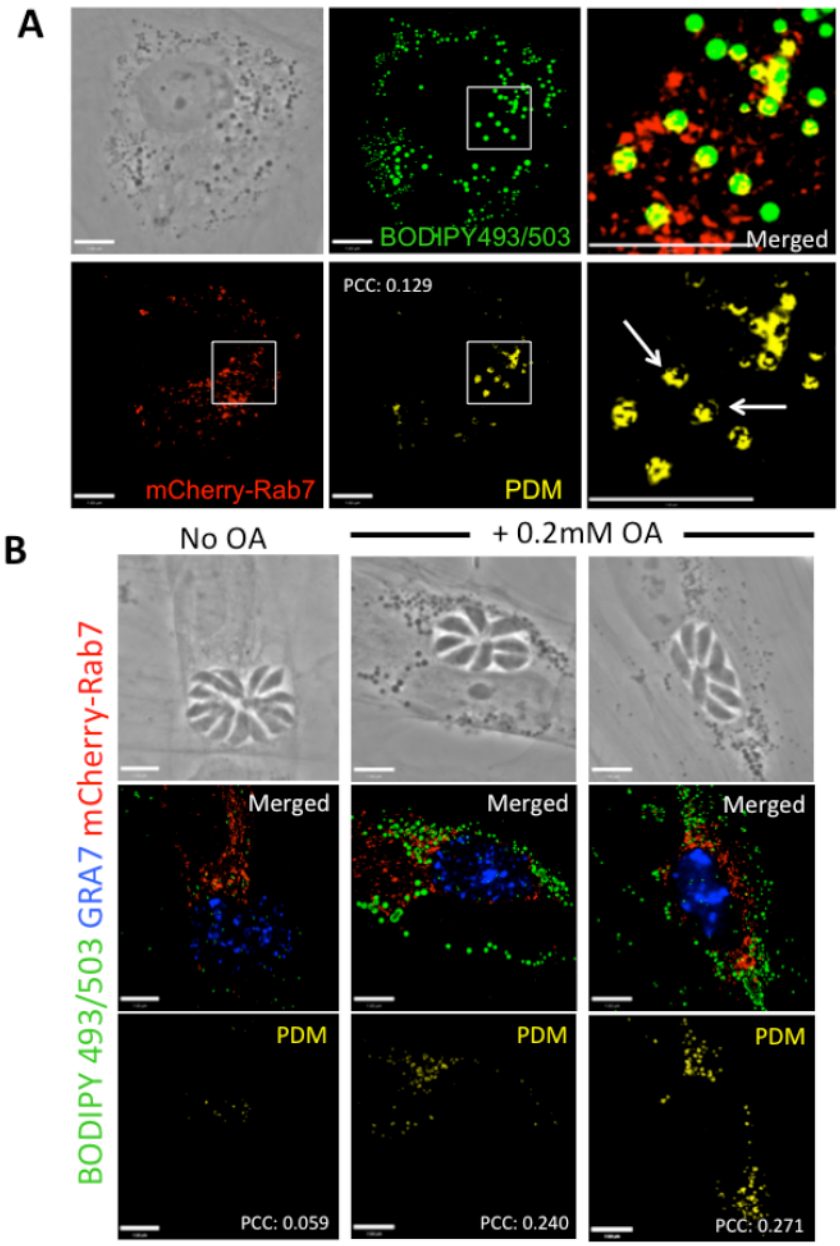

Figure 3-17. Codistribution of host Rab7 vesicles with BODIPY 493/503-stained structures in mammalian cells.

A. Fluorescence microscopy of HFF expressing mCherry-Rab7. HFF expressing the mCherry Rab7 constructs were fixed and stained with BODIPY 493/503. Extended-focus images are shown for the BODIPY 493/503 (green), mCherry Rab7 (red) and the positive PDM (yellow, indicating colocalization, Pearson's Correlation Coefficient: 0.129). A subset of host LD colocalize with mCherry-Rab7 indicating that some host LD possess Rab7 at their surface (white boxes highlighting areas of colocalization, arrows). Scale bars, 7 µm. **B.** Fluorescence microscopy of infected HFF expressing mCherry Rab7 grown in normal α-MEM medium, or in the presence of 0.2 mM OA. Transfected mCherry-Rab7 HFF were infected with *Toxoplasma* and incubated with 0.2 mM OA for 24 h, fixed and stained with BODIPY 493/503 (green) and anti-GRA7 antibodies (blue, PV). Two representative extended focus images of merged and PDM (yellow) show increased colocalization events between mCherry Rab7 and BODIPY 493/503 when cells were incubated with 0.2 mM OA. Colocalization foci were confirmed by analyzing the Z-slices. Scale bars, 7 µm.

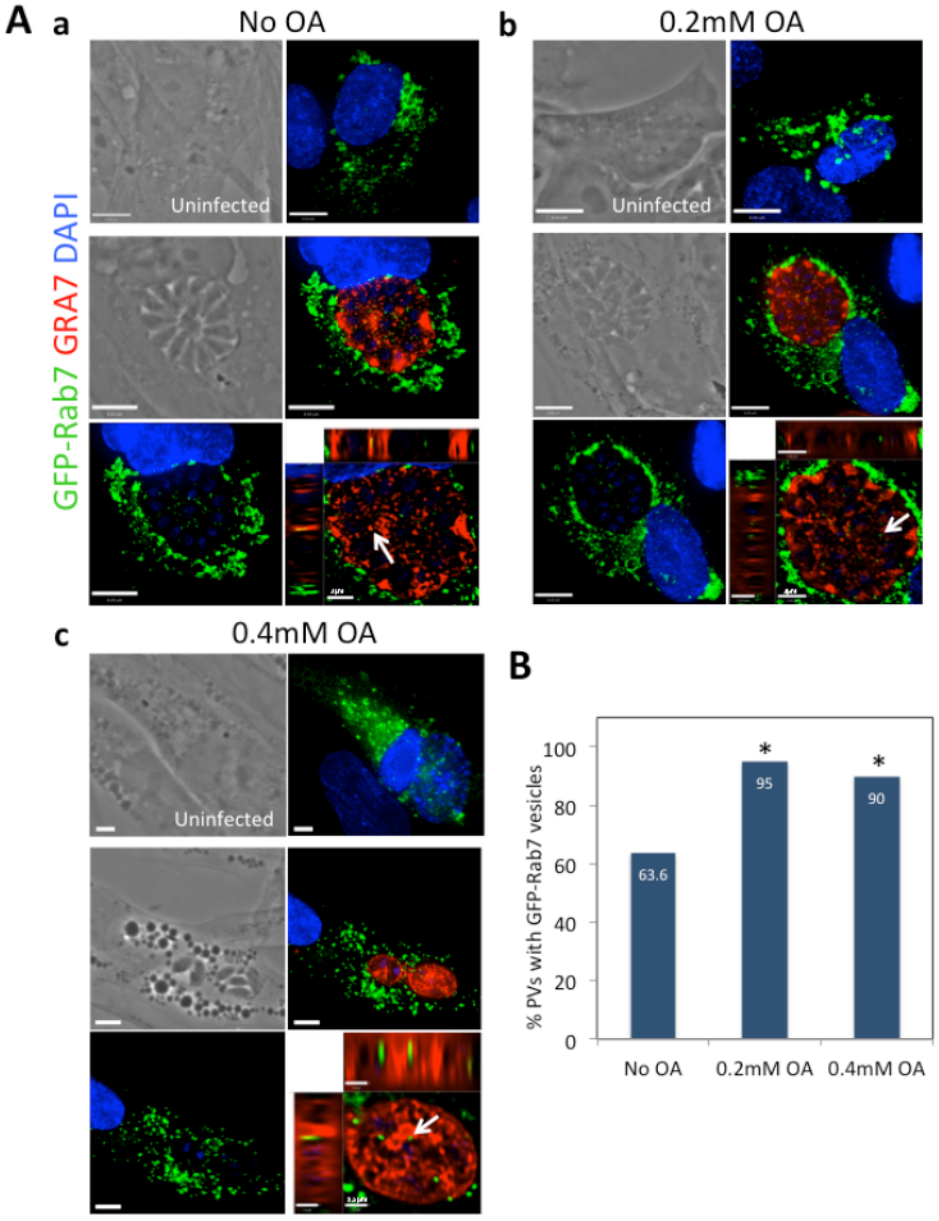

Figure 3-18. Detection of host Rab7 vesicles in the PV.

A. Fluorescence microscopy of uninfected or *Toxoplasma*-infected HFF expressing GFP-Rab7 grown without OA (a), with 0.2 mM OA (b) or 0.4 mM OA (c). GFP-Rab7 transfected HFF were infected with *Toxoplasma* and incubated for 24 h in the indicated concentrations of OA. Coverslips were fixed and stained with antibodies for GRA7 (red, parasite PVM and PV lumen) and 4-,6-diamidino-2-phenylindole (DAPI; blue, nucleus). The distribution of GFP-Rab7-positive vesicles (green) is shown in these extended-focus images in both uninfected and infected cells. Cropped images of the *Toxoplasma* PV is also shown in an optical XYZ slice to highlight the localization of host-derived GFP-Rab7 vesicles inside the PV of *Toxoplasma* (arrows). Scale bar, 7 µm unless specified. **B.** Quantification of the percentage of PVs positively containing GFP-Rab7 vesicles from (A). The percent of PVs containing Rab7 foci, determined by XYZ visualization of cropped PVs in GFP-Rab7 transfected HFF, increases when cells were incubated in the presence of 0.2 or 0.4 mM OA. Representative of duplicate experiments, n>20 in each experiment; Chi-squared test, $p^* < 0.05$.

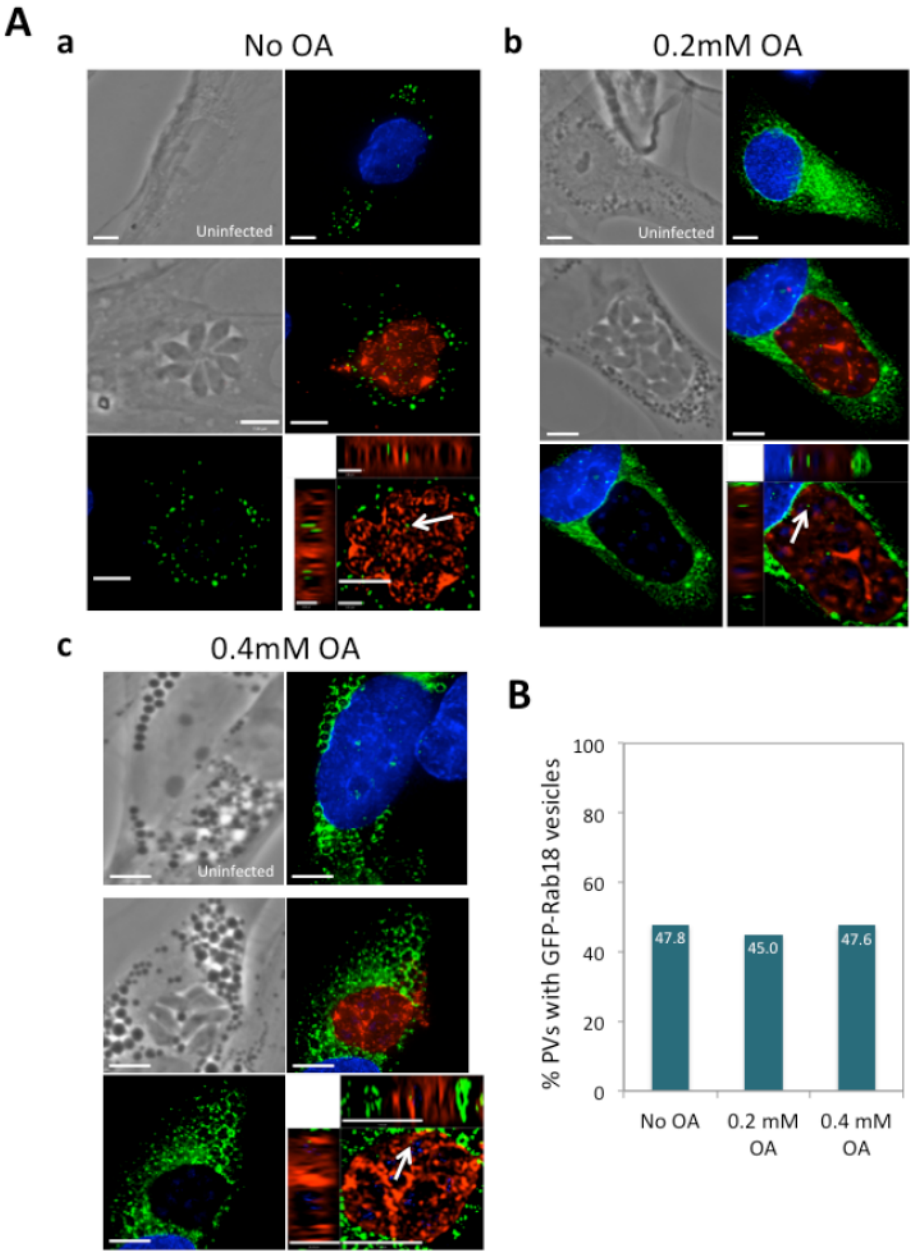

Figure 3-19. Detection of host Rab18 vesicles in the PV.

A. Fluorescence microscopy of uninfected or *Toxoplasma*-infected HFF expressing GFP-Rab18 grown without OA (a), with 0.2 mM OA (b), or 0.4 mM OA (c). GFP-Rab18-transfected HFF were infected with *Toxoplasma* and incubated for 24 h in the indicated concentrations of OA. Fixed cells were stained with antibodies for GRA7 and 4-,6--diamidino-2-phenylindole (DAPI; blue, nucleus). The distribution of GFP-Rab18-positive vesicles (green) is shown in these extended-focus images in both uninfected and infected cells. A cropped image of the *Toxoplasma* PV at various OA concentrations is also shown in an optical XYZ slice to highlight the localization of host-derived GFP-Rab18 vesicles inside the PV, arrows. Scale bar, 7 µm. **B.** Quantification of the percentage of PVs containing GFP-Rab18 vesicles. XYZ visualization of cropped PVs was used to determine the presence of GFP-Rab18 inside the PV, and plotted in the histograms. There is no statistical difference in the uptake of GFP-Rab18 to *Toxoplasma* PVs when incubated with OA. Representative of duplicate experiments, n>20; Chi-squared test, non significant.

3.4.10. Upon excess OA incubation, *Toxoplasma* shows endocytic activities

Compelling morphological evidence revealed that host Rab vesicles, organelles and LD are sequestered into the PV of *Toxoplasma* (Coppens *et al,* 2000; Coppens *et al,* 2006; Romano *et al*, 2013). We hypothesize that this feature is orchestrated by the parasite to usurp their nutrient content. To acquire nutrients present in the PV, the parasite expresses several transporters or translocators on its PM that can mediate the internalization of lipids, amino acids or sugars by simple diffusion or active transport (reviewed in Robibaro *et al*., 2001). In regard to endocytic mechanisms for the uptake of macromolecules, *Toxoplasma* is an intriguing organism since no internalization gates have been identified so far for this pathogen, and the question whether *Toxoplasma* is able to incorporate large extracellular material into an internal membrane system is still disputable since the parasite is lacking canonical lysosome-like compartments and digestive enzymes. One intriguing feature of the PM of the parasites is the presence of a small cup-shaped invagination (20 nm in diameter), the micropore, that is covered by filamentous coat material (Nichols *et al*, 1994). While this structure brings to mind endocytic-like PM invaginations, the micropore is static and its physiological role e.g. in nutrient uptake, has not yet been demonstrated. The genome of *Toxoplasma* contains homologues coding for the AP2 complex, and the light and heavy chains of clathrin but does not express these proteins at the PM to form clathrin-coated pits (reviewed in Field *et al*, 2007). No caveolin homologues can be retrieved from the parasite genome data, and therefore *Toxoplasma* lacks PM domains with the characteristic features of caveolae. In conclusion, the current dogma is that *Toxoplasma* is refractory to endocytosis, and solely relies on transport activities across the PM to have access to nutrients.

During our in-depth scrutiny of the ultrastructure of *Toxoplasma* exposed to 0.2 mM OA, we observed a very large invagination of the parasite PM, with a narrow neck and a diameter of,

on average, 250 nm. This open structure was usually located at the anterior pole of the mother parasite, close to the apex, and was never found on dividing parasites during endodyogeny (Fig. 3-20, panels a and b). This structure was distinct from the micropore by its larger size and more post-nuclear localization. Based on the following observations, we hypothesize that this structure may represent an endocytic gate as opposed to an exocytic cup: 1) the content of the invagination was identical to that of the PV lumen indicative of a connection between these structures and the PV milieu, and 2) their cytoplasmic surface was often coated with a radiating bristle-like structure, reminiscent of the clathrin coat of mammalian coated pits (Fig. 3-20, all panels). Moreover, although the presence of these structures were not a rare occurrence when incubated with excess OA, they were exclusively detected in these conditions i.e., gavage conditions, since *Toxoplasma* cannot regulate nutrient intake.

If these structures contribute to the endocytosis of PV material, we might expect the presence of endocytic structures within the parasite's cytoplasm. Our EM studies reveal several structures intriguingly similar in electron-density and morphology to those found in the close vicinity of the parasite in the PV, like membrane whorls (Fig. 3-21, all panels), suggestive of endocytic vesicles. These data may represent the first evidence of an endocytic event associated with an intravesicular system within the parasite, likely involved in nutrient uptake and delivery to the *Toxoplasma* interior. This also might imply that endocytic processes must be particularly fast in this parasite, due to the untrackability of these endocytic profiles under normal conditions.

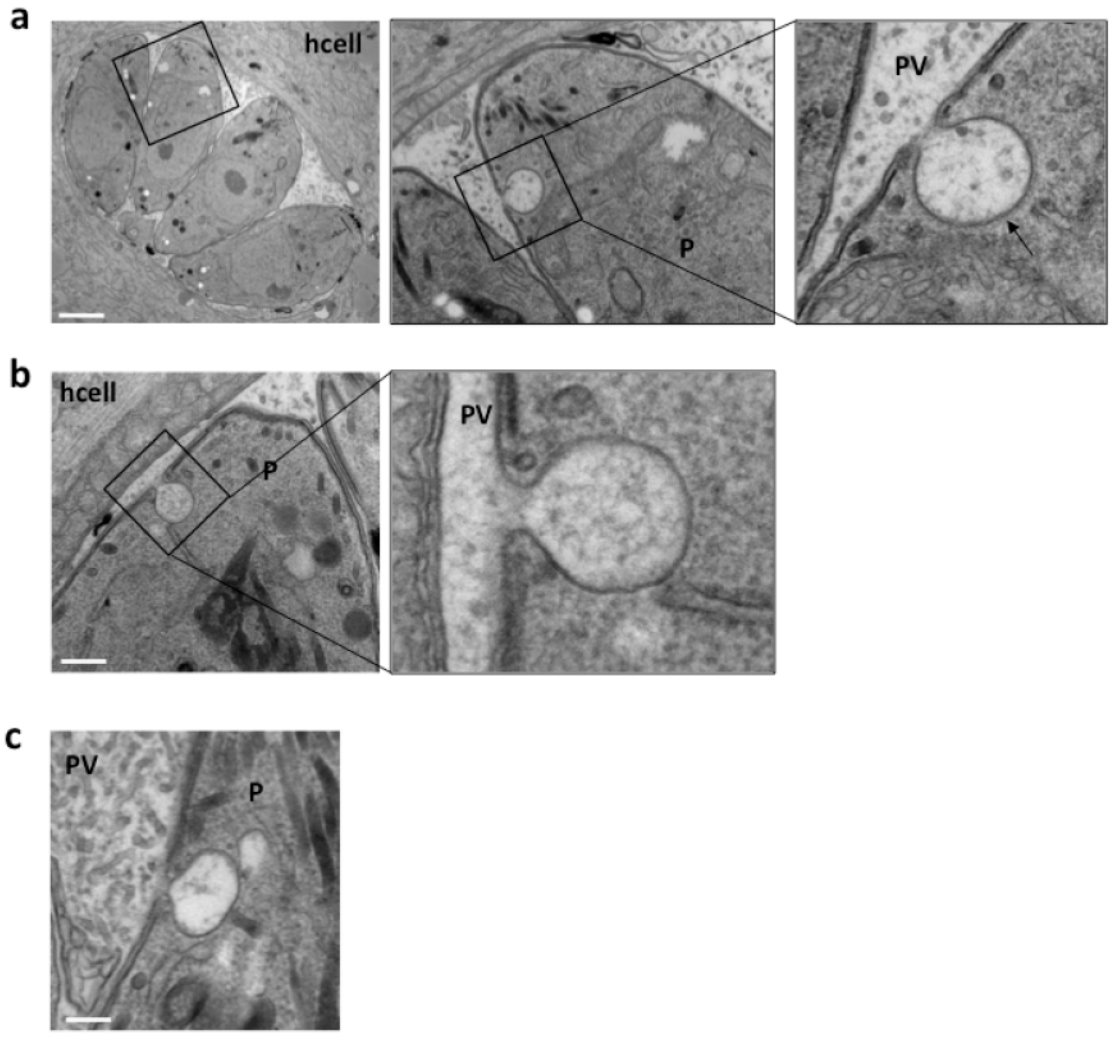

Figure 3-20. Ultrastructural detection of endocytic pits on the parasite plasma membrane.
EM of parasites in HFF incubated with 0.2 mM OA for 24 h. Structures resembling endocytic pits docked onto the parasite plasma membrane are observed at the apical end of the parasite. The double-membraned pits appear to be coated with protein (arrow) indicating an endocytic event, and appear to be in the process of pinching off (a, b) or nearly completely pinched off (c). The content of the pits display a striking resemblance to the material present in the PV lumen. Scale bars, 1 µm (a), 0.3 µm (b) and 0.4 µm (c).

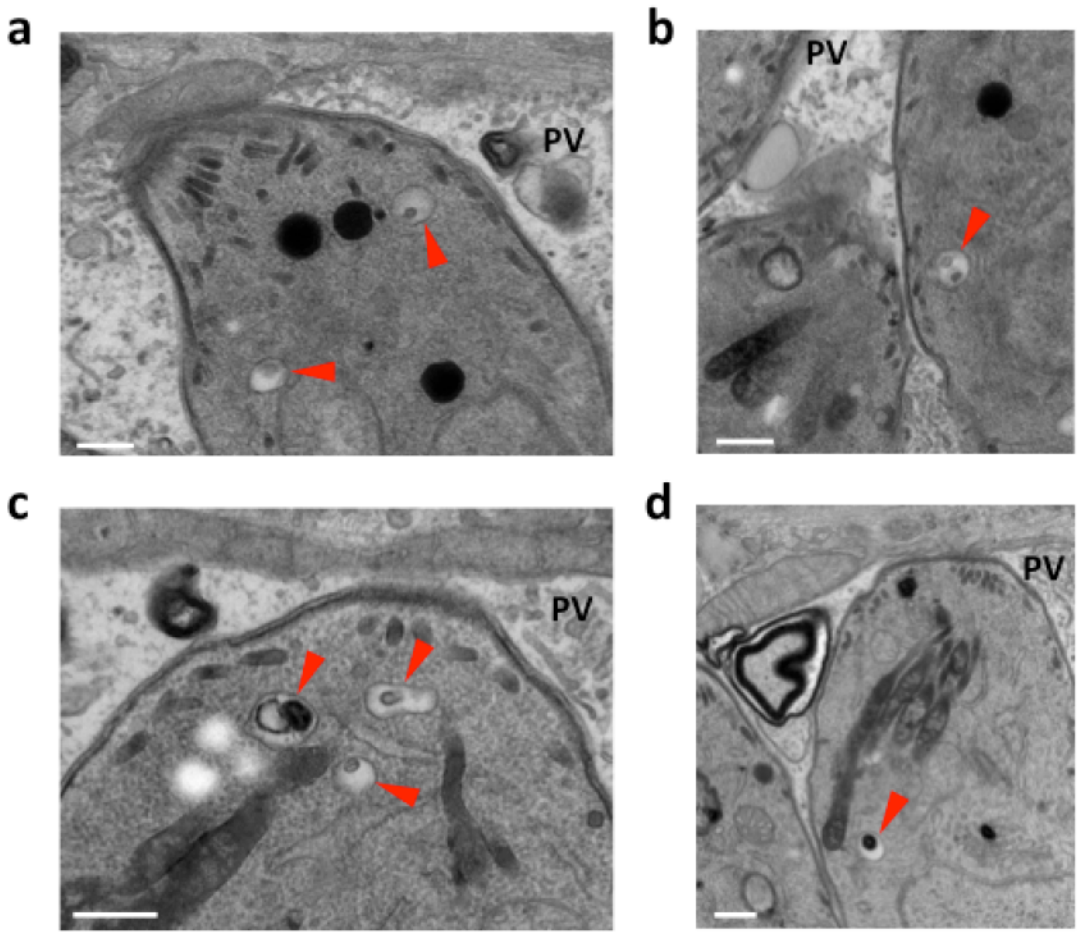

Figure 3-21. Ultrastructural detection of PV lumen material inside endocytic vesicles in *Toxoplasma*. **a-d.** EM of parasites in HFF incubated with 0.2 mM OA for 24 h showing intraparasitic vesicles containing lipophilic material similar to that present in the PV lumen (red arrowheads). These structures are hypothesized to have originated from an endocytic process of PV lumen material. Scale bar, 0.3 µm.

3.5. DISCUSSION

Toxoplasma gondii requires vast amounts of lipids for the biogenesis of new membranes for its daughter cells during replication, which occurs every 6-8 h in cell culture. One way *Toxoplasma* obtains these needed lipids is to scavenge lipids species such as cholesterol, fatty acids, sphingolipids or lipid precursors from host organelles such as endolysosomes or the Golgi (Charron and Sibley, 2002; Quittnat *et al,* 2004; Coppens *et al*, 2006; Romano *et al*, 2013). In this study, we demonstrated that *Toxoplasma* has the capacity to scavenge NL; e.g., fatty acids (FA) from host lipid droplets (LD). These NL, present in LD, may not solely provide the building blocks of membranes but may also function as energy sources as some lipids like FA are substrates for β-oxidation in mitochondria and ATP generation.

One of the most abundant FA in humans and animals is the monounsaturated 18:1 cis9 fatty acid, oleic acid (OA). OA is present in the blood (complexed to albumin), is highly abundant in adipose tissue, and is associated with membranes in many cell types (Baylin *et al*, 2002; Hodson and Fielding 2013; Lopez e*t al*, 2014). Human serum contains around 7.5 mM of FA, of which OA is the most profuse FA species at 38 %, followed by palmitic acid (25 %), linoleate acid (22 %) and stearic acid (10 %) (Richieri and Kleinfeld,1995). Adipose tissue is composed of adipocytes, highly specialized cells for the storage of energy and fat, particularly in the form of TAG. In these cell types, OA makes up over 40% of all fatty acids, predominantly in membranes and in a single enormous LD (Seidelin, 1995; Baylin *et al*, 2002). In the plasma membrane (PM) of human cells, the concentration of free OA is between 1-2%, on average, of all lipids, a number that can rise nearly two-fold in individuals on a Mediterranean diet, rich in olive oil. Oleic acid is the main constituent of olive oil, accounting for up to 83% of its composition (Vicario *et al*, 1998;

Funari *et al*, 2002; Lopez *et al*, 2014). In human fibroblasts, one of the major cell types most commonly used in *Toxoplasma* research, up to 3% of total lipids is OA (Schroeder *et al*, 1984).

The molecular structure of OA affects the organization, structure and function of membranes. The kink in the structure of OA at the 9th carbon helps organize membranes into non-lamellar phase, induces negative curvature and therefore helps govern the fluidity of the membrane matrix (Khandoker *et al*, 1997; Funari *et al*, 2003; Lopez *et al*, 2014). At higher OA concentrations in the membrane, membrane fluidity is increased. Other FA like palmitic or stearic acid do not affect membrane fluidity to the same extent due to their molecular structure. The saturation of these FA causes them to be tightly packed together in the PM (Funari *et al*, 2003). As well as influencing membrane fluidity, OA can act as a signaling molecule at the plasma or nuclear membrane, affecting various cellular and protein functions directly. OA can signal through G-protein-coupled receptors leading to cellular transcriptional changes, activation of ERK1/2, PI3K or Akt, or cause an increase of cytosolic calcium levels (Funari *et al*, 2003; Hara *et al*, 2011).

The addition of OA to cell culture has several downstream effects including increased LD-related transcriptional and metabolic activities, increased OA in membranes, and the upregulation of autophagy. Adding exogenous OA to cells leads to an increase in LD biogenesis due to an accumulation of intracellular TAG levels as a result of increased *DGAT* and *ADRP* expression (Listenberger *et al,* 2003; Fujimoto *et al*, 2006; Thörn and Bergsten, 2010; Mei *et al*, 2011; Ahn *et al*, 2013). Membranes are also affected by excess OA which tends to accumulate within the bilayer, increasing the baseline level of OA in membranes from 18% to 39% of all FA in human macrophage cell lines and Caco-2 epithelial cells (Nowak *et al*, 2011; Jackson *et al*, 2009). Addition of OA can also lead to an upregulation of autophagy in order to catabolize free FA. The buildup of free FA such as OA can be harmful for cells and cause lipotoxicity. This results

in cellular dysfunction and death by apoptosis via the generation of reactive oxygen species (ROS) and nitric oxide (NO) (Shimabukuro *et al*, 1997; Ostrander *et al*, 2001; Listenberger *et al*, 2003; Ricchi *et al*, 2009; Mei *et al*, 2011).

In *Toxoplasma*-infected cells (HFF or HeLa), host LD grouped around the PV of *Toxoplasma*. This perivacuolar localization became more obvious upon the addition of 0.2 mM OA that increases the numbers of LD in the host cell and LD clustered around the PV. The detection of host LD around the PV is consistent with other studies reporting such events around the PV in skeletal muscle cells and macrophages infected with *Toxoplasma* at 2 h, 6 h, and 24 h p.i., even though these studies did not use OA (Mota *et al*, 2014, Gomes *et al*, 2014). It seems unlikely that this process is triggered by the host cell in HFF for immune protection as OA lacks the carbon unsaturation at the omega-6 position, and therefore cannot contribute to the synthesis of eicosanoids, the primary immune modulator related to LD (Bartelli *et al*, 2000; Zhou and Nilsson, 2001). Eicosanoid production requires the FA linoleic acid, a 20-carbon polyunsaturated FA, the precursor to arachidonic acid. These findings suggest that the parasite may be mediating the observed clustering of host LD around the PV for lipid acquisition, a hypothesis supported by the detection of host LD in the PV lumen.

The number of LD in the host cell is not constant during *Toxoplasma* infection. Although the number of host LD initially doubles during the first 24 h of infection, the number of host LD then returns to levels observed prior to infection. An increase in host LD numbers has been reported in *Toxoplasma*-infected skeletal cells at 6 h, 24 h and 48 h p.i, but no decrease in LD number was reported by 48 h p.i. (Gomes *et al*, 2014). In contrast to HFF, skeletal muscle cells contain fewer LD at baseline (5 LD per cell) which may affect LD dynamics during the late stages of infection. Indeed, in these cell types, the number of LD rose only by 10 over the entire course of infection, which is less than our observed increase by 25 in HFF (Gomes *et al*, 2014).

Furthermore, *Toxoplasma* may undergo spontaneous stage conversion to bradyzoites in skeletal muscle cells, so the dynamics of the host cell and the parasite differs from our cell culture system (Ferreira-da-Silva *et al*, 2009). However, these experiments do suggest that *Toxoplasma* infection interferes with the host cell lipid metabolism. Indeed, large scale microarrays of HFF gene expression following *Toxoplasma* infection for 24 h revealed changes in host cell metabolism. An increase in host metabolic activities, such as glycolysis and the melavonate and squalene biosynthesis pathways was observed (Blader *et al*, 2001). Both of these pathways supply nutrients for the parasite, suggestive of the parasite boosting their activity. On the other hand, the host cell may be upregulating the activity of these enzymes to ensure it has enough nutrients for itself due to excessive scavenging by the parasite. The dynamic variation in LD numbers upon in *Toxoplasma*-infected HFF may therefore be a consequence of *Toxoplasma* infection in specific cell types. The decrease in LD by 24 h p.i. may be attributed to the deviation of lipid stores to the *Toxoplasma* PV. As the parasite replicates, its nutritional needs increase proportionally, and must scavenge lipids accordingly from the host cell. The progressive decline in host LD numbers could be due to the translocation and consumption of LD by *Toxoplasma*.

Addition of OA to cell culture leads to transcriptional changes in enzymes involved in LD metabolism. Incubation of MIN6 pancreatic cells with 0.5 mM OA for 6 h leads to a two-fold increase in *DGAT2* expression, and a 2-fold increase in intracellular TAG levels whereas in hepatocytes, TAG levels rose 3-fold (Mei *et al*, 2011; Thörn and Bergsten, 2010). Interestingly, 0.25 mM OA incubation of pancreatic AR42J cells leads to a slight, but significant increase in *DGAT2* expression (1.2x), similar to *DGAT* transcription in HFF with 0.2 mM OA (Ahn *et al*, 2013). An increase in *ADRP* expression in HFF with 0.2 mM OA incubation is detected but no change in *ACAT* expression is observed. The lack of *ACAT* expression is due to the preferential esterification of DAG over cholesterol with OA in mammalian embryonic fibroblasts,

hepatocytes and pancreatic cells (Ahn *et al*, 2013; Mei *et al*, 2011; Listenberger *et al*, 2003). In *Toxoplasma*-infected cells, the decrease in transcription of *ACAT, DGAT* and *ATGL* is surprising and could be explained by a dysregulation of the NL cycle in host cells upon parasite assault. Nevertheless, the decrease in *ACAT* and *DGAT* upon *Toxoplasma* infection mirrors our observation of a dwindling of host LD numbers 24 h p.i.

In the same fashion as in mammalian cells, *Toxoplasma* is responsive to excess OA. Incubation of infected HFF with 0.2 mM leads to the increase in expression of *TgDGAT*, concomitant with increased numbers of LD in the parasite, likely as means to store TAG or free OA. However, *Toxoplasma* seems incapable of regulating OA intake as exposure with OA up to 0.5 mM forces to parasite to store excessive lipids, resulting in a massive accumulation of numerous LD that occupy a large space in the cytoplasm, and even protruding out from the parasite. Another similar example of the unrelentless lipid scavenging activities of *Toxoplasma* is illustrated with cholesterol (Coppens *et al*, 2000). In host cells incubated with excess LDL (the source of cholesterol for the parasite), *Toxoplasma* takes up cholesterol in quantities that exceed its needs and must store the excess in LD that accumulate in the cytoplasm (Coppens *et al*, 2000; Nishikawa *et al*, 2005; Coppens *et al*, 2006) This can be detrimental to the parasite if incubated with ACAT inhibitors, which block cholesterol esterification into CE and consequently, LD formation (Coppens and Vielemeyer, 2005). The free cholesterol becomes toxic as it accumulates in the membranes of *Toxoplasma,* which are destabilized, leading to the destruction of the parasite (Nishikawa *et al*, 2005). Lipidomics studies may prove fruitful to investigate how excess OA affects the total lipid composition of the parasite to provide insights on lipid homeostasis in *Toxoplasma*.

Intact host LD were detected inside the PV of *Toxoplasma*. By tracking the movement of lipids such as C4-BODIPY-C9, BODIPY 493/503 or radiolabeled OA stored in host LD in

Toxoplasma-infected cells, we provide evidence that *Toxoplasma* can have access to these host cell-derived lipids. The mechanism of lipid acquisition by *Toxoplasma* was investigated by EM which hinted at the engulfment of intact host LD by *Toxoplasma*. Indeed, despite the PVM providing a safe haven for the parasite, it also creates a barrier for nutrient uptake. However, this membrane is permeable to small solutes (Schwab *et al*, 1994) and is composed of lipids derived from the host PM, and is therefore very dynamic and deformable. Indeed, the PVM can form long protruding tubules that pervade the host cytoplasm (Coppens *et al*, 2006) and invaginations in the PV. With the sharing of these characteristics, it is possible that the PVM functions as a PM and may be able to "phagocytose" or translocate larger structures such as vesicles, endolysosomes, and potentially LD. In fact, intact endolysosomes have been observed in the PV and are surrounded by the PVM, suggestive of a phagocytosis-like process (Coppens *et al*, 2006). Further confirmation of the presence of host LD in the PV would necessitate immunogold staining for a protein marker of LD such as ADRP. We have previously shown that both *Toxoplasma* and a closely related protozoan, *Neospora caninum* can take up host Rab vesicles (Rab14, Rab30, Rab43) containing lipids, possibly also via a phagocytosis-like mechanism (Romano *et al*, 2013; Nolan *et al*, 2015: Fig. 2-9, Chapter 2). This present study has added Rab7 and Rab18 to the list of Rab structures that *Toxoplasma* can reroute to its PV, with potentially NL as contents if these Rab proteins are present on LD leaflet. Other Rab proteins like Rab5, Rab7 and Rab10 are also associated to subsets of LD (Ozeki *et al*, 2005). It could be interesting to investigate if *Toxoplasma* can also hijack these Rab associated to the LD to assess the selectivity of this process of LD translocation.

Host LD trapped in the PV lumen are wrapped by the intravacuolar network (IVN), which is a membranous tubular network derived from vesicles exported by the parasite. The IVN contains mainly lipids derived from the host cell and dense granule proteins secreted by the

parasite (GRA2, GRA4, GRA6) (Caffaro and Boothroyd, 2011; Mercier *et al*, 2002; Labruyere *et al*, 1999). Analysis of the IVN by EM revealed that host LD in the PV lumen are completely surrounded by membranous tubules of the IVN, a process proposed to play a role in nutrient uptake and lipid scavenging. Interestingly, a recent study identified a phospholipase secreted by *Toxoplasma*, TgLCAT, which is distributed in the IVN and PM (Pszenny *et al*, 2015). This finding leads to the possibility that this enzyme could be implicated in the degradation of organelles or structures derived from the host cells such as LD, allowing the parasite to have access to their nutrients liberated in the PV lumen. Interference with the IVN using parasites lacking GRA2 and GRA6 proteins would be an interesting direction to investigate if translocation of host LD still occurs.

The intravacuolar bacterium *Chlamydia trachomatis* has similar post-invasion events as *Toxoplasma* such as association with the host ER, mitochondria, Golgi apparatus and host endolysosomes. The bacterium also scavenges lipids from the host cell such as cholesterol and ceramide (Romano and Coppens, 2013). Moreover, host cytoplasmic LD are translocated into the inclusion body of the bacterium, which adds another analogous feature shared between the two pathogens (Romano and Coppens, 2013; Cocchiaro *et al*, 2008). Similarly to the data shown here, intact host LD are detected within the replicative niche of the bacterium. Interestedly, in *Chlamydia*-infected cells, ADRP is cleaved off the host LD prior to translocation to the inclusion of *C. trachomatis*. *C. trachomatis* secretes 3 bacterial proteins that interact with ADRP to form a complex prior to LD translocation to the inclusion body named LC1, LC2 and LC3 (Cocchiaro *et al*, 2008). It would be interesting to test to what extent the activities of *Toxoplasma* mirrors *Chlamydia* spp. The parasite effector on the PVM that mediates the recognition and internalization of host LD remains to be identified by cross-linking assays and co-immunoprecipitation with a host LD protein.

The mechanism by which *Toxoplasma* takes up lipids internalized to the PV is unknown. *Toxoplasma* contains several protein transporters located on the PM for the active transport of lipids, nucleotides, amino acids or hexoses (reviewed in Blader and Saeij, 2010). Exposure of *Toxoplasma* to 0.2 mM OA revealed previously unreported large invaginations of the parasite PM, containing material present in the PV lumen, as well as intra-parasitic vesicles. This highlights that *Toxoplasma* may also able to endocytose macromolecules and vesicles present in the PV. The identification of these endocytic structures solely under conditions of oversaturation of the parasite with large amount of fatty acids may suggest that this hypothesized process of endocytosis occurs much faster in *Toxoplasma* cultivated under normal nutritional conditions. Actually, the process might occur too fast to have ever been captured before. Alternatively, it is possible that these proposed endocytic structures are normally present in *Toxoplasma* but are too small to be noticed, and that the ingested fatty acids in large quantities can subsequently modify the properties of the PM, e.g. fluidity or curvature, which leads to the formation of endocytic structures of considerable size and capacity. Nevertheless, this discovery will open new prospects in the study of the endocytic trafficking machinery in *Toxoplasma*.

CHAPTER 4

INFLUENCE OF EXCESS MONO-UNSATURATED FATTY ACIDS ON THE INTRACELLULAR DEVELOPMENT OF *TOXOPLASMA*

4.1. ABSTRACT

The obligate intravacuolar Apicomplexan parasite, *Toxoplasma gondii*, develops in a parasitophorous vacuole from where it scavenges lipids such as cholesterol, ceramides, phospholipids and fatty acids from the host cell. Previous studies have shown that high amounts of cholesterol and ceramides added to the culture medium stimulate parasite replication. Nothing is known about the influence of excess fatty acids on *Toxoplasma*'s growth. Surprisingly, we show that addition of the monounsaturated 18:1 cis9 fatty acid oleic acid (OA) at harmless concentrations for the mammalian host cell (0.2 to 0.4 mM), has a detrimental effect on *Toxoplasma* development, impairing both the replication and egress of the parasite. We document that OA does not hinder the parasite's ability to associate with host organelles, nor does it act as a stressor inducing stage conversion to the parasite cyst form or bradyzoite. Increased autophagic activities in the host mediated by excess OA do not seem to harm the parasite. We hypothesize that the cause of the developmental defect of intravacuolar *Toxoplasma* is likely due to a particularly high sensitivity of the parasite to OA, leading to lipotoxic damage. At the morphological level, we observed numerous lipid deposits including excess, large lipid droplets that filled the parasite cytoplasm and a variety of lamellar lipid structures accumulated within the PV. This reflects a dysregulation in lipid metabolism and intracellular trafficking due to ectopic overaccumulation of lipids in intravacuolar parasites.

4.2. BACKGROUND

This section includes a brief synopsis of Chapter 3 plus general background information on the intracellular development of *Toxoplasma* and fatty acid metabolism that is relevant for the studies in this chapter on the influence of host fatty acid on *Toxoplasma* infectivity.

4.2.1. Synopsis of Chapter 3

The focus of chapter 3 was to determine whether the Apicomplexan *Toxoplasma gondii* could manipulate host cell LD and scavenge neutral lipids (NL) from them as previously observed for other lipid-filled organelles. Previous studies have reported the scavenging of many different lipid species by the parasite including cholesterol, ceramides, phospholipids, sphingolipids and fatty acids (Coppens *et al*, 2006; Romano *et al*, 2013; Quittnat *et al,* 2004; Nishikawa *et al*, 2005; Charron and Sibley, 2002; Tomavo *et al*, 1989). Neutral lipids (NL), e.g. triacylglycerols (TAG) or sterol esters (SE) are the primary lipids for energy storage across the tree of life. TAG consists of 3 fatty acids (FA) and a glycerol molecule, and SE consists of a steryl conjugated to a FA. Addition of the fatty acid oleic acid (OA) at a concentration of 0.2 mM to cells leads to a dramatic accumulation of LD (Listenberger *et al,* 2003; Fujimoto *et al*, 2006; Mei *et al*, 2011; Thörn and Bergsten, 2010; Ahn *et al*, 2013), and is therefore a useful technical tool to track host LD and monitor NL uptake by the parasite.

Our previous data suggests that *Toxoplasma* attracts host LD to its PV, has access to the host's NL reserves and stores the NL in its own LD. This salvage process may involve the internalization of host LD into the PV as observed by electron microscopy, and by visualizing the distribution of Rab proteins associated with LD inside the PV by fluorescence microcopy.

Interestingly, the results from chapter 3 highlight that *Toxoplasma* is unable to regulate its uptake of OA by feedback mechanisms, making it potentially vulnerable to lipotoxic damage. Moreover, the work from chapter 3 has also hypothetically identified novel endocytic events and vesicles in the parasite under the conditions of lipid gavage.

With the knowledge that excess OA leads to LD accumulations in the parasite, at least partially via NL uptake from host LD, our focus was shifted to the potential benefit of this process for the parasite. In fact, the addition of other lipid species such as excess cholesterol or ceramides leads to a boost in *Toxoplasma* replication (Coppens *et al*, 2000; Nishikawa *et al*, 2005; Romano *et al*, 2013). Therefore we hypothesize that excess FA may also be beneficial for parasite replication.

4.2.2. Intracellular development of *Toxoplasma*

Toxoplasma gondii is an Apicomplexan parasite capable of infecting any mammalian nucleated cell. There are 3 major steps involved in the intracellular development of *Toxoplasma*: invasion, replication and egress (reviewed in Blader *et al*, 2015).

Active invasion of a cell by *Toxoplasma* is a parasite-mediated event, as opposed to a cell-induced process or phagocytosis. Following host cell penetration, the parasite is surrounded by a parasitophorous vacuolar membrane (PVM), derived from lipids from the plasma membrane (PM) of the cell of which host cell PM proteins were excluded. The PV is resistant to fusion with host cell organelles such as endolysosomes and evades the cytosolic immune surveillance pathways. The PV therefore serves as a protective compartment for *Toxoplasma* in which to replicate. The PV localizes to the perinuclear region of the cell and associates with host

organelles and structures such as mitochondria, the ER, the Golgi, microtubules and the microtubule-organizing center (MTOC) (reviewed in Romano and Coppens, 2013). Very shortly after cell invasion, the host rough ER distribution is intensely altered by *Toxoplasma* (Sinai *et al*, 1997). Within 4 h following invasion, the PV of *Toxoplasma* is covered with host ER elements and is localized to the perinuclear region of the cell, a process mediated by the anchoring of the PVM to the ER envelope (Sinai *et al*, 1997; Romano *et al*, 2008). Similarly, close association and concentration of host mitochondria around the PV is also apparent 4 h p.i. (Sinai *et al*, 1997). The recruitment of mitochondria to the PV is, at least in part, mediated by a secreted parasite protein, TgMAF1 (Pernas *et al*, 2014). Association of the PV with host cell organelles is hypothesized to facilitate nutrient transfer and acquisition by the parasite. Nutrient acquisition from the host cell is imperative to ensure optimal growth rates. For example, *Toxoplasma* cannot synthesize cholesterol *de novo*, and must scavenge it from the host cells, in part by endolysosome uptake to the PV (Coppens *et al*, 2000; Coppens *et al*, 2006).

Within the PV, *Toxoplasma* replicates every 6-8 h *in vitro* by a process termed endodyogeny whereby two daughter cells are formed within one mother cell. The small remnants of the mother cells are collected in a structure called the residual body, located in the center of the PV, whose contents are expelled into the PV lumen prior to degradation by an unknown mechanism. When the PV is full of parasites and the host cell can no longer support the growth of the parasite, egress ensues. This is a parasite-mediated event dependent on calcium signaling, leading first to the destruction of the PVM, then the host cell PM and finally the emergence of fresh parasites ready to invade another cell.

Further details on the intracellular development of *Toxoplasma* can be found in the first chapter of this thesis.

4.2.3. Fatty acids overview

Lipids are non-polar organic molecules that are distinguished by their high solubility in non-polar solvents and insolubility in water due to the presence of long hydrophobic hydrocarbon chains. These chains can be saturated between carbon atoms (all single bonds) or unsaturated (double of triple covalent bonds). Lipids are a diverse group of compounds including oils, waxes, fats, sterols and phospholipids and are amphipatic molecules as they have both hydrophobic and hydrophilic regions.

The functions of lipids are very broad but their three primary roles are: 1) membrane constituents, 2) energy storage, and 3) hormone production. Firstly, lipids are found in all cell membranes of all prokaryotes and eukaryotes organisms. Membranes are the defining feature of the basic unit of life, the cell, and also form all the subcellular compartments in eukaryotes. Secondly, lipids tend to be reduced molecules and so oxidation of these compounds releases vast amounts of energy. Thirdly, lipids are the building blocks of hormones, essential for many signal transduction events in the body and between cells.

4.2.3.1. Fatty acids

Among lipids, fatty acids (FA) are long chain hydrocarbon molecules with a carboxylic moiety at one end (Fig. 4-1). FA are essential for life as they perform 3 roles: 1) they are the building blocks of more complex membrane and non-membrane lipids, 2) they can be stored as energy in the form of TAG, and 3) they are the precursors for the synthesis of bioactive lipids involved in signaling.

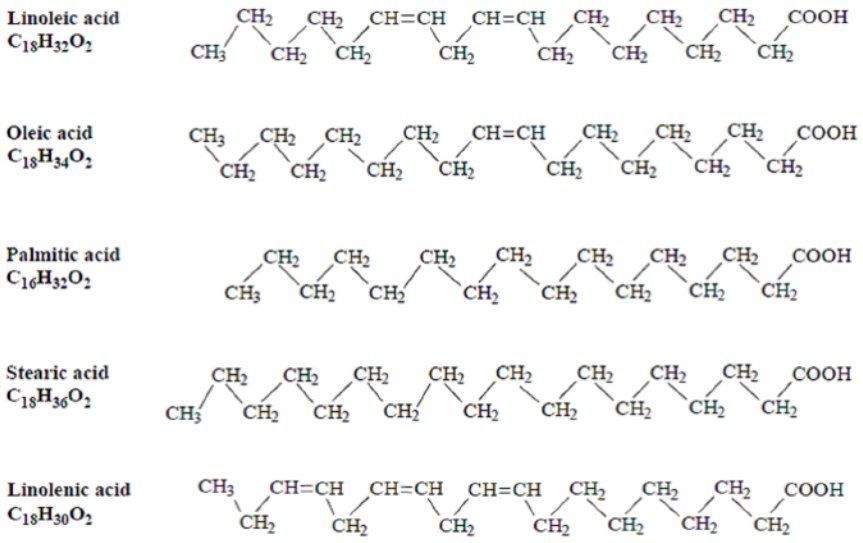

Figure 4-1. Chemical formula and structure of the most common fatty acids in mammals. Diagram from Karacor and Cam, 2015.

FA are major constituents of membranes, usually bound to phospholipids or cholesterol esters but around 1-2% of lipids in membranes are free FA (FFA) (Funari *et al*, 2003). Of all the FFA in membranes, the most abundant in fibroblasts are 42% OA, 22% palmitic acid (PA), 13% stearic acid and 9% palmitoleic acid (Maziere *et al*, 1980).

4.2.3.2. Endogenous FA synthesis and degradation

The synthesis of FA occurs in the cytosol, whereas their degradation occurs primarily in the mitochondrial matrix (Berg *et al*, 2002). The synthesis of FA involves several enzymes collectively named fatty acid synthases (FAS) that perform several reactions. The first committed step to FA synthesis is acetyl-CoA carboxylation to generate malonyl-CoA. Several more reactions take place in the cytosol using intermediates linked to the sulfhydryl groups of an acyl carrier protein (ACP), and eventually ending with the 16-carbon palmitic acid (PA). The majority of the acetyl-CoA for the initial FA synthesis step originates from pyruvate by the enzyme pyruvate dehydrogenase (PDH) within the glycolytic cycle in the mitochondrion. Pyruvate is therefore a critical molecule linking the conversion of carbohydrates to FA. As an aside, the glycerol molecule needed for TAG generation is also produced in the glycolytic pathway.

FA degradation occurs in the mitochondria or peroxisomes by β-oxidation. This involves the activation and transport of FFA bound to CoA to the mitochondrion, followed by cleavage of two carbons every cycle, generating acetyl-CoA. The degradation of FA is not simply a reversal of FA synthesis since the acetyl-CoA generated cannot re-enter the FA synthesis pathway in the cytosol, and instead enters the citric acid cycle in the mitochondrion. Additionally, the two processes use two distinctive sets of enzymes, occur in distinct cellular locations and are mutually inhibitory.

4.2.3.3. Fatty acid uptake by mammalian cells

Most of the FA present in the serum is esterified but 2-5 % of FFA are bound to albumin (Wang *et al*, 2008). FFA in the serum are generated via the hydrolysis of TAG-rich lipoproteins by lipases within the endothelial lumen, and subsequently bound to albumin (Doege and Stahl, 2006). The mechanism by which FFA are released from albumin is unknown but increased albumin levels in the serum can stimulate FFA release (Richieri and Kleinfeld, 1995). Transport of FFA across plasma membrane can occur either by passive diffusion, or binding to protein carriers such as fatty acid transport protein complexes (FATP), as well as binding to cell-surface proteins such as CD36 which deliver the FFA to the FATP. Following the binding of FA to proteins in the PM, albumin dissociates from the FA prior to cell entry (Doege and Stahl, 2006). FFA may also be incorporated into cellular PM, which also necessitates albumin removal. FFA can also act as signal transducers on the cell surface e.g. by binding toll-like receptors (TLR) in the innate immune response, or binding G-protein-coupled receptors in the PM.

4.2.3.4. Fatty acid destinations in mammalian cells

Upon cell entry, fatty acid binding proteins (FABP) help remove FFA carriers bound to FFA such as FATP and bind FFA themselves. FABP then mediates the trafficking of FFA to many different cellular compartments (Doege and Stahl, 2005) (Fig. 4-2). Alternatively, FFA may be activated by CoA, yielding acyl-CoA destined for oxidative degradation. The coupling of FFA to CoA is performed by long-chain fatty acyl-CoA synthetases in the cytosol. Acyl-CoA can then be transported throughout the cell by acyl-CoA binding protein (ACBP) (Rustan and Drevon, 2005; Furuhashi and Hotamisligil, 2008).

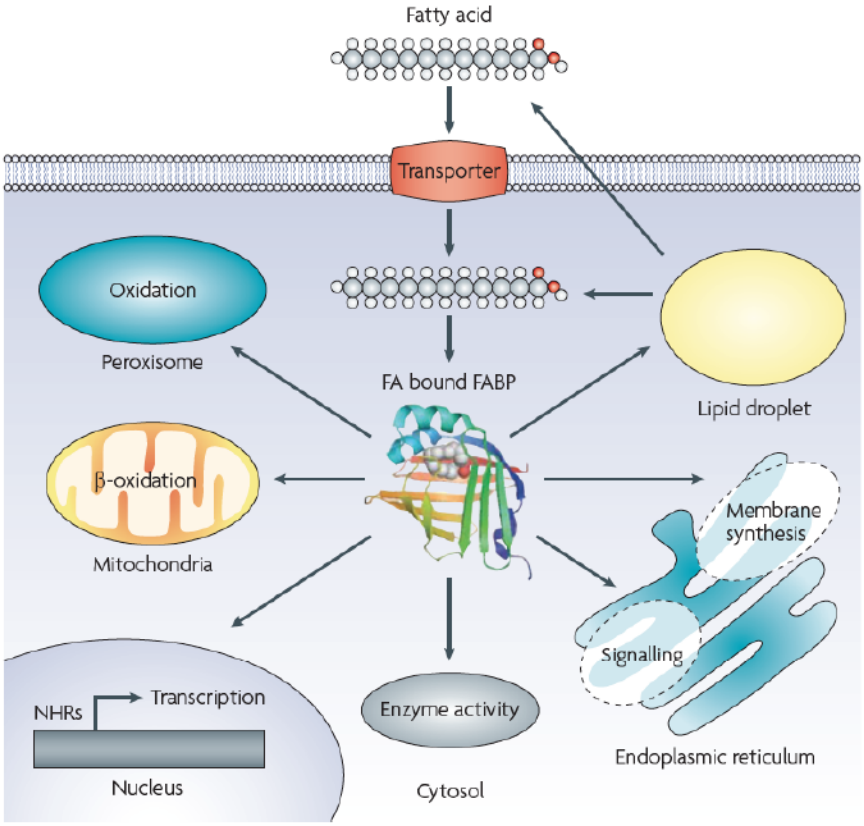

Figure 4-2. Cellular fatty acid trafficking by fatty acid binding proteins.

Following the intracellular uptake of fatty acid (FA), fatty acid binding proteins (FABP) bind FA for subsequent trafficking throughout the cell. Organellar destinations include the mitochondria and peroxisomes for β-oxidation, lipid droplets for storage, the endoplasmic reticulum for membrane synthesis and signaling, and the nucleus for the control of FA-mediated transcriptional programs.

Image from Furuhashi and Hotamisligil, 2008.

FA, such as OA, can be trafficked to the LD, ER, mitochondria, peroxisomes, and the nucleus. The fate of OA upon entering the cell depends on whether OA binds FABP directly or is activated by CoA first. In the former scenario, OA bound to FABP is shuttled to LD for its incorporation within these confines, particularly in order to prevent lipotoxicity. In the latter case, OA-CoA can then be bound by either FABP or ACBP, both of which can transport OA-CoA to mitochondria or peroxisomes for β-oxidation, or the endoplasmic reticulum (ER) for esterification to phospholipids, TAG or CE (McArthur *et al*, 1999). Alternatively in the ER, FA such as OA may be incorporated into membranes or signaling molecules also via esterification of DAG. Finally, FA can be converted into signaling molecules such as eicosanoids within LD or transported to the nucleus for the modulation of transcription factors that are mediated by lipids through nuclear hormone receptors (Furuhashi and Hotamisligil, 2008).

4.2.4. Effects of excess oleic acid on mammalian cells: lipolysis and lipophagy

4.2.4.1. Effects of oleic acid.

Oleic acid (OA) is a monounsaturated 18:1 cis9 fatty acid and is the most common FA in human serum, cellular membranes and adipose tissue (Baylin *et al*, 2002; Hodson and Fielding 2013; Lopez e*t al*, 2014). The kink at the 9^{th} carbon of OA helps organize membranes into non-lamellar phase, induces negative curvature and helps govern the fluidity of the membrane matrix (Khandoker *et al*, 1997; Funari *et al*, 2003; Lopez *et al*, 2014). The influence on membrane fluidity is specific to monounsaturated FA such as OA or linoleic acid since saturated FA like PA are not kinked and therefore tightly pack together in membranes (Funari *et al*, 2003). As well as influencing membranes fluidity, OA can act directly as a signaling molecule at the PM or the nuclear envelope through G-protein-coupled receptor binding which may lead to transcriptional

changes, activation of ERK1/2, PI3K or Akt, or increase of cytosolic calcium levels (Funari *et al*, 2003; Hara *et al*, 2011).

Addition of OA to the medium leads to the accumulation of intracellular TAG, an increase in DGAT activity and stimulation of LD biogenesis (Listenberger *et al,* 2003; Fujimoto *et al*, 2006; Mei *et al*, 2011; Thörn and Bergsten, 2010; Ahn *et al*, 2013; Dupont *et al*, 2014). In addition to changes in lipid metabolism, treatment of cells such as macrophages or epithelial cells with OA increases the baseline levels of this FA in membranes to nearly 40% of all FA (Nowak *et al*, 2011; Jackson *et al*, 2009).

4.2.4.2. Lipolysis and lipophagy

Lipids stored within LD can be metabolized by cytosolic neutral lipases, such as ATGL, by a process of lipolysis (reviewed in Chapter 1). Another process that leads to LD depletion from the cell is lipophagy, a selective form of autophagy targeting LD. LD containing NL and FA can be engulfed by autophagosomes and delivered to lysosomes for degradation by hydrolases (Liu and Czaja, 2013). The FA liberated from the LD can then be used for mitochondrial β-oxidation. Thus, lipophagy helps regulate energy homeostasis by modifying intracellular lipids supplies and FFA levels.

Lipotoxicity can severely damage the cell through the generation of reactive oxygen species (ROS) and nitric oxide (NO), leading to cellular and mitochondrial dysfunction, and cell death by apoptosis (Shimabukuro *et al*, 1997; Ostrander *et al*, 2001; Listenberger *et al*, 2003; Ricchi *et al*, 2009; Mei *et al*, 2011). Lipophagy has also been implicated as a critical pathway for the prevention of lipotoxicity. Different FA have different effects on cells in relation to LD metabolism and lipophagy.

Conflicting reports on the ability of OA or PA to induce lipophagy have been published, indicating cell type specificity in the ability of these FFA to induce lipophagy. Addition of palmitic acid to various cell types (fibroblasts, hepatocytes) inhibits lipophagy whereas addition of OA stimulates lipophagy (Singh *et al*, 2009; Las *et al*, 2011; Mei *et al*, 2011; Dupont *et al*, 2014). Another study described lack of lipophagy in hepatocytes treated with both 0.25 mM OA or 0.25 mM PA (Koga *et al*, 2010). Other studies have shown that OA does not stimulate lipophagy in pancreatic β-cells and fibroblasts, whereas it does in hepatocytes (Choi *et al*, 2009; Las *et al*, 2011; Tan *et al*, 2012; Tu *et al*, 2014). In general however, the induction of lipophagy is critical for resistance against lipotoxicity from FFA. Lipotoxicity occurs more readily with PA incubation as cells cannot efficiently sequester excess PA into LD or increase TAG biogenesis. Indeed, in hepatocytes and fibroblasts, no increase in LD numbers were observed when incubated with PA, in contrast to OA (Singh *et al*, 2009; Mei *et al*, 2011; Tan *et al*, 2012).

4.2.5. Chapter goals:

In this chapter, we investigated the effects of excess OA on the intracellular development of *Toxoplasma* in mammalian fibroblasts. *Toxoplasma* scavenges from the host cell many lipid species such as cholesterol and ceramides. When these lipids are introduced in excess to the host cells, the replication of *Toxoplasma* is stimulated. However, in response to excess cholesterol in the medium, the parasite needs to store this lipid in LD (Nishikawa *et al*, 2005), as a safe mechanism to prevent damage from free cholesterol (Coppens *et al*, 2000; Romano *et al*, 2013).

In this chapter, the following questions will be addressed:

- Does excess OA introduced to the medium impact the development of *Toxoplasma*, e.g., its replication rate or ability to egress?
- Does the parasite exhibit signs of lipotoxicity upon incubation with excess OA?
- Is *Toxoplasma* still capable of recruiting host organelles, e.g., ER, mitochondria and Golgi to its PV, despite the accumulation of host LD around the PV?
- Does increased autophagy in the host cell upon excess OA affect the development of *Toxoplasma*?

4.3. MATERIALS AND METHODS

4.3.1. Reagents and antibodies

All chemicals were obtained from Sigma (St Louis, MO) or Fisher (Waltham, MA) unless otherwise stated. 4-Difluoro-1,3,5,7,8-Pentamethyl-4-Bora-3a,4a-Diaza-*s*-Indacene (BODIPY 493/503) was purchased from Life Technologies (Carlsbad, CA). The following primary antibodies were used: rabbit polyclonal anti-giantin (Covance, Emeryville, CA); rabbit polyclonal anti-GRA7 antibodies (Coppens *et al.*, 2006); mouse anti-KDEL (Stressgen, Assay Designs, Farmingdale, NY); rabbit monoclonal anti-TOM20 mouse polyclonal (Santa Cruz, CA). Secondary antibodies used for immunofluorescence were conjugated to Alexa^{488}, Alexa^{594} or Alexa^{350} (Invitrogen, Carlsbad, CA). For oleic acid (OA) preparations, sodium oleate was dissolved in H_2O at a concentration of 100 mM, then thoroughly mixed by vortexing (3 minutes) with 5% Fatty Acid Free BSA for a final concentration of 10mM to ensure BSA-OA complexes formation and stored in the dark at 4°C. For palmitic acid (PA) preparations, sodium palmitate was dissolved in 50% ethanol at a concentration of 100 mM and prepared subsequently identically as OA. Cells were incubated in medium with various final OA or PA concentrations.

4.3.2. Cell lines and culture conditions

Human foreskin fibroblasts (HFF) and HeLa cells were obtained from the American Type Culture Collection (Manassas, VA). GFP-ADRP HeLa cells were kindly provided by Raphael Valdivia (Duke University, North Carolina, USA; originally made by P. Targett-Adams and J. McLauchlan, Glasgow, UK). All cell lines were grown as monolayers and cultivated in α-minimum essential medium (MEM) supplemented with 10% fetal bovine serum (FBS), 2 mM glutamine and

penicillin/streptomycin (100 units/ml per 100 µg/ml), and maintained at 37°C in 5% CO_2 unless specified otherwise.

4.3.3. Parasite cultivation

The tachyzoites from the RH strain (Type I lineage) were used throughout this study. In one set of experiments, the Prugniaud (Type II lineage) strain of *Toxoplasma gondii* was used (kindly provided by David Roos, University of Pennsylvania, PA). *Toxoplasma* stably expressing RFP was generously provided by Florence Dzierszinski (McGill University, Montreal, Canada). The parasites were propagated *in vitro* by serial passage in monolayers of HFF (Roos *et al.*, 1994).

4.3.4. Mammalian cell transfection with LC3 constructs

The GFP-LC3 construct was a gift from Jennifer Lippincott-Schwartz, NIH, Rockville, MD. HFF were transfected using the Amaxa nucleofector kit V according to the manufacturer's protocol (Lonza, Basel, Switzerland) with 2.5 µg of plasmid DNA, and 16 h later infected with *Toxoplasma* for 30 minutes at 37°C, washed with PBS to remove extracellular parasites, and incubated for 24 h at 37°C.

4.3.5. Parasite assays

4.3.5.1. Development

For plaque assays, HFF were grown until confluence in a 6-well plate, infected with one hundred *Toxoplasma* RH parasites per well and the plates were incubated at 37°C for 5 days, with 0.2

mM OA, 0.4 mM OA or 0.2 mM palmitic acid, or in the absence of FA as a control. The cells were fixed and stained as described previously (Striepen and Soldati-Favre, 2013). The plates were scanned (ScanWizard 5, Microtek). The average area of the plaques was calculated using Volocity software and graphed in Excel (Microsoft).

4.3.5.2. Replication

Coverslips with confluent HFF were infected with RFP-expressing *Toxoplasma* RH for 30 minutes, thoroughly washed with PBS to remove extracellular parasites, and incubated without OA (control), 0.1 mM, 0.2 mM, 0.3 mM, 0.4 mM or 0.5 mM OA for 24 h. Coverslips were fixed with 4% formaldehyde plus 0.02% glutaraldehyde in PBS for 15 minutes and viewed with a Nikon Eclipse 90i equipped with an oil-immersion plan Apo 100x NA 1.4 objective and a Hamamatsu GRCA-ER camera (Hamamatsu Photonics, Hamamatsu, Japan). The number of parasites was recorded for at least 1000 PVs on the coverslip for each OA condition. The means of means for each condition is graphed as a percentage of all PVs recorded with standard deviations using Excel (Microsoft).

4.3.5.3. Egress

For natural egress assays, HFF were grown until confluence in a 6 well plate and $5x10^6$ parasites per well were allowed to invade cells for 1 h. Non-invading parasites were then washed away and infected cells were incubated up to 76 h in the presence of 0.2 mM or 0.4mM OA. Cells were fixed and observed using an inverted Microscope (Nikon, TE200) using a DIC filter. Images were taken using Spot Advanced Software (Diagnostic Instruments, Inc) and processed using

iMovie (Apple). For induced egress assays, HFF were grown until confluence in a 6 well plate and $5x10^6$ parasites per well were allowed to invade cells for 1 h, washed and incubated with 0.2 mM, 0.4 mM OA or without OA for 24 h. Egress was induced by adding the Calcium ionophore A23187 and time taken to egress was recorded by live image capture using an inverted microscope (Nikon, TE200). The time (in seconds) taken for individual PVs to egress from their host cells was recorded using Spot Advanced Software, and graphed as a ratio to control conditions (no OA) in Excel using the means of means and standard deviations.

4.3.5.4. Differentiation

To monitor tachyzoite-bradyzoite stage conversion, coverslips with confluent HFF were infected with *Toxoplasma* RH or *Toxoplasma* Prugniaud strain for 24 h with or without 0.2 mM OA at 5% CO_2, or in the absence of CO_2 as a condition control for differentiation induction. Coverslips were fixed and stained for lectin with TRITC-conjugated lectin from *Dolichos biflorus*, 4-,6-diamidino-2-phenylindole (DAPI) (Boothroyd *et al*, 1997, Prandovszky *et al*, 2011) and for the PV with antibodies against GRA7.

4.3.6. Fluorescence microscopy

Immunofluorescence assays (IFA) on HFF were performed as described previously (Karsten *et al*, 2004) with a 5 minute permeabilization step with 0.3% TritonX-100 in PBS following fixation with 4% formaldehyde (Polysciences, Warrington, PA) plus 0.02% glutaraldehyde in PBS for 15 minutes. Specific IFA with BODIPY 493/503 labeling was performed after the secondary incubation step for 30 minutes at 1:100 dilution in PBS, followed by three 5 minute PBS washes

prior to staining with 4-,6-diamidino-2-phenylindole (DAPI). Coverslips were mounted using ProLong Diamond Antifade Mountant (Life Technologies) to minimize bleaching during microscopy. Cells were viewed with a Nikon Eclipse 90i equipped with an oil-immersion plan Apo 100x NA 1.4 objective and a Hamamatsu GRCA-ER camera (Hamamatsu Photonics, Hamamatsu, Japan). Optical z-sections with 0.2 µm spacing were acquired using Volocity software (PerkinElmer, Waltham, MA). The images were deconvolved using an iterative restoration algorithm and the registry was corrected using Volocity software. Volocity and Photoshop (Adobe) were used to adjust brightness levels, cropping and resizing of the images obtained. To quantify host organelle-PV interaction, we used the quantitative image analysis software MetaScopics using the "Intensity by Distance" algorithm or the "Centroid to Surface Distance" algorithm as described (Nolan et al, 2015).

4.3.7. Electron microscopy

For transmission EM, HFF cells infected with *T. gondii* for 24 h or 72 h were fixed in 2.5% glutaraldehyde (EM grade; Electron Microscopy Sciences, Hatfield, PA) in 0.1 M sodium cacodylate buffer (pH 7.4) for 1 h at room temperature, and processed as described (Fölsch *et al.*, 2001) before examination with a Philips CM120 Electron Microscope (Eindhoven, the Netherlands) under 80 kV.

2.3.8. Uracil incorporation assay

HFF, Hela or ADRP-GFP HeLa cells were grown until confluent in 24-well plates before infection with $5x10^4$ parasites for 4 h at 37°C, washed with PBS and incubated for 21 h in MEM medium

containing 0.1, 0.2 or 0.4 mM OA or PA. Cells were then incubated with 1 µCi of [^{3}H]uracil for 2 h at 37°C and the samples were processed as described previously (Roos *et al*, 1994).

4.3.9. Statistical methods

Data were displayed in box plots using Kaleidagraph software (Synergy Software) or graphed in Excel (Microsoft). Means and standard deviations were calculated from three independent experiments using Excel (Microsoft). P-values were calculated using student's *t*-test in Excel.

4.4. RESULTS

4.4.1. Excess oleic acid impairs the intracellular development of *Toxoplasma*

Although *Toxoplasma gondii* can synthesize *de novo* many of the lipids required for its intracellular growth, it must also scavenge others from the host cell. The latter include lipids that the parasite is unable to synthesize as well as lipids that, despite being produced *de novo* by the parasite, are not synthesized in large enough amounts to satisfy the parasite's needs (Charron and Sibley, 2002; Quittnat *et al,* 2004; Coppens *et al*, 2006; Sampels *et al*, 2012; Romano *et al*, 2013). This is emphasized by the fact that the addition of large amounts of lipids such as ceramides and cholesterol to the medium of infected cells has been shown to boost the replication of *Toxoplasma in vitro* (Coppens *et al*, 2000; Romano *et al*, 2013), presumably by favoring membrane biogenesis for replication. In fact, *Toxoplasma* takes up various fatty acids from the medium for incorporation into lipids and proteins (Tomavo *et al*, 1989; Charron and Sibley, 2002; Nishikawa *et al*, 2005; Romano *et al*, 2013; Chapter 3). In this study, we investigated the effects of exposure of the parasite to 20-times excess oleic acid (OA), exogenously added to the medium, on parasite growth. We hypothesize that such a large supply of FA would be beneficial for the parasite

The development of *Toxoplasma* was first examined by plaque assays in the presence of 0.2 and 0.4 mM OA over 5 days allowing for several cycles of invasion, growth and egress of the parasite (Fig. 4-3.A). The presence of OA in the medium led to significantly smaller plaques, correlating to OA concentration, as we observed a 50 % and 65 % reduction in average plaques sizes following incubation with 0.2 mM and 0.4 mM OA, respectively (Fig. 4-3.B). These data demonstrated that there is a global impairment of parasite development with OA incubation. To assess if this detrimental effect of excess OA on parasite development is specific for this FA, we

performed the same assay with 0.2 mM palmitic acid (PA) added to the medium. There was no change in parasite development with excess PA, as the average plaque size was not significantly altered as compared to treatment without excess FA. Only plaque size, not the number of plaques, were altered with OA incubation, suggesting that invasion is not affected by this FA.

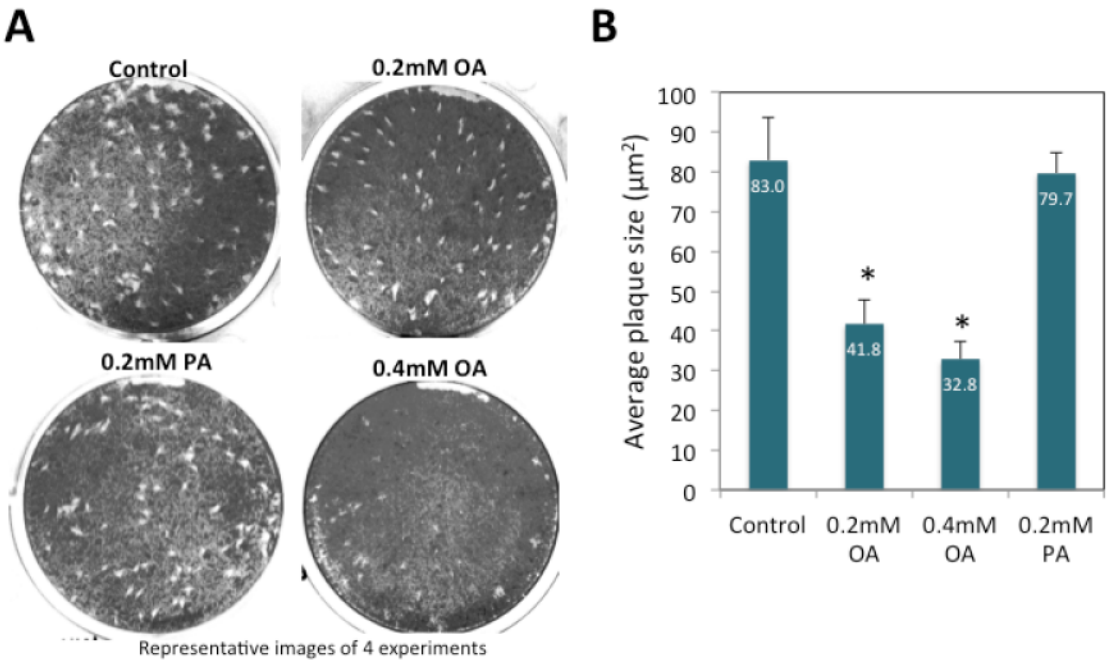

Figure 4-3. *Toxoplasma* development with incubation of fatty acids.

A. Plaque assays comparing the development of *Toxoplasma* grown with oleic acid (OA) or palmitic acid (PA). Cell monolayers of HFF were infected with 100 parasites and allowed to grow for 5 days at the indicated concentrations of fatty acids (no FA supplement; 0.2 and 0.4 mM OA; 0.2 mM PA). Representative images of each condition are shown. **B.** Histogram of the mean area of plaques (in μm^2) from the assays in (**A**). Means ± SD of 4 independent experiments. Indicated statistical differences are between control (no OA) and 0.2 mM OA and 0.4 mM OA-treated HFF. p^* <0.002, Student's t test.

4.4.2. *Toxoplasma* replication is hindered with excess OA introduced into the medium

To distinguish at which individual step OA affects the development of the parasite, the effect of OA on *Toxoplasma* replication and egress *in vitro* were investigated separately. We evaluated if the parasite's ability to replicate was influenced by the presence of excess OA in the medium. Infected HFF were incubated with control medium (no added FA), 0.1 mM, 0.2 mM or 0.4 mM OA for 24 h and parasite multiplication was measured by radioactive uracil incorporation (Fig. 4-4.A, panel a). Addition of OA resulted in a significant reduction of uracil incorporation into the parasites in a concentration-dependent manner (0.2 mM vs 0.4 mM), as compared to control parasites i.e. 0.4 mM OA led to 35 % less uracil incorporation as compared to control (Fig. 4-4.A, panel a). This replication defect was specific to OA, since incubation with PA at identical concentrations did not result in significant variations of uracil incorporation into the parasites (Fig. 4-4.A, panel b). The same replication deficiency was observed in infected HeLa cells incubated with 0.2 mM OA (29 % decreased uracil incorporation) indicating that this effect is not cell type specific (Fig. 4-4.B). Interestingly, *Toxoplasma* replication in ADRP-GFP-expressing HeLa cells without any OA addition to the medium was also impaired, suggestive of a role of increased LD numbers on *Toxoplasma* development (Fig. 4-4.B). The addition of 0.2 mM OA to ADRP-GFP HeLa cells did not lead to significant difference as compared to without OA in these cells. In parallel, we counted the number of parasites per PV to investigate whether the lower levels of uracil incorporation coincided with the presence of fewer parasites in the PV knowing that *Toxoplasma* has a doubling time of 6-8 h *in vitro*. We infected HFF with RFP-expressing *Toxoplasma* for 24 h with concentrations of OA ranging from 0 to 0.5 mM in 0.1 mM increments (Fig. 4-4.C). A gradual shift towards smaller PV sizes was detected as OA concentrations increased. At 0.4 mM and 0.5 mM OA, most of the PVs contained 1, 2 or 4 parasites.

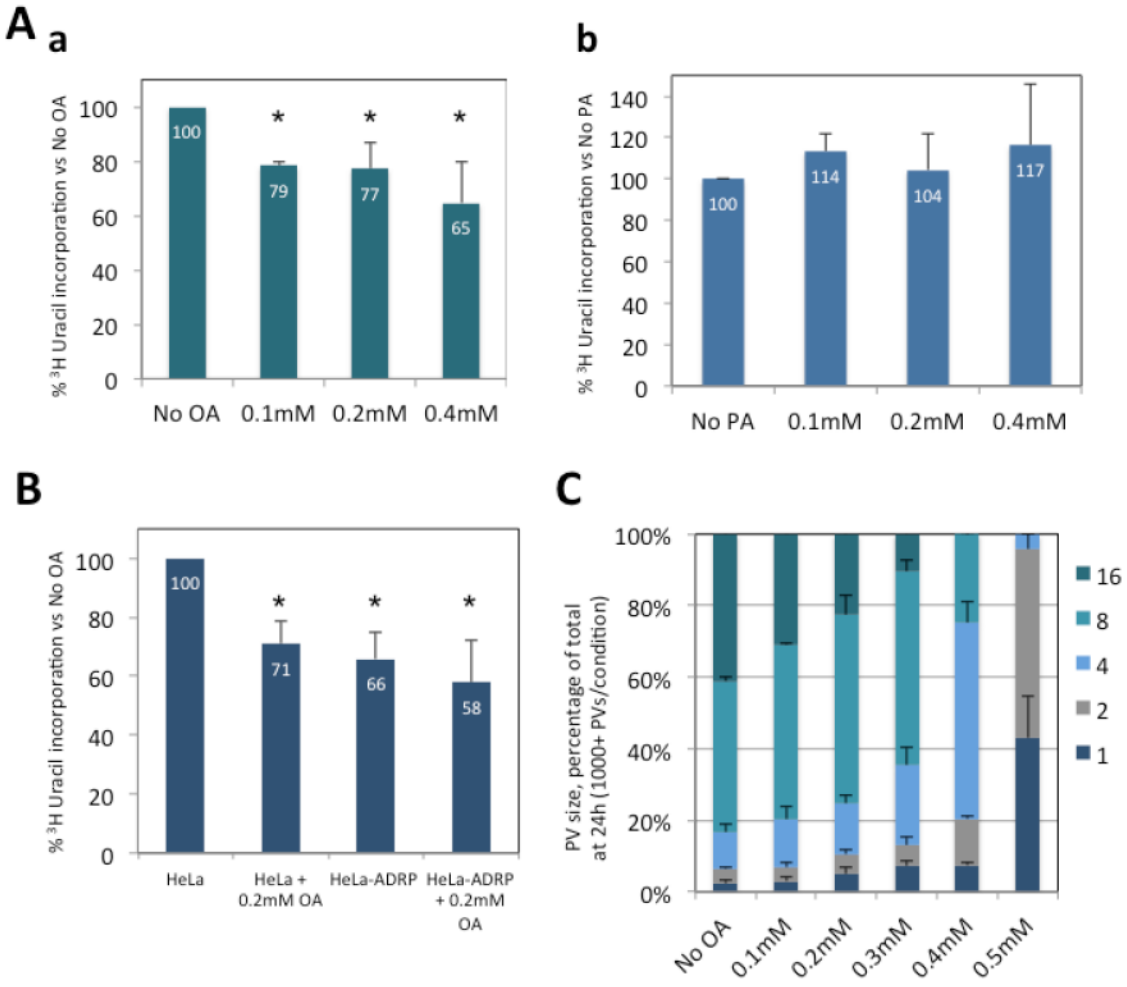

Figure 4-4. Influence of FA on *Toxoplasma* replication.

A-B. Influence of OA or PA addition on *Toxoplasma* replication. Uracil incorporation by *Toxoplasma* at 24 h p.i. in: (A) HFF incubated with 0.1 mM, 0.2 mM or 0.4 mM OA (panel a) or PA (panel b); (B) HeLa and GFP-ADRP HeLa cells ± 0.2 mM OA and. Data are percentages ± SD relative to control (No OA; set as 100%) of experimental triplicates. p^* <0.05, Student's t test. **C.** *Toxoplasma* replication assessed by PV size at 24 h p.i. grown with OA concentrations ranging from 0 to 0.5 mM, in 0.1 mM increments. The number of parasites per PV in *Toxoplasma*-infected HFF 24 h p.i. with various OA concentration are displayed as percentages of all PVs. At low or no OA, the majority of PVs contain **8** or **16** individual parasites. At higher [OA], most PVs contain 1, 2 or 4 parasites. Data show means ± SD from at least 1000 randomly selected vacuoles from 3 independent experiments.

4.4.3. Egress of *Toxoplasma* from the host cell is delayed upon incubation with excess OA

We next determined the effect of excess OA on *Toxoplasma* egress. In HFF with a MOI of 2, egress usually occurs around 40-44 h p.i. We performed microscopy studies 76 h p.i. in HFF incubated with 0.4 mM OA and noticed that the PV eventually grew excessively large and the parasites were still retained in their PV (Fig. 4-5.A, panel a-b). Based on data from Fig. 4-4.C, at 24 h p.i., there are mainly 8-16 parasites per PV, indicating 3 or 4 replication events, consistent with the doubling time of 6-8 h *in vitro*. In 0.4 mM treated cells, there are mainly 4 parasites in the PV (2 replications), indicating a doubling time of 10-12 h. At 76 h p.i. in untreated cells, we therefore calculate that there would be in theory 512-1024 parasites whereas in 0.4 mM treated cells, there would be 64-256 parasites per PV. This latter number is consistent with our observations. Egress in untreated cell usually occurs when the PV reaches 64-128 parasites. Electron microscopy (EM) of infected cells incubated with 0.4 mM OA showed parasites sequestered into the host cells, apparently unable to breach the host plasma membrane (PM) (Fig. 4-5.B). Further evidence of an egress defect in parasites exposed to excess OA was demonstrated by their delay in escaping host cells even upon chemical induction with the calcium ionophore, A23817 (Endo *et al*, 1982) as compared to control parasites. Indeed, following the addition of this ionophore, egress occurred by 30 seconds in normal medium while parasites exposed to 0.2 mM and 0.4 mM OA, the time to egress increased 1.6 fold and 2.2 fold, respectively.

To further investigate this delayed egress phenotype, we conducted additional EM studies on parasites incubated with 0.4 mM OA for 72 h. Different stages in the process of egress could be observed (Fig. 4-6). The rosette structure characteristic of replicating parasites

(Fig. 4-6, panel a) started to disassemble, a sign of parasite motility within the PV (Fig 4-6, panels b and c). Despite host cell depletion of organelles and therefore nutrients, many parasites were observed still encased in their PV (Fig. 4-6, panel e). The next step involves the rupture of the PVM, leaving the parasites free in the host cytosol (Fig. 4-6, panel e).

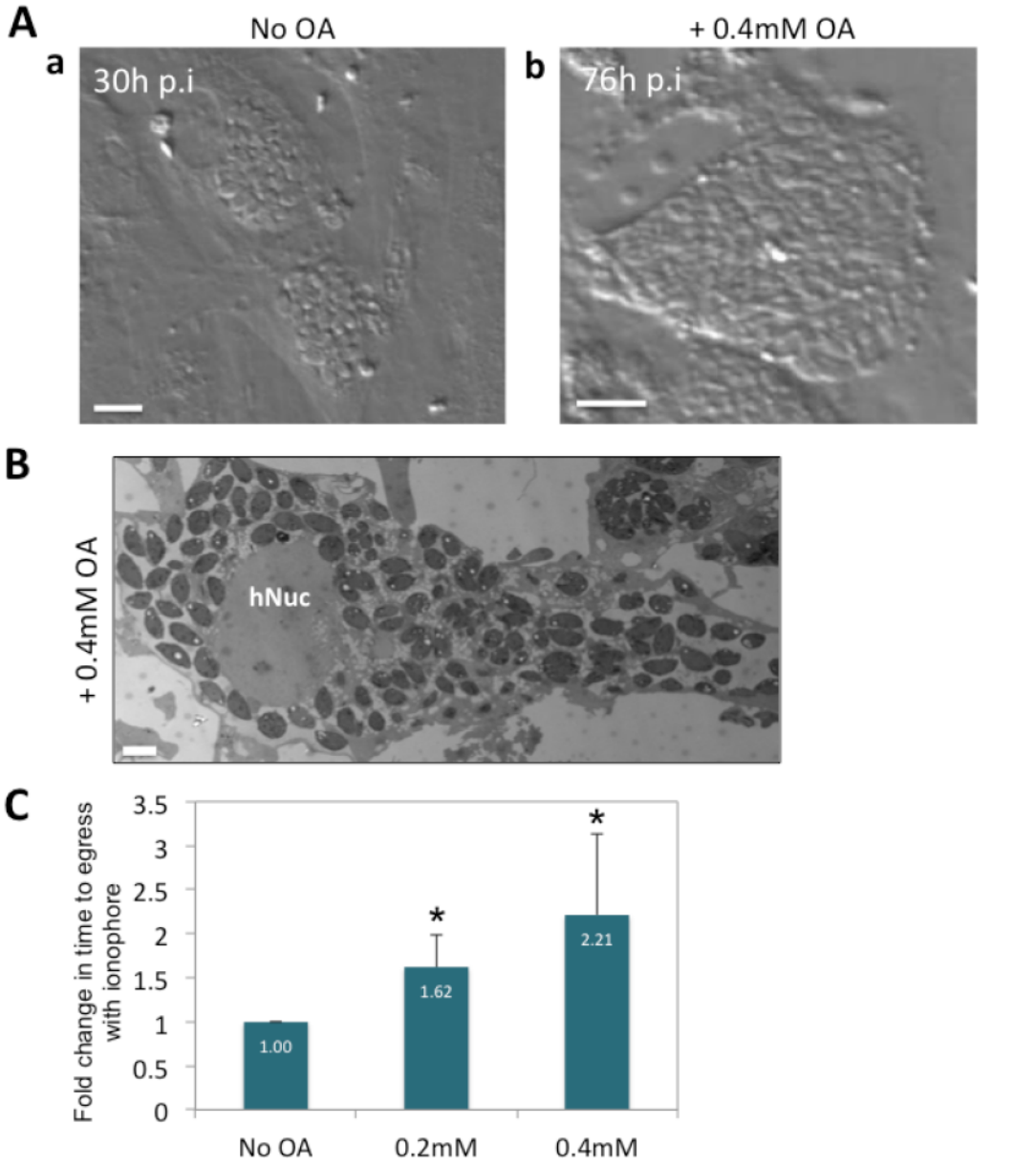

Figure 4-5. Influence of OA on *Toxoplasma* egress from the host cell.

A. Live DIC phase microscopy of HFF infected with *Toxoplasma* without OA at 30 h p.i. (a) and with 0.4 mM OA at 76 h p.i. (b). Scale bars, 10 µm. **B.** EM of *Toxoplasma*-infected HFF with 0.4 mM OA for 76 h p.i. The parasites appear unable to breach the HFF plasma membrane. Scale bars, 7 µm. **C.** Histogram of the quantification of the capability of *Toxoplasma* to egress following growth with OA in the medium. At 24 h p.i. in HFF, egress was induced with an ionophore as described in the *Materials and Methods*. Incubation with 0.2 or 0.4 mM OA during infection time caused a delay in *Toxoplasma* egress upon ionophore-stimulated egress. Time-taken to egress was recorded in seconds and the ratio to the control was calculated and plotted as means ± SD of three independent experiments. Indicated statistical differences are between control (no OA) and 0.2 mM OA and 0.4 mM OA-treated HFF. $p^* < 0.05$, Student's t test.

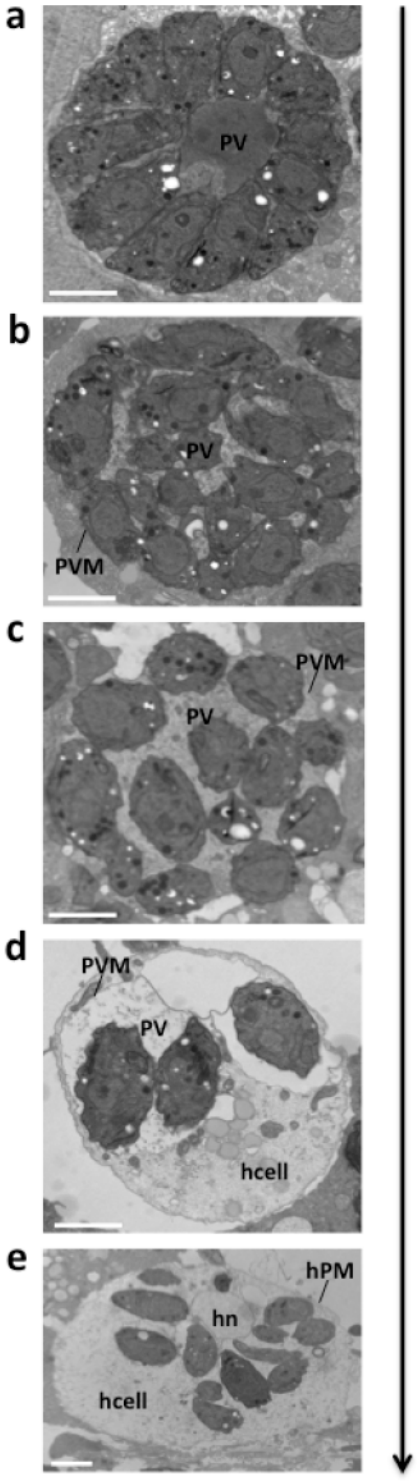

Figure 4-6. Retention of *Toxoplasma* within their host cells with excess OA.
EM of parasites in HFF incubated with 0.4 mM OA for 72 h. Panels a through e show different stages of egress: panel a shows a normal rosette which begins to lose structure (b, c), followed by depletion of host cell organelles (c, d, e), a dwindling of the PVM (d) and eventual loss of the PVM (e). Scale bar, 7 µm.

4.4.4. The slow growth of *Toxoplasma* in the presence of excess OA is not due to parasite differentiation into the latent cyst form

We next investigated whether OA may act as a stressor on the parasite, causing the differentiation of *Toxoplasma* to the latent, cyst form. The conversion of the *Toxoplasma* tachyzoite (highly proliferative) to bradyzoite (slow growing cyst) form can spontaneously occur *in vitro* in some cell types (Ferreira-da-Silva *et al*, 2009), but can also be induced in response to stressors such as changes in temperature, alkaline pH, amino acid deprivation and lower CO_2 levels (Dzierszinski *et al*, 2004; Skariah *et al*, 2010). The bradyzoite phenotype is characterized by slower growth and the incorporation of carbohydrates into the PVM, which develops into a thick cyst wall (Boothroyd *et al*, 1997). As excess OA in the medium leads to a decrease in parasite replication (Fig. 4-4), we investigated whether OA could be a trigger of parasite stress, resulting in tachyzoite to bradyzoite conversion. We evaluated the ability of OA to induce stage differentiation by incubating infected HFF with 0.2 mM OA for 24 h and monitoring, using TRITC labeled lectin, the formation of the cyst wall (Fig. 4-7). No fluorescent staining was observed on the PVM of parasites grown with OA (Fig. 4-7, panel c, blue arrow). As a positive control, we incubated infected cells in the absence of CO_2, and a TRITC lectin signal was clearly apparent on the PVM (Fig. 4-7, panel b, yellow arrow). The Prugniaud strain is cystogenic and therefore more sensitive to external stressors (Skariah *et al*, 2010; Asgari *et al*, 2013). When cells were infected with Prugniaud parasites with excess OA and stained with TRITC lectin, no fluorescence was detected on the PVM, in contrast to CO_2-deprived conditions in which Prugniaud parasites exhibited a very strong fluorescent signal as a sign of cyst wall formation and bradyzoite conversion. These results indicate that parasite growth impairment following incubation with excess OA in the medium is not attributable to a shift in the developmental program of the parasite from tachyzoite to bradyzoite forms.

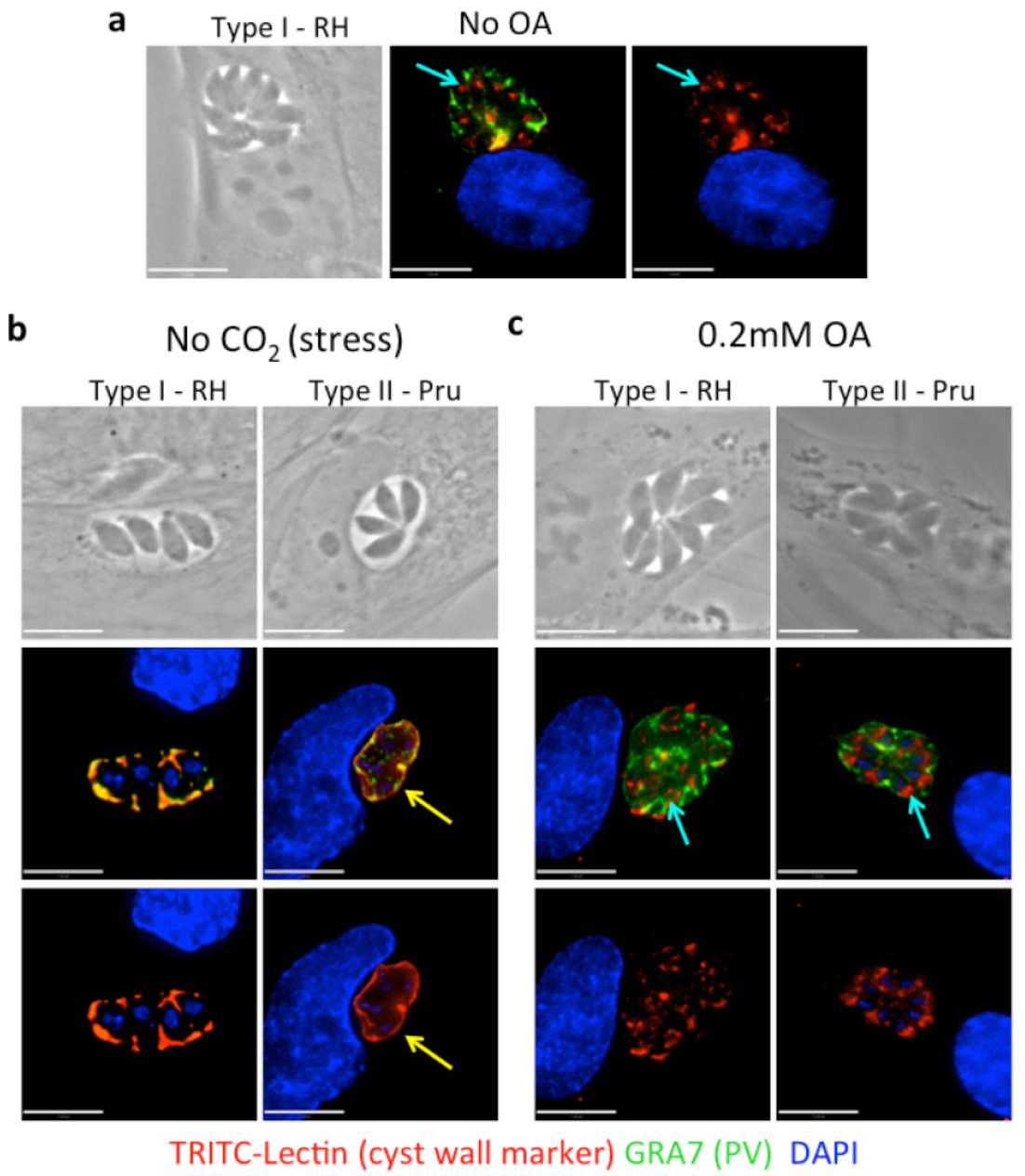

Figure 4-7. No detection of parasite stage differentiation induced by OA.
Fluorescence microscopy of HFF infected with *Toxoplasma* RH (type 1 strain) or Prugniaud (type 2 strain) with 0.2 mM OA. HFF were infected with *Toxoplasma* RH or Prugniaud for 24 h with α-MEM medium (a), without CO_2 (b) or with 0.2 mM OA in the medium (c). Coverslips were fixed and stained with 4-,6-diamidino-2-phenylindole (DAPI; nucleus, blue), TRITC-lectin (red) and antibody for GRA7 (parasite PVM and PV lumen, green). Upon stage conversion of tachyzoite to bradyzoite, TRITC-lectin stains the cyst wall (yellow arrows in panel b) instead of the parasite's Golgi apparatus (blue arrows in panels a and c). Scale bars, 10 µm.

4.4.5. Upon excess OA incubation, *Toxoplasma* accumulates large deposits of lipids in the PV and organelles

To gain further insight into the impairment of parasite development with OA incubation, we examined the parasites at the EM level. Upon treatment with 0.2 mM OA, we observed the presence of large osmiophilic (electron-dense) materials in the PV lumen, squeezed between individual parasites and along the PVM, seemingly in random locations (Fig. 4-8.A, panels a and b). At high magnification we could resolve multilamellar stuctures with a striking compaction and circular organization, as seen in the cross-section, reminiscent of the close-packing of lipid membrane sheaths (Fig. 4-8.A, panels c to d). This suggests there is an overaccumulation of lipid materials within the PV, which is likely a result of the massive uptake of OA by the parasite. Lipid deposits were also observed within the parasite, associated and within several structures including membrane-bound organelles such as the mitochondrion, the apicoplast and the vesicles of the Golgi apparatus (Fig. 4-8.B, panels a and b).

Previously, we showed that parasites incubated with 0.4 mM OA stimulated LD biogenesis to store the excess NL (Fig. 3-7 through 3-9 in Chapter 3). Although LD represent a safe mechanism to avoid cell lipotoxicity, their high number and large size could also compromise cellular functions and the formation of *Toxoplasma* progeny. Indeed, our EM observations reveal many parasites with severe cytopathies, including defects in organelle formation and endodyogeny, when exposed to 0.4 mM OA for 24 h (Fig. 4-9). Endodyogeny is a form of replication where two daughters are formed within the confines of the mother. When the daughters emerge, a small residual body is left in the PV, containing the remnants of the mother (Anderson-White *et al*, 2012). Dividing parasites were observed exporting lipid-overloaded organelles and excess LD to the residual body of the mother cell for evacuation (Fig.

4-9.A, and B). Under normal conditions, the residual body is detached from the two newly formed parasites and reabsorbed within the PV. However, under 0.4 mM OA conditions we observed, by EM, some enormous residual bodies occupying a very large space in the PV, more than likely interfering with the normal process of *Toxoplasma* division. Additionally, in many instances small PVs containing only a single parasite were observed, supporting our previous observations of replication defects (Fig. 4-4). These parasites occupying small PVs showed signs of lipotoxicity due to the presence of uncharacterized cytoplasmic structures, such as lipid deposits and membrane whorls. Altogether these studies highlight that parasites are capable of relentlessly salvaging exogenous OA. This FA accumulates in the PV and is internalized into the parasite and its organelles, leading to membrane defects and lipid overload. The consequence of this is likely cellular dysfunction and death.

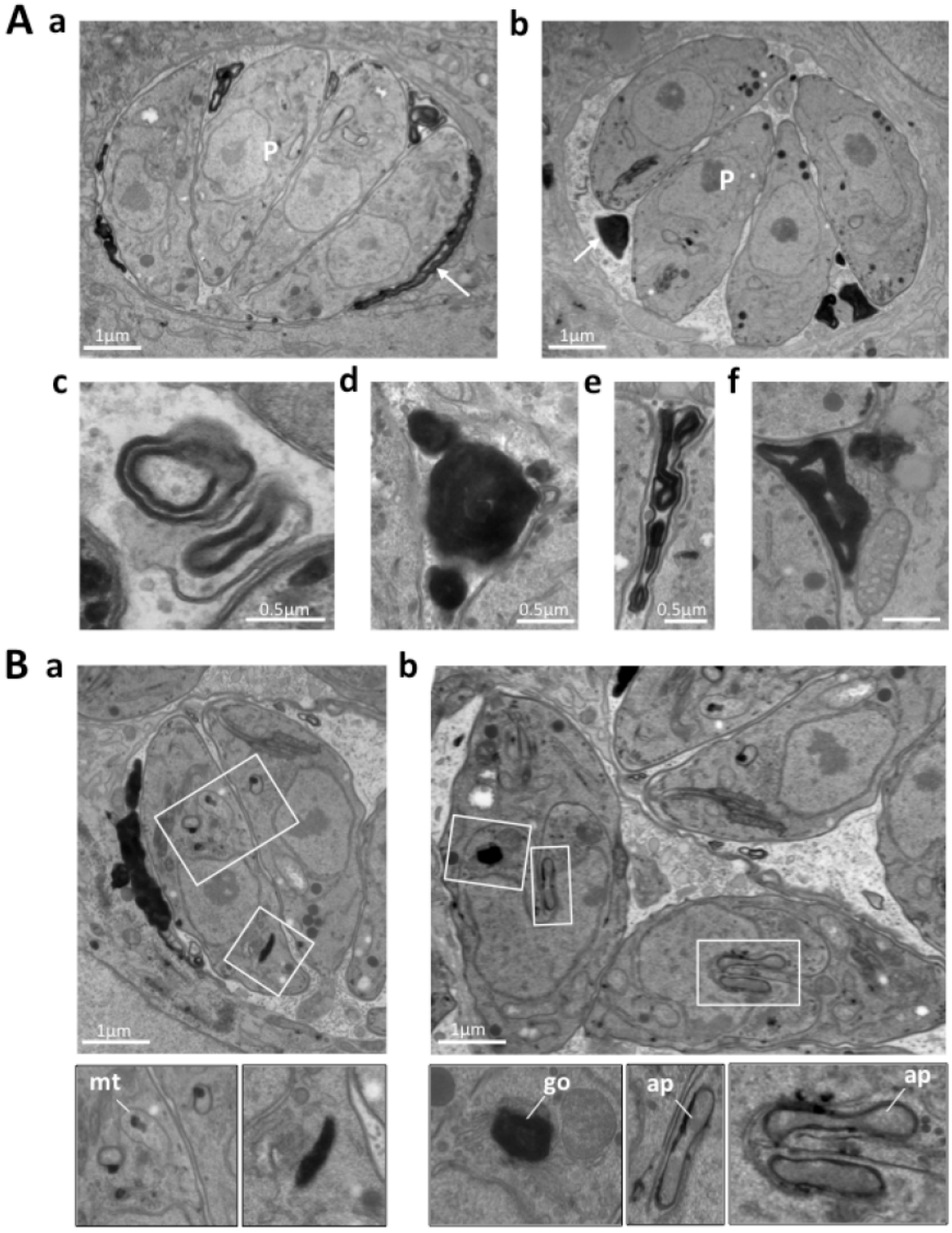

Figure 4-8. Lipid accumulation in *Toxoplasma* PV and organelles upon OA incubation.

A-B. EM of HFF infected with *Toxoplasma* for 24 h with 0.2 mM OA. Large deposits of osmiophilic material (**A, panels a, b**) and the accumulation of multilamellar structures (**A, panels c-f**) were observed in the PV lumen. Within individual parasites, lipid deposits were observed in mitochondria (mt), Golgi (go) and apicoplast (ap) (**B, panels a, b**).

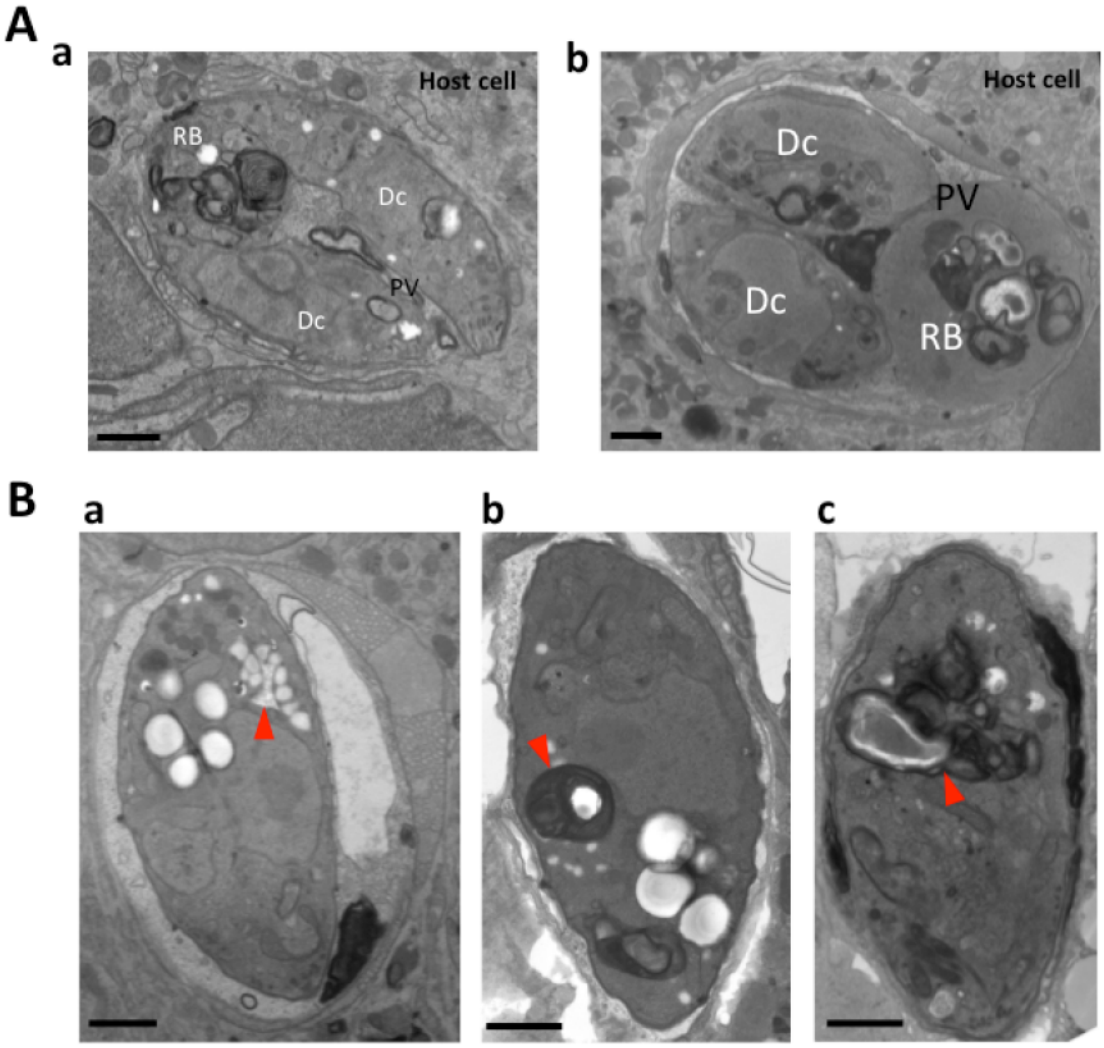

Figure 4-9. Cytopathies of *Toxoplasma* incubated with 0.4 mM OA

A-B. EM of intravacuolar parasites exposed to 0.4 mM OA for 24h. Panels a and b in **A** each show a large residual body (RB) containing lipid material and still attached to the daughter cells (Dc). Panels a to c in **B** illustrate dying parasites by lipotoxicity with accumulated lipid deposits (arrows). Scale bars, 1 µm.

4.4.6. Perivacuolar LD accumulation does not hinder host organelle association to the PV of *Toxoplasma*

Our data showed that excess OA leads to the dramatic accumulation of host LD around the PV, which may result in impaired association to the PV of host cellular organelles, such as the ER, Golgi apparatus and mitochondria. The interaction between these host organelles and the PV is most likely important for *Toxoplasma* growth as this proximity may facilitate the delivery of their nutrient content to the parasite (Sinai *et al*, 1997; Quittnat *et al,* 2004; Coppens *et al*, 2006; Walker *et al*, 2008; Romano *et al*, 2008; Wang *et al*, 2010; Romano *et al*, 2013; Pernas *et al*, 2014). Perturbation of host organelle-PV recruitment may therefore be detrimental for parasite viability.

To determine whether excessive host LD numbers disturb the association of the host ER to the PV, we analyzed in infected cells treated with 0.2 mM OA the distribution of the host ER to the PV by fluorescence microscopy using anti-KDEL antibodies and by electron microscopy (Fig. 4-10.A and 4-8.B). Uninfected and infected HFF displayed an altered ER network, likely due to the numerous LD throughout the cytoplasm (Fig. 4-10.A). However, despite LD gathering around the PV, we observed ER association with all the PV to the same extent as found for PV in normal medium with 70% of the PVM covered by the ER. EM observations illustrate a close physical apposition of host ER elements with the PVM, with ER-bound ribosomes facing the host cytoplasm (Fig. 4-10.B) as previously reported (Sinai *et* al, 1997). Upon incubation with excess OA, the host LD were located behind the layer of host ER attached to the PVM, indicating that the parasite could recruit and form intimate associations with the host ER independent of the presence of abundant LD in the host cell.

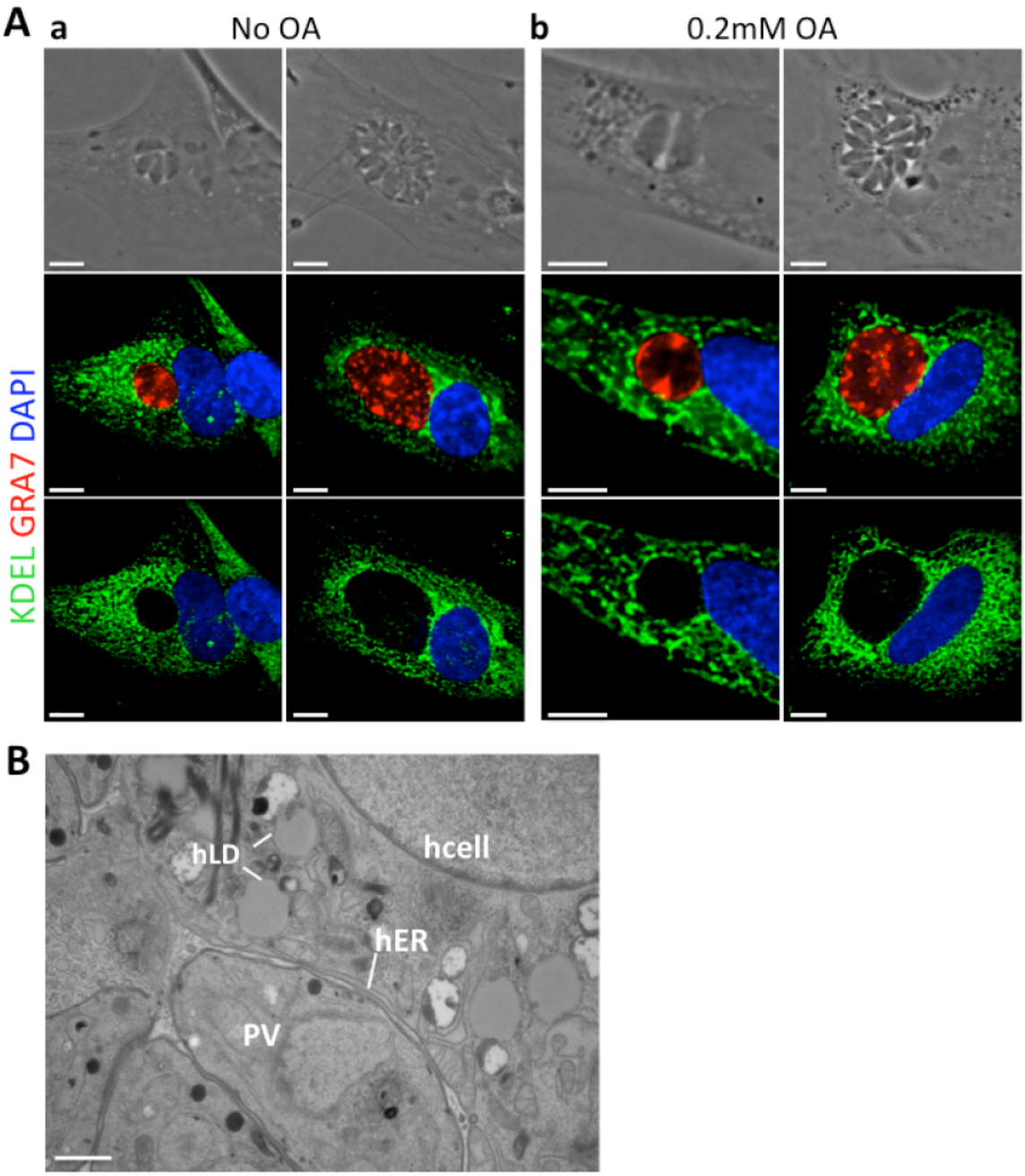

Figure 4-10. ER recruitment to *Toxoplasma* PV upon OA incubation.

A. Fluorescence microscopy of ER in HFF infected with *Toxoplasma* for 24 h ± 0.2 mM OA. HFF were infected with *Toxoplasma* for 24 h without OA (a) or with 0.2 mM OA (b), fixed and stained with 4-,**6**-diamidino-2-phenylindole (DAPI; nucleus, blue), and antibodies for KDEL (host ER, green) and GRA7 (PVM and PV lumen, red). Association of host ER with *Toxoplasma* PV still occurs in the presence of OA. Scale bars, 7 µm. **B.** Ultrastructural analysis by EM of host ER association with *Toxoplasma* PV with 0.2 mM OA in HFF. The host cell's ER (hER) associates with the PV of *Toxoplasma* 24 h p.i. when incubated in medium with 0.2 mM. Host LD (hLD) are observed in close proximity to the hER and PV. Scale bars, 1 µm.

We next investigated whether the clustering of host Golgi ministacks still occur around the PV of *Toxoplasma* with excess OA. Infection of fibroblasts with *Toxoplasma* induces dramatic alterations in the morphology and distribution of the host Golgi apparatus. Early during infection, the host Golgi surrounds the PV of *Toxoplasma*, which then fragments into functional ministacks, that all gather around the PV (Romano *et al*, 2013).

To assess the influence of LD accumulation on Golgi recruitment to the *Toxoplasma* PV, we inspected the morphology of the Golgi by IFA using anti-giantin antibodies in infected HFF in the presence of 0.2 mM OA. (Fig. 4-11.A, panels a-b). In both small and large PVs, the host Golgi was recruited. We used MetaScopics to quantify the association of the host Golgi to the *Toxoplasma* PV at different developmental timepoints based on PV size. In the presence of 0.2 mM OA, the centroid-to-surface distance of the host Golgi to small PVs (1, 2 and 4 parasites in the vacuole) was significantly longer than observed in conditions without added OA (Fig. 4-11.B), suggesting a slightly delayed accumulation of host Golgi ministacks around the PV. This does not imply that there is no Golgi clustering around the PV, as the Golgi is observed in close proximity to the PV regardless of OA presence. Later during infection, the recruitment of the Golgi to the PV with OA incubation matched that of control medium. Despite a significant delay in the surrounding of the PV byvhost Golgi elements early during infection with OA treatment, eventually clustering did occur, suggesting that perivacuolar LD did not affect the accumulation of Golgi ministacks to the PV.

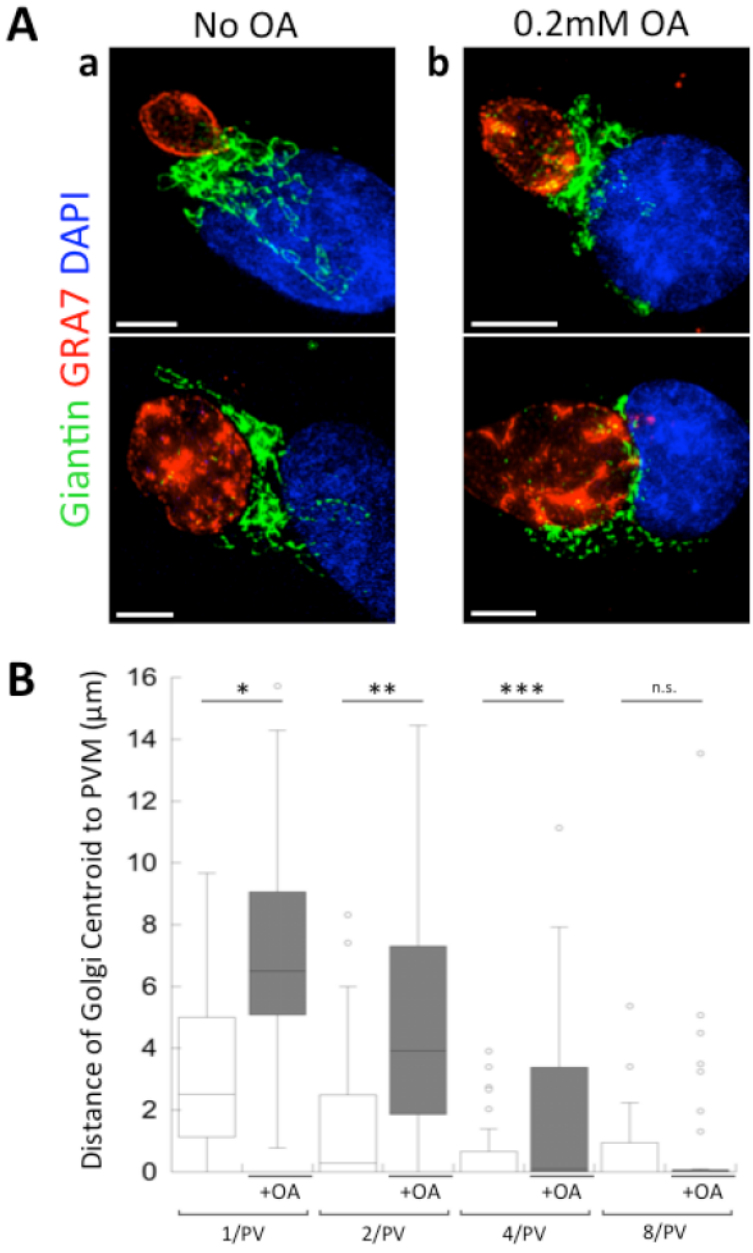

Figure 4-11. Golgi accumulation around the *Toxoplasma* PV upon OA incubation.

A. Fluorescence microscopy of the Golgi apparatus in HFF infected with *Toxoplasma* for 24 h ± 0.2 mM OA. HFF were infected with *Toxoplasma* for 24 h without OA (a) or with 0.2 mM OA (b), fixed and stained with 4-,6-diamidino-2-phenylindole (DAPI; nucleus, blue), and antibodies for Giantin (Golgi, green) and GRA7 (PVM and PV lumen, red). The host cell's Golgi clusters around the PV of *Toxoplasma* in both conditions and becomes segmented around larger PVs. Scale bars, 7 µm. **B.** Quantification of Golgi apparatus recruitment by *Toxoplasma* using MetaScopics with 0.2 mM OA. Boxplot shows the average distance from the host Golgi complex centroid to the nearest PV boundary. In smaller PVs (1, 2 or 4 parasites per PV), the centroid distance to the PV is significantly larger when grown with 0.2 mM OA but by 8 parasites per PV, there is no difference between OA-treated and control samples (n >30 per condition). p^* <0.001; p^{**} <0.03; . p^{***} <0.02, Student's t test.

Shortly after penetrating the cell, *Toxoplasma* induces a dramatic change in the spatial distribution of host mitochondria. We wanted to determine whether large numbers of host LD hinder the association of mitochondria to the PV. In infected cells incubated with 0.2 mM OA ,we probed the distribution of host mitochondria and their association with the PVM by IFA using antibodies against TOM20. A concentric fluorescent signal was detected around the PV similar to that observed in control conditions (Fig. 4-12.A). We used MetaScopics to determine the intensity-weighted distances of host mitochondria to the PV of *Toxoplasma* in both conditions. There was no significant difference in the recruitment of this organelle to the PV regardless of OA presence, as calculated within an arbitrary delineated area of 7 µm radiating from the PV (Fig. 4-12.B).

We performed ultrastructural analysis to verify the association of host mitochondria around the PV in infected cells treated with 0.2 mM OA. We confirmed that host mitochondria were closely apposed to the PVM. However, the morphology of these organelles was profoundly altered, as they appeared enlarged. These swollen mitochondria were characterized by an increase in area, a rounded shape, a loss of matrix density, and a distortion of cristae (Fig. 4-13.A). The mitochondria in infected cells not associated with the PV, however, showed no morphological abnormalities suggesting a relationship mediated by the parasite between host mitochondria and excess OA.

Jointly these data illustrate that, despite significant LD accumulation around the PV, host organelles are still recruited to the PV as previously reported. In the case of ER and mitochondria, these two organelles still form intimate association with the PVM. Nevertheless, the abnormally enlarged mitochondria attached to the PV strongly suggests mitochondrial

dysfunction, and such a degeneration may also account for a reduction in parasite growth with excess OA.

To ensure that the abnormal morphology of the mitochondria around the PV is specific to OA incubation and subsequent LD accumulation, we treated cells with 0.2 mM PA. Addition of 0.2mM PA to infected cells does not affect *Toxoplasma* growth (Fig. 4-4) nor lead to excessive LD accumulation. However, it is known that PA can alter mitochondrial function; at 0.1 mM, PA induces mitochondrial ROS generation, mitochondrial membrane potential loss and DNA damage (Rachek *et al*, 2007; Yuzefovych *et al*, 2010; Cheon and Cho, 2014). PA can also modify the shape and distribution of the mitochondrial network in uninfected cells as shown by IFA using anti-TOM antibodies (Fig. 4-14.A). We next investigated whether host mitochondria could be recruited by *Toxoplasma* in the presence of 0.2 mM PA. In infected HFF grown with 0.2 mM PA and stained with TOM20, a concentric fluorescent signal was detected around both small and large PV (Fig. 4-14.B), comparable to that of PV incubated with 0.2 mM OA. This suggests that the parasite is still able to recruit host mitochondria despite their altered morphology. Excess PA leads to universal morphological changes to the host mitochondrial network while excess OA leads to morphological changes to the host mitochondria associated with the PV.

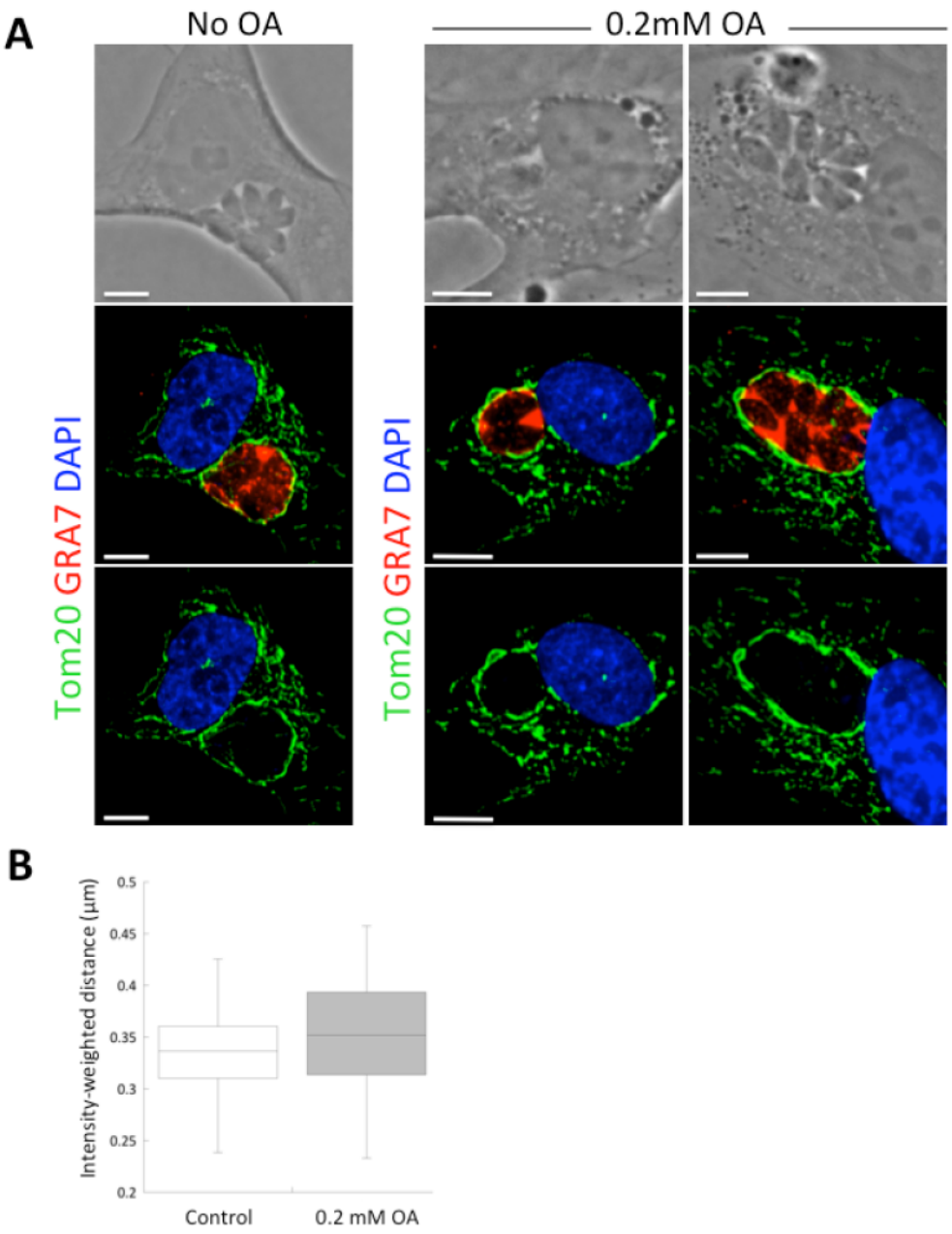

Figure 4-12. Mitochondria morphology around *Toxoplasma* PV with OA incubation.
A. Fluorescence microscopy of mitochondria in HFF infected with *Toxoplasma* for 24 h ± 0.2 mM OA. HFF were infected with *Toxoplasma* for 24 h without OA or with 0.2 mM OA, fixed and stained with 4-,**6**-diamidino-2-phenylindole (DAPI; nucleus, blue), and antibodies for Tom20 (mitochondria, green) and GRA7 (PVM and PV lumen, red). The morphology of the mitochondria is altered when treated with OA, especially those directly associated with the PV as they appear more swollen. Scale bars, 7 µm. **B.** Quantification of host mitochondria association to *Toxoplasma* PV by MetaScopics analysis. Boxplots show the average distances, weighted by intensity, of the host mitochondria to the PV boundary, as calculated for host mitochondrial profiles within a 7 µm radius of the PV (data from >40 infected HFF per condition at 24 h p.i.). A comparison between the treatments is not statistically significant.

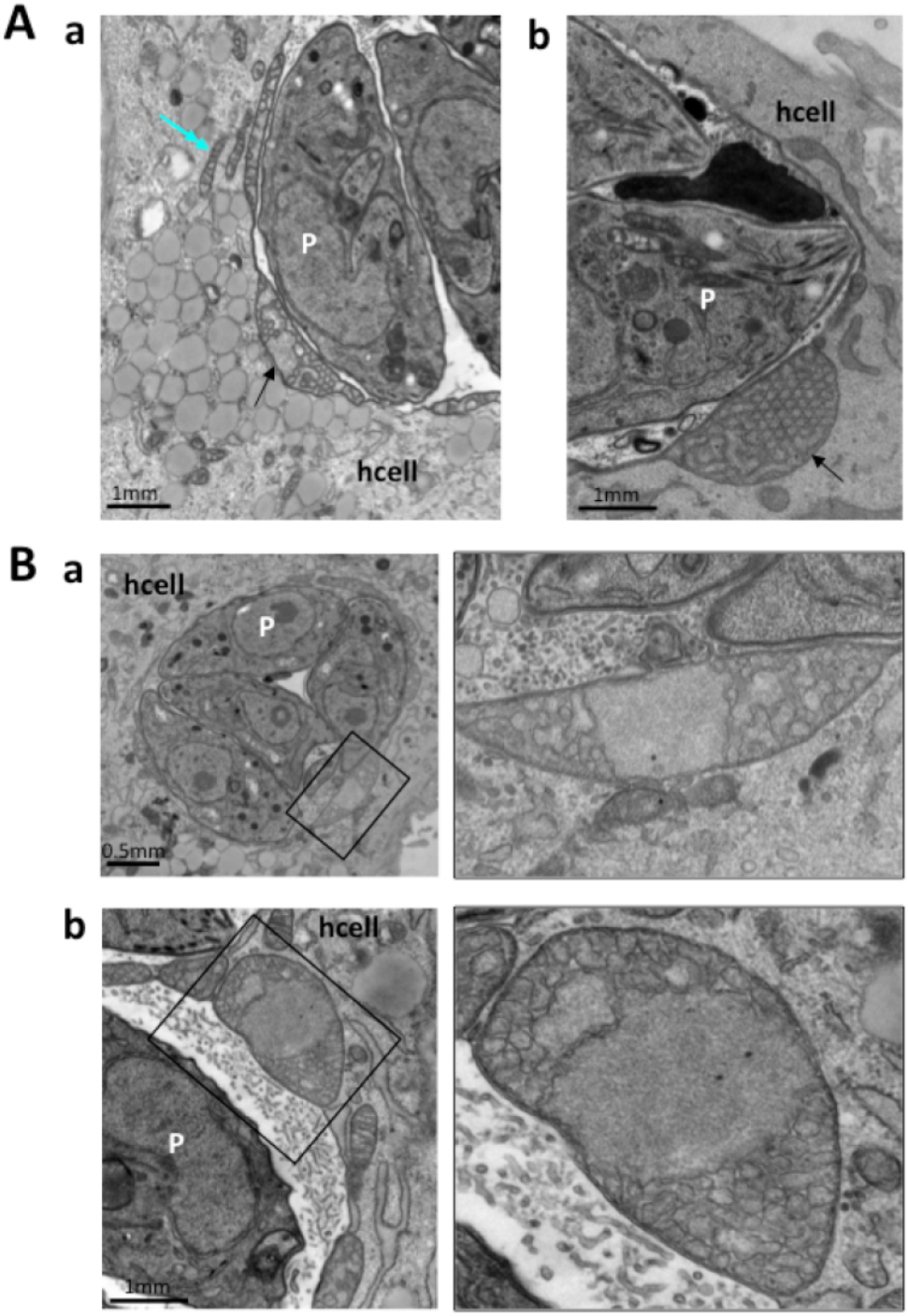

Figure 4-13. Ultrastructure of PV-associated mitochondria incubated with 0.2mM OA.
A-B. Electron micrographs of *Toxoplasma*-infected HFF for 24 h with 0.2 mM, focusing on the host mitochondria associated to the PV. Mitochondria in the host cell associated with the PV membrane exhibited distorted cristae (**A, panel b**), were misshapen and enlarged (**A-B, all panels**), and lost matrix density (**B**). Host cell mitochondria unassociated to the PV appear healthy (double blue arrow in **A**).

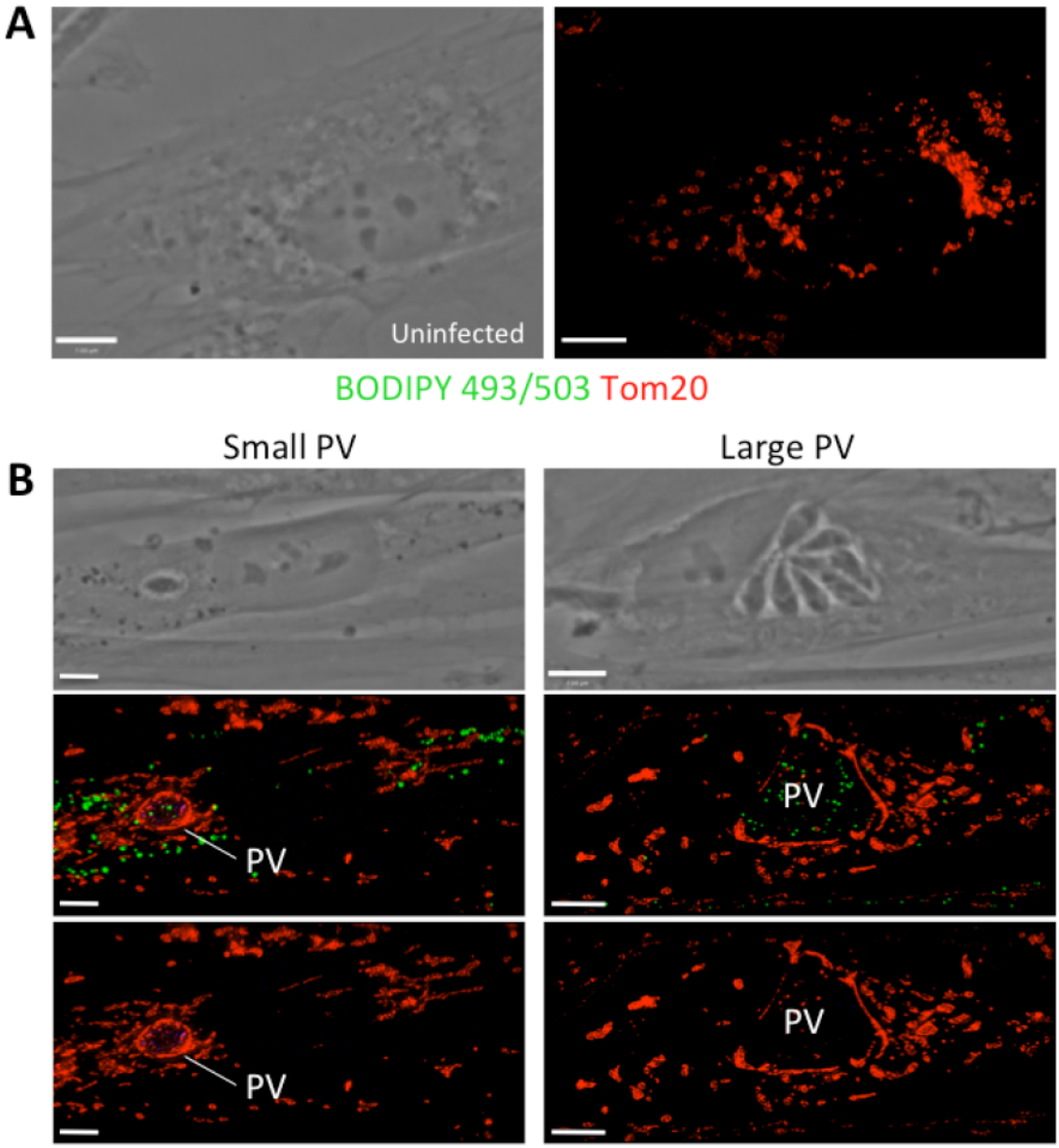

Figure 4-14. Mitochondria morphology around *Toxoplasma* PV with PA incubation.
Fluorescence microscopy of mitochondria in uninfected (**A**) and infected HFF (**B**), both incubated with 0.2 mM PA. HFF were infected with *Toxoplasma* for 24 h with 0.2 mM PA. Coverslips were fixed antibodies for Tom20 (host mitochondria, red) (**A-B**) and stained with BODIPY 493/503 (lipid droplets, green) (**B**). Incubation with PA leads to abnormal mitochondrial morphology in the host cell (**A**, uninfected; **B**, infected with small and large PVs). There is association of mitochondria to the PV in the presence of PA. Scale bars, 7 µm.

4.4.7. Increased autophagy in cells incubated with excess OA is not involved in reducing *Toxoplasma* development

Upon incubation with excess OA (up to 1 mM), lipophagy is stimulated. This is an important process for regulating lipid metabolism and homeostasis by preventing the aggregation of toxic FA and LD in the cytoplasm (Singh *et al*, 2009). In cells such as hepatocytes, excess OA triggers autophagy and these lipids are mobilized to generate phagosomal membranes and autophagosomes. We therefore wanted to investigate the role of lipophagy in hampering parasite growth as parasites in cells incubated in the presence of 0.2 mM OA may be exposed to a harmful environment characterized by elevated autophagic activities. Degradation of the PV via autophagy has not been reported for *Toxoplasma* Type I strains, such as RH, however Type II and III strains are susceptible to immune-mediated autophagy induction. In such strains, this cellular process involves the ubiquitination of the PVM, LC3 deposition around the PV, as well as the formation of multiple membranes enclosing the PV (Selleck *et al*, 2015).

We first wanted to confirm that OA could induce autophagy in fibroblasts. HFF expressing a GFP-LC3 construct were incubated with 0.2 mM or 0.4 mM OA to monitor, by microscopy, the formation of LC3-containing autophagic structures. Similarly to amino acid depletion (Wang *et al*, 2009), our data show that excess OA induced large GFP-LC3 puncta in the cytosol, in contrast to control medium showing diffuse LC3 staining (Fig. 4-15.A). These assays were repeated in infected cells transfected with GFP-LC3. We detected the accumulation of LC3-GFP puncta, likely corresponding to autophagic profiles, (Fig. 4-15.B) surrounding the PV. This gathering of autophagosomal structures around the PV was confirmed by EM (Fig. 4-15.C). However, fusion events of LC3-positive structures with the PV were never observed, making the destruction of the PV by autophagy unlikely, even in host cells with many autophagosomes.

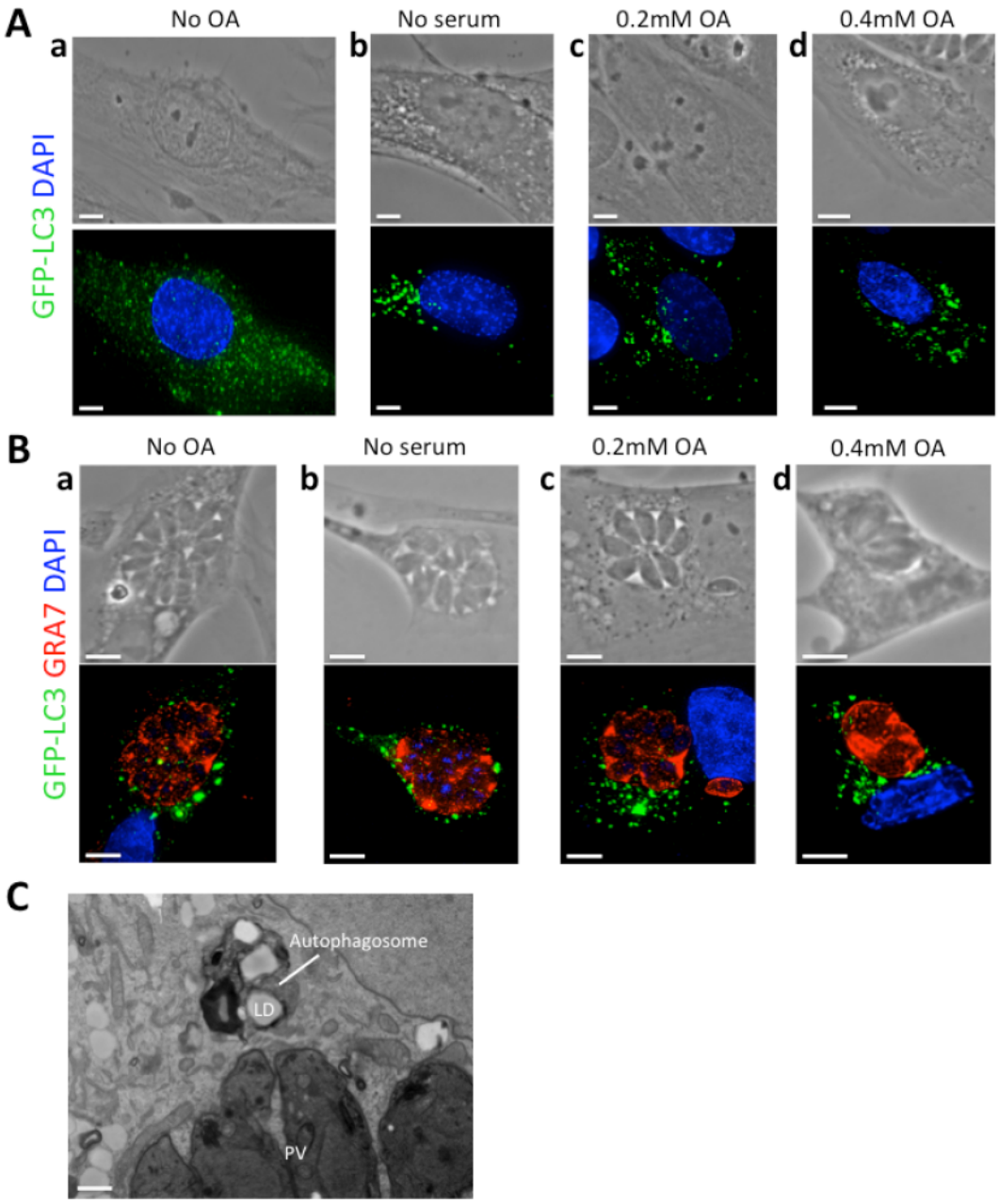

Figure 4-15. Distribution of GFP-LC3 structures around *Toxoplasma* PV.

A-B. Fluorescence microscopy of uninfected (A) or *Toxoplasma*-infected (B) HFF expressing GFP-LC3 grown without OA (a), without serum (starvation condition) (b), 0.2 mM OA (c) or 0.4 mM OA (d). GFP-LC3-transfected HFF were infected with *Toxoplasma* and incubated for 24 h without serum in the medium or with 0.2 mM or 0.4 mM OA. Uninfected fixed cells were stained with 4-,**6**-diamidino-2-phenylindole only (DAPI; nucleus, blue) (A) whereas infected cells were stained with DAPI (nucleus, blue) and antibodies against GRA7 (PVM and PV lumen, red). The distribution of GFP-LC3-positive vesicles (green) is shown in these extended-focus images in both uninfected and infected cells. Scale bars, 7 µm. **C.** Ultrastructural analysis of a host autophagosome with hLD in the process of digestion, in close proximity to *Toxoplasma* PV. HFF were infected with *Toxoplasma* for 24 h with 0.2 mM OA to observe the occurrence of autophagy. Scale bars, 0.5 µm.

4.5. DISCUSSION

The intracellular lifestyle of *Toxoplasma gondii* requires lipids either synthesized *de novo* by the parasite or scavenged from the host cell. The exogenously acquired lipids include those that the parasites cannot synthesize (e.g., cholesterol) or lipids produced by the parasite but in insufficient amounts to accommodate the parasite's needs for fast replication (e.g., ceramides, phospholipids) (Charron and Sibley, 2002; Quittnat *et al,* 2004; Gupta *et al*, 2005; Coppens *et al*, 2006; Romano *et al*, 2013; Hartmann *et al*, 2014). The concentration in the medium of lipids that *Toxoplasma* needs to salvage directly influences its growth rate. For example, the replication of *Toxoplasma* is boosted by high amounts of exogenous cholesterol or ceramides whereas removal of cellular cholesterol sources leads to a severe decline in parasite replication (Coppens *et al*, 2000; Nishikawa *et al*, 2005; Ihara and Nishikawa, 2014). In this study, we examined the impact of the fatty acids oleic acid (OA) and palmitic acid (PA), added in excess to the medium, on *Toxoplasma* development. We showed that the development of the parasite is impaired in the presence of excess OA while PA has no effect. Our investigations into the cause of the parasite's developmental defect observed with excess OA reveal impairment in both the parasite's ability to replicate and to egress. These failures seem likely to be due to lipotoxicity from excess OA as we observed abnormally large lipid deposits inside the PV as well as inside the parasite, which in turn could affect the proper functioning of the parasite at many levels. Additionally, we noticed major morphological abnormalities in the host mitochondria associated with the PV, which may also interfere with proper parasite development.

Unlike excess cholesterol or ceramides that are beneficial for the replication of *Toxoplasma*, excess OA, unexpectedly, is detrimental for its growth. This defect is specific to OA since incubation at the same concentrations of PA did not impair the development of

Toxoplasma. The replication defect with excess OA was also surprising in light of studies on *Chlamydia trachomatis* for which 0.1 mM OA addition to the medium positively affected the growth of the bacterium whereas deletion of host LD enzymatic machinery (i.e. *DGAT*) led to a dramatic growth reduction (Hatch and McClarty, 1998; Cocchiaro *et al*, 2008). The effect of excess OA or PA (0.03 to 0.4 mM) on the Apicomplexan parasite *Plasmodium falciparum* is also favorable as a 3 to 5 fold increase in growth rate was observed in parasite infected hepatocytes and erythrocytes (Lombard et al, 1998; Mi-Ichi *et a*l, 2007). As a matter of fact, OA is absolutely essential for the proper development of *P. falciparum* in erythrocytes (Vielemeyer *et al*, 2004; Mi-Ichi *et a*l, 2007).

The egress defect observed for *Toxoplasma* exposed to excess OA may be due to different factors: 1) impaired calcium signaling, 2) changes in lipid membrane composition, and/or 3) parasite weakness due to toxicity. In OA-overloaded cells, parasites take more time to escape naturally from their host cells and are retained in the host cytosol for up to 3 days. *Toxoplasma* egress is a calcium-dependent event as incubation with calcium ionophores triggers the rapid exit of parasites from the PV and its host cell (Endo *et al*, 1982). Cytoplasmic levels of calcium in mammalian cells are affected by OA. OA, bound to albumin, causes a cellular influx of calcium leading to cytoplasmic calcium accumulation in many cell types (Zaloga *et al*, 1987; Katsura *et al*, 2005; Katsuta *et al*, 2009; Carrillo *et al*, 2016). The effect of OA on calcium stores in *Toxoplasma* is unknown but OA may also affect calcium signaling within the parasite, thus impairing egress. The egress defect may also be due to changes in the lipid composition of the PVM and/or host PM. It is not yet known whether the composition of lipids, FA or FA-derived lipids, in the PVM or host PM affects *Toxoplasma* egress, but excess OA leads to increased membrane fluidity following incorporation within the bilayer (Lopez *et al*, 2014). Finally, the

egress defect may be a symptom of a general malfunction related to the inability of parasites to regulate OA influx, leading to massive lipid accumulation in the PV and parasite.

Risk of toxicity from elevated FFA levels occurs in mammalian cells, with repercussions at the organismal level, of hypertension, diabetes, insulin resistance and heart failure (Wende and Abel, 2010; Yang and Li, 2012; Tuder *et al*, 2014; Karpe *et al*, 2011). Adipocytes and adipose tissue are well equipped to manage excess FFA but the accumulation of elevated levels of FFA in all other cell types with a limited capacity to store surplus lipids tends to cause severe lipotoxicity, a phenomenon leading to cellular dysfunction and cell death by apoptosis (Listenberger *et al*, 2003). The cellular consequences of lipotoxicity vary depending on cell type but generally include the generation of ceramide, ROS and NO (Shimabukuro *et al*, 1997). Caspase activation, along with altered mitochondrial structure and dysfunction is also a well-documented consequence of excessive FFA levels in the cell (Ostrander *et al*, 2001; Listenberger *et al*, 2003; Ricchi *et al*, 2009). The saturation of the FA correlates with the degree of lipotoxicity, as saturated FA such as palmitic acid (PA) tend to more readily lead to lipotoxicity than unsaturated FA such as oleic acid (OA) (Ricchi *et al*, 2009), presumably because unsaturated FA like OA are incorporated to TAG more efficiently than saturated FA, and subsequently sequestered in LD, thus preventing the onset of lipotoxicity (Listenberger *et al*, 2003; Jackson *et al*, 2009; Mei *et al*, 2011; Nowak *et al*, 2011; Ibarguren *et al*, 2014; Garcia-Ruiz *et al*, 2015). Lipotoxicity from saturated FA (PA) can be partially rescued by supplementation with unsaturated FA (OA). The mechanism is yet unknown but is thought to involve better channeling of PA towards TAG storage in the presence of OA (Listenberger *et al*, 2003). In our hands, HFF could tolerate OA up to a concentration of 0.7 mM as 0.8 mM led to cell death, potentially by apoptosis. Many studies on the effects of OA in mammalian cells are performed between 0.5 mM and 1.2 mM OA without any apparent cytotoxicity (Dwight *et al*, 1992; Mei *et al*, 2011;

Thörn and Bergsten, 2010). OA is a poor inducer of lipotoxicity in mammalian cells due to its ability to be rapidly and efficiently converted to TAG and stored in LD (Mei *et al*, 2011), however, *Toxoplasma* seems extremely vulnerable to high amounts of OA present in its environment, with a much lower threshold for OA concentration. Colossal osmiophilic deposits, unrelated to LD, are visible by electron microscopy in the PV and within individual parasites when incubated with 0.2 mM OA. Increasing OA concentrations up to 0.4 mM led to intensified osmiophilic deposits, despite the parasite's ability to upregulate enzymes for NL synthesis and storage in LD in response to excess OA (Chapter 3).

One consequence of incubating mammalian cells with OA is the biogenesis of many cytoplasmic LD (Listenberger *et al,* 2003; Fujimoto *et al*, 2006; Thörn and Bergsten, 2010; Mei *et al*, 2011; Ahn *et al*, 2013). The presence of numerous host LD accumulated in the host cytosol upon OA treatment may negatively affect *Toxoplasma*'s growth by posing a physical hindrance on the parasite's ability to recruit host organelles (Coppens *et al*, 2006; Sinai *et al*, 1997; Walker *et al*, 2008; Romano *et al*, 2008; Wang *et al*, 2010; Romano *et al*, 2013b; Pernas *et al*, 2014); the intimate association between the PV and host organelles is hypothesized to facilitate nutrient uptake to the PV (Charron and Sibley, 2002; Quittnat *et al,* 2004; Coppens *et al*, 2006; Sampels *et al*, 2012; Romano *et al*, 2013). Even though the ER is the site of LD biogenesis, ER function is not compromised in mammalian cells upon incubation with excess OA at 0.5 mM. In fact, in OA-incubated cells, the ER helps prevent lipotoxicity by increasing LD biogenesis and ER stress is avoided, whereas saturated FA like PA causes both of these detrimental processes (Shimabukuro *et al*, 1997; Ostrander *et al*, 2001; Listenberger *et al*, 2003; Ricchi *et al*, 2009; Mei *et al*, 2011). However, there seems to be a threshold for OA, as incubation with 1.2 mM OA for prolonged periods has been shown to induce ER stress *in vitro* and *in vivo* in murine hepatocytes (Ota *et al*, 2008). In our hands, the host ER appears unaffected by 0.2 mM OA, and still

associates with the PV, thus likely not impacting *Toxoplasma*'s growth. Another organelle that clusters around the PV is the Golgi apparatus. With OA in the medium, our quantitative studies reveal a slight delay in the clustering of the host Golgi around the PV at the onset of infection. Further studies investigating the normal functionality of the host Golgi upon OA incubation (e.g., monitoring ceramide transport from the host Golgi to the parasite) may prove useful. Finally, we investigated the association of mitochondria to the *Toxoplasma* PV. The intimate apposition of host mitochondria to the PV is well documented although the significance of this association is still unknown (Sinai *et al*, 1997; Pernas *et al*, 2014). In fact, only type I stains of *Toxoplasma* recruit mitochondria to the PV, and these strains tend to be more virulent *in vivo*. *Neospora caninum*, a very closely related Apicomplexan is less virulent, but also recruits mitochondria to its PV, but in a much diminished capacity (Nolan *et al*, 2015). It is therefore possible that mitochondrial recruitment may only play a role in virulence *in vivo*. Interestingly, the morphology of mitochondria associated with the *Toxoplasma* PV is altered upon incubation with OA while mitochondria in the rest of the cell appear normal. This may be important as there must be something about the mitochondria's attachment to the PV that is altered with OA treatment. This may help in future to provide insight about interactions between the PV and host mitochondria. Alterations in the shape and ultrastructure of mitochondria are well documented in lipid-related diseases, such as neurodegeneration, aging, and cellular lipid overdose (Su *et al*, 2009; Reddy and Reddy, 2011; Galloway and Yoon, 2013; Galloway and Yoon, 2015; 2013; Yoon et al, 2011). Since mitochondria must import FA for β-oxidation, it is not surprising that excess FA may alter mitochondrial functions and disrupt mitochondrial membrane integrity. Incubation with low concentrations of PA (0.1 mM) induces mitochondrial ROS generation, mitochondrial membrane potential loss and DNA damage in hepatocytes and skeletal muscles cells (Rachek *et al*, 2007; Yuzefovych *et al*, 2010; Cheon and Cho, 2014). In

contrast, 1 mM OA did not induce these effects in these cells (Yuzefovych *et al*, 2010). Furthermore, apoptosis is not induced when treated with 1 mM OA, whereas Caspase 3 cleavage occurs with just 0.1 mM PA incubation leading to apoptosis, as well as ROS generation (Turpin *et al*, 2006; Yuzefovych *et al*, 2010; Egnatchik *et al*, 2014). Interestingly, despite PA incubation clearly affecting mitochondrial morphology and its network, no difference in *Toxoplasma* growth is detected. We cannot discount the fact that the alteration of host mitochondria next to the PV in OA treated cells may affect parasite growth. However, it is possible that host mitochondria association to the PV may not be critical for the intracellular development of *Toxoplasma* RH *in vitro*, as observed with type II and III strains.

Host autophagy could be involved in the decrease in growth of *Toxoplasma* upon OA incubation as excess of this FA triggers autophagy. Degradation of the PV via autophagy has not been reported for Type I strains of *Toxoplasma,* such as RH, however Type II and III strains are susceptible to immune-mediated autophagy induction. This process involves ubiquitination of the PVM, accumulation of LC3 around the PV, as well as enclosure of the PV by multiple membranes (Selleck *et al*, 2015). This complex does not fuse with lysosomes and endosomes and, as such, is not xenophagy, a form of autophagy occurring in the control of intracellular pathogens. Canonical autophagy occurs during periods of limited resources, i.e. starvation. *In vitro* studies have shown that incubation of fibroblasts in starvation medium leads to an increase in LD numbers, which in turn associate with mitochondria. This action enables FA, released from LD by ATGL lipolysis to enter the mitochondria for β-oxidation (Rambold *et al*, 2015). The opposite scenario, i.e. treatment with excess OA (up to 1 mM) stimulates lipophagy, the catabolism of LD by autophagy. This is an important process for the regulation of lipid metabolism to prevent toxic LD aggregation in the cytoplasm (Singh *et al*, 2009; Liu and Czaja, 2013). In mammalian cells, including HeLa cells and hepatocytes, excess OA triggers lipophagy

whereby OA and LD lipids contribute to the generation of the phagosomal membranes and autophagosomes via ATGL-mediated LD lipolysis (Dupont *et al*, 2014; Shpilka and Elazar, 2015). Interestingly, *Toxoplasma* appears to disrupt host cell lipid metabolism as a decrease in *ATGL* expression is observed, even with OA incubation (Chapter 3), which further suggests that *Toxoplasma* alters the host cell's metabolic activities (Blader *et al*, 2001). Previous studies have reported that *Toxoplasma* induces autophagy in HeLa cells and HFF, allowing optimal proliferation for the parasite and increased nutrient scavenging (Wang *et al*, 2009; Lee *et al*, 2013; Gao *et al*, 2014). Despite autophagic activity upon OA incubation, the increase was not dissimilar to that seen under normal *Toxoplasma*-infected conditions without OA. This suggests that autophagy induction by OA may not affect *Toxoplasma*'s development in our cell culture conditions. Additionally, *Toxoplasma* may disrupt the host cell's autophagic capacity by altering lipolysis enzymatic activity and therefore may also dampen the extent of global cellular autophagy. Further studies investigating the extent of LC3-II protein accumulation in the cytosol would confirm our microscopy results that autophagy is not highly induced with OA treatment in *Toxoplasma*-infected cells.

CHAPTER 5

FUTURE DIRECTIONS AND PERSPECTIVES

5.1. Exploitation of Apicomplexan auxotrophies as a potential therapeutic approach

The large Apicomplexa phylum comprises unicellular protozoa and, among them, obligate intracellular parasites that cause disease worldwide in animals and humans such as malaria, toxoplasmosis, cryptosporidiosis, babesiosis and neosporosis. These parasites are able to synthesize many metabolites, however, they also rely on nutrients they salvage from the host cell to support their development.

Presently, all the anti-Apicomplexa drugs target biosynthetic pathways that are unique to the parasites (e.g., fatty acid type II or folate synthesis) but these drugs such as chloroquines, macrolides, pyrimethamine, sulfadiazine, and artemisins, are not without their shortcomings. These drugs tend to cause many side effects, affect the host cell's physiology, may be expensive, are not very efficient at curing the proliferative parasite stages, have poor potency against the chronic parasite stages and are prone to drug resistance by the parasites. One promising direction in the search for new chemotherapeutics may be the development of drugs targeting the parasite's salvaging activities as a powerful way to essentially "starve" Apicomplexa. The rationale for this approach is based on the following arguments:

1. As obligate intracellular parasites, Apicomplexa have lost their ability to live independently from their host organism and cannot replicate axenically; they require nutrients from their host cell to effectively replicate.
2. They express many transporters and few metabolic enzymes, implying that salvaging is critical for survival.

3. Parasites should be particularly sensitive to inhibitors of transporters or enzymes in their salvage pathways.
4. Subversive substrate analogs internalized by the parasite might be metabolized into toxic metabolites.
5. As there is a large phylogenetic separation between Apicomplexa and their mammalian hosts, parasite transporters must have some specificity in their mechanism of action and sensitivities that may be exploited.

The problem of redundancy in salvage, recycling and biosynthetic pathways in Apicomplexa may limit this chemotherapeutic approach. Nevertheless, perturbing one salvaging pathway may have metabolic consequences despite possible redundancies by reducing global cellular biosynthesis. This may, in turn, result in parasite attenuation or loss of virulence *in vivo*. As such, identifying the most vulnerable facets of the parasite's scavenging mechanisms may aid in the discovery of better drug targets. Alternatively, a multiple step attack using a combination of drugs directed against more than one target in salvaging pathways may be beneficial to avoid the development of a single drug resistance.

This thesis focuses on two Apicomplexa: *Toxoplasma gondii* and *Neospora caninum*, very closely related parasites residing within a parasitophorous vacuole (PV) in mammalian cells (Sibley, 2003). Their sequestration in a PV provides them with a protective environment in which to replicate but the PV membrane also isolates them from the nutrients present in the host cytosol and organelles. However, both of these parasites have evolved strategies to circumvent this barrier as we have shown in chapter 2. One example is the recruitment and clustering of host organelles, like the Golgi apparatus or endolysosomes, around the PV to facilitate nutrient scavenging (Fig. 5-1) (Coppens *et al*, 2006; Romano *et al*, 2013; Nolan *et al*, 2015).

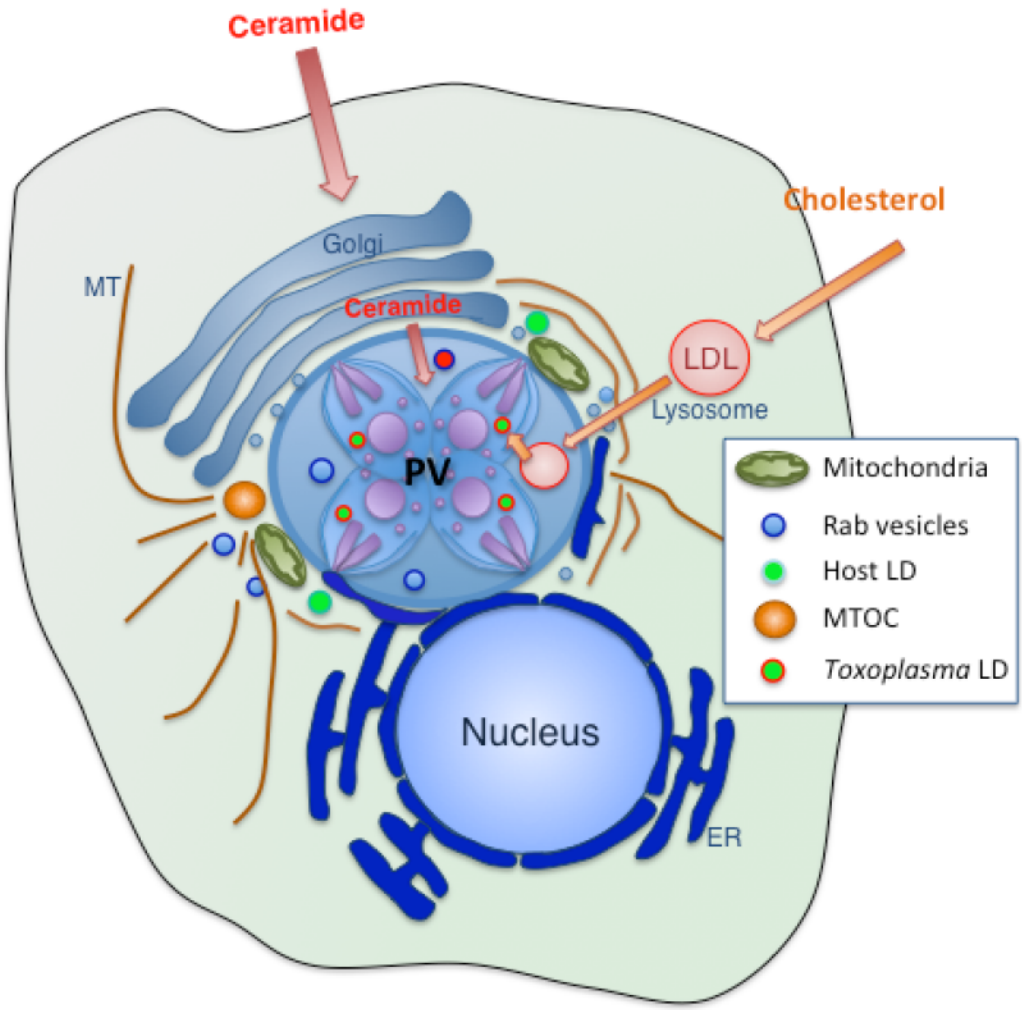

Figure 5-1. Recruitment of host organelles and structures to the PV of *Toxoplasma* and *N. caninum*
Both *Toxoplasma* and *N. caninum* recruit host cell structures and organelles to their PV, such as the endoplasmic reticulum (ER), Golgi apparatus, mitochondria, lipid droplets (LD), microtubule organizing center (MTOC), microtubules and Rab vesicles. In addition, both parasites can scavenge ceramide via the translocation of Golgi-derived Rab vesicles, loaded with ceramide. Exogenously added cholesterol is scavenged by *Toxoplasma* via the translocation of LDL-loaded lysosomes to its PV. Although *N. caninum* also scavenges cholesterol, the mechanism is unknown. Excess cholesterol salvaged by both parasites is eventually visible in labeled structures within the parasites, likely LD.

Toxoplasma has increased the number of genes that promote nutrient scavenging for auxotrophic or insufficiently synthesized metabolites, such as cholesterol, choline, polyamines, amino acids (arginine, tryptophan, histidine, methionine, threonine, leucine, isoleucine, valine), and purines (Fig 5-2, for complete list of metabolites scavenged) (reviewed in Coppens, 2013). The host cytosol and organelles represent a valuable source for these nutrients and *Toxoplasma* contains a variety of transporters for these compounds. e.g. for purines and folate, which will be discussed in greater detail. Many transporters have been either hypothesized, uncharacterized or have yet to be identified (e.g. those mediating lipoate, isoprenoid, or pyrimidine salvaging). The purine salvaging pathway in *Toxoplasma* has been extensively studied as the parasite is auxotrophic for this metabolite. *Toxoplasma* contains 3 purine transporters: TgAT1 (high affinity for adenosine and inosine); TgAT2 (purines and pyrimidines); and TgNBT1 (hypoxanthine, xanthine, guanine). Only TgAT1 has been cloned and its inactivation is not lethal, indicating redundancy in purine uptake (Chiang *et al*, 1999; De Koning *et al*, 2003). The addition of purine nucleoside analogs causes toxicity for the parasite following their internalization into the parasite via the TgAT2 transporter (Illzsch *et al*, 1995; Kim *et al*, 2010b). Drug targeting to the purine salvaging pathway is feasible since enzymes involved in purine metabolism in *Toxoplasma* vary sufficiently from mammalian enzymes in terms of substrate specificity. The drugs would have to target multiple transporters or, at the very least, not TgAT1 alone because inactivation of TgAT1 is not lethal. In addition to nucleosides, the parasite contains transporters for polyamines derived from arginine, such as ornithine and putrescine, although they have yet to be fully described (Cook *et al*, 2007). The cofactor, folate, is important for DNA synthesis and methionine metabolism and the folate pathway is the target of current *Toxoplasma* drugs such as pyrimethamine and trimethoprim. Both of these drugs target *de novo* folate metabolism by inhibiting dihydrofolate reductase (DHFR) and folate recycling in the parasite. In contrast to

mammalian cells, *Toxoplasma* can synthesize folate *de novo* but also scavenges it from the host cell using transporters similar to the BT1 family of proteins (Anderson *et al*, 2005; Massimine *et al*, 2005). Many other transporters are known to exist based on research using analogs and inhibitors, but are still largely uncharacterized. These transporters include, but are not limited to those mediating the uptake of amino acids, lipoate, pyrimidines, isoprenoids, and phospholipids (reviewed in Coppens, 2013). Targeting the aforementioned salvaging pathways may be promising in the search for novel drugs, however, more efforts needs to be deployed to better characterize these transporters in order to find their specificities for a selective intervention against the parasites.

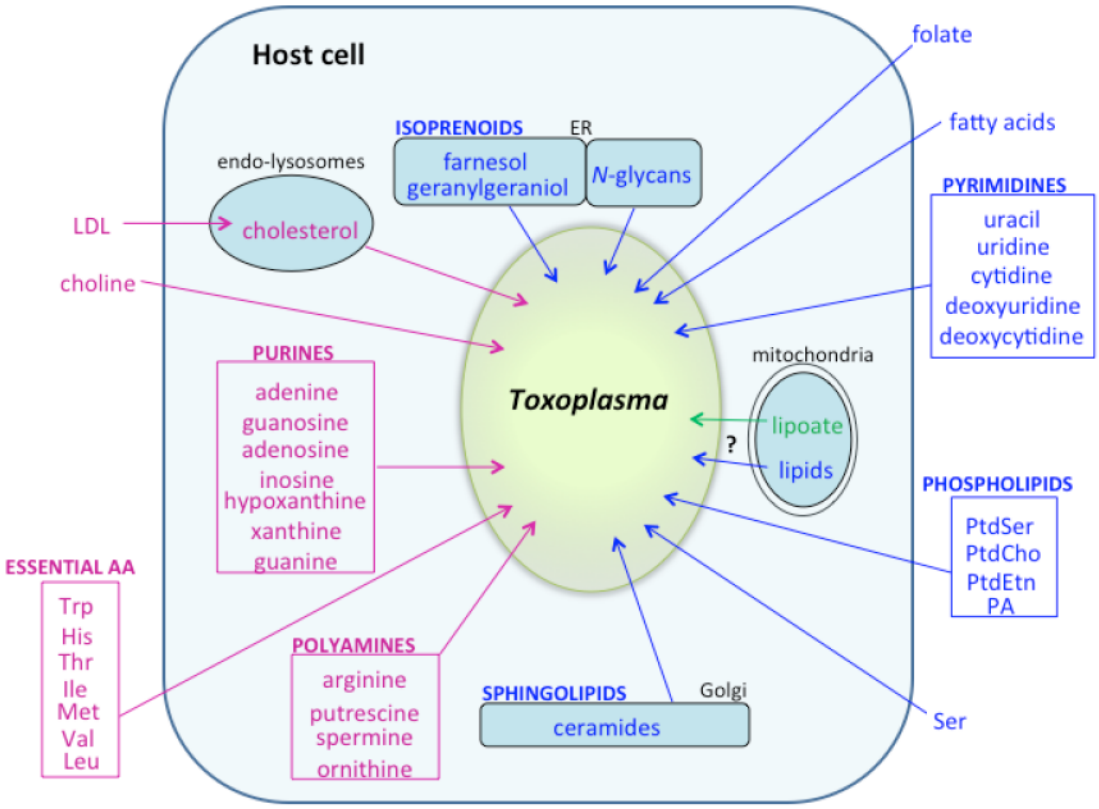

Figure 5-2. Diagram highlighting the salvage activities mediated by intracellular *Toxoplasma*
Metabolites and substrates that must be scavenged by the parasite are in pink, whereas those that are synthesized and scavenged by *Toxoplasma* are in blue. Lipoate, in green, is synthesized and scavenged by the parasite but its fate depends on its origin. The transport of lipoate or lipids from mitochondria is hypothesized but not yet proven. Abbreviations: ER, endoplasmic reticulum; LDL, low-density lipoprotein; AA, amino acids; PA, phosphatidic acid. Image from Coppens, 2013.

5.2. Lipid salvage pathways in *Toxoplasma* as potential drug targets

Toxoplasma has a very rapid replication rate. To this end, the parasite must either synthesize or scavenge large amounts of lipids for membrane generation. Targeting lipid salvage pathways may thus provide an effective avenue for future drug generation.

5.2.1. Cholesterol

Cholesterol is essential for organizing signaling lipids and proteins in membranes, as well as regulating general membrane fluidity. It is the main sterol in mammalian membranes and the only sterol present in *Toxoplasma*'s membranes despite the parasite's inability of synthesizing cholesterol *de novo* (Coppens *et al*, 2000). *Toxoplasma* acquires this lipid from host endosomes containing plasma low-density lipoproteins (LDL) (Coppens *et al*, 2006). Interfering with the parasite's access to cholesterol has a detrimental effect on *Toxoplasma,* as its growth is impaired and stage conversion to the slow-growing cyst form is stimulated (Nishikawa *et al*, 2005; Lige *et al*, 2010; Ihara and Nishikawa, 2014).

Our laboratory has identified several transporters involved in cholesterol metabolism in *Toxoplasma* e.g. ATP-binding cassette (ABC) G family (ABCG), Niemann-Pick type C1-related protein (NPC1) and sterol carrier protein 2 (SCP2). ABCG transporters have been identified in *Toxoplasma* and are located in the PV membrane, the parasite membrane and on vesicles in the PV lumen (Ehrenmann *et al*, 2010). Out of the six identified, five of these are upregulated upon sterol exposure and may represent a fruitful drug target particularly as one ABCG has been classified as a cholesterol importer. Another transporter involved in cholesterol homeostasis is the Niemann-Pick type C1-related protein (NPC1). This protein is localizes to the endolysosome membrane in mammalian cells and modulates the export of sterols and sphingolipids (Liscum

and Sturley, 2004). *Toxoplasma* contains a homologue, TgNCR1, located in the inner membrane complex (IMC) that plays a role in lipid homeostasis (Lige *et al*, 2010). Parasites lacking TgNCR1 contain large amounts of cholesteryl esters and divide rapidly, indicating a role in lipid uptake regulation. This further suggests that it is possible to disrupt lipid metabolism in *Toxoplasma*. The sterol carrier protein 2 (SCP2) is localized to the peroxisome membrane in mammalian cells. This protein helps in the transport of not only sterols, but fatty acids, fatty acyl-CoA, and phospholipids between membranes (Gallegos *et al*, 2001). *Toxoplasma* contains a D-bifunctional protein containing two SCP2 domains involved in the trafficking of phospholipids, cholesterol and fatty acids between parasite organelles and the plasma membrane (Lige *et al*, 2009). Overexpression of this protein leads to increased growth and enhanced cholesterol uptake, which makes this protein another potential target for disruption.

Once internalized in *Toxoplasma*, cholesterol can be esterified into cholesterol esters in lipid droplets using two acyl-CoA:cholesterol acyltransferases, TgACAT1 and TgACAT2. Incubation with ACAT inhibitors arrests *Toxoplasma*'s growth due to lipotoxicity from cholesterol accumulation in membranes (Nishikawa *et al*, 2005; Lige *et al*, 2013). These findings suggest that the acquisition, trafficking and storage of cholesterol is essential for the parasite's physiology and as such, may represent fruitful drug targets. Future research could involve studying the virulence *in vivo* of TgACAT1 and TgACAT2 knockout *Toxoplasma*. If cholesterol storage ability has an effect *in vivo*, perhaps TgACAT could represent a potential drug target. If successful, drug screens will be performed to help identify candidates, followed by *in vivo* efficacy testing.

5.2.3. Sphingolipids

All eukaryotic cells contain sphingolipids in their membranes to provide a stable and chemically resistant outer membrane for protection again harmful environmental factors. Sphingolipids and their precursors are also important for neighboring-cell recognition and signaling, as well as signaling cascades during cellular development and stress response (ceramides).

Lipidomics studies reveal that *Toxoplasma* contains over 20 types of sphingolipids (Welti *et al*, 2007; Lige *et al*, 2010). *Toxoplasma*'s growth can be severely impaired by molecules targeting host sphingolipid synthesis and salvage pathways. For example, treatment of infected cells with the sphingolipid analogs *threo*-phenyl-2-palmitoylamino-3-morpholino-1-propanol (PPMP) and $_{L}$-cycloserin, impairs the growth of *Toxoplasma* (Azzouz *et al*, 2002). Aureobasidin A, a inositol phosphorylceramide synthase inhibitor, also blocks *Toxoplasma* growth by reducing complex sphingolipid synthesis without affecting the host cell although no gene coding for inositol phosphorylceramide synthase has been identified in the *Toxoplasma* genome, in this case the mechanism of action remains puzzling (Sonda *et al*, 2005). Moreover, evidence of *de novo* synthesis of this lipid by the parasite, based on pharmocological inhibitors, remains argumentative.

The parasite also salvages sphingolipids from the host Golgi (de Melo and De Souza, 1996; Pratt *et al*, 2013; Romano *et al*, 2013). We have previously shown that *Toxoplasma* and *N. caninum* scavenge ceramides via the internalization of ceramide-loaded Golgi-associated Rab vesicles (Romano *et al*, 2013; Nolan *et al*, 2015). Examples include Rab14, which mediates the trafficking between the trans-Golgi network, endosomes and the plasma membrane and Rab30, involved in Golgi structure maintenance and vesicular trafficking (de Leeuw *et al*, 1998; Junutula *et al*, 2004; Proikas-Cezanne *et al*, 2006; Kitt *et al*, 2008; Sinka *et al*, 2008; Thomas *et al*, 2009;

Kelly *et al*, 2011). This is mediated by the selective translocation of Rab-vesicles into the PV. This implies that host Rab proteins are either recognized by *Toxoplasma* prior to translocation to the PV, or are present on structures/vesicles that the PV internalizes. Identifying potential candidates involved in the recognition and internalization of Rab vesicles via genetic screens on temperature sensitive mutants may prove fruitful in characterizing the *Toxoplasma* machinery involved in Rab vesicle uptake. Another suitable method of identifying this machinery could involve infecting stable cell lines expressing BirA, fused with specific Rab proteins. Proteins in close proximity to host Rab proteins would be biotinylated, which could then be isolated followed by mass spectrometry identification.

5.2.3. Fatty acids

Fatty acids (FA) are essential for all life as they are the building blocks of membranes, are important for energy storage in lipid droplets and have physiological roles such as signaling and post-translational protein modifications. *Toxoplasma* has three FA synthase (FAS) pathways: 1) a FAS II pathway in the apicoplast producing lipoic, myristic and palmitic acid; 2) FA elongation pathway in the ER for long-chain monounsaturated FA synthesis; 3) FAS I pathway, similar to that found in mammalian cells (Waller *et al*, 1998; Crawford *et al* 2003; Seeber *et al*, 2003; Ramakrishnan *et al*, 2012). Targeting the FAS I pathway is not a viable approach due to the homologous enzymes in the host cell. The FAS II pathway, found primarily in prokaryotes, has been extensively studied and involves different sets of enzymatic reactions, not found in eukaryotic cells (Goodman and McFadden, 2007). The apicoplast is a relict, nonphotosynthetic plastid resulting from secondary endosymbiosis. As such, the reactions taking place are

prokaryotic in nature and are ideal drug targets as the host cell would be unaffected by targeted disruptions in this pathway.

Toxoplasma is not auxotrophic for FA but it can also scavenge FA such as palmitic, oleic, linoleic, or arachidonic acids from the host cell for incorporation into more complex lipids or neutral lipids, or degradation by β-oxidation in the parasite's mitochondrion (Tomavo *et al*, 1989; Charron and Sibley; 2002; Quittnat *et al*, 2004; Polonais and Soldati-Favre; 2010; Nishikawa *et al*, 2005). Deletion of FAS II synthase in the parasite impairs growth, a phenotype that can be reversed with exogenous addition of FA to the medium (Ramakrishnan *et al*, 2012) signifying FA synthesis and uptake can be offset. Due to the dual sources of FA for *Toxoplasma*, interference with FA pathways need to occur at multiple points in order to affect *Toxoplasma* development. The work in this thesis revealed that *Toxoplasma* readily scavenges FA such as oleic acid from the host cell. FA uptake by *Toxoplasma* is part of its parasitism, and therefore should be studied in greater depth. Host lipid droplets represent a prominent source of FA and neutral lipids for the parasite, so a greater understanding of their interaction with *Toxoplasma* may help reveal novel points of disruption in the parasite's FA metabolism.

5.3. Perturbation of lipid salvaging pathways in *Toxoplasma*

As previously discussed, the optimal growth of *Toxoplasma* relies on salvaging of lipids from the host cell. This is evidenced by the boost in growth following addition of ceramides and cholesterol to the medium (Coppens *et al*, 2000; Nishikawa *et al*, 2005; Romano *et al*, 2013). Conversely, depletion of these lipids from the medium leads to *Toxoplasma* growth impairment (Nishikawa *et al*, 2005; Ihara and Nishikawa, 2014). In this thesis, we explored the effect of excess oleic acid (OA) on parasite growth, hypothesizing that it would be beneficial for the parasite's infectivity. Surprisingly, there appears to be a deluge of the parasite's salvaging pathways leading to cytotoxic damage in the parasite. This was evidenced by: 1) a reduction in replication rate; 2) delayed egress from the host cells; 3) the over-accumulation of large-sized lipid droplets in the parasite, often protruding out of the cytoplasm; 4) the presence of lipidic deposits in the PV lumen, the cytosol, organelles and residual bodies of the parasite; 5) morphological defects in host mitochondria associated with the PVM (Fig 5-3).

Clarifying why the parasite is affected to such an extent at OA concentrations in the medium that are subtoxic for mammalian cells is essential for a better understanding of *Toxoplasma*'s physiology. One direction we could take is performing lipidomics studies will be relevant in order to examine lipid profiles in the lipid-overloaded parasites, particularly analyzing the nature of the NL accumulated in the large LD. In parallel, analyzing the enzymatic activities of TgACATs and TgDGAT in these parasites would be interesting to reveal unique properties, e.g. in their kinetics, velocity, or avidity. Down the road, this may help designing specific pharmacological ligands as potential drugs.

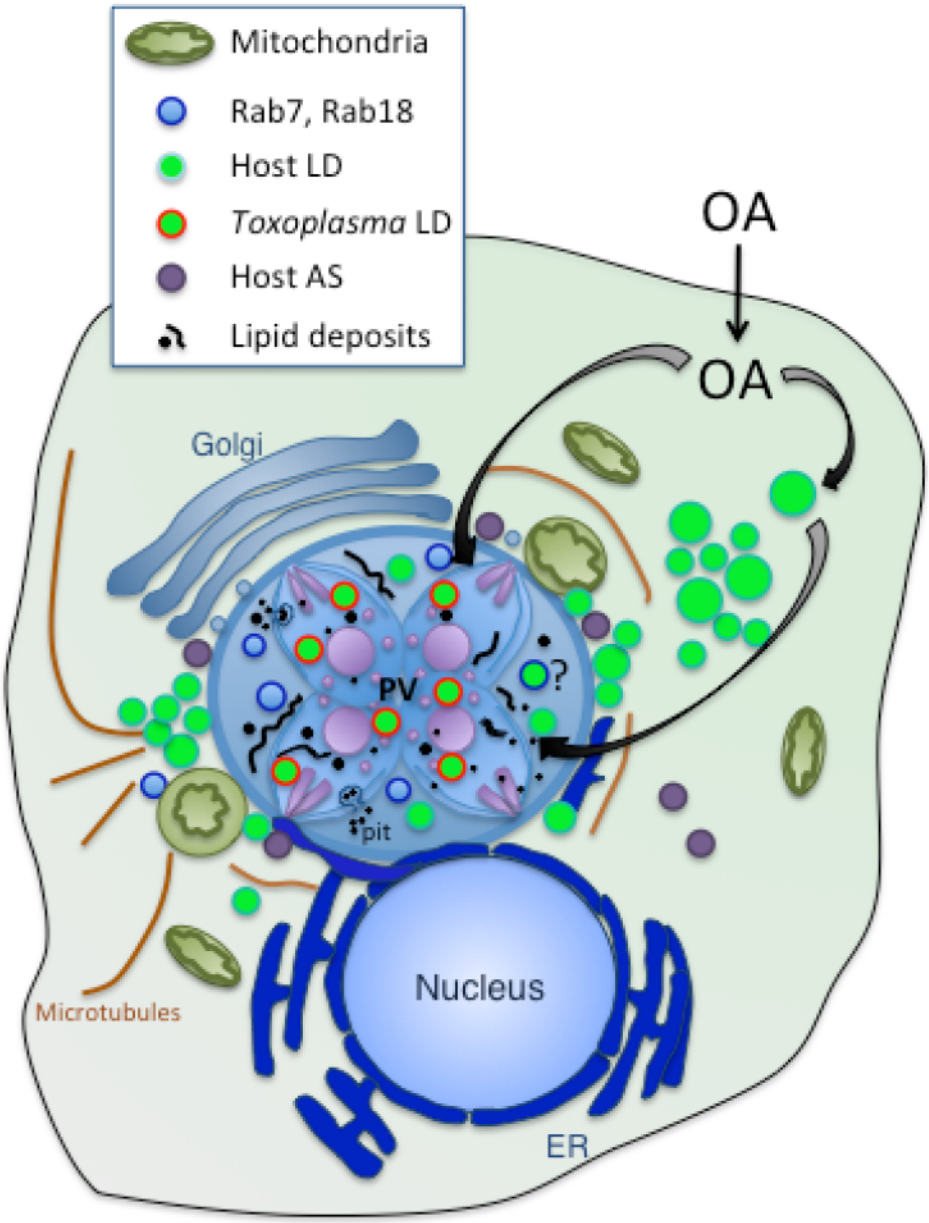

Figure 5-3. Summary of findings in chapters 3 and 4: Distribution of host organelles and *Toxoplasma* development with 0.2 mM OA.

Addition of oleic acid (OA) to the medium of infected cells leads to lipid droplet (LD) accumulation in the host cytosol, some of which are translocated to the *Toxoplasma* PV, along with the biogenesis of parasite LD. The Despite the amassing of host LD around the PV, the host ER, Golgi, autophagic structures (AS) and mitochondria are normally recruited by the parasite to the PV or associated with the PV. However, PV-associated mitochondria display morphological abnormalities. Intact host LD were observed in the PV lumen, as were as host-derived LD-associated Rab vesicles. Endocytic pits observed near the apex of the parasite are apparent with incubation with 0.2 mM OA. OA concentrations greater than 0.2 mM led to the massive accumulation of lipid deposits in the PV lumen, the parasite cytosol and the residual body (not shown).

Additionally, RNA-Seq analysis comparing transcriptional profiles of parasites cultivated with excess OA and under normal conditions, as well as Protein DIGE (Difference Gel Electrophoresis) would provide essential information in identifying the molecular components implicated in lipid uptake (at 0.2 mM OA). These include proteins that may be forming the coat of the endocytic structures, FA binding proteins or transporters including potentially a PLIN homologue despite The *Toxoplasma* genome not containing a homologue for LD-associated proteins like such as PLIN2 (ADRP) or PLIN5. The LD protein PLIN5 helps mediate LD association with mitochondria, has recently been implicated in promoting NL lipid storage and preventing lipotoxicity (reviewed in Kimmel and Sztalryd, 2014). Further digging into identifying proteins found in *Toxoplasma* involved in LD maturation, expansion, fusion/fission, motility and contact with organelles would also be essential in order to gain a better understanding of lipid metabolism in the parasite. Furthermore, it will help elucidate the mechanisms behind the lipotoxicity observed in the presence of > 0.2 mM OA. In non-adipose cells, several lipotoxic pathways have been identified including omega-oxidation, lipid peroxidation and, oxidative and ER stress. The lipotoxic-response elicited by *Toxoplasma*, incapable of storing and utilizing excess FA would likely reveal unique mechanisms by which the parasite channels excess FA to alternate fates than storage in LD. The consequence of which leads to alterations of organelle membrane structure/function, production of toxic metabolites and parasite death.

The gluttonous nature of *Toxoplasma* could be exploited by incubating the parasite with FA analogs, not toxic for the mammalian host. Previous studies on obesity therapies have shown that plant phytosterol treatment can reduce the pool of available cholesterol in humans, thereby lowering LDL-cholesterol (reviewed in Ostlund, 2004). Addition of FA analogs may trick the parasite into using these FA, potentially to detrimental effects. The synthetic OA analog, 2-hydroxylated OA (2OHOA), has a longer half life than OA as it is not degraded through β-

oxidation but by the α-oxidation pathway (Vögler *et al*, 2008). Currently, OA is being extensively researched by the cancer community as it appears that OA possesses natural anti-proliferative activities. Addition of 2OHOA enhances these activities and inhibits growth of tumors and cancer cells *in vitro* and *in vivo* (Terés *et al*, 2012). The mechanism is unknown but may be related to changes in membrane lipid composition and membrane biophysical properties (Prades *et al*, 2008; reviewed in Ibarguren *et al*, 2014). Considering the detrimental effect of OA on the parasite, 2OHOA may also prove to be a valuable tool to study OA toxicity in *Toxoplasma* and potentially open up new drug opportunities.

A naturally occurring FA analog derived from plants, jasmonic acid, may prove to be a useful therapeutic approach for *Toxoplasma*. JA originates from α-linoleic acid and its production is induced in response to stressors (UV radiation, osmotic stress, temperature, pathogens) and mediates the production of reactive oxygen species (ROS) and downstream defense responses in plants (Sembdner and Parthier, 1993; Vasyukova *et al*, 2009). This FA has no effect on normal, dividing mammalian cells (EPA, 2013) but is toxic for many different human and murine cancer cells (e.g. breast, cervical, colorectal, gastric, hepatoma, lung, lymphoma, melanoma, leukemia, prostate, neuroblastoma and sarcoma) (reviewed in Cesari *et al*, 2014). JA has been shown to be toxic to cancer cells by inducing ROS generation, MAP kinase signaling, cell cycle arrest, decrease in mitochondrial membrane potential, and apoptosis. The cause of JA selective toxicity on some cancer cells is still unknown but it may be interesting to investigate its effect on *Toxoplasma*.

Finally, considering the evolutionary closeness of *Toxoplasma* with *N. caninum*, it may be interesting to investigate if *N. caninum* is affected by OA to the same extent as *Toxoplasma*. As opposed to *Toxoplasma* that possesses two TgACAT enzymes, *N. caninum* only has one,

which shares 71% identity with TgACAT1. *N. caninum* has the ability to form lipid droplets but it is not known whether only possessing NcACAT may be even more detrimental upon OA excess. No NcDGAT enzyme has yet been identified in *N. caninum*, but bioinformatics searches reveal a putative *NcDGAT* with 87% identity with *TgDGAT* (NCLIV_032680). This suggests that both parasites have similar capabilities for triacylglycerol (TAG) generation but requires further studies to elucidate the capacity of *N. caninum* to form TAG upon OA excess. Since *N. caninum* does not seem to cause disease in humans, any biological and physiological differences between the two parasites may highlight differences in infectivity.

The focus of this thesis was to examine the ability of the Apicomplexa *Toxoplasma* and *N. caninum* to recruit host organelles (mitochondria, lipid droplets, Golgi, endolysosomes), potentially in order the salvage nutrients for their intracellular development. The more we learn about the parasite pathways involved in the salvage of key nutrients and the metabolism of key factors, the better equipped we will be to develop effective therapies. Such therapies may in future combine inhibitors that disrupt both the salvage and biosynthetic pathways, at multiple targets. The identification of weak points in *Toxoplasma*, such as excessive OA salvaging may also provide novel drug identification opportunities. Moreover, considering the similarities shared between *Toxoplasma* and *N. caninum*, it is feasible that intervention efforts could also target more than one Apicomplexa species. There is therefore a need for extensive efforts in the fundamental research on Apicomplexa. In particular, acquiring more detailed knowledge of their nutritional needs, metabolic deficiencies and nutrient transport system may help in the development of antiparasitic therapies.

REFERENCES

Ahn JH, Kim MH, Kwon HJ, Choi SY, Kwon HY. 2013. Protective Effects of Oleic Acid Against Palmitic Acid-Induced Apoptosis in Pancreatic AR42J Cells and Its Mechanisms. Korean J. Physiol. Pharmacol. **17**(1):43-50.

Alaeddine F, Hemphill A, Debache K, Guionaud C. 2013. Molecular cloning and characterization of NcROP2Fam-1, a member of the ROP2 family of rhoptry proteins in *Neospora caninum* that is targeted by antibodies neutralizing host cell invasion *in vitro*. Parasitology. **140:**1033-1050.

Alexander DL, Mital J, Ward GE, Bradley P, Boothroyd JC. 2005. Identification of the moving junction complex of Toxoplasma gondii: a collaboration between distinct secretory organelles. PLoS Pathog. **1**(2):e17.

Almería S, Lópes-Gatius F. 2013. Bovine neosporosis: clinical and practical aspects. Res. Vet. Sci. **95**(2):303-309.

Anand SK, Tikoo SK. 2013. Viruses as modulators of mitochondrial functions. Adv. Virol. **2013:**738-794.

Anderson-White BR, Beck JR, Chen CT, Meissner M, Bradley PJ, Gubbels MJ. 2012. Cytoskeleton assembly in Toxoplasma gondii cell division. Int. Rev. Cell Mol. Biol. **298**:1-31.

Andrade RM, Wessendarp M, Gubbels MJ, Striepen B, Subauste CS. 2006. CD40 induces macrophage anti-*Toxoplasma gondii* activity by triggering autophagy-dependent fusion of pathogen-containing vacuoles and lysosomes. J. Clin. Investig. **116**:2366-2377.

Asgari Q, Keshavarz H, Shojaee S, Motazedian MH, Mohebali M, Miri R, Mehrabani D, Rezaeian M. 2013. In vitron and in vivo potential of RH strain of *Toxoplasma gondii* (Type I) in tissue cyst forming. Iran J. Parasitol. **8**(3):367-375.

Ashida H, Mimuro H, Ogawa M, Kobayashi T, Sanada T, Kim M, Sasakawa C. 2011. Cell death and infection: a double-edged sword for host and pathogen survival. J. Cell Biol. **195:**931-942.

Athenstaedt K, Daum G. 2006. The life cycle of neutral lipids: synthesis, storage and degradation. Cell. Mol. Life Sci. **63**:1355-1369.

Azzouz N, Rauscher B, Gerold P, Cesbron-Delauw MF, Dubremetz JF, Schwarz RT. 2002. Evidence for de novo sphingolipid biosynthesis in *Toxoplasma gondii*. Int. J. Parasitol. **32:**677-684.

Barber J, Trees AJ, Owen M, Tennant B. 1993. Isolation of *Neospora caninum* from a British dog. Vet. Rec. **133:**531-532.

Barisch C, Paschke P, Hagedorn, M, Maniak M, Soldati T. 2014. Lipid droplet dynamics at early stages of *Mycobacterium marinum* infection in *Dictyostelium*. Cellular Microb. **17**:1332-1349.

Bartoli R, Fernandez-Banares F, Navarro E, Castellà E, Mañé J, Alvarez M, Pastor C, Cabré E, Gassull MA. 2000. Effect of olive oil on early and late events of colon carcinogenesis in rats: modulation of arachidonic acid metabolism and local prostaglandin E(2) synthesis. Gut. **46**:191-199.

Baylin A, Kabagambe EK, Siles X, Campos H. 2002. Adipose tissue biomarkers of fatty acid intake. Am. J. Clin. Nutr. **76**:750-757.

Beatty WL. 2006. Trafficking from CD63-positive late endocytic multivesicular bodies is essential for intracellular development of *Chlamydia trachomatis*. J. Cell Sci. **119:**350-359.

Berg JM, Tymoczko JL, Stryer L. Biochemistry, 5th edition. New York: WH Freeman. Section 22.4.

Bickel PE, Tansey JT, Welte MA. 2010. PAT proteins, an ancient family of lipid droplet proteins that regulate cellular lipid stores. Biochim. Biophys. Acta. **1791**(6):419-440.

Beatty WL. 2008. Late endocytic multivesicular bodies intersect the chlamydial inclusion in the absence of CD63. Infect. Immun. **76:**2872-2881.

Bjerkås I, Mohn SF, Presthus J. 1984. Unidentified cyst-forming sporozoon causing encephalomyelitis and myositis in dogs. Z. Parasitenkd. **70**:271-274

Binder EM, Kim K. 2004. Location, location, location: trafficking and function of secreted proteases of *Toxoplasma* and *Plasmodium*. Traffic. **5:**914-924.

Binns D, Januszewski T, Chen Y, Hill J, Markin VS, Zhao Y, Gilpin C, Chapman KD, Anderson RG, Goodman JM. 2006. An intimate collaboration between peroxisomes and lipid bodies. J. Cell Biol. **173**:719-731.

Bisanz C, Bastien O, Grando D, Jouhet J, Maréchal E, Cesbron-Delauw MF. 2006. *Toxoplasma gondii* acyl-lipid metabolism: de novo synthesis from apicoplast-generated fatty acids versus scavenging of host cell precursors. Biochem. J. **394:**197-205.

Blader IJ, Manger ID, Boothroyd JC. 2001. Microarray analysis reveals previously unknown changes in *Toxoplasma gondii*-infected Human cells. J. Biol. Chem. **276**:24223-24231.

Blader IJ, Saeij JP. 2010. Communication between *Toxoplasma gondii* and its host: impact on parasite growth, development, immune evasion, and virulence. APMIS. **117**:458-476.

Blader IJ, Coleman BI, Chen CT, Gubbels MJ. 2015. Lytic cycle of *Toxoplasma gondii*: 15 years alter. Annu. Rev. Microbiol. **69**:463-485.

Black MW, Boothroyd JC. 2000. Lytic cycle of *Toxoplasma gondii*. Microbiol. Mol. Biol. Rev. **64**(3):607-623.

Blais J, Tardif C, Chamberland S. 1993. Effect of clindamycin on intracellular replication, protein synthesis, and infectivity of *Toxoplasma gondii*. Antimicrob. Agents Chemother. **37:**2571-2577.

Boothroyd JC, Black M, Bonnefoy S, Hehl A, Knoll LJ, Manger ID, Ortega-Barria E, Tomavo S. 1997. Genetic and biochemical analysis of development in *Toxoplasma gondii*. Philos. Trans. R. Soc. **352**:1347-1354.

Boothroyd JC, Dubremetz JF. 2008. Kiss and spit: the dual roles of *Toxoplasma* rhoptries. Nat. Rev. Microbiol. **6**(1):79-88.

Bottova I, Hehl AB, Stefanić S, Fabriàs G, Casas J, Schraner E, Pieters J, Sonda S. 2009. Host cell P-glycoprotein is essential for cholesterol uptake and replication of *Toxoplasma gondii*. J. Biol. Chem. **284**:17438-17448.

Bougnères L, Helft J, Tiwari S, Vargas P, Chang BH, Chan L, Campisi L, Lauvau G, Hugues S, Kumar P, Kamphorst AO, Dumenil AM, Nussenzweig M, MacMicking JD, Amigorena S, Guermonprez P. 2010. A role for lipid bodies in the cross-presentation of phagocytozed antigens by MHC class I in dendritic cells. Immunity. **31**:232-244.

Bradley PJ, Sibley LD. 2007. Rhoptries: an arsenal of secreted virulence factors. Curr. Opin. Microbiol. **10:**582-587.

Brasaemle D. 2007. The perilipin family of structural lipid droplet proteins: stabilization of lipid droplets and control of lipolysis. J. Lipid Res. **48**:2547-2559.

Buhman KF, Accad M, Farese RV Jr. 2000. Mammalian acyl-CoA:cholesterol acyltransferases. Biochim. Biophys. Acta. **1529**:142-154.

Bushkin GG, Ratner DM, Cui J, Banerjee S, Duraisingh MT, Jennigs CV, Dvorin JD, Gubbels MJ, Robertson SD, Steffen M, O'Keefe BR, Robbins PW, Samuelson J. 2010. Suggestive evidence for Darwinian Selection against asparagine-linked glycans of *Plasmodium falciparum* and *Toxoplasma gondii*. Eukar. Cell. **9**: 228-241.

Caffaro CE, Boothroyd JC. 2011. Evidence for host cells as the major contributor of lipids in the intravacuolar network of *Toxoplasma*-infected cells. Eukar. Cell. **10**(8):1095-1099.

Carrillo , Giraldo M, Cavia MM, Alonso-Torre SR. 2016. Effect of oleic acid on store-operated calcium entry in immune-competent cells. Eur. J. Nutr. PMID: 26830415.

Carruthers VB, Blackman MJ. 2005. A new release on life: emerging concepts in proteolysis and parasite invasion. Mol. Microbiol. **55:**1617-1630.

Carruthers V, Boothroyd JC. 2007. Pulling together: an integrated model of Toxoplasma cell invasion. Curr. Opin. Microbiol. **10**(1):83-89.

Carruthers VB, Tomley FM. 2008. Microneme proteins in apicomplexans. Subcell. Biochem. **47:**33-45.

Cases S, Smith SJ, Zheng YW, Myers HM, Lear SR, Sande E, Novak S, Collins C, Welch CB, Lusis AJ, Erickson SK, Farese RV Jr. 1998. Identification of a gene encoding an acyl CoA:diacylglycerol

acyltransferase, a key enzyme in triacylglycerol synthesis. Proc. Natl. Acad. Sci. USA. **95**:13018-13023.

CDC. Centers for Disease Control. 2013. Epidemiology and Risk Factors.

Cesari IM, Carvalho E, Figueiredo Rodrigues MF, Mendonça Bdos S, Amôedo ND, Rumjanek FD. 2014. Methyl jasmonate: putative mechanisms of action on cancer cells cycle, metabolism, and apoptosis. Int. J. Cell Biol. **2014**:572097.

Cesbron-Delauw MF, Lecordier L, Mercier C. 1996. Role of secretory dense granule organelles in the pathogenesis of toxoplasmosis. Curr. Top. Microbiol. Immunol. **219:**59-65.

Cesbron-Delauw MF, Gendrin C, Travier L, Ruffiot P, Mercier C. 2008. Apicomplexa in mammalian cells: trafficking to the parasitophorous vacuole. Traffic. **9**:657-664.

Charron AJ, Sibley LD. 2002. Host cells: mobilizable lipid resources for the intracellular parasite *Toxoplasma gondii*. J. Cell. Sci. **115:**3049-3059.

Chang BH, Li L, Paul A, Taniguchi S, Nannegari V, Heird WC, Chan L. 2006. Protection against fatty liver but normal adipogenesis in mice lacking adipose differentiation-related protein. Mol. Cell. Biol. **26**:1063-1076.

Chang TY, Chang CC, Lin S, Yu C, Li BL, Miyazaki A. 2001. Roles of acyl-coenzymeA:cholesterol acyltransferase-1 and -2. Curr. Opin. Lipidol. **12**:289-296.

Chaudhary K, Darling JA, Fohl LM, Sullivan WJ, Donald RG, Pfefferkorn ER, Ullman B, Roos DS. 2004. Purine salvage pathways in the apicomplexan *Toxoplasma gondii*. J. Biol. Chem. **279**:31221-31227.

Cheon HG, Cho YS. 2014. Protection of palmitic acid-mediated lipotoxicity by arachidonic acid via channeling of palmitic acid into triglycerides in C2C12. J. Biomedic. Sci. **21**:13.

Chiang CW, Carter N, Sullivan Jr. WJ, Donald RG, Roos DS, Naguib FN, el Kouni MH, Ullman B, Wilson CM. 1999. The adenosine transporter of *Toxoplasma gondii*. Identification by insertional mutagenesis, cloning, and recombinant expression. J. Biol. Chem. **274**:35255-35261.

Choi SE, Lee SM, Lee YJ, Li LJ, Lee SJ, Lee JH, Kim Y, Jun HS, Lee KW, Kang Y. 2009. Protective role of autophagy in palmitate-induced INS-1 beta cell death. Endocrinology. **150:**126-134.

Choi J, Park S, Biering SB, Selleck E, Liu CY, Zhang X, Fujita N, Saitoh T, Akira S, Yoshimori T, Sibley LD, Hwang S, Virgin HW. 2014. The Parasitophorous Vacuole Membrane of *Toxoplasma gondii* is Targeted for Disruption by Ubiquitin-like Conjugation Systems of Autophagy. Immunity. **40**(6):924-935.

Cocchiaro JL, Kumar Y, Fischer ER, Hackstadt T, Valdivia RH. 2008. Cytoplasmic lipid droplets are translocated into the lumen of the *Chlamydia trachomatis* parasitophorous vacuole. Proc. Natl. Acad. Sci. USA. **105**:9379-9384.

Cole NB, Sciaky N, Marotta A, Song J, Lippincott-Schwartz J. 1996. Golgi dispersal during microtubule disruption: regeneration of Golgi stacks at peripheral endoplasmic reticulum exit sites. Mol. Biol. Cell. **7**:631-650.

Cole NB, Murphy DD, Grider T, Rueter S, Bramaemle D, Nussbaum RL. 2002. Lipid droplet binding and oligomerization properties of the Parkinson's disease protein alpha-synuclein. J. Biol. Chem. **277**:6344-6352.

Collazo CM, Yap GS, Sempowski GD, Lusby KC, Tessarollo L, Van de Woude GF, Sher A, Taylor, GA. 2001. Inactivation of LRG-47 and IRG-47 reveals a family of interferon gamma-inducible genes with essential, pathogen-specific roles in resistance to infection. J. Exp. Med. **194**:181-188.

Cook T, Roos D, Morada M, Zhu G, Keithly JS, Feagin JE, Wu G, Yarlett N. Divergent polyamine metabolism in the Apicomplexa. Microbiology. **153**:1123-1130.

Coppens I, Opperdoes FR, Courtoy PJ, Baudhuin P. 1987. Receptor-mediated endocytosis in the bloodstream form of *Trypanosoma brucei*. J. Protozool. **34:**465-473.

Coppens I, Sinai AP, Joiner KA. 2000. *Toxoplasma gondii* exploits host low-density lipoprotein receptor-mediated endocytosis for cholesterol acquisition. J. Cell Biol. **149**:167-180.

Coppens I, Joiner KA. 2003. Host but not parasite cholesterol controls *Toxoplasma* cell entry by modulating organelle discharge. Mol. Biol. Cell. **14:**3804-3820.

Coppens I, Vielemeyer O. 2005. Insights into unique physiological features of neutral lipids in Apicomplexa: from storage to potential mediation in parasite metabolic activities. Int. J. Parasitology. **35**:597-615.

Coppens I, Dunn JD, Romano JD, Pypaert M, Zhang H, Boothroyd JC, Joiner KA. 2006. *Toxoplasma gondii* sequesters lysosomes from mammalian hosts in the vacuolar space. Cell. **125:**261-274.

Coppens I. 2013. Targeting lipid biosynthesis and salvage in apicomplexan parasites for improved chemotherapies. Nat. Rev. Microbiol. **11**:823-835.

Coppens I. 2014. Exploitation of auxotrophies and metabolic defects in *Toxoplasma* as therapeutic approaches. Int. J. Parasit. **44**:109-120.

Cornelissen AW, **Overdulve JP**, **van der Ploeg M**. 1984. Determination of nuclear DNA of five eucoccidian parasites, *Isospora* (*Toxoplasma*) *gondii*, *Sarcocystis cruzi*, *Eimeria tenella*, *E. acervulina* and *Plasmodium berghei*, with special reference to gamontogenesis and meiosis in *I.* (*T.*) *gondii*. Parasitology. **88**:531-553.

Costes SV, Daelemans D, Cho EH, Dobbin Z, Pavlakis G, Lockett S. 2004. Automatic and Quantitative Measurement of Protein-Protein Colocalization in Live Cells. Biophys. J. **86:**3993-4003.

Crawford MJ, Thomsen-Zieger N, Ray M, Schachtner J, Roos DS, Seeber F. 2006. *Toxoplasma gondii* scavenges host-derived lipoic acid despite its *de novo* synthesis in the apicoplast. EMBO J. **25**:3214-3222.

Dahl NK, Reed KL, Daunais MA, Faust JR, Liscum L. 1992. Isolation and characterization of Chinese hamster ovary cells defective in the intracellular metabolism of LDL-derived cholesterol. J. Biol. Chem. **267**:4889-4896.

D'Avila H, Freire-de-Lima CG, Roque NR, Teixeira L, Barja-Fidalgo C, Silva AR, Melo RC, Dosreis GA, Castro-Faria-Neto HC, Bozza PT. 2011. Host cell lipid bodies triggered by Trypanosoma cruzi infection and enhanced by the uptake of apoptotic cells are associated with prostaglandin E generation and increased parasite growth. J. Infect. Dis. **204**: 951-961.

De Koning HP, Al-Salabi MI, Cohen AM, Coombs GH, Wastling JM. 2003. Identification and characterisation of high affinity nucleoside and nucleobase transporters in *Toxoplasma gondii*. Int. J. Parasitol. **33**:821-831.

de Leeuw HP, Koster PM, Calafat J, Janssen H, van Zonneveld AJ, van Mourik JA, Voorberg J. 1998. Small GTP-binding proteins in human endothelial cells. Br. J. Haematol. **103:**15-19.

Dejgaard SY, Murshid A, Erman A, Kizila O, Verbich D, Lodge R, Dejgaard K, Ly-Hartig TB, Pepperkok R, Simpson JC, Presley JF. 2008. Rab18 and Rab43 have key roles in ER-Golgi trafficking. J. Cell Sci. **121:**2768-2781.

Dellarupe A, Regidor-Cerrillo J, Jiménez-Ruiz E, Schares G, Unzaga JM, Venturini MC, Ortega-Mora LM. 2014. Comparison of host cell invasion and proliferation among *Neospora caninum* isolates obtained from oocysts and from clinical cases of naturally infected dogs. Exp. Parasitol. **145**:22-28.

Delorme-Walker V, Abrivard M, Lagal V, Anderson K, Perazzi A, Gonzalez C, Page C, Chauvet J, Ochoa W, Volkmann N, Hanein D, Tardieux I. 2012. Toxofilin upregulates the host cortical actin cytoskeleton dynamics, facilitating *Toxoplasma* invasion. J. Cell Sci. **125**:4333-4342.

de Melo EJ, de Souza W. 1996. Pathway of C6-NBD-Ceramide on the host cell infected with *Toxoplasma gondii*. Cell Struct. Funct. **21:**47-52.

Doege H, Stahl A. 2005. Protein-Mediated Fatty Acid Uptake: Novel Insights from In Vivo Models. Physiology. **21**:259-268.

Dowse TJ, Soldati D. 2005. Rhomboid-like proteins in Apicomplexa: phylogeny and nomenclature. Trends Parasitol. **21:**254-258.

Dubey JP, Miller NL, Frenkel JK. 1970. Characterization of the new fecal form of *Toxoplasma gondii*. J. Parasitol. **56**(3):447-456.

Dubey JP, Carpenter JL, Speer CA, Topper MJ, Uggla A. 1988. Newly recognized fatal protozoan disease of dogs. J. Am. Vet. Med. Assoc. **192:**1269-1285.

Dubey JP, **Lindsay DS**, **Speer CA.** 1998. Structures of *Toxoplasma gondii* tachyzoites, bradyzoites, and sporozoites and biology and development of tissue cysts. Clin. Microbiol. Rev. **11**:267-299.

Dubey JP, Barr BC, Barta JR, Bjerkas I, Bjorkman C, Blaqburn BJ, Bowman DD, Buxton D, Ellis JT, Gottstein B, Hemphill A, Hill DE, Howe DK, Jenkins MC, Kobayashi Y, Koudela B, Marsh AE, Mattsson JG, McAllister MM, Modrý D, Omata Y, Sibley LD, Speer CA, Trees AJ, Uggla A, Upton SJ, Williams DJ, Lindsay DS. 2002. Redescription of *Neospora caninum* and its differentiation from related coccidia. Int. J. Parasitol. **32:**929-946.

Dubey JP, Schares G, Ortega-Mora LM. 2007. Epidemiology and control of Neosporosis and *Neospora caninum*. Clin. Microbiol. Rev. **20**(2):323-367.

Ducharme NA, Bickep PE. 2008. Lipid droplets in lipogenesis and lipolysis. Endocrinology. **149**(3):942-949.

Dupont N, Chauhan S, Arko-Mensah J, Castillo EF, Masedunskas A, Weigert R, Robenek H, Proikas-Cezanne T, Deretic V. 2014. Neutral lipid stores and lipoase PNPLA5 contribute to autophagosome biogenesis. Curr. Biol. **24**(6):609-620.

Dwight JF, Mendes Ribeiro AC, Hendry BM. 1992. Membrane incorporation of non-esterified fatty acids and effects on the sodium pump of human erythrocytes. Clin. Sci. **82**:99-104.

Dzierszinski F, Nishi M, Ouko L, Roos DS. 2004. Dynamics of *Toxoplasma gondii* differentiation. Eukaryot.Cell. **3**:992-1003.

Egan JJ, Greenberg AS, Chang MK, Londos C. 1990. Control of endogenous phosphorylation of the major cAMP-dependent protein kinase substrate in adipocytes by insulin and beta-adrenergic stimulation. J. Biol. Chem. **265**:18769-18775.

Egnatchik RA, Leamy AK, Noguchi Y, Shiota M, Young JD. 2014. Palmitate-induced activation of mitochondrial metabolism promotes oxidative stress and apoptosis in H4IIEC3 rat hepatocytes. Metabolism. **63**:283-295.

Ehrenman K, Sehgal A, Lige B, Stedman TT, Joiner KA, Coppens I. 2010. Novel roles for ATP-binding cassette G transporters in lipid redistribution in *Toxoplasma*. Mol. Microbiol. **76:**1232-1249.

Ehrenman K, Wanyiri JW, Bhat N, Ward HD, Coppens I. 2013. *Cryptosporidium parvum* scavenges LDL-derived cholesterol and micellar cholesterol internalized into enterocytes. Cell. Microbiol. **15:**1182-1197.

El Hajj H, Lebrun M, Arold ST, Vial H, Labesse G, Dubremetz JF. 2007. ROP18 is a rhoptry kinase controlling the intracellular proliferation of *Toxoplasma gondii*. PLoS Pathog. **3:**e14.

Elwell CA, Jiang S, Kim JH, Lee A, Wittmann T, Hanada K, Melancon P, Engel JN. 2011. *Chlamydia trachomatis* co-opts GBF1 and CERT to acquire host sphingomyelin for distinct roles during intracellular development. PLoS Pathog. **7:**e1002198.

Endo T, Sethi KK, Piekarski G. 1982. *Toxoplasma gondii*: calcium ionophore A23187-mediated exit of trophozoites from infected murine macrophages. Exp. Parasitol. **53**(2):179-188.

Environmental Protection Agency (EPA). 2013. Methyl Jasmonate: exemption from the requirement of a tolerance. Federal Register. **78**(74):22789-22794.

Esteban-Redondo I, Innes EA. 1997. *Toxoplasma gondii* infection in sheep and cattle. Comp. Immunol. Microbiol. Infect. Dis. **20:**191-196.

Farese RV Jr, Walther TC. 2009. Lipid droplets finally get a little R-E-S-P-E-C-T. Cell. **139**(5):855-860.

Fentress SJ, Behnke MS, Dunay IR, Mashayekhi M, Rommereim LM, Fox BA, Bzik DJ, Taylor GA, Turk BE, Lichti CF, Townsend RR, Qiu W, Hui R, Beatty WL, Sibley LD. 2010. Phosphorylation of immunity-related GTPases by a *Toxoplasma gondii* secreted kinase promotes macrophage survival and virulence. Cell Host Microbe. **8:**484-495.

Ferreira-da-Silva MF, Takács AC, Barbosa HS, Gross U, Lüder CG. 2009. Primary skeletal muscle cells trigger spontaneous *Toxoplasma gondii* tachyzoite-to-bradyzoite conversion at higher rates than fibroblasts. Int. J. Med. Microbiol. **299**:281-288.

Field MC, Gabernet-Castello C, Dacks JB. 2007. Reconstruction the evolution of the endocytic system: insights from genomics and molecular cell biology. Adv. Exp. Med. Biol. **607**:84-96.

Fölsch H, Pypaert M, Schu P, Mellman I. 2001. Distribution and function of AP-1 clathrin adaptor complexes in polarized epithelial cells. J. Cell Biol. **152:**595-606.

Foussard F, Leriche MA, Dubremetz JF. 1991. Characterization of the lipid content of *Toxoplasma gondii* rhoptries. Parasitology. **102:**367-370.

Fox BA, Ristuccia JG, Gigley JP, Bzik DJ. 2009. Efficient gene replacements in *Toxoplasma gondii* strains deficient for nonhomologous end joining. Eukaryot. Cell. **8**(4): 520-529.

Fujimoto T, Ohsaki Y, Cheng J, Suzuki M, Shinohara Y. 2008. Lipid droplets: a classic organelle with new outfits. Histochem. Cell. Biol. **130**:263-279.

Fujimoto T and Ohsaki Y. 2006. The proteasomal and autophagic pathways converge on lipid droplets. Autophagy. **2**:299-301.

Fujimoto Y, Onoduka J, Homma KJ, Yamaguchi S, Mori M, Higashi Y, Makita M, Kinoshita T, Noda J, Itabe H, Takanoa T. 2006. Long-chain fatty acids induce lipid droplet formation in a cultured human hepatocyte in a manner dependent of Acyl-CoA synthetase. Biol. Pharm. Bull. **29**(11):2174-2180.

Funari SS, Barceló F, Escribá PV. 2003. Effects of oleic acid and its congeners, elaidic and stearic acids, on the structural properties of phosphatidylethanolamine membranes. J. Lipid Res. **44**:567-575.

Furuhashi M, Hotamisligil GS. 2008. Fatty acid-binding proteins: role in metabolic diseases and potential as drug targets. Nat. Rev. Drug Discov. **7**(6):489-503.

Furuyashiki T, Narumiya S. 2011. Stress responses: the contribution of prostaglandin E2 and its receptors. Nat. Rev. Endocrinol. **7**:163-175.

Gallegos AM, Atshaves BP, Storey SM, Starodub O, Petrescu AD, Huang H, McIntosh AL, Martin GG, Chao H, Kier AB, Schroeder F. 2001. Gene structure, intracellular localization, and functional roles of sterol carrier protein-2. Prog. Lipid Res. **40**(6):498-563.

Galloway CA, Yoon Y. 2013. Mitochondrial morphology in metabolic diseases. Antioxid. Redox. Signal. **19**(4):415-430.

Galloway CA, Yoon Y. 2015. Mitochondrial dynamics in diabetic cardiomyopathy. Antioxid. Redox. Signal. **22**(17):1545-1562.

Gao D, Zhang J, Zhao J, Wen H, Pan J, Zhang S, Fang Y, Li X, Cai Y, Wang X, Wang S. 2014. Autophagy activated by *Toxoplasma gondii* infection in turn facilitates *Toxoplasma gondii* proliferation. Parasitol. Res. **113**(6):2053-2058.

Garcia-Ruiz I, Solis-Muñoz P, Fernandez-Moreira D, Muñoz-Yagüe T, Solis-Herruzo JA. 2015. *In vitro* treatment of HepG2 cells with saturated fatty acids reproduces mitochondrial dysfunction found in nonalcoholic steatohepatitis. Disease Models and Mechanisms. **8**:183-191.

Garénaux E, Shams-Eldin H, Chirat F, Bieker U, Schmidt J, Michalski JC, Cacan R, Guérardel Y, Schwarz RT. 2008. The dual origin of *Toxoplasma gondii* N-glycans. Biochem. **47:**12270-12276.

Gillingham AK, Sinka R, Torres IL, Lilley KS, Munro S. 2014. Towards a comprehensive map of the effectors of Rab GTPases. Dev. Cell. **31**(3):358-373.

Goldstein JL, Brown MS. 1990. Regulation of the mevalonate pathway. Nature. **343:**425-430.

Goldszmid RS, Coppens I, Lev A, Caspar P, Mellman I, Sher A. 2009. Host ER-parasitophorous vacuole interaction provides a route of entry for antigen cross-presentation in *Toxoplasma gondii*-infected dendritic cells. J. Exp. Med. **206**:399-410.

Gomes AF, Magalhães KG, Rodrigues RM, de Carvalho L, Molinaro R, Bozza PT, Barbosa HS. 2014. *Toxoplasma gondii*-skeletal muscle cells interaction increases lipid droplet biogenesis and positively modulates the production of IL-12, IFN-g and PGE2. Parasit. Vectors. **7**:47.

Goodman DS, Deykin D, Shiratori T. 1964. The formation of cholesterol esters with rat liver enzymes. J. Biol. Chem. **239**:1335-1345.

Goodman CD, McFadden GI. 2007. Fatty acid biosynthesis as a drug target in Apicomplexan parasites. Curr. Drug Targets. **8**:15-30.

Goodman JM. 2008. The gregarious lipid droplet. J. Biol. Chem. **283**:28005-28009.

Graham DA, Calvert V, Whyte M, Marks J. 1999. Absence of serological evidence for human *Neospora caninum* infection. Vet. Rec. **144:**672-673.

Greenberg A, Egan JJ, Wek S, Garty N, Blanchette-Mackie E, Londos C. 1991. Perilipin, a major hormonally regulated adipocyte-specific phosphoprotein associated with the periphery of lipid storage droplets. J. Biol. Chem. **266**:11341-11346.

Greenberg AS, Coleman RA., Kraemer FB, McManaman, JL, Obin MS, Puri V, Yan QW., Miyoshi H, Mashek DG. 2011. The role of lipid droplets in metabolic disease in rodents and humans. J. Clin. Invest. **121**:2102-2110.

Gross DN, Miyoshi H, Hosaka T, Zhang HH, Pino EC, Souza S, Obin M, Greenberg AS, Pilch PF. 2006. Dynamics of lipid droplet-associated proteins during hormonally stimulated lipolysis in engineered adipocytes: stabilization and lipid droplet binding of adipocyte differentiation-related protein/adipophilin. Mol. Endocrinol. **20**:459-466.

Gupta N, Zahn MM, Coppens I, Joiner KA, Voelker, DR. 2005. Selective disruption of phosphatidylcholine metabolism of the intracellular parasite *Toxoplasma gondii* arrests its growth. J. Biol. Chem. **280**:16345-16353.

Hackstadt T, Scidmore MA, Rockey DD. 1995. Lipid metabolism in *Chlamydia trachomatis*-infected cells: directed trafficking of Golgi-derived sphingolipids to the chlamydial inclusion. Proc. Natl Acad. Sci. USA. **92:**4877-4881.

Hackstadt T, Rockey DD, Heinzen RA, Scidmore MA. 1996. *Chlamydia trachomatis* interrupts an exocytic pathway to acquire endogenously synthesized sphingomyelin in transit from the Golgi apparatus to the plasma membrane. EMBO J. **15:**964-977.

Hara T, Hirasawa A, Ichimura A, Kimura I, Tsujimoto G. 2011. Free fatty acid receptors FFAR1 and GPR120 as novel therapeutic targets for metabolic disorders. J. Pharm. Sci. **100**(9):3594-3601.

Hartmann A, Hellmund M, Lucius R, Voelker DR, Gupta N. 2014. Phosphatidylethanolamine synthesis in the parasite mitochondrion is required for efficient growth but dispensible for survival of *Toxoplasma gondii*. J. Biol. Chem. **289**(10):6809-6824.

Hatch GM, McClarty G. 1998. Phospholipid composition of purified *Chlamydia trachomatis* mimics that of the eucaryotic host cell. Infect Immun. **66**(8):3727-3735.

Heaton NS, Randall G. 2010. Dengue virus-induced autophagy regulates lipid metabolism. Cell Host Microbe. **8**:422-432.

Hemphill A, Gajendran N, Sonda S, Fuchs N, Gottstein B, Hentrich B, Jenkins M. 1998. Identification and characterisation of a dense granule-associated protein in *Neospora caninum* tachyzoites. Int. J. Parasitol. **28:**429-438.

Hemphill A, Gottstein B. 2000. A European perspective on *Neospora caninum*. Int. J. Parasitol. **30:** 877-924.

Hemphill A, Vonlaufen N, Naguleswaran A. 2006. Cellular and immunological basis of the host-parasite relationship during infection with *Neospora caninum*. Parasitology. **133:**261-278.

Heuer D, Rejman Lipinski A, Machuy N, Karlas A, Wehrens A, Siedler F, Brinkmann V, Meyer TF. 2009. *Chlamydia* causes fragmentation of the Golgi compartment to ensure reproduction. Nature. **457:**731-735.

He XL, Grigg ME, Boothroyd JC, Garcia KC. 2002. Structure of the immunodominant surface antigen from the *Toxoplasma gondii* SRS superfamily. Nat. Struct. Biol. **9**:606-611.

Hill DE, Chirukandoth S, Dubey JP. 2005. Biology and epidemiology of *Toxoplasma gondii* in man and animals. Anim. Health Res. Rev. **6**(1):41-61.

Hodson L, Fielding BA. 2013. Stearoyl-CoA desaturase: rogue or innocent bystander? Prog. Lipid Res. **52**(1):15-42.

Hu K, Johnson J, Florens L, Fraunholz M, Suravajjala S, DiLullo C, Yates J, Roos DS, Murray JM. 2006. Cytoskeletal components of an invasion machine—the apical complex of *Toxoplasma gondii*. PLOS Pathog. **2**:e13.

Huang B, Hubber A, McDonough JA, Roy CR, Scidmore MA, Carlyon JA. 2010. The *Anaplasma phagocytophilum*-occupied vacuole selectively recruits Rab-GTPases that are predominantly associated with recycling endosomes. Cell Microbiol. 1;**12**(9):1292-307.

Hunn JP, Feng CG, Sher A, Howard JC. 2011. The immunity-related GTPases in mammals: a fast-evolving cell-autonomous resistance system against intracellular pathogens. Mamm. Genome. **22**:43-54.

Huynh,MH, Carruthers VB. 2009. Tagging of endogenous genes in a *Toxoplasma gondii* strain lacking Ku80. Eukaryot. Cell. **8**(4):530-539.

Ibarguren M, López DJ, Escribá PV. 2014. The effect of natural and synthetic fatty acids on membrane structure, microdomain organization, cellular functions and human health. Biochim. Biophys. Acta. **1838**:1518-1528.

Ibrahim HM, Huang P, Salem TA, Talaat RM, Nasr MI, Xuan X, Nishikawa Y. 2009. Prevalence of *Neospora caninum* and *Toxoplasma gondii* Antibodies in Northern Egypt. Am. J. Trop. Med. Hyg. **80:**263-267.

Ihara F, Nishikawa Y. 2014. Starvation of low-density lipoprotein-derived cholesterol induces bradyzoite conversion in *Toxoplasma gondii*. Parasit. Vectors. 7:248.

Iltzsch MH, Uber SS, Tankersley KO, el Kouni MH. 1995. Structure-activity relationship for the binding of nucleoside ligands to adenosine kinase from *Toxoplasma gondii*. Biochem. Pharmacol. **49**:1501-1512.

Jackson KG, Bateman PA, Yaqoob P, Williams CM. 2009. Impact of saturated, polyunsaturated and monounsaturated fatty acid-rich micelles on lipoprotein synthesis and secretion in Caco-2 cells. Lipids. **44**:1081-1089.

Jackson AJ, Clucas C, Mamczur NJ, Ferguson DJ, Meissner M. 2013. *Toxoplasma gondii* Syntaxin 6 is required for vesicular transport between endosomal-like compartments and the Golgi complex. Traffic. **14**(11):1166-1181.

Imamura M, Inoguchi T, Ikuyama S, Taniguchi S, Kobayashi K, Nakashima N, Nawata H. 2002. ADRP stimulates lipid accumulation and lipid droplet formation in murine fibroblasts. Am. J. Physiol. Endocrinol. Metab. **283**:775-783.

Jackson KE, Klonis N, Ferguson DJ, Adisa A, Dogovski C, Tilley L. 2004. Food vacuole-associated lipid bodies and heterogeneous lipid environments in the malaria parasite, Plas*modium falciparum*. Mol Microbiol. **54**:109-122.

Jones PJH, Pencharz PB, Clandinin MT. 1985. Whole body oxidation of dietary fatty acids: Implications for energy utilization. Am. J. Clin. Nutr. **42**:769-777.

Junutula JR, De Maziére AM, Peden AA, Ervin KE, Advani RJ, van Dijk SM, Klumperman J, Scheller RH. 2004. Rab14 is involved in membrane trafficking between the Golgi complex and endosomes. Mol. Biol. Cell. **15:**2218-2229.

Jung C, Lee CY, Grigg ME. 2004. The SRS superfamily of *Toxoplasma* surface proteins. Int. J. Parasitol. **34:**285-296.

Kafsack BF, Pena JD, Coppens I, Ravindran S, Boothroyd JC, Carruthers VB. 2009. Rapid membrane disruption by a perforin-like protein facilitates parasite exit from host cells. Science. **323**:530-533.

Karacor K, Cam M. 2015. Effects of oleic acid. Medical Sci. and Discov. **2**(1):125-132.

Karpe F, Dickmann JR, Frayn KN. 2011. Fatty acids, obesity and insulin resistance: time for a reevaluation. Diabetes. **60**(10):2441-2449.

Karsten V, Hegde RS, Sinai AP, Yang M, Joiner KA. 2004. Transmembrane domain modulates sorting of membrane proteins in *Toxoplasma gondii*. J. Biol. Chem. **279**:26052-26057.

Katsuta Y, Iida T, Inomata S, Denda M. 2005. Unsaturated fatty acids induce calcium influx into keratinocytes and cause abnormal differentiation of epidermis. J. Invest. Dermatol. **124**(5):1008-1013.

Katsuta Y, Iida T, Hasegawa K, Inomata S, Denda M. 2009. Function of oleic acid on epidermal barrier and calcium influx into keratinocytes is associated with N-methyl D-aspartate-type glutamate receptors. **160**(1):69-74.

Katze MG, He YP, Gale M. 2002. Viruses and interferon: a fight for supremacy. Nat. Rev. Immunol. **2**:675-687.

Keeley A, Soldati D. 2004. The glideosome: a molecular machine powering motility and host-cell invasion by Apicomplexa. Trends Cell Biol. **14**(10):528-532.

Kelly EE, Giordano F, Horgan CP, Jollivet F, Raposo G, McCaffrey MW. 2011. Rab30 is required for the morphological integrity of the Golgi apparatus. Biol. Cell. **104:**84-101.

Kernohan EA, Lepherd EE. 1969. Size distribution of fat globules in cow's milk during milking, measured with a Coulter counter. J. Dairy Res. **36**:177-182.

Khandoker MAM, Tsujii H, Karasawa D. 1997. Fatty acid compositions of oocytes, follicular, oviductal and uterine fluids of pig and cow. Asian Australas. J. Anim. Sci. **10**(5):523-527.

Khor VK, Shen WJ, Kraemer FB. 2013. Lipid droplet metabolism. Curr. Opin. Clin. Nutr. Metab. Care. **16**(6):632-637.

Kieffer F, Wallon M. 2013. Congenital Toxoplasmosis. Handb. Clin. Neurol. **112:**1099-1101.

Kim K. 2004. Role of proteases in host cell invasion by *Toxoplasma gondii* and other Apicomplexa. Acta Trop. **91:**69-81.

Kim JY, Ahn HJ, Ryu KJ, Nam HW. 2008. Interaction between parasitophorous vacuolar membrane-associated GRA3 and calcium modulating ligand of host cell endoplasmic reticulum in the parasitism of *Toxoplasma gondii*. Korean J. Parasitol. **46:**209-216.

Kim MJ, Wainwright HC, Locketz M, Bekker LG, Walther GB, Dittrich C, Visser A, Wang W, Hsu FF, Wiehart U, Tsenova L, Kaplan G, Russell, DG. 2010. Caseation oh human tuberculosis granulomas correlate with elevated host lipid metabolism. EMBO Mol. Med. **2**:258–274.

Kim YA, Rawal RK, Yoo J, Sharon A, Jha AK, Chu CK, Rais RH, Al Safarjalan ON, Naguib FN, El Kouni MH. 2010b. Structure-activity relationships of carbocyclic 6-benzylthioinosine analogues as subversive substrates of *Toxoplasma gondii* adenosine kinase. Bioorg. Med. Chem. **18**:3403-3412.

Kitt KN, Hernández-Deviez D, Ballantyne SD, Spiliotis ET, Casanova JE, Wilson JM. 2008. Rab14 regulates apical targeting in polarized epithelial cells. Traffic. **9:**1218-1231.

Ko DC, Gordon MD, Jin JY, Matthew P, Scott MP. 2001. Dynamic Movements of Organelles Containing Niemann-Pick C1 Protein: NPC1 Involvement in Late Endocytic Events. Mol. Biol. Cell. **12:**601-614.

Kornmann B. 2013. The molecular hug between the ER and the mitochondria. Curr. Opin. Cell Biol. **25:**443-448.

Krahmer N, Guo Y, Wilfling F, Hilger M, Lingrell S, Heger K, Newman HW, Schmidt-Supprian M, Vance DE, Mann M, Farese RV Jr. 2011. Phophatidylcholine synthesis for lipid droplet expansion is mediated by localized activation of CTP:phophocholine cytidyltransferase. Cell Metabolism. **14**:504-515.

Labesse G, Gelin M, Bessin Y, Lebrun M, Papoin J, Cerdan R, Arold ST, Dubremetz JF. 2009. ROP2 from *Toxoplasma gondii*: a virulence factor with a protein-kinase fold and no enzymatic activity. Structure. **17:**139-146.

Labaied M, Jayabalasingham B, Bano N, Cha SJ, Sandoval J, Guan G, Coppens I. 2011. *Plasmodium* salvages cholesterol internalized by LDL and synthesized *de novo* in the liver. Cell. Microbiol. **13:**569-586.

Labruyere E, Lingnau M, Mercier C, Sibley LD. 1999. Differential membrane targeting of the secretory proteins GRA4 and GRA6 within the parasitophorous vacuole formed by *Toxoplasma gondii*. Mol. Biochem. Parasitol. **102**:311-324.

Lartigue L, Faustin B. 2013. Mitochondria: metabolic regulators of innate immune responses to pathogens and cell stress. Int. J. Biochem. Cell. Biol. **45:**2052-2056.

Layerenza JP, Gonzalez P, Garcia de Bravo MM, Polo MP, Sisti MS, Ves-Losada, A. 2013. Nuclear lipid droplets: a novel nuclear domain. Biochim. Biophys. Acta **1831**:327-340.

Lee Yj, Song HO, Lee YH, Ryu JS, Ahn MH. 2013. Proliferation of *Toxoplasma gondii* suppresses host cell autophagy. Korean J. Parasitol. **51**(3):279-287.

Lei T, Wang H, Liu J, Nan H, Liu Q. 2014. ROP18 is a key factor responsible for virulence difference between *Toxoplasma gondii* and *Neospora caninum*. PLoS One. **9:**e99744.

Levine T. 2004. Short-range intracellular trafficking of small molecules across endoplasmic reticulum junctions. Trends Cell Biol. **14**:483-490.

Li Z, Thiel K, Thul PJ, Beller M, Kühnlein RP, Welte MA. 2012. Lipid droplets control the maternal histone supply of Drosophila embryos. Curr. Biol. **22**:2104-2113.

Li ZH, Ramakrishnan S, Striepen B, Moreno SNJ. 2013. *Toxoplasma gondii* relies on both host and parasite isoprenoids and can be rendered sensitive to atorvastatin. PLoS Pathog. **9**:e1003665.

Lige B, Jayabalasingham B, Zhang H, Pypaert M, Coppens I. 2009. Role of an ancestral d-bifunctional protein containing two sterol-carrier protein-2 domains in lipid uptake and trafficking in *Toxoplasma*. Mol. Biol. Cell. **20**:658-672.

Lige B, Romano JD, Bandaru VVR, Ehrenman K, Levitskaya J, Sampels V, Haughey NJ, Coppens I. 2010. Deficiency of a Niemann-Pick, type C1-related protein in *Toxoplasma* is associated with multiple lipidoses and increased pathogenicity. PLoS Pathog. **7:**e1002410.

Lige B, Sampels V, Coppens I. 2013. Characterization of a second sterol-esterifying enzyme in *Toxoplasma* highlights the importance of cholesterol storage pathways for the parasite. Mol. Microbiol. **87:**951-967.

Lipsky NG, Pagano RE. 1985. Intracellular translocation of fluorescent sphingolipids in cultured fibroblasts: endogenously synthesized sphingomyelin and glucocerebroside analogues pass through the Golgi apparatus en route to the plasma membrane. J. Cell Biol. **100:**27-34.

Liscum L, Sturley SL. 2004. Intracellular trafficking of Niemann-Pick C proteins 1 and 2: obligate components of subcellular lipid transport. Biochim. Biophys. Acta. **1685**:22-27.

Listenberger LL, Han X, Lewis SE, Cases S, Farese RV Jr; Ory DS, Schaffer JE. 2003. Triglyceride accumulation protects against fatty acid-induced lipotoxicity. Proc. Natl. Acad. Sci. U.S.A. **100**(6):3077-3082.

Listenberger LL, Ostermeyer-Fay AG, Goldberg EB, Brown WJ, Brown DA. 2007. Adipocyte differentiation-related protein reduces lipid droplet association of adipose triglyceride lipase and slows triacylglycerol turnover. J. Lipid Res. **48**:2751-2761.

Liu P, Bartz R, Zehmer JK, Ying YS, Zhu M, Serrero G, Anderson RG. 2007. Rab-regulated interaction of early endosomes with lipid droplets. Biochim. Biophys. Acta. **1773**:784-793.

Liu K, Czaja MJ 2013. Regulation of lipid stores and metabolism by lipophagy. Cell death and Diffentiation. **20**:3-11.

Liu J, Pace D, Dou Z, King TP, Guidot D, Li ZH, Carruthers VB, Moreno SN. 2014. A vacuolar-H(+) -pyrophosphatase (TgVP1) is required for microneme secretion, host cell invasion, and extracellular survival of *Toxoplasma gondii*. Mol. Microbiol. **93**(4):698-712.

Lobato J, Silva DA, Mineo, TW, Amaral JD, Segundo GR, Costa-Cruz JM. Ferreira MS, Borges AS, Mineo JR. 2006. Detection of immunoglobulin G antibodies to *Neospora caninum* in humans: high seropositivity rates in patients who are infected by human immunodeficiency virus or have neurological disorders. Clin. Vaccine Immunol. **13:**84-89.

Lombard M-N, Bazin R, Durand D, Beauge F, Baccam D, Milgen F, Landau I. 1998. Rodent *Plasmodium* development in livers of genetically obese Zucker rats (fa/fa). Eur. J. Prot. **34**:78-81.

Lopez S, Bermudez B, Montserrat-de la Paz S, Jaramillo S, Varela LM, Ortega-Gomez A, Abia R, Muriana FJG. 2014. Membrane composition and dynamics: a target of bioactive virgin olive oil constituents. Biochim. Biophys. Acta. **1838**(6):1638-1656.

Luft BJ, Remington JS. 1992. Toxoplasmic encephalitis in AIDS. Clin. Infect. Dis. **15:**211-222.

Magnusson B, Asp L, Bostrom P, Ruiz M, Stillemark-Billton P, Linden D, Boren J, Olofsson SO. 2006. Adipocyte differentiation-related protein promotes fatty acid storage in cytosolic triglycerides and inhibits secretion of very low-density lipoproteins. Arterioscler. Thromb. Vasc. Biol. **26**:1566-1571.

Massimine KA, Doan LT, Atreya CA, Stedman TT, Anderson KA, Joiner KA, Coppens I. 2005. *Toxoplasma gondii* is capable of exogenous folate transport: A likely expansion of the BT1 family of transmembrane proteins. Mol. Biol. Parasit. **144**:44-54.

Martin S, Parton RG. 2005. Caveolin, cholesterol, and lipid bodies. Cell Dev. Biol. **16**:163-174.

Maxfield FR, Tabas I. 2005. Role of cholesterol and lipid organization in disease. Nature. **438**:612-621.

Maziere C, Maziere JC, Polonivski J. 1980. Fatty acid composition and metabolism in normal and SV40 transformed hamster fibroblasts. Biochimie. **62**(4):283-285.

McArthur MJ, Atshaves BP, Frolov A, Foxworth WD, Kier AB, Schroeder F. 1999. Cellular uptake and intracellular trafficking of long chain fatty acids. J. Lipid Res. **40**:1371-1383.

Mei S, Ni H, Manley S, Bockus A, Kassel KM, Luyendyk JP, Copple BL, Ding W. 2011. Differential roles of unsaturated and saturated fatty acids on autophagy and apoptosis in hepatocytes. J. Pharma. Exp. Therap. **339**(2):487-498.

Meissner M, Schlüter D, Soldati D. 2002. Role of *Toxoplasma gondii* myosin A in powering parasite gliding and host cell invasion. Science. **298**(5594):837-840.

Melo RCN, D'Avila H, Fabrino DL, Almeida PE, Bozza PT. 2003. Macrophage lipid body induction by Chagas disease *in vivo*: putative intracellular domains for eicosanoid formation during infection. Tissue Cell. **35**:59-67.

Mercier C, Dubremetz JF, Rauscher B, Lecordier L, Sibley LD, Cesbron-Delauw MF. 2002. Biogenesis of nanotubular network in *Toxoplasma* parasitophorous vacuole induced by parasite proteins. Mol. Biol. Cell. **13**:2397-2409.

Mi-Ichi F, Kano S, Mitamura T. 2007. Oleic acid is indispensable for intraerythrocytic proliferation of *Plasmodium falciparum*. Parasitology. **134**(12):1671-1677.

Molestina RE, El-Guendy N, Sinai AP. 2008. Infection with *Toxoplasma gondii* results in dysregulation of the host cell cycle. Cell. Microbiol. **10:**1153-1165.

Mordue DG, Hakansson S,Niesman I, Sibley LD. 1999. *Toxoplasma gondii* resides in a vacuole that avoids fusion with host cell endocytic and exocytic vesicular trafficking pathways. Exp. Parasitol. **92**:87-99.

Moriishi K, Matsuura Y. 2012. Exploitation of lipid components by viral and host proteins for hepatitis C virus infection. Front. Microbiol. **3**(54):1-14.

Morris MT, Cheng WC, Zhou XW, Brydges SD, Carruthers VB. 2004. *Neospora caninum* expresses an unusual single-domain Kazal protease inhibitor that is discharged into the parasitophorous vacuole. Int. J. Parasitol. **34:**693-701.

Mota LA, Roberto Neto J, Monteiro VG, Lobato CS, Oliveira MA, Cunha Md, D'Ávila H, Seabra SH, Bozza PT, DaMatta RA. 2014. Culture of mouse peritoneal macrophages with mouse serum induces lipid bodies that associate with the parasitophorous vacuole and decrease their microbicidal capacity against *Toxoplasma gondii*. Mem. Inst. Oswaldo Cruz. **109**(6):767-774.

Muniz-Feliciano L, Van Grol J, Portillo JA, Liew L, Liu B, Carlin CR, Carruthers VB, Matthews S, Subauste CS. 2013. *Toxoplasma gondii*-induced activation of EGFR prevents autophagy protein-mediated killing of the parasite. PLOS Pathog. **9**:e1003809.

Murphy D, Martin S, Parton RG. 2009. Lipid droplet-organelle interactions; sharing the fats. Biochim. Biophys. Acta. **791**:441-447.

Nagamune K, Hicks LM, Fux B, Brossier F, Chini EN, Sibley LD. 2008. Abscisic acid controls calcium dependent egress and development in *Toxoplasma gondii*. Nature. **451**:207-210.

Nagamune K, Moreno SN, Chini EN, Sibley LD. 2008. Calcium regulation and signaling in apicomplexan parasites. Subcell. Biochem. **47**:70-81

Naguleswaran A, Müller N, Hemphill A. 2003. *Neospora caninum* and *Toxoplasma gondii*: a novel adhesion/invasion assay reveals distinct differences in tachyzoite-host cell interactions. Exp. Parasitol. **104:**149-158.

Nam HW. 2009. GRA proteins of *Toxoplasma gondii*: maintenance of host-parasite interactions across the parasitophorous vacuole membrane. Korean J. Parasitol. **47**:S29-S37.

Neyrolles O. 2014. Mycobacteria and the Greasy Macrophage: Getting Fat and Frustrated. Infect. Immun. **82**:472-475.

Nichols BA, Chiappino ML, Pavesio CE. 1994. Endocytosis at the micropore of *Toxoplasma gondii*. Parasitol. Res. **80**(2):91-98.

Nicolle C, Manceaux L. 1908. Sur une infection a corps de Leishman (ou organismes voisins) du gondi. CR Acad. Sci. **146**:2207-2209.

Nishikawa Y, Quittnat F, Stedman TT, Voelker DR, Choi JY, Zahn M, Yang M, Pypaert M, Joiner KA, Coppens I. 2005. Host cell lipids control cholesteryl ester synthesis and storage in intracellular *Toxoplasma*. Cell. Microbiol. **7:**849-867.

Nishikawa Y, Ibrahim HM, Kameyama K, Shiga I, Hiasa J, Xuan X. 2011. Host cholesterol synthesis contributes to growth of intracellular *Toxoplasma gondii* in macrophages. J. Vet. Med. Sci. **73:**633-639.

Nolan SJ, Romano JD, Luechtefeld T, Coppens I. 2015. *Neospora caninum* recruits host cell structures to its parasitophorous vacuole and salvages lipids from organelles. Eukaryot. Cell. **14**(5):454-473.

Nowak M, Tardivel S, Sayegrih K, Robert V, Abreu S, Chaminade P, Vicca S, Grynberg A, Lacour B. 2011. Impact of polyunsaturated fatty acids on oxidized low density lipoprotein-induced U937 cell apoptosis. J. Atheros. and Thromb. **18**(6):494-503.

Ohsaki Y, Kawai T, Yoshikawa Y, Cheng J, Jokitalo E, Fujimoto T. 2016. PML isoform II plays a critical role in nuclear lipid droplet formation. J. Cell Biol. **212**:29-38.

Olofsson SO, Böstrom P, Andersson L, Rutberg M, Perman J, Boren J. 2009. Lipid droplets as dynamic organelles connecting storage and efflux of lipids. Biochim. Biophys. Acta. **1791**:448-458.

Ong YC, Reese ML, Boothroyd JC. 2010. *Toxoplasma* rhoptry protein 16 (ROP16) subverts host function by direct tyrosine phosphorylation of STAT6. J. Biol. Chem. **285:**28731-28740.

Ostlund RE Jr. 2004. Phytosterols and cholesterol metabolism. Curr. Opin. Lipidol. **15**(1):37-41.

Ostrander, DB, Sparagna GC, Amoscato AA, McMillin JB, Dowhan W. 2001. Decreased cardiolipin synthesis corresponds with cytochrome c release in palmitate-induced cardiomyocyte apoptosis. J. Biol. Chem. **276:**38061-38067.

Ota T, Gayet C, Ginsberg HN. 2008. Inhibition of apolipoprotein B100 secretion by lipid-induced hepatic endoplasmic reticulum stress in rodents. J. Clin. Invest. **118**:316-332.

Ouimet M, Franklin V, Mak E, Liao X, Tabas I, Marcel YL. 2011. Autophagy regulates cholesterol efflux from macrophage foam cells via lysosomal acid lipase. Cell. Metab. **13**:655-667.

Ozeki S, Cheng J, Tauchi-Sato K, Hatano N, Taniguchi H, Fujimoto T. 2005. Rab18 localizes to lipid droplets and induces their close apposition to the endoplasmic reticulum-derived membrane. J. Cell Sci. **188**:2601-2611.

Pagano RE, Martin OC, Kang HC, Haugland RP. 1991. A novel fluorescent ceramide analogue for studying membrane traffic in animal cells: accumulation at the Golgi apparatus results in altered spectral properties of the sphingolipid precursor. J. Cell Biol. **113:**1267-1279.

Pagliarini DJ, Rutter J. 2013. Hallmarks of a new era in mitochondrial biochemistry. Genes Dev. **27:**2615-2627.

Palacpac NM, Hiramine Y, Mi-ichi F, Torii M, Kita K, Hiramatsu R, Horii T, Mitamura T. 2004. Developmental-stage-specific specific triacylglycerol biosynthesis, degradation and trafficking as lipid bodies in Plasmodium falciparum-infected erythrocytes. J. Cell Sci. **117**:1469-1480.

Palanisamy GS, Kirk NM, Ackart DF, Obregon-Henao A, Shanley CA, Orme IM, Basaraba RJ. 2012. Uptake and accumulation of oxidized low-density lipoprotein during *Mycobacterium tuberculosis* infection in guinea pigs. PLoS ONE. **7**(3):e34148.

Pérez-Chacón G, Astudillo AM, Balgoma D, Balboa MA, Balsinde J. 2009. Control of free arachidonic acid levels by phospholipases A2 and lysophospholipid acyltransferases. Biochim. Biophys. Acta. **1791**:1103-1113.

Pernas L, Boothroyd JC. 2010. Association of host mitochondria with the parasitophorous vacuole during *Toxoplasma* infection is not dependent on rhoptry proteins ROP2/8. Int. J. Parasitol. **40:**1367-1371.

Pernas L, Adomako-Ankomah Y, Shastri AJ, Ewald SE, Treeck M, Boyle JP, Boothroyd JC. *Toxoplasma* effector MAF1 mediates recruitment of host mitochondria and impacts the host response. PLoS One. **12**(4):e1001845.

Perrotta J, Keister DB, Gelderman AH. 1971. Incorporation of precursors into *Toxoplasma* DNA. J. Protozool. **18**:470-473.

Pfefferkorn ER. 1984. Interferon gamma blocks the growth of *Toxoplasma gondii* in human fibroblasts by inducing the host cells to degrade tryptophan. PNAS. **81**:908-912.

Plattner H, Sehring IM, Mohamed IK, Miranda K,De Souza W, Billington R, Genazzani A, Ladenburger EM. 2012. Calcium signaling in closely related protozoan groups (Alveolata): non-parasitic ciliates (*Paramecium*, *Tetrahymena*) versus parasitic Apicomplexa (*Plasmodium*, *Toxoplasma*). Cell Calcium. **51**:351-382.

Persson EK, Agnarson AM, Lambert H, Hitziger N, Yagita H, Chambers BJ, Barragan A, Grandien A. 2007. Death receptor ligation or exposure to perforin trigger rapid egress of the intracellular parasite *Toxoplasma gondii*. J. Immunol. **179**:8357-8365.

Polonais V, Soldati-Favre D. 2010. Versatility in the acquisition of energy and carbon sources by the Apicomplexa. Biol. Cell. **102**:435-445.

Prades J, Alemany R, Perona JS, Funari SS, Vögler O, Ruíz-Gutiérrez V, Escribá PV, Barceló F. 2008. Effects of 2-hydroxyoleic acid on the structural properties of biological and model plasma membranes. Mol. Membr. Biol. **25**:46-57.

Prandovszky E, Gaskell E, Martin H, Dubey JP, Webster JP, McConkey GA. 2011. The Neurotropic Parasite *Toxoplasma Gondii* Increases Dopamine Metabolism. PLoS One. **6**(9): e23866.

Pratt S, Wansadhipathi-Kannangara NK, Bruce CR, Mina JG, Shams-Eldin H, Casas J, Hanada K, Schwarz RT, Sonda S, Denny PW. 2013. Sphingolipid synthesis and scavenging in the intracellular apicomplexan parasite, *Toxoplasma gondii*. Mol. Biochem. Parasitol. **187**:43-51.

Proikas-Cezanne T, Gaugel A, Frickey T, Nordheim A. 2006. Rab14 is part of the early endosomal clathrin-coated TGN microdomain. FEBS Lett. **580**:5241-5246.

Pszenny V, Ehrenman K, Romano JD, Kennard A, Schultz A, Roos DS, Grigg ME, Carruthers VB, Coppens I. 2015. A lipolytic lecithin:cholesterol acyltransferase secreted by *Toxoplasma* facilitates parasite replication and egress. J. Biol. Chem. PMID: 26694607.

Pulido-Mendez M, Finol HJ, Giron ME, Aguilar I. 2006. Ultrastructural pathological changes in mice kidney caused by *Plasmodium berghei* infection. J. Submicrosc. Cytol. Pathol. **38**:143-148.

Quittnat F, Nishikawa Y, Stedman TT, Voelker DR, Choi JY, Zahn MM, Murphy RC, Barkley RM, Pypaert M. Joiner KA, Coppens I. 2004. On the biogenesis of lipid bodies in ancient eukaryotes: synthesis of triacylglycerols by a*Toxoplasma* DGAT1-related enzyme. Mol. Biochem. Parasitol. **138**:107-122.

Rachek LI, Musiyenko SI, LeDoux SP, Wilson GL. 2007. Palmitate induced mitochondrial deoxyribonucleic acid damage and apoptosis in l6 rat skeletal muscle cells. Endocrinology. **148**: 293-299.

Ramakrishnan S, Docampo MD, Macrae JI, Pujol FM, Brooks CF, van Dooren GG, Hiltunen JK, Kastaniotis AJ, McConville MJ, Striepen B. 2012. Apicoplast and endoplasmic reticulum cooperate in fatty acid biosynthesis in apicomplexan parasite *Toxoplasma gondii*. J. Biol. Chem. **287**:4957-4971.

Rambold AS, Cohen S, Lippincott-Schwartz J. 2015. Fatty acid trafficking in starved cells: regulation by lipid droplet lipolysis, autophagy, and mitochondrial fusion dynamics. Dev. Cell. **32**(6):678-692.

Reddy PH, Reddy TP. 2011. Mitochondria as a therapeutic target for aging and neurodegenerative diseases. Curr. Alzheimer Res. **8**(4):393-409.

Reese ML, Zeiner GM, Saeij JP, Boothroyd JC, Boyle JP. 2011. Polymorphic family of injected pseudokinases is paramount in *Toxoplasma* virulence. PNAS. **108**:9625-9630.

Reid AJ, Vermont SJ, Cotton JA, Harris D, Hill-Cawthorne GA, Könen-Waisman S, Latham SM, Mourier T, Norton R, Quail MA, Sanders M, Shanmugam D, Sohal A, Wasmuth JD, Brunk B, Grigg ME, Howard JC, Parkinson J, Roos DS, Trees AJ, Berriman M, Pain A, Wastling JM. 2012. Comparative genomics of the apicomplexan parasites *Toxoplasma gondii* and *Neospora caninum*: Coccidia differing in host range and transmission strategy. PLoS Pathog. **8:**e1002567.

Ricchi M, Odoardi MR, Carulli L, Anzivino C, Ballestri S, Pinetti A, Fantoni LI, Marra F, Bertolotti M, Banni S, Lonardo A, Carulli N, Loria P. 2009. Differential effect of oleic and palmitic acid on lipid accumulation and apoptosis in cultured hepatocytes. J. Gastroent. Hepatol. **24**(5):830-840.

Richieri GV, Kleinfeld AM. 1995. Unbound free fatty acid levels in human serum. J. Lipid Res. **36**:229-240.

Robibaro B, Hoppe HC, Yang M, Coppens I, Ngô HM, Stedman TT, Paprotka K, Joiner KA. 2001. Endocytosis in different lifestyles of protozoan parasitism: role in nutrient uptake with special reference to *Toxoplasma gondii*. Int. J. Parasitol. **31**(12):1343-1353.

Robert-Gangneux F, Dardé ML. 2012. Epidemiology of and diagnostic strategies for toxoplasmosis. Clin. Microbiol. Rev. **25**(2):264-296.

Rohloff P, Miranda K, Rodriguez JC, Fang J, Galizzi M, Plattner H, Hentschel J, Moreno SN. 2011. Calcium uptake and proton transport by acidocalcisomes of *Toxoplasma gondii*. PLoS One. **6**(4):e18390.

Rohwedder A, Zhang Q, Rudge SA, Wakelam MJO. Lipid droplet formation in response to oleic acid in Hyg-7 cells is mediated by the fatty acid receptor FFAR4. J. Cell Science. **127**:3104-3115.

Roiko MS, Svezhova N, Carruthers VB. 2014. Acidification activates *Toxoplasma gondii* motility and egress by enhancing protein secretion and cytolytic activity. PLOS Pathog. **10**:e1004488.

Romano JD, Bano N, Coppens I. 2008. New host nuclear functions are not required for the modifications of the parasitophorous vacuole of *Toxoplasma*. Cell Microbiol. **10**:465-476.

Romano JD, Coppens I. 2013. Host Organelle Hijackers: a similar modus operandi for *Toxoplasma gondii* and *Chlamydia trachomatis*: co-infection model as a tool to investigate pathogenesis. Pathog. Dis. **69**(2):72-86.

Romano JD, Sonda S, Bergbower E, Smith ME, Coppens I. 2013. *Toxoplasma gondii* salvages sphingolipids from the host Golgi through the rerouting of selected Rab vesicles to the parasitophorous vacuole. Mol. Biol. Cell **24:**1974-1995.

Roos DS, Donald RG, Morrissette NS, Moulton AL. 1994. Molecular tools for genetic dissection of the protozoan parasite *Toxoplasma gondii*. Method Cell Biol. **45:**27-63.

Rustan AC, Drevon CA. 2005. Fatty acids: structures and properties. Encyclopedia of life sciences. John Wiley and Sons.

Saka HA, Valdivia R. 2012. Emerging roles for lipid droplets in immunity and host-pathogen interactions. Annu. Rev. Cell Dev. Biol. **28**:411-437.

Saka HA, Thompson JW, Chen YS, Dubois LG, Haas JT, Moseley A, Valdivia RH. 2015. *Chlamydia trachomatis* Infection Leads to Defined Alterations to the Lipid Droplet Proteome in Epithelial Cells. PLoS One. **10**(4):e0124630.

Sampels V, Hartmann A, Dietrich I, Coppens I, Sheiner L, Striepen B, Herrmann A, Lucius R, Gupta N. 2012. Conditional mutagenesis of a novel choline kinase demonstrates plasticity of phosphatidylcholine biogenesis and gene expression in *Toxoplasma gondii*. J. Biol. Chem. **287**:16289-16299.

Schneider AG, Abi Abdallah DS, Butcher BA, Denkers EY. *Toxoplasma gondii* Triggers Phosphorylation and Nuclear Translocation of Dendritic Cell STAT1 while Simultaneously Blocking IFNγ-Induced STAT1 Transcriptional Activity. PLoS One. **8**(3):e60215.

Schrader M, Godinho LF, Costello JL, Islinger M. 2015. The difference facets of organelle interplay – an overview of organelle interactions. Front. Cell. Dev. Biol. **3**(56):1-22.

Schroeder F, Goetz I, Roberts E. 1984. Sex and age alter plasma membranes of cultured fibroblasts. Eur. J. Biochem. **142**:183-191.

Schroeder B, Schulze RJ, Weller SG, Sletten AC, Casey CA, McNiven MA. 2015. The small GTPase Rab7 as a central regulator of hepatocellular lipophagy. Hepatology. **61**(6):1896-1907.

Schwab JC, Beckers CJM, Joiner KA. 1994. The parasitophorous vacuole membrane surrounding intracellular *T. gondii* functions as a molecular sieve. Proc. Natl. Acad. Sci. USA. **91**:509-513.

Seeber F. 2003. Biosynthetic pathways of plastid-derived organelles as potential drug targets against parasitic apicomplexa. Curr. Drug Targets Immune Endocr. Metabol. Disord. **3**:99-109.

Seeber F, Soldati-Favre D. 2010. Metabolic pathways in the apicoplast of Apicomplexa. Int. Rev. Cell. Mol. Biol. **281**:161-228.

Seidelin KN. 1995. Fatty acid composition of adipose tissue in humans. Implications for the dietary fat-serum cholesterol-CHD issue. Progress in Lipid Res. **34**(3):199-217.

Selleck EM, Orchard RC, Lassen KG, Beatty WL, Xavier RJ, Levine B, Virgin HW, Sibley LD. 2015. A Noncanonical Autophagy Pathway Restricts *Toxoplasma gondii* Growth in a Strain-Specific Manner in IFN-γ-Activated Human Cells. Mol. Bio. **6**(5):e01157-15.

Sembdner G, Parthier B. 1993. The biochemistry and the physiological and molecular actions of jasmonates. Annual Rev. of Plant Phys. and Plant Mol. Biol. **44**(1):569-589.

Shanmugasundram A, Gonzalez-Galarza FF, Wastling JM, Vasieva O, Jones AR. 2013. Library of Apicomplexan Metabolic Pathways: a manually curated database for metabolic pathways of apicomplexan parasites. Nucleic Acids Res. **41**:D706-D713.

Shaw CS, Jones DA, Wagenmakers AJ. 2008. Network distribution of mitochondria and lipid droplets in human muscle fibers. Histochem. Cell. Biol. **129**:65-72.

Shimabukuro M, Ohneda M, Lee Y, Unger RH. 1997. Role of nitric oxide in obesity-induced beta cell disease. J. Clin. Invest. **100:**290-295.

Shpilka T, Elazar Z. 2015. Lipid droplets regulate autophagosome biogenesis. Autophagy. **11**(11):2130-2131.

Sibley LD, Niesman IR, Asai T, Takeuchi T. 1994. *Toxoplasma gondii*: secretion of a potent nucleoside triphosphate hydrolase into the parasitophorous vacuole. Exp. Parasitol .**79**:301-311.

Sibley LD. 2003. *Toxoplasma gondii*: perfecting an intracellular life style. Traffic. **4**:581-586.

Sinai AP, Webster P, Joiner KA. 1997. Association of host cell endoplasmic reticulum and mitochondria with the *Toxoplasma gondii* parasitophorous vacuole membrane: a high affinity interaction. J. Cell Sci. **110:**2117-2128.

Sinai AP, Joiner KA. 2001. The *Toxoplasma gondii* protein ROP2 mediates host organelle association with the parasitophorous vacuole membrane. J. Cell Biol. **154:**95-108.

Sinai AP, Payne TM, Carmen JC, Hardi L, Watson SJ, Molestina RE. 2004. Mechanisms underlying the manipulation of host apoptotic pathways by *Toxoplasma gondii*. Int. J. Parasitol. **34:**381-391.

Sinai AP. 2008. Biogenesis of and activities at the *Toxoplasma gondii* parasitophorous vacuole membrane. Subcell. Biochem. **47:**155-164.

Singh R, Kaushik Y, Wang Y, Xiang Y, Novak I, Komatsu M, Tanaka K, Cuervo AM, Czaja MJ. 2009. Autophagy regulates lipid metabolism. Nature. **458**:1131-1135.

Sinka R, Gillingham AK, Kondylis V, Munro S. 2008. Golgi coiled-coil proteins contain multiple binding sites for Rab family G proteins. J. Cell Biol. **183:**607-615.

Shaughnessy DT, McAllister K, Worth L, Haugen AC, Meyer JN, Domann FE, Van Houten B, Mostoslavsky R, Bultman SJ, Baccarelli AA, Begley TJ, Sobol R, Hirschey MD, Ideker T, Santos JH, Copeland WC, Tice RR, Balshaw DM, Tyson FL. 2014. Mitochondria, Energetics, Epigenetics, and Cellular Responses to Stress. Environ. Health Perspect. **122**:1271-1278.

Sheiner L, Vaidya AB, McFadden GI. 2013. The metabolic roles of the endosymbiotic organelles of *Toxoplasma* and *Plasmodium* spp. Curr. Opin. in Microb. **16**(4):452-458.

Sibley LD, Boothroyd JC. 1992. Virulent strains of *Toxoplasma gondii* comprise a single clonal lineage. Nature. **359**(6390):82-85.

Sirakova TD, Dubey VS, Deb C, Daniel J, Korotkova TA, Abomoelak B, Kolattukudy PE. 2006. Identification of a diacylglycerol acyltransferase gene involved in accumulation of triacylglycerol in *Mycobacterium tuberculosis* under stress. Microbiology. **152**:2717-2725.

Skariah S, McIntyre MK, Mordue DG. 2010. *Toxoplasma gondii*: determinants of tachyzoite to bradyzoite conversion. Parasitol. Res. **107**(2):253-260.

Smirnova E, Goldberg EB, Makarova KS, Lin L, Brown WJ, Jackson CL. 2006. ATGL has a key role in lipid droplet/adiposome degradation in mammalian cells. EMBO Rep. **7**(1):106-113.

Sohn CS, Cheng TT, Drummond ML, Peng ED, Vermont SJ, Xia D, Cheng SJ, Wastling JM, Bradley PJ. 2011. Identification of novel proteins in *Neospora caninum* using an organelle purification and monoclonal antibody approach. PLoS One. **6:**e18383.

Sonda S, Sala G, Ghidoni R, Hemphill A, Pieters J. 2005. Inhibitory effect of aureobasidin A on *Toxoplasma gondii*. Antimicrob. Agents Chemother. **49:**1794-1801.

Speer CA, Dubey JP, McAllister MM, Blixt JA. 1999. Comparative ultrastructure of tachyzoites, bradyzoites, and tissue cysts of *Neospora caninum* and *Toxoplasma gondii*. Int. J. Parasitol. **29:**1509-1519.

Steinfeldt T, Konen-Waisman S, Tong L, Pawlowski N, Lamkemeyer T, Sibley LD, Hunn JP, Howard JC. 2010. Phosphorylation of mouse immunity-related GTPase (IRG) resistance proteins is an evasion strategy for virulent *Toxoplasma gondii*. PLoS Biol. **8:**e1000576.

Striepen B, Soldati-Favre D. 2013. Genetic Manipulation of *Toxoplasma gondii*. In *Toxoplasma Gondii* The Model Apicomplexan: Perspectives and Methods, Weiss, L.M., and Kim, K. eds. (London, UK: Academic Press), pp. 408-409.

Su B, Wang X, Zheng L, Perry G, Smith MA, Zhu X. 2009. Abnormal mitochondrial dynamics and neurodegenerative diseases. Biochim. Biophys. Acta. **1802**(1):135-142.

Sweeney KR, Morrissette NS, LaChapelle S, Blader IJ. 2010. Host cell invasion by *Toxoplasma gondii* is temporally regulated by the host microtubule cytoskeleton. Eukaryot. Cell. **9:**1680-1689.

Szymanski KM, Binns D, Bartz R, Grishin NV, Li WP, Agarwal AK, Garg A, Anderson RGW, Goodman JM. 2007. The lipodystrophy protein seipin is found at endoplasmic reticulum lipid droplet junctions and is important for droplet morphology. Proc. Natl. Acad. Sci. USA. **104**:20890-20895.

Tan SH, Shui G, Zhou J, Li JJ, Bay BH, Wenk MR, Shen HM. 2012. Induction of autophagy by palmitic acid via protein kinase C-mediated signaling pathway independent of mTOR (mammalian target of rapamycin). J. Biol. Chem. **287**(18):14364-14376.

Tansey JT, Sztalryd C, Gruia-Gray J, Roush DL, Zee JV, Gavrilova O, Reitman ML, Deng CX, Li C, Kimmel AR, Londos C. 2001. Perilipin ablation results in a lean mouse with aberrant adipocyte lipolysis, enhanced leptin production, and resistance to diet-induced obesity. Proc. Natl. Acad. Sci. USA. **98**:6494-6499.

Targett-Adams P, Chambers D, Gledhill S, Hope RG, Coy JF, Girod A, McLauchlan J. 2003. Live cell analysis and targeting of the lipid droplet-binding adipocyte differentiation-related protein. J. Biol. Chem. **278**(18):15998-16007.

Tauchi-Sato K, Ozeki S, Houjou T, Taguchi T, Fujimoto T. 2002. The surface of lipid droplets is a phospholipid monolayer with a unique Fatty Acid composition. J. Biol. Chem.**277**:44507–44512.

Tenter AM, Heckeroth AR, Weiss LM. 2002. *Toxoplasma gondii*: from animals to humans. Int. J. Parasitol. **30:**1217-1258.

Terés S, Lladó V, Higuera M, Barceló-Coblijn G, Martin ML, Noguera-Salva MA, Marcilla-Etxenike A, García-Verdugo JM, Soriano-Navarro M, Saus C, Gómez-Pinedo U, Busquets X, Escribá PV. 2012. 2-Hydroxyoleate, a nontoxic membrane binding anticancer drug, induces glioma cell differentiation and autophagy. Proc. Natl. Acad. Sci. U.S.A. **109**:8489-8494.

Thomas C, Rousset R, Noselli S. 2009. JNK signalling influences intracellular trafficking during Drosophila morphogenesis through regulation of the novel target gene Rab30. Dev. Biol. **331:**250-260.

Thörn K, Bergsten P. 2010. Fatty acid-induced oxidation and triglyceride formation is higher in insulin-producing MIN6 cells exposed to oleate compared to palmitate. J. Cell. Biochem. **111**:497-507.

Tomavo S, Schwarz RT, Dubremetz JF. 1989. Evidence for glycosylphosphatidylinositol anchor of *Toxoplasma gondii* major surface antigens. Mol. Cell. Biol. **9**:4576-4580.

Tomavo S. 2001. The differential expression of multiple isoenzyme forms during stage conversion of *Toxoplasma gondii*: an adaptive developmental strategy. Int. J. Parasitol. **31:**1023-1031.

Tu Q, Zheng R, Li J, Hu L, Chang Y, Li L, Li M, Wang R, Huang D, Wu M, Hu H, Chen L, Wang H. 2014. Palmitic acid induces autophagy in hepatocytes via JNK2 activation. Acta Pharm. Sinica. **35**:504-512.

Tuder RM, Robinson JC, Graham BB. 2014. Fat and cardiotoxicity in hereditary pulmonary hypertension. Am. J. Respir. Crit. Care Med. **189**(3):247-249.

Turpin SM, Lancaster GI, Darby I, Febbraio MA, Watt MJ. 2006. Apoptosis in skeletal muscle myotubes is induced by ceramides and is positively related to insulin resistance. Am. J. Physiol. Endocrinol. Metab. **291**:1341-1350.

Tyler JS, Treeck M, Boothroyd JC. 2011. Focus on the ringleader: the role of AMA1 in apicomplexan invasion and replication. Trends Parasitol. **27**(9):410-420.

Ueno M, Shen WJ, Patel S, Greenberg AS, Azhar S, Kraemer FB. 2013. Fat-specific protein 27 modulates nuclear factor of activated T cells 5 and the cellular response to stress. J. Lipid Res. **54**:734-743.

Uzbekov R, Roingeard P. 2013. Nuclear lipid droplets identified by electron microscopy of serial sections. BMC Res. **Notes 6**, 386.

Vance JE, Vance DE. 2004. Phospholipid biosynthesis in mammalian cells. Biochem. Cell Biol. **82**:113-128.

Vasyukova NI, Zinovieva SV, Udalova ZV, Gerasimova NG, Ozeretskovskaya OL, Sonin MD. 2009. Jasmonic acid and tomato resistance to the root-knot nematode *Meloidogyne incognita*. Doklady Biological Sciences. **428**:448-450.

Vicario IM, Malkova D, Lund EK, Johnson IT. 1998. Olive oil supplementation in healthy aldults: effects in cell membrane fatty acid composition and platelet function. Ann. Nutri. Metab. **42**:160-169.

Vielemeyer O, McIntosh MT, Joiner KA, Coppens I. 2004. Neutral lipid synthesis and storage in the intraerythrocytic stages of Plasmodium falciparum. Mol. Biochem. Parasitol. **135**(2):197-209.

Vögler O, López-Bellán A, Alemany R, Tofe S, González M, Quevedo J, Pereg V, Barceló F, Escribá PV. 2008. Structure-effect relation of C18 long-chain fatty acids in the reduction of body weight in rats. Int. J. Obes. **32**:464-473.

Volpon L, Lancelin J. 2000. Solution NMR structures of the polyene macrolide antibiotic filipin III. FEBS Lett. **478:**137-140.

Vonlaufen N, Guetg N, Naguleswaran A, Müller N, Björkman C, Schares G, von Blumroeder D, Ellis J, Hemphill A. 2004. *In vitro* induction of *Neospora caninum* bradyzoites in Vero cells reveals differential antigen expression, localization, and host-cell recognition of tachyzoites and bradyzoites. Infect. Immun. **72:**576-583.

Walker ME, Hjort EE, Smith SS, Tripathi A, Hornick JE, Hinchcliffe EH, Archer W, Hager KM. 2008. *Toxoplasma gondii* actively remodels the microtubule network in host cells. Microbes Infect. **10:**1440-1449.

Waller RF, Keeling PJ, Donald RG, Striepen B, Handman E, Lang-Unnasch N, Cowman AF, Besra GS, Roos DS, McFadden GI. 1998. Nuclear-encoded proteins target to the plastid in *Toxoplasma gondii* and *Plasmodium falciparum*. Proc. Natl. Acad. Sci. USA. **95**:12352-12357.

Walther TC, Farese RV Jr. 2012. Lipid droplets and cellular lipid metabolism. Annu. Rev. Biochem. **81**:687-714.

Wang DZ, Dubois RN. 2010. Eicosanoids and cancer. Nat. Rev. Cancer. **10**:181–193.

Wang S, Soni KG, Semache M, Casavant S, Fortier M, Pan L, Mitchell GA. 2008. Lipolysis and the integrated physiology of lipid energy metabolism. Mol Genet. Metab. **95**(3)**:**117-126.

Wang Y, Weiss LM, Orlofsky A. 2009. Host cell autophagy is induced by *Toxoplasma gondii* and contributes to parasite growth. J. Biol. Chem. **284**:1694-1701.

Wang Y, Weiss LM, Orlofsky A. 2010. Coordinate control of host centrosome position, organelle distribution, and migratory response by *Toxoplasma gondii* via host mTORC2. J. Biol. Chem. **285:**15611-15618.

Wang CW. 2015. Lipid droplets, lipophagy, and beyond. Biochim. Biosphys. Acta. In press.

Welte MA. 2009. Fat on the move: Intracellular motion of lipid droplets. Biochem. Soc. Trans. **37**:991-996.

Welte MA. 2015. Expanding roles for lipid droplets. Curr. Biol. **25**:470-481.

Welti R, Mui E, Sparks A, Wernimont S, Isaac G, Kirisits M, Roth M, Roberts CW, Botté C, Maréchal E, McLeod R. 2007. Lipidomic analysis of *Toxoplasma gondii* reveals unusual polar lipids. Biochem. **46:**13882-13890.

Wende AR, Abel ED. 2010. Lipotoxicity in the heart. Biochim. Biophys. Acta. **1801**(3):311-319.

WHO. World Health Organization. 2015. World Malaria Report.

Wilfling F, Wang H, Haas JT, Krahmer N, Gould TJ, Uchida A, Cheng J, Graham M, Christiano R, Fröhlich F, Liu X, Buhman KK, Coleman RA, Bewersdorf J, Farese RJ Jr, Walther TC. 2013. Triacylglycerol synthesis enzymes mediate lipid droplet growth by relocalizing from the ER to lipid droplets. Dev. Cell. **24**:384-399.

Wolins NE, Brasaemle DL, Bickel PE. 2006. A proposed model of fat packaging by exchangeable lipid droplet proteins. FEBS Lett. **580**:5484–5491.

Wymann MP, Schneiter R. 2008. Lipid signalling in disease. Nat. Rev. Mol. Cell Biol. **9**:162-76.

Yang H, Cromley D, Wang H, Billheimer JT, Sturley SL. 1997. Functional expression of a cDNA to human acyl-coenzyme A:cholesterol acyltransferase in yeast. Species-dependent substrate specificity and inhibitor sensitivity. J. Biol. Chem. **272**:3980-3985.

Yang H, Li X. 2012. The role of fatty acid metabolism and lipotoxicity in pancreatic β-cell injury: Identification of potential therapeutic targets. Acta Pharmac. Sinica. **2**(4):396-402.

Yang L, Ding Y, Chen Y, Zhang S, Huo C, Wang Y, Yu J, Zhang P, Na H, Zhang H, Ma Y, Liu P. 2012. The proteomics of lipid droplets: structure, dynamics, and functions of the organelle conserved from bacteria to humans. J. Lipid Res. **53**(7):1245-1253.

Yen CE, Stone SJ, Koliwad S, Harris C, Farese RV Jr. DGAT enzymes and triacylglycerol biosynthesis. J. Lipid Res. **49**:2283-2301.

Yuzefovych L, Wilson G, Rachek L. 2010. Different effects of oleate vs. palmitate on mitochondrial function, apoptosis, and insulin signaling in L6 skeletal muscle cells: role of oxidative stress. Endocrinology and Metabolism. **299**(6):1096-1105.

Zaloga GP, Willey S, Tomasic P, Chernow B. 1987. Free fatty acids alter calcium binding: a cause for misinterpretation of serum calcium values and hypocalcemia in critical illness. J. Clin. Endocrinol. Metab. **64**(5):1010-1014.

Zhou L, Nilsson . 2001. Sources of eicosanoid precursor fatty acid pools in tissues. J. Lipid Res. **42**:1521-1542.

Zinecker CF, Striepen B, Geyer H, Geyer R, Dubremetz JF, Schwartz RT. 2001. Two glycoforms are present in the GPI-membrane anchor of the surface antigen 1 (P30) of *Toxoplasma gondii*. Mol. Biochem. Parasitol. **116**(2):127-135.

CURRICULUM VITAE

SABRINA JANE NOLAN

Work: 615 N. Wolfe St, Rm E2209 – Baltimore 21205, MD. Tel: 443 287 1588
Personal: 3001 O'Donnell St, Apt 2 – Baltimore 21224, MD. Tel: 443 345 7499
Email: snolan9@jhu.edu - LinkedIn: /sabrinanolan

Dual Nationality : UK and Ireland – Born in Italy, October 20 1983
Currently holding US F1 visa until May 2016, with option for OPT

EDUCATION:

- August 2011 – present: PhD candidate at the Johns Hopkins Bloomberg School of Public Health (JHSPH) in the Molecular Microbiology and Immunology department, Baltimore MD. GPA: 3.91.

  Currently pursuing thesis research in Dr. Isabelle Coppens laboratory (July 2012 – present):

  - Investigation of host cell interactions with *Toxoplasma gondii* and *Neospora caninum* analyzing cellular organelle recruitment, lipid scavenging and vesicle uptake to the parasitophorous vacuole (Published work, March 2015).
  - Analysis of the role of host lipid droplets to *T. gondii* replication and development in mammalian cells.
  - Investigation of the effect of excess oleic acid on the intracellular development of *T. gondii* in mammalian cells
  - Techniques include (but not limited to) live microscopy, immunofluorescence assays and microscopy, electron microscopy, western blotting, cell culture, plaque assays, protein and RNA extraction, radioactivity assays, PCR, RT-PCR and mammalian cell/parasite transfections.
- January 2008 – August 2010: MSc in Biology at American University (NW D.C.) in collaboration with the National Institutes of Health. GPA: 3.8
  - Under the supervision of Dr. Jonathan Wiest (now director of Center for Cancer Training, NCI), and my advisor, Dr. K. DeCicco-Skinner (American University), we looked at different signaling pathways being expressed in *tpl2* knockout mice to account for increased tumorigenesis in a 2-step skin carcinogenesis model.
  - Techniques include: Extracting keratinocytes from mice and protein isolation, cell culture, protein assays, western blotting, in *vivo* mousework, immunoassays and immunohistochemistry.
- October 2002 – June 2006: Bachelor Degree for Biological Sciences from Edinburgh University, Scotland. Components of interest: Immunology, Medical Microbiology and Infection & Diseases.

PUBLICATIONS AND CONFERENCE ABSTRACTS:

- **Nolan SJ, Romano JD, Luechtefeld T and Coppens I. *Neospora caninum* recruits host cell structures to its parasitophorous vacuole and salvages lipids from organelles (2015). *Eukaryotic Cell* 14(5):4554-73**
- **DeCicco* K, Nolan* SJ (* co- first author), Deshpande MM, Trovato EL, Dempsey TA, Wiest JS. Altered prostanoid signaling contributes to increased skin tumorigenesis in tpl2 knockout mice. *PLoS One*. 2013;8(2):e56212**

- Nolan SJ, Romano JD, Ehrenman K and Coppens I. Changes in Lipid Droplet Dynamics in *Toxoplasma*-infected cells. June 2015, 13th International Conference on Toxoplasma, Gettysburg, Pennsylvania, USA.
- Romano JD, Nolan SJ, Porter C, Hartman E, Ehrenman K, Strong J, Hsia R, Coppens I. Characterization of *Toxoplasma gondii* Interception of Host Vesicles. June 2015, 13th International Conference on Toxoplasma, Gettysburg, USA.
- Romano JD, Nolan SJ, Porter C and Coppens I. Scavenging of host lipids and vesicles by the parasite *Tonxoplasma gondii*. Abstract and poster for American Society of Cell Biology meeting, December 2013, New Orleans, Louisiana, USA.
- Nolan SJ, Romano JD, Luechtefeld TH and Coppens I. Comparative study on lipid scavenging and host organelle association of *Neospora caninum* and *Toxoplasma gondii*. Abstract and poster for Molecular Parasitology Meeting, September 2013, Woods Hole, Massachussetts.
- DeCicco-Skinner K, Nolan SJ, Dempsey TA, Lepage P, Trovato EL, and Wiest JS. Tumor progression locus 2 (Tpl2) knockout mice have a dysregulation in COX-2 signaling in two-stage skin carcinogenesis. American Association for Cancer Research, Orlando, Fl, 2011.
- Dempsey TA, Nolan SJ, Wiest JS and DeCicco-Skinner K. Tumor progression locus 2 (Tpl2) knockout mice have heightened expression of transcription factors and nuclear receptors in keratinocytes stimulated with 12-*O*-tetradecanoylphorbol-13-acetate (TPA). American Association for Cancer Research, Washington, DC, 2010.

CURRENT SIDE PROJECTS AND PAST EXPERIENCE:

Side Projects:

- October 2015 – present: Collaboration with Dr. Arturo Casadevall's laboratory investigating the influence of excess fatty acid on the development of the fungi *Cryptosporidium neoformans* in macrophages.
- March 2013 – present: Co-founder/creator of an Image Quantification Software: MetaScopics
  - Image analysis: Advanced microscopy techniques with image analysis algorithms
    - Microscopy analysis is often limited to qualitative, rather than quantitative conclusions. MetaScopics creates new algorithms to independently achieve quantifiable data from sets of images www.metascopics.com.

        - Proof of concept and functionality published in 2015, *Eukaryotic Cell*, Nolan SJ. *et al.*
- August 2012 – present: Teaching assistant for the graduate level course, Evolution of Infectious Diseases.
    - Classroom organization, administration, grading, pedagogy, technology, evaluation, student-faculty communication and problem solving.
    - Professors: Drs. Sabra Klein, Richard Markham and Doug Norris.

Professional Experience:

- February 2011 – August 2011: Research technician at the Center for Alternatives to Animal Testing at Johns Hopkins Bloomberg School of Public Health, under the supervision of Dr H. Högberg and Dr. Thomas Hartung. Duties include RNA extraction and identification, astrocyte and neuron extraction from rats, mass spectrometry, cell culture, western blotting and immunoassays. Contact: Dr. Thomas Hartung, Director.
- August 2010 – February 2011: Expanding on research completed for Masters' thesis at American University and NIH. Contact: Dr. Kathleen DeCicco-Skinner.
- June 2009 – August 2010: Special Volunteer at the National Cancer Institute at NIH, Bethesda. In *vivo* and in *vitro* laboratory research for Masters' thesis. Contact: Dr. Jonathan Wiest.
- April 2007 – May 2007: Internship at the French Embassy, in the mission for Sciences and Technology as a communications writer. Contact: Dr. Hedi Haddada.
- February 2007 – March 2007: Internship at Coeus International School (NW D.C.). Teaching assistance in French and sciences/maths, data organization. Contact: Noel Sheppard.
- June – September 2005 and July – September 2006: Research experience at the Institute for Infection & Immunology Research, Edinburgh University, Scotland, UK. Contact: Dr Francisca Mutapi.

CERTIFICATIONS, ORGANIZATIONS AND OTHER:

Certifications:

- Vaccine Science and Policy, JHSPH Department of International Health, March 2015
- Clinical Vaccine Trials and Good Clinical Practice, JHSPH Department of International Health, May 2013 – present
- Responsible Conduct of Research, JHSPH, August 2013 – present
- IACUC Rodent Handling and Surgery Course, JHU, March 2012 – present

Organizations:

- JHSPH Student Assembly officer: Member-at-Large, officer in the Honors & Awards, and Social & Cultural committees.

- MMI Student Group Organization, Student Assembly
  - AY 2015-2016: President Ex-Officio
  - AY 2014-2015: President – Chairing and organizing student committees, interacting with faculty, logistics, conveying information between students and faculty, organizing and chairing meetings, inviting and hosting outside speakers (Dr. Feng Zhang, MIT; Dr. William Fischer, UNC), organizing events, distributing meeting reports to students, working with faculty to update the curriculum.
  - AY 2013-2014: Vice-president and treasurer
  - 2011 – present: Recruitment committee
- American Society for Microbiology: student member since 2011
- American Association for the Advancement of Science: student member since 2011
- Golden Key International Honour Society: member since 2008

Scholarships & Honors:

- May 2013: Hegner, Cort, Root Memorial Fellowship in Immunology and Infectious Disease
- May 2012: Dr. J. Harold Drudge Scholarship
- April 2009: Helmlinge Summer Stipend Grant and Research Supply Grant
- Summer 2005: Nuffield Summer Stipend Grant

Languages:

- English and French spoken and written bilingually
- Moderate understanding of German and Spanish